Assessment and Reduction of Seismic Vulnerability of Art Objects

Dissertation

submitted to and approved by the

Department of Architecture, Civil Engineering and Environmental Sciences
University of Braunschweig – Institute of Technology

and the

Faculty of Engineering
University of Florence

in candidacy for the degree of a

Doktor-Ingenieur (Dr.-Ing.) /
Dottore di Ricerca in "Riduzione del Rischio da Catastrofi Naturali su Strutture ed Infrastrutture"

by

Tommaso Favaretto

Born 22 May 1983

from Jesolo (VE), Italy

Submitted on	18 March 2012
Oral examination on	07 May 2012
Professorial advisors	Prof. A. Saetta
	Prof. H. Budelmann

2012

Ai miei genitori

To my parents

Acknowledgments

I would like to express my gratitude to the coordinators of this doctorate school, Prof. Claudio Borri and Prof. Udo Peil for giving me the chance to join this school and challenge myself with this fantastic international experience. Thanks to professor Harald Budelmann, for the precious advices and the patience. A special thank is due to my Italian tutor, prof. Anna Saetta, for so many things that they would require an entire chapter.

I cannot forget to thank Prof. Renato Vitaliani, who has always stimulated my curiosity towards engineering issues and life in general; many thanks also to Dr. Luisa Berto for the technical (and not only) support to this work and the interesting long chats about it. Thanks to former student of the Ph.D. school, Paola, Giuseppe and Laura for their precious support and help.

Thanks to Dr. Gianmario Benzoni, for letting me challenge myself with experimental part of research. I really appreciated this opportunity furthermore his help was fundamental in this work.

Thanks to Eng. Samuele Infanti of FiP group and Dr. Jerry Podany of Getty museum for the helpful hints and support, for material and knowledge that you shared with passion.

Last but not least, the most important “thank you” goes to my mum and dad who supported me with love and patience every single day of my life. I will never thank you enough.

Pictures of Test at FiP facilities are available with courtesy of FIP industriale; pictures and details of tests at San Diego facility are available with courtesy of Dr. Gianmario Benzoni.

Contents

Introduction

In the last decade seismic protection of structures and infrastructures has become a topic of significant importance. Recent experiences have highlighted the need for proficient tools to approach this issue, that can provide an efficient assessment of the safety condition of a structure, for different structural and nonstructural types. This is the reason why decision makers need effective instruments to deal with the problem of the assessment and reduction of seismic vulnerability. Italy in particular has recently proposed a standard, the so called "*Guidelines for assessment and reduction of seismic risk on cultural heritage*"; this standard deals in particular with masonry structures, and suggests a possible approach to assess and reduce the seismic vulnerability of different structural types (palaces, bell towers and churches). The results obtained from the application of this standard on the Italian territory was so encouraging, both in terms of applicability and reliability, that it lead to the proposal of an extension of these principles to other targets, objects classified as "historical", and that do not belong to the category of masonry: reinforced concrete buildings, archeological sites and movable art objects.

In this perspective the main aim of this dissertation is to propose an extension of the principles adopted by Guidelines for masonry structures to the particular case of movable art objects. This project is conducted within the context of a research project granted by the Italian Ministry of Culture, as they constitute an important and considerable part of the national heritage in need to be studied and protected, as much as other cultural goods typologies.

This work is divided into three fundamental parts, and each one of them is subdivided into different steps: a general introduction to the normative side of the problem, with a description of the existing norms is provided; a proposal for the assessment of seismic vulnerability of art objects is described and, last but not least, the mitigation phase is dealt with. The theoretical results of the methodology are tested on the case study of the "Galleria dell'Accademia in Florence" with particular attention to "Sala dell'Ottocento" and to " Galleria dei Prigioni", which contain two different typologies of art objects, both interesting for the developments resulting from this work.

The first part discussed in this work is about the normative framework involved. The problem is approached via a logical path that first of all provides the general background knowledge of the existing standards and their conceptual "backbone". Guidelines for masonry structures are then applied to the case study of 85 bell towers placed in the city of Venice. This application is intended to be an introduction to the criteria contained in this code, and it wants to provide a proficient reading key for its extension to the case of art objects. Immediately afterwards a comparison between the main framework of the Guidelines, the framework of risk management (also known as the "risk chain") and the proposed framework is made. This comparison highlights common points and differences between the approaches, and provides a clearer overview of problems related to the extension procedure and to the contents of this work in general.

Then the vulnerability assessment of art objects is presented in detail. Each step of the proposed procedure is described, discussed and applied to the chosen cases of study located in the halls of the "Galleria dell'Accademia". Particular attention is paid to the step of geometrical and material surveys: different levels of accuracy are considered by means of traditional tools and also with the application of the advanced methods of 3D laser scanning. Moreover a new methodology for the survey of stone materials is proposed. Then the methodology deals with the definition of mechanical models, in which two main approaches are assumed: the first one considers the targeted body as a rigid block and it involves in particular the rocking and the overturning phenomena. In this case the dynamic response is initially studied by means of simplified static formulas that take into account the possibility of a non symmetric target object as well as the presence of a vertical action. Afterwards the problem is studied in a more accurate way by means of the application of time history analyses. These results are obtained with a specifically developed Matlab program for the integration of the non linear rocking equations. This numerical tool is hence applied as a tool to obtain a reliable feedback for the proposed static formulas but also to study the dynamic response of a single specific object subjected to a ground motion input. The second approach discusses the case in which the object is firmly connected to the floor, and is meant to analyze the stress level induced in the target by a ground motion. Indeed, whenever from the previous analyses the possibility of triggering of some dynamic phenomena is found, one of the possible considered solutions is to restrain it to the "ground". This analysis method aims to underline possible situations of excessive stress that may damage the object, considering the "health conditions" emerged from the material survey . The methodology is described step-by-step and it is applied to the case study of the Galleria dell'Accademia, in particular the "static analyses" were applied both to "Sala dell'Ottocento" and to "Galleria dei Prigioni", while the second level of analyses (integration of rocking equations and FE modeling) were applied to the case of "Galleria dei Prigioni".

The third phase presented is the one about mitigation, which is a fundamental aspect of the Guidelines and of any procedure that aims to an aware dealing with problems of seismic vulnerability reduction. As it will be shown, there are several possibilities to approach this is issue: from rough and quick technical solutions, aimed to large scale applications, to very detailed ones, that involve the application of anti seismic devices. This dissertation particularly focuses on this aspect; indeed the third part contains, besides a general discussion of quick mitigation measures, a proposal for the extension of an existing technology for antiseismic devices (i.e. double concave friction pendulum) designed "ad hoc" for the case of statues. The purpose of this work is to study and extend an already established technology and adapt it to the different conditions of light weight objects, in turn remedy a gap in the current market. This objective is pursued, in collaboration with an international firm (F.I.P. Industriale) that produces antiseismic devices, by means of an accurate redesign phase, in which it was taken care of including all the different conditions that make the response different from the traditional one, and afterwards an experimental phase. Two different series of experimental tests were carried out: the first one at F.I.P. facility aimed to identify the mechanical parameters of the devices and to verify the correspondence between it and the one expected from the traditional theory; the second series of tests, carried out at San Diego SRMD lab, were aimed to study the interaction between these new devices and a system resembling an art object, also including presence of bidirectional and vertical inputs, that are not often considered. These experiments also highlighted some unexpected behaviors that are connected with the particular geometry and features of the system itself; some of these aspects will be commented and justified in the mitigation part.

Finally, in the mitigation part, the effects of seismic isolation on statues will be tested and evaluated by means of three dimensional finite element models, with the double purpose of understanding whether there is a correspondence between the existing mechanical models and the actual behavior of these reshaped devices, and to understand the effectiveness of such technical choices in terms of reduction of the vulnerability of the system.

1. Risk Management Framework

1.1 Introduction

In the last two decades, there has been an increasing awareness that part of the resources given by our world are non-renewable, such as materials and energy, but some are also limited, like drinking water, clean air, etc.. The resources spent on the analysis of such a problem have brought to the conclusion that a sustainable development is necessary; "sustainable development" means a development "that meets the need of the present without compromising the ability of future generations to meet their own needs"(1). The concept of sustainable decision making has thus become the base for joint consideration of society, economy and environment. The implications of sustainable planning are immediately clear in regard to environmental impacts: the first targets are energy saving, pollution reduction, non renewable energy saving and much more.

For civil engineers also the financial aspect is important. Facilities are financed by the community with taxes charges or other, with the purpose to serve the community with benefits that increase people's quality of life. Engineering has to give an optimal solution in terms of cost, not using more financial resources than those available, and also in terms of durability: the present generation must not leave a burden of maintenance or replacement of too short lived structures. This concept ,that can be summarized with the definition of intergenerational equity, has become the basis for societal decision making that aims to fulfill requirements not only from a technological point of view but also from a sustainability point of view.

Moreover, during the last decades, we have experienced an exponential growth of the social consciousness of the direct relationship between decision makings and consequences on society. Speed of information and mass media diffusion made the common attention more and more focused on the impacts of strategic policies and plans on environment and individuals' quality of life; hence governments interest in developing more and more reliable strategies to improve their efficiency increased.

This tough issue lead to the development of policies oriented to solving complex problems, influenced by possible consequences of actions and probabilities that these consequences will occur; the result of this approach is also known as *risk*.

Risk is an intrinsic concept for human beings: everyone is aware that the introduction of a new input into a process gives back a certain degree of risk, as a counterpart of expected benefits. This clear concept though is not always easily applicable to predict consequences in advance and, often, it is not always possible to quantify the level of risk, given the large amount of variables of different nature involved in the problem. However taking into account risk becomes an intrinsic issue in actions that a policy maker, a researcher, a manager or an engineer have to deal with.

In daily conversation risk is a common notion used interchangeably with words like chance, likelihood and probability to indicate an uncertainty about the state of activity, item or issue under discussion (1). For instance talks are made about the risk of getting cancer to cigarette smoking, the chance of succeeding in developing a vaccine against the HIV virus in 2007, the likelihood of getting a "Royal Flush" in a Poker game and the probability of a major earthquake occurring in Italy within the next decade.

Even though it may be understandable from the context of discussion what is meant by the different words, in engineering decision making risk has to be specifically addressed and understood as the expected consequences of an event associated with a given activity, e.g. the construction, operation and decommissioning of a power plant.

Considering an activity with only one event with potential consequences C, the risk R is the probability P that this event will occur multiplied with the consequences given the event occurs i.e.:

$$\mathrm{R} = P \times C \tag{1.1}$$

If n events with consequences C_i and occurrence probabilities P_i may result from the activity, the total risk associated with the activity is simply assessed through the sum of the risks from the individual events:

$$\mathrm{R} = \sum_{i=1}^{n} P_i \times C_i \tag{1.2}$$

The definition of risk is consistent with the interpretation of risk used in the insurance industry and from the socio economic point of view. Risk may be quantified in a *currency*, like Dollars or Euro, and also in terms of victims, both killed or affected by the event; risk values can mostly be converted in the amount of money necessary to restore and recovery failures or in the price for a belated reached goal; similarly, in case of environmental impact, it can be expressed as the amount of money needed to restore the damage or to heal people involved. However the value of risk is the starting point for developing managing strategies.

Different risk analysis approaches were proposed through years by the scientific community, they basically propose logical path for an objective and quantitative analysis aimed to evaluate the risk connected to a certain event; in this work the aspect of geophysical risk will be dealt with, with particular attention to *seismic risk*; a first and rough definition of a logical path for assessing risk is:

CATASTROPHE → LOSSES

Although the simplicity the above mentioned correlation is the basis for each procedure of risk assessment that can be applied and, as it will be shown in the following, it represents the main concepts of norms and codes that deal with this issue. According to (2) a risk management procedure can be defined with the flowchart depicted in Figure 1.1.

This risk management procedure is divided into three macro parts: *Identification*, *Assessment* and *Treatment*. These three steps allow to identify the risk, then to define a model capable to assess the risk itself and, in case, to treat the risk in order to mitigate it.

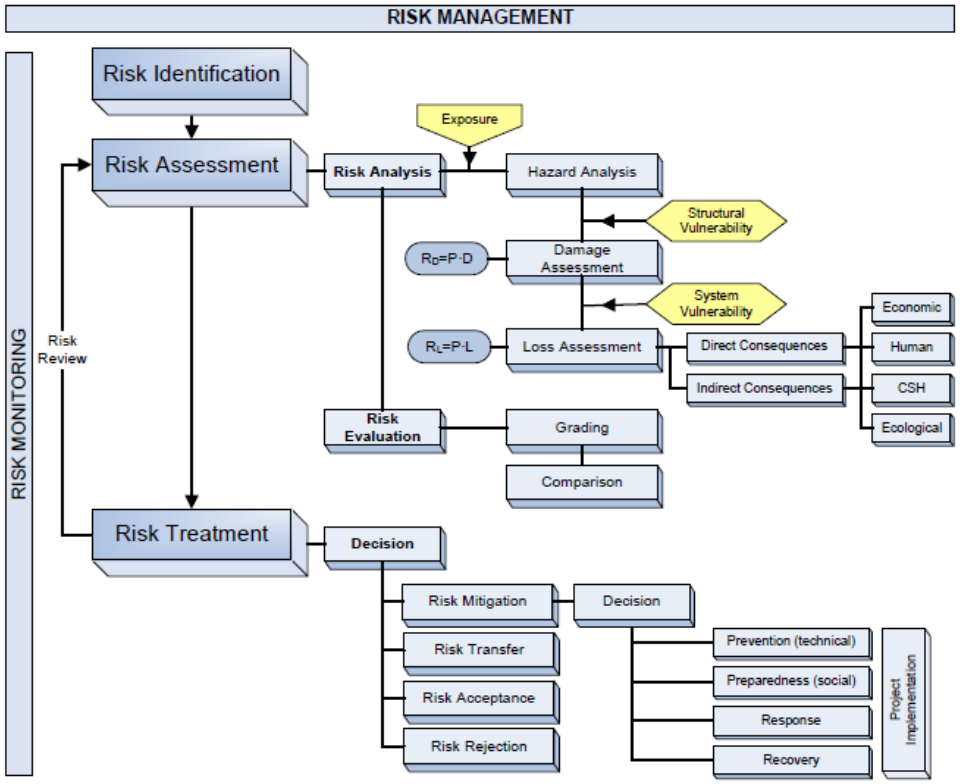

Figure 1.1 - Risk management framework (2)

1.2 Catastrophic events: earthquakes

According to CRED terminology a disaster is:

"*A situation or event which overwhelms local capacity, necessitating a request to the national or international level for external assistance, or is recognized as such by a multilateral agency or by at least two sources, such as national, regional or international assistance groups and the media*".

The definition of disaster is not as simple as it seems, indeed an event can be catastrophic for a single individual but not for the community or for the society. In addition categorization also depends on the particular aspect assumed as evaluation parameter.

The classification of natural disasters given by CRED divides them into four macro groups, namely Climatological, Geophysical, Hydrological and Meteorological; according to (CRED 2004), more than 9'000 natural disasters have been registered since 1900. Of these, about 80% have occurred over the last 30 years. More than 255 million people were affected by natural disasters globally each year, on average, between 1994 and 2003, ranging from of 68 million to 618 million. During the same period, these disasters claimed an average of 58'000 lives annually, with a range of 10'000 to 123'000. During the last decade disasters caused damage of an estimated US$ 67 billion per year on average, with a maximum of US$ 230 billion and a minimum of US$ 28 billion. The economic cost associated with natural disasters has increased 14-fold since the 1950s.

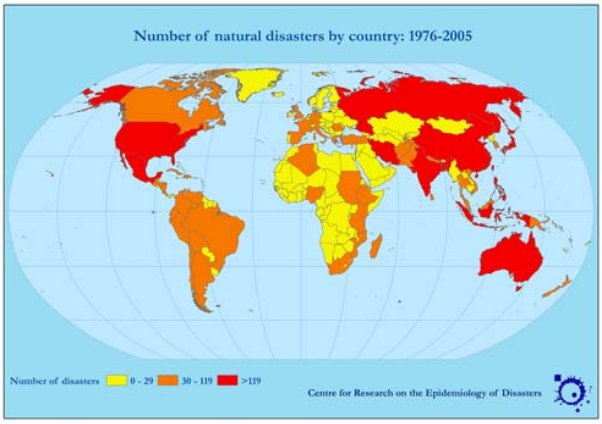

Figure 1.2 - number of disasters by country 1976 – 2005

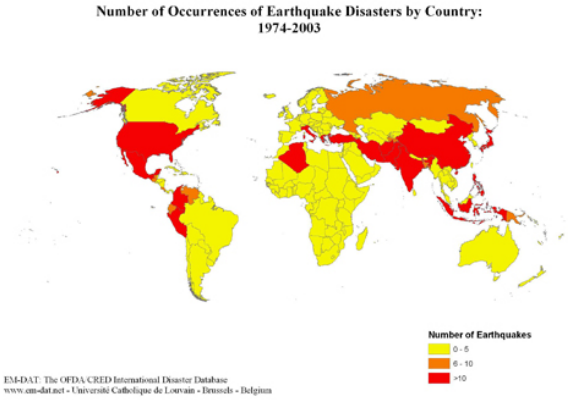

Figure 1.3 - number of earthquakes by country 1974 – 2003 (source www.emdata.be)

Table 1.1 - highest number of victims earthquakes

Country	Date	N° Killed
Haiti, Earthquake (ground shaking)	12/01/2010	222570
Indonesia, Tsunami	26/12/2004	165708
China P Rep, Earthquake (ground shaking)	12/05/2008	87476
Pakistan, Earthquake (ground shaking)	08/10/2005	73338
Sri Lanka, Tsunami	26/12/2004	35399
Iran Islam Rep, Earthquake (ground shaking)	26/12/2003	26796
Japan, Tsunami	11/03/2011	20319
India, Earthquake (ground shaking)	26/01/2001	20005
Turkey, Earthquake (ground shaking)	17/08/1999	17127
India, Tsunami	26/12/2004	16389

In 2010, 385 natural disasters killed more than 297000 people, affected over 217 million and caused US$ 123.9 billion of damages. A total of 131 countries were hit by natural disasters, though only 10 countries accounted for 120 of the 385

disasters (31.2%). (EM-DAT 2011). These data refer to disasters belonging to the four afore mentioned macro groups. In particular Haiti had over 39.1% of its population affected by the January 12th earthquake; the Chilean earthquake on February 27th caused 2.7 million victims, which represent 15.7% of the country's population. The earthquake ranked the highest in terms of economic damages caused by natural disasters in 2010, with a total of US$ 30 billion of reported damages (24.4% of the global reported damage). However the Haitian earthquake was especially destructive in view of the already impoverished economy. It is worth to note that the cost of that event surpassed the country GDP, the estimated US$ 8 billion represented 123.5% of the countries' GDP.

1.3 Catastrophic events: modeling the risk frame work

Procedures to predict and model natural and man induced disasters have been proposed by several authors, even if through different approaches, they all aim to describe these catastrophic events in a way they are manageable for the risk evaluations. In their management approach Grossi and Kunreuther (3) identify four elements that can completely describe the model: hazard, inventory, vulnerability and losses. The flowchart depicted in Figure 1.4 describes their mutual interaction.

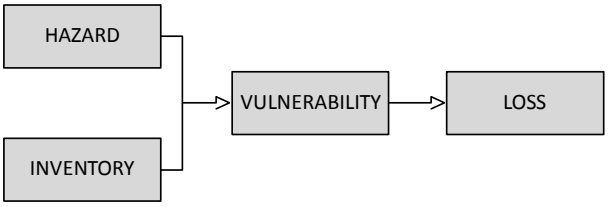

Figure 1.4 - catastrophe modeling

Basically the first phase of acquiring knowledge about the problem consists into the hazard evaluation, for instance, when dealing with a seismic risk assessment analysis, the seismic characteristic of the site needs to be taken into account. On the other hand the inventory phase consists into the collection of the available information about the structures and of its *Elements at Risk (EaR)*. Building a consistent portfolio of elements at risk and of their position is fundamental for the following step which is evaluation of *vulnerability*. Measures of vulnerability can be used as tools for decision makers, that can apply the risk management framework for tailoring the intervention policies: for instance assessing seismic vulnerability of a category of buildings, in a certain area, allows to rank the priority of interventions; on the other hand it can be used as a measure of the effectiveness of a potential intervention: "does the evaluated reduction of vulnerability justify the cost of the intervention?".

This step allows quantifying the effect of the hazardous event on the system. The last step is then the evaluation of the losses, according to the measure of vulnerability; in risk management, as it is shown in Figure 1.1 consequences can be direct or indirect depending on the temporal scale: when consequence are directly related to the failure they are considered *direct*, otherwise, when they are characterized by a shift in time they are defined *indirect*. According to (2) losses can also be categorized, four types can be distinguished: economic losses, humanitarian losses, CSH (cultural, social and historical) losses; since all these losses can be converted in a monetary value they will be considered *tangible*, other classes are defined *intangible*.

As it was stated above many standards and norms provide, even though it is not directly mentioned, procedures and methodologies that apply these risk assessment features; it is the case of the "Guidelines for assessment and reduction of seismic risk on cultural heritage", which propose a procedure of assessment and mitigation of the seismic risk on historical masonry buildings.

1.4 Computation of Risk

In many everyday life situations, probability is calculated according to the frequency probability definition, counting the number of times an event occurs and dividing it by the number of experiments that are carried out. This approach is normally used in quality tests in the industry. When considering larger scale approaches, e.g. when studying buildings, infrastructures, dams, in engineering, but also in economy and social sciences applications, it is impossible to statistically estimate the probability of a given event. A statistically significant number of comparable events are indeed lacking. Modern structural reliability and risk analysis assume the Bayesian idea of probability, where the lack of knowledge is dealt with like other categories of uncertainties.

Applying the theorem of total probability and the Bayesian theory (see Appendix A), when assigning the conditional probabilities of the single events, it becomes possible to calculate the risk for the system as the sum of all possible loss levels, multiplied by their probability to happen.

$$\mathrm{R} = \sum_i \mathrm{L}_i \cdot P(\mathrm{L}_i) \tag{1.3}$$

Covering the risk chain (2) in the opposite direction, it is further possible to define the probability of a loss level $P(L_i)$ after determining all the conditional probabilities $P(\cdot \mid \cdot)$ of the different chain rings, explicating the mobility relationships yet hinted, multiplied by the probability of the hazard at the beginning of the framework.

$$P(\mathrm{L}_i) = \sum_j P\big(\mathrm{L}_i \cap \mathrm{D}_j\big) = \sum_j P\big(\mathrm{L}_i|\mathrm{D}_j\big) \cdot P\big(\mathrm{D}_j\big) \tag{1.4}$$

$$P\big(\mathrm{D}_j\big) = \sum_k P\big(\mathrm{D}_j \cap \mathrm{EDP}_k\big) = \sum_k P\big(\mathrm{D}_j|\mathrm{EDP}_k\big) \cdot P(\mathrm{EDP}_k) \tag{1.5}$$

$$P(\mathrm{EDP}_k) = \sum_m P(\mathrm{EDP}_k \cap \mathrm{HL}_m) = \sum_m P(\mathrm{EDP}_k|\mathrm{HL}_m) \cdot P(\mathrm{HL}_m) \tag{1.6}$$

$$P(\mathrm{HL}_m) = \sum_n P(\mathrm{HL}_m \cap \mathrm{H}_n) = \sum_n P(\mathrm{HL}_m|\mathrm{H}_n) \cdot P(\mathrm{H}_n) \tag{1.7}$$

Substituting (1.4) – (1.7) in (1.3), it is possible to obtain the complete formula for the calculatio

n of the risk due to natural catastrophes in continuous terms:

$$\mathrm{R} = \int \mathrm{L} \cdot f(\mathrm{L}|\mathrm{D})\, f(\mathrm{D}|\mathrm{EDP})\, f(\mathrm{EDP}|\mathrm{HL})\, f(\mathrm{HL}|\mathrm{H})\, d\mathrm{H}\, d\mathrm{HL}\, d\mathrm{EDP}\, d\mathrm{D}\, d\mathrm{L} \tag{1.8}$$

Equation (1.8) is the integral formula of the risk, where all the conditional probabilities $P(\cdot \mid \cdot)$ have been substituted with the conditional probability density function $f(\cdot \mid \cdot)$. The formula, as here reported, with a multiple integral with the same number of values of the number of the chain rings, has been firstly reported by PEER, in the study of earthquakes' effects (4), but due to its general nature can be applied in other different fields (5).

2. Guidelines D.P.C.M 09/02/2011

2.1 Abstract

The following chapter includes a general overview of the main contents associated with the Guidelines ("Guidelines for assessment and reduction of seismic risk on cultural heritage", DPCM 09.02.2011 referred to NTC, hereon Guidelines) as well as an overview of their principles and criteria with the aim to facilitate a descriptive comparison between the risk framework and the "Guidelines" .

Moreover a critical analysis of their contents will be presented as an introduction to the main topic of this dissertation, which aims to an extension of the above mentioned principles to the case of museum contents and art objects.

The main aspects and criteria of the Guidelines for masonry structures will be presented and described, with particular attention to those that give them an innovative perspective for the evaluation of seismic vulnerability, and design of interventions to reduce it; next a quick comparison between the general risk framework will be presented, pointing out differences and similarities between the two approaches. Afterwards the application of the "territorial scale" approach on a sample of 85 Venetian bell towers will be discussed: this example will give the chance to better understand the criteria contained into these standards by means of a practical application. In the end the proposal of extension of this standards from masonry buildings to art objects and museum contents with the aim to obtain as a result a procedure to approach the problem of seismic vulnerability assessment for this category will be discussed.

2.2 General Description of Guidelines Principles and criteria

Guidelines are codes that are published by the Italian Government to specifically address issues of assessment and mitigation of seismic vulnerability on cultural heritage. As the majority of the Italian heritage constitutes works of masonry structures, the first draft deals in particular with this structural type. Since they introduce some innovative aspects, but they also apply well known and proved technical concepts, their normative placement is framed among different previous codes: they refer to *Technical Constructions Regulations* (hereon "*NTC*") and more specifically to *Annex 2* of "Technical regulations for designing, evaluating and seismic upgrading of buildings" of the P.C.M. Ordinance no. 3274/03 (hereon "Ordinance").

"*The Cultural Heritage and Landscape Code*" established that the functions of protecting national and cultural heritage is attributed to the state and carried out by the Ministry of Cultural Heritage and Activities, as already stated by Article 16 of Decreed law no.64 of February 2nd 1974. As far as interventions on historical landmarks are concerned, article 29 of the Code states that for building in areas with relevant seismic risk, restoration must also include interventions of

strengthening. Furthermore, the Ministry states that these codes shall be implemented in collaboration with universities and research institutions, which shall establish guidelines, regulations, criteria and models regarding the conservation of cultural heritage. Such a robust background is though headed to future developments, in order to provide useful tools and methods for guaranteeing an adequate safety level to all those buildings classified as historical".

Guidelines were established with the intention to provide a reliable and easy-to-use set of tools for formulating objective judgment on the safety and conservation of the "state of art" and of the strengthening interventions. The aim is to delineate specifications about the e building, to evaluate seismic safety and to define interventions by means of particular analysis tools specifically defined for the case of cultural heritage. In particular the conservation of historical buildings is taken into account at two different levels: the evaluation of seismic vulnerability on a territorial scale and the evaluation of vulnerability and the design of strengthening interventions for the single building.

Even though the contents of the documents are not binding in the design and intervention phases they give a useful and reliable procedure for approaching the study of a category of particularly complicated and multifaceted objects.

This procedure is described in six chapters of Guidelines that start with safety requirements and definition of new reference limits states, not only connected to the safeguard of people and of functionality, but also to the loss or damage of the artistic assets contained in the building. Then seismic action is defined, with particular attention to the level of action to use.

The fourth chapter of the Guidelines deals with the information about the building. In that a procedure to acquire the greatest number of details possible about the structure is discussed, in order to have a clear and defined overview of "state of the art" of its conditions.

The fifth chapter, describes the mechanical models that can be adopted to evaluate the seismic vulnerability of the structure, according to the category it belongs to, and to the level of analysis that is performed. About this particular aspect Guidelines define three different increasing complexity levels respectively namely LV1, for the territorial approach, LV2 and LV3, for the single building approach. The sixth and last chapter finally describes the interventions to reduce the identified vulnerabilities and to improve the safety condition of the building.

Generally, the study of historical buildings includes the evaluation of the extent of necessary improvements and the level of safety while at the same time fulfilling the objective of conservation. Various analysis tools suggested by the Guidelines were developed for these purposes. First the territorial approach aims to put mitigation policies into practice on a wide scale, not to assess the absolute condition of safety of buildings, but to draw a priority list, based both on qualitative and quantitative features, that can be acquired and calculate quickly and easily to pinpoint the most critical situations, and establish priorities for future interventions. The calculated values, used in the ranking phase are seismic indexes that are defined as follows.

If the safety index is significantly lower than the expected limit for the site it simply means that more accurate investigations must be carried out. Methods proposed for this level are in general simple and based on a limited number of geometrical and mechanical parameters. On the other hand, when critical situations are pointed out, some interventions might be necessary. The objective of an efficient design of intervention can be reached with more detailed analyses aimed to evaluate both the feasibility and the effectiveness of improvement interventions. In this case the obvious difficulty is to define a procedure to verify safety requirements for historical buildings, given their typological variety and specific singularity that make them classified as "monuments". It is also difficult to quantify the effectiveness of an intervention with a purely quantitative procedure, since it is often very useful to join also a qualitative judgment that helps with the global assessment. The procedure proposed in the code indicates a path in which the judgment of level of risk and validity of intervention emerge from the comparison between structural capacity and seismic hazard. It is worth noting that such a comparison should not be seen as mandatory verification between capacity and demand in the way of common safety verifications, but more as a quantitative element that must be taken into account with other qualitative aspects for obtaining a global reliable result.

Another key concept is the idea of minimum intervention, i.e. to avoid unnecessary interventions that do not significantly improve the safety of the structure, but strongly modify its appearance; furthermore an analysis also has to highlight situations in which it is proper to intervene.

Strengthening interventions might deal with single parts of the building or also to involve the entire structure. This is the reason why two different levels of approaches for detailed analyses are indicated in the Guidelines: approach with LV2 level is proposed for evaluations of local interventions on limited zones of the building; approach with LV3 level, is required when interventions that modify the structural behavior are designed. More details will be presented in the following part.

As it was stated above the aim of the Guidelines is predominantly to safeguard the occupants of the building (ultimate limit state, SLU), and then also the protection of the building itself from damage (damage limit state, SLD). Moreover, since cultural heritage protection is discussed, Guidelines propose a specific limit state to protect works contained in the building: works of art such as frescoes, stuccos, etc. ; an appropriate special limit state needs then to be defined: Artistic Limit State (SLA). Limit states are defined as follows:

- **SLU** (ultimate limit state) : Under the effect of a reference seismic event, which is characterized by a probability of exceeding 10% in 50 years. It is opportunely modulated in terms of the differing probabilities of excess or the importance factor. The structure even when submitted to grave damage, maintains a residual resistance and stiffness when confronted with lateral shifting and the entire load capacity when under vertical stress.
- **SLD** (limit state of damage) : Under the effect of a seismic event, characterized by a probability of exceeding limits by 50% in 50 years. It is opportunely modulated in terms of the differing probabilities of excess or a coefficient of importance. The building as a whole is not greatly damaged in a way that justifies the interruption of use following an earthquake that has a major probability of occurring with respect to reference values for the last limit state.
- **SLA** (limit state of damage for works of art) : Works of art contained in a building (decorated walls, etc.) which during an earthquake of a certain level are submitted to modest damage and can be restored without significant loss of their cultural value.

Ultimate limit state analyses are always required, since they guarantee the safeguard of occupants of the building. Damage limit state ones, however, are required either when the functionality of the building needs to be guaranteed and also when, at a local level, the presence of important works of art requires a higher level of seismic protection. Concerning the Artistic Limit State, which can be compared to a damage limit state, but is specifically referred to art works, it is required in situations defined by the Administrative competency.

Two safety indexes to evaluate the seismic vulnerability condition can be calculated: the first one is the ratio between the return period of the critical action and the return period for the reference action, named I_s, and the second one is the ratio between the capacity of the structure and the expected acceleration on the site for a defined return period is called f_a.

One of the fundamental aspects of the procedure defined in the Guidelines is the path of knowledge, which is intended as a mean of reliable evaluation of the current seismic vulnerability as well as a mean to define effectiveness of strengthening interventions; the path of knowledge is defined as a set of operations that aim to reduce the great level of uncertainty connected to the knowledge of historical constructions: the lack of information and the high number of changes that the structure has experienced in its lifetime (anthropic transformations, aging of materials, damaging in general, etc.) represent a source of uncertainties and variability that reduces the reliability of assessment operations, but the application of this procedure allows to improve the quantity and the quality of the information about the building or part of it; it can be divided into different “steps” each one aimed to acquire data about the main aspects of the structure:

- identification of the building aims to a correct and complete identification of the structure and its location on the territory;
- geometrical relief is a fundamental part of the path of knowledge , it must refer both to the complete geometry of the building and also to its structural parts, including the interaction with adjacent buildings;
- historical characterization and definition of the evolution of the building;
- identification of the resisting structural elements;
- identification of materials, their conservation conditions and mechanical properties: construction materials need to be investigated in detail, because the quality of data available can strongly affect the outcome of the seismic risk assessment phase, it is nonetheless true that all surveys should satisfy the principle of minimum

invasiveness, hence it is suggested to adopt mostly non destructive techniques of survey or, at least, to limit the destructive test to a minimum number to join with non destructive or indirect survey techniques;

- knowledge about foundations: as well as the previous step, the interaction between the bearing structures and the ground is fundamental for a complete and satisfactory knowledge of the building, in particular with the aim of assessing the seismic risk for the structure; a correct investigation about the typology of soil can be carried out both with in situ investigation and with archive researches.

After the structure has been identified and described, with a more or less accurate level of detail, designer has to assign a "confidence factor" to take into account the actual level of accuracy of the data collected, before using them for the analytical investigation with the mechanical models; indeed "confidence factor", which varies from the value of 1 to the value of 1.35, grades the reliability of the structural analyses and of the evaluation of the seismic safety index; it is differently applied according to the adopted model for the evaluation of the seismic safety.

Basically the models belong to two categories: models which consider the deformability and resistance of materials of structural elements and models which consider the limit equilibrium condition of the single elements of the structures defined as rigid blocks. In the first case the confidence factor is applied to the mechanical characteristics of the material reducing both the plastic model and the resistance; it is worth noting that the reference values for masonry resistance are given by Ordinance tables 11.D.1 and 11.D.2. In the second case, in which resistance of materials is not involved in the calculations, the "confidence factor" is applied to the structural capacity, reducing the corresponding acceleration of the different limit states. The confidence factor is obtained as the sum of partial factors that are referred to the different steps of the path of knowledge and, combined together, give the final factor to apply in the analyses. Values of the confidence factor are summarized in Table 2.1.

Once the partial confidence factors are assigned the global confidence factor can be evaluated as follows:

Table 2.1 - partial confidence factors

<table>
<tr><th>Geometric survey</th><th>Identification of historical and constructive specificities</th><th>Mechanical properties of the material</th><th>Terrain and foundations</th></tr>
<tr><td rowspan="2">The geometrical survey has been completed
$\mathbf{F_{c1} = 0.05}$</td><td>Hypothetic render of constructive phases based on a limited survey of materials and constructive elements, connected to the awareness of transformations
$\mathbf{F_{c2} = 0.12}$</td><td>Mechanical parameters deduced from available data
$\mathbf{F_{c3} = 0.12}$</td><td>Limited survey of terrain and foundations, in absence of geological data or availability of information about the foundation
$\mathbf{F_{c4} = 0.06}$</td></tr>
<tr><td rowspan="2">Partial render of constructive phases and interpretation of structural behavior based on: a) limited material and structural elements survey; b) extended material survey connected to transformations of the building
$\mathbf{F_{c2} = 0.06}$</td><td rowspan="2">Limited research of mechanical parameters of materials
$\mathbf{F_{c3} = 0.06}$</td><td rowspan="2">Geological data and information regarding the foundation structure is available; limited research on terrain foundation
$\mathbf{F_{c4} = 0.03}$</td></tr>
<tr><td>The geometrical survey has been completed along with the graphic rendering of cracking and deformities
$\mathbf{F_{c1} = 0}$</td></tr>
<tr><td></td><td>complete render of constructive</td><td>Extensive research of</td><td>Extensive or</td></tr>
</table>

Geometric survey	**Identification of historical and constructive specificities**	**Mechanical properties of the material**	**Terrain and foundations**
	phases and structural behavior based on an exhaustive material and structural elements survey **F_{c2} = 0**	mechanical parameters of materials **F_{c3} = 0**	exhaustive research on the terrain and foundation **F_{c4} = 0**

$$F_c = 1 + \sum_{k=1}^{4} F_{ck}$$

The next step constitutes the assessment of the condition of the structure. This is a delicate and difficult step because historical masonry buildings possess a combination of numerous variables and complexities in regards to typology and construction techniques.

As such defining seismic behavior models becomes very difficult, especially considering that one has to take into account all these variables that impact the problem: for example the interaction between the structural elements or the conditions of materials. Furthermore, there are other relevant aspects that hinder the individuation of a proper mechanical model to be adopted for the evaluation. First of all, in the past construction of historical buildings was not based on building codes, but rather followed basic “rules of thumb” that changed and were refined during the years. Second, historical buildings have experienced changes and structural modifications throughout the years and there are inevitable changes to the materials and their properties and quality over time. It is evident that this sum of factors affects the seismic safety of the building and its evaluation.

The choice for a mechanical model depends on the level of analyses that is carried out. As previously stated, Guidelines suggest three different levels of complexity for the assessment of seismic safety ranging from territorial to single building levels. The complexity and the detail of analyses increase in precision: the territorial level of approach is based on simple and quick models that can be used to establish intervention priorities, it is between a qualitative and a quantitative evaluation and, with only a reduced number of mechanical and geometrical parameters involved, allows the evaluation of seismic index. It is clear that with such diffused heritage, tools belonging to this category must be sufficiently rigorous and at the same time agile and easy-to-use. The next level of complexity LV2 is applied when restorations which involve parts of the buildings are designed; these interventions do not modify the global behavior of the structure but are limited to autonomous structural parts (macro elements), and in general do not modify the original function of the building; in these situations it would be excessively burdensome to perform an analysis on the whole structure, and it is more efficient to investigate each single part within the global context; Guidelines suggest to perform linear and non linear kinematic analyses, or to apply finite element models to the considered portions; at the same time, since a global evaluation is required before and after the intervention, the LV1 safety index can be used. The third and most detailed level of complexity is the so called LV3 level which is used to evaluate the seismic safety of the entire construction; this level of analysis is applied when interventions modify the final use of the structure or whenever the restoration involves a building of strategic importance. Guidelines also underline the fact that an assessment of the whole building does not necessarily require the creation of a global model but it is possible to proceed with the division of the structure in macro elements that can be singularly considered with the same tools used for LV2 modeling.

The approach described in the Guidelines also provides some mechanical models, for the evaluation of the seismic safety at level LV1, according to the structural type. Even though the concept of “structural type” does not perfectly fit historical buildings because of the way they were designed, built and modified through years; Guidelines point out the main characteristics of each category and also suggest a procedure to evaluate the seismic response of each one of them with a LV1 approach, as examples to clarify the criteria that they suggest; the four categories considered are palaces and villas, churches and cult buildings, towers and bell towers, bridges and arches. In the following an example of the application of LV1 territorial approach will be described and results will be discussed.

2.3 A parallel between "Guidelines" and the Risk Framework

The risk management framework proposed and described in chapter 1 is a general approach to problems of different nature and it aims to an evaluation of the condition of risk of a system. The affinity of such an approach with the main target of Guidelines is clearly visible from the first line of the regulation: " *Herewith directions for assessment and reduction of seismic risk on cultural heritage are provided […]*"; as it was widely discussed in the previous part the main purpose of these standards is to define a procedure, by means of which, technicians and operators in the cultural heritage field can easily assess seismic risk on historical buildings and, in case, consider the possibility to prescribe and design specific interventions of reduction of exceptional events' effects. The two approaches, even though with some differences, have a common starting point and a common goal: the assessment and the reduction of risk.

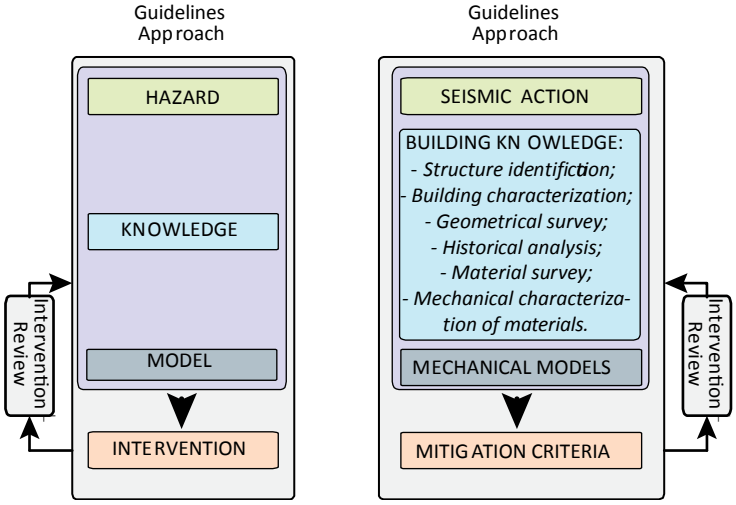

Figure 2.1 - Guidelines approach framework

Guidelines methodology can be summarized as in the previous chart (Figure 2.1):

It can be described by means of four macro parts , namely: *Hazard*, *Knowledge*, *Model* and *Intervention*, the first three steps can be clustered in a general wider group, which represents the assessment phase. The first is *Hazard*, intended as "*all the possible sources that can endanger the system*"; in this case only earthquake is considered. Hazard evaluation includes an Hazard Analysis phase, performed to identify the intensity and frequency of the event that can occur; a first observation needs to be made: in Guidelines the choice for the hazard level is connected to the kind of analysis that is performed and, as it will be explained in the following, to the "*consequences*" assumed as a threshold; therefore it is related also to the following phase of modeling, even though it is treated as a separate block. The parallel between Guidelines and risk framework is simple, but some remarks need to be made; the comparison is depicted in Figure 2.2:

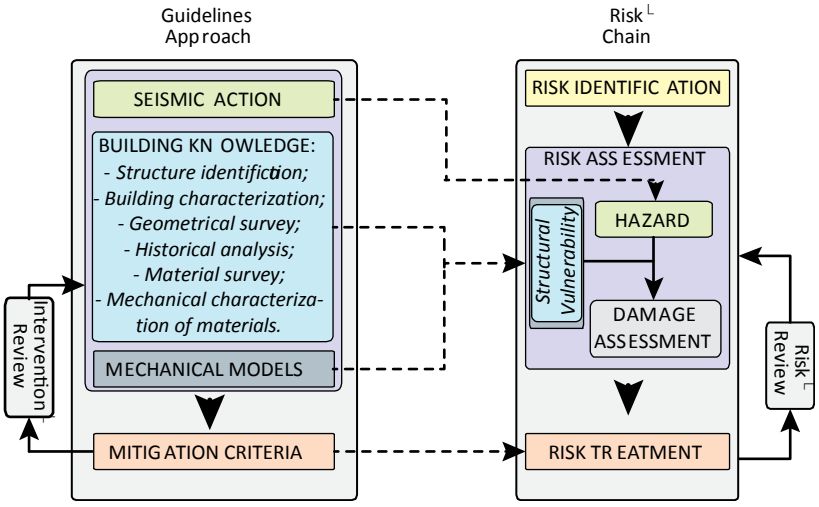

Figure 2.2 - Comparison Guidelines-Risk Framework

It is important to note that Guidelines do not consider the Risk Identification phase but rather it is treated as a pre evaluation phase which has the main objective to answer the question of "*What can happen and where*?" Based on the fact that an investigation is required, it is assumed that a potentially risky situation has already been identified. Nonetheless, an evaluation is required to fully address the question.

The phase of "*knowledge*" is subdivided into different steps that are necessary for gathering all data needed for the system identification and for elements at risk (*EaR*). *EaR* are elements exposed to risk; in a risk framework all these elements' condition concur to the evaluation of *structural vulnerability* or rather a quantification of the susceptibility of all *EaR* towards the impact of the Hazard. Different aspects and characteristics of the system's elements might be considered and may be involved in the evaluation combining both quantitative and qualitative aspects of the system under analysis.

Guidelines, from this point of view, provide a very detailed path to follow in order to achieve an optimal framing of the structure or object of study. The other fundamental aspect for vulnerability assessment is the choice of the model: an entire block is dedicated to this important phase: the selection of an appropriate mechanical model is lead by an accurate understanding of the structural behavior of the system, and it also allows to convert all data gathered in the knowledge phase, both qualitative and quantitative, to a concrete evaluation of structural vulnerability. Different solutions are proposed to model the structural system according to the accuracy of the information available and based on the objective of the analyses. The assessment of vulnerability can hence be summarized as:

KNOWLEDGE + MODELS → VULNERABILITY

Despite the fact it is simple, the concept summarized in the relation above, encompasses the basics of the vulnerability assessment analysis as proposed by the Guidelines. Indeed they mostly focus their attention on this step of the risk framework and they explain and detail each single step aimed for an accurate investigation.

Once hazard and vulnerability are defined, the damage can be assessed and analyzed in terms of "*Structural vulnerability the relation between hazard and damage*":

VULNERABILTY + HAZARD → DAMAGE

Unlike the approach proposed by (2), the Guidelines do not directly involve the *consequences* that might go in line with a given damage, subdivided into *Direct* and *Indirect Consequences*. The concept of consequence is intrinsic in the methodology. Actually the outcome of a vulnerability analysis with the Guidelines approach is a coefficient, or better a safety index which "quantifies" the vulnerability of the structure. It is interesting to note that, even though the consequences are not directly involved in the risk analysis phase, as it was stated above, they are indirectly considered when the choice of the hazard level is made: indeed the selection of a reference limit state instead of another, practically means to set different levels of acceptance of the consequences produced by an earthquake event.

For the Guidelines risk evaluation is therefore limited to an analysis for the assessment of the vulnerability of a given system. Vulnerability, as stated above, is quantified with an index. Even if this procedure does not calculate the total risk, either in currency or in other terms, the potential of the seismic safety indexes in the decision making field is big. Indeed they can be applied with two main purposes: the first one is to draw lists of priority of interventions, after large scale analyses; when a category of building in a certain area is analyzed, interventions can be planned according to the values of the safety index; moreover a first rough distinction can be made between buildings that may require further investigations and buildings that can be considered reasonably safe. The second application is an evaluation of efficiency of the intervention; when a detailed analysis is performed the seismic safety index can help to point out whether the designed solution is justified by an improvement of the seismic capacity of the structure, just comparing the index before and after the potential intervention; this helps to avoid unnecessary actions with respect for the criterion of minimum modification.

2.4 An example of application of the territorial level LV1, the case study of Venetian bell towers

In this section a practical example of application of the above described guidelines is given. This allows one to point out those aspects and details that are often hidden between the lines of a simple theoretical description and emerge only when the procedure is applied. A complete and deep comprehension of all facets of the issue will be useful for the further step of extension of the existing Guidelines to the case of museum contents.

As it was stated above Guidelines identify three different levels of analysis characterized by an improvement of the evaluation level. The first step of investigation (LV1) is based on a territorial approach of the concept of vulnerability, which needs to be extended to a wide sample of structures. The structures belong to the same structural category, of which a priority list of intervention needs to be drawn, in order to define a protection plan. This paragraph in particular refers to the LV1 model, concerning “Towers and Bell towers and other tall and slender structures” given by the guidelines in the section relative to mechanical simplified models.

The model for this structural category assumes slender structures can behave as vertical cantilever beams when subjected to seismic loads; the main failure mechanism considered involves both flexural and axial resistance, and the safety level is evaluated by comparing the design bending moment to the ultimate flexural moment of the structure, evaluated under the assumption of no tensile strength for masonry, joined with a proper non linear distribution of compressive stress.

The verification is carried out considering the two principal axes and the seismic load that induces the bending moment acts only along one of the main direction at time, furthermore the main directions need to be checked both because difference of stiffness can induce different levels of the seismic demand. Moreover verifications are performed at different levels of height of the structure and, since it is not possible to pinpoint critical sections “a priori”, because of the variability of geometry and material characteristics of the structure (tapering in wall thickness, openings), the object is divided in *n* significant sectors characterized by averagely similar characteristics; then each sector safety is checked at level where the characteristics change. The assumed distribution of force is coherent with a linear distribution of displacements, and the force, evaluated at the barycenter of each sector (where it is applied) is given by:

$$F_i = \frac{W_i\, z_i}{\sum_{k=1}^{n} W_k z_k} F_h \qquad (2.1)$$

where:

- $F_h = 0.85 S_e(T_1) W/qg$ (assuming that the fundamental period of a tower is always higher than T_B, corresponding to the first point of the peak spectral acceleration plateau);

- W_i and W_k are the weight of the i^{th} and k^{th} sector respectively;

- z_i and z_k are the heights of the barycentre of the i^{th} and k^{th} sector with respect to the foundation;

- $S_e(T_1)$ is the elastic response spectrum, which is function of the first period of the structure (T_1) according to a given direction;

- $W=\Sigma W_i$ is the total weight of the structure;

- q is the structural performance factor that can be assumed (in absence of a more accurate estimation and according to the building provisions) equal to 3 for the structures with regular shape along the height, or reduced up to 2.25 if obvious stiffness changes along the height or an adjacent building are present;

- g is gravitational acceleration.

The seismic force in the i^{th} section is given by:

$$F_{hi} = \frac{\sum_{k=i}^{n} z_k W_k}{\sum_{k=1}^{n} z_k W_k} F_h \tag{2.2}$$

The height z_{Fi}, to which the force F_{hi} has to be applied, is evaluated through the following formula:

$$z_{Fi} = \frac{\sum_{k=i}^{n} z_k^2 W_k}{\sum_{k=1}^{n} z_k W_k} - z_{i^*} \tag{2.3}$$

where:

z_{i^*} is the height of the i^{th} section in reference to the base;

By imposing equality between the design bending moment and the ultimate flexural resistance:

$$M_{u_i} = F_{hi} z_{Fi} \tag{2.4}$$

It is possible to evaluate the lowest return period T_{SLV} between the different analyses sections corresponding to the achievement of the ultimate limit state (SLU); in this way it is possible to evaluate a safety index defined as the ratio between the return period of the seismic load and the corresponding return period $T_{R,SLV}$:

$$I_{s,SLV} = \frac{T_{SLV}}{T_{R,SLV}} \tag{2.5}$$

Similarly it is possible to evaluate an acceleration factor defined as the ratio between the peak ground acceleration related to the achievement of the LLS and the acceleration corresponding to the reference return period $T_{R,SLV}$, both referring to soil type A:

$$f_{s,SLV} = \frac{a_{SLV}}{a_{R,SLV}} \tag{2.6}$$

The approach proposed for bell towers and described above appears very simple and quick, moreover it is necessary a reasonable amount of geometrical parameters to obtain the seismic safety index. As it was explained before the problem of monumental buildings is connected to a great number of variability and uncertainties; the example of application to the sample of venetian bell towers that is described immediately in the following points out this strong heterogeneity in a sample of the same category type; the dataset available was complete, with detailed descriptions and reference about the different main features (roof, belfry shape, masonry properties and some other important aspects) this dataset permitted the application of the mechanical models proposed by the Guidelines. Just as an example, in Figure 2.3 and Figure 2.4, statistical distributions about the roof shapes and the characteristics of masonry are shown:

Pitched roof	44	
Dome	6	
Cusp	6	
Tambour and dome	26	
Tambour and cusp	20	
Flat roof	2	
Tambour and pitched roof	9	
Cusp with circular base	1	
Tambour and lowered cusp	2	

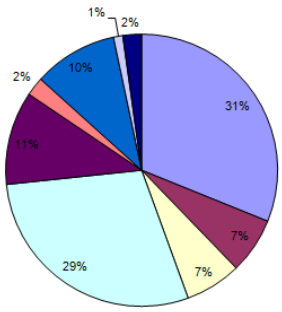

Figure 2.3 - Statistical distribution of the analyzed sample: roof type

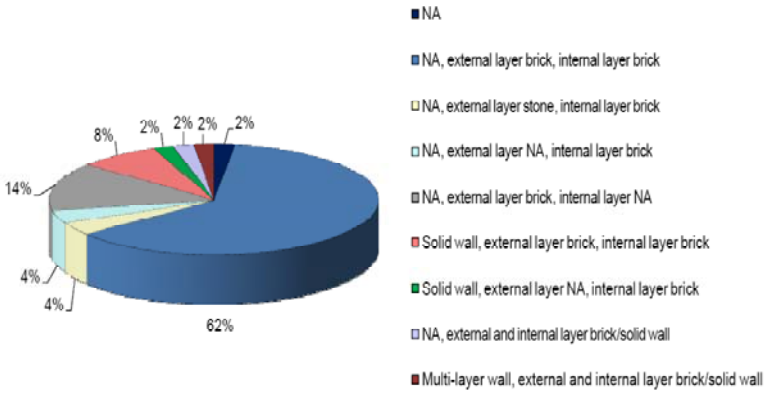

Figure 2.4 - Statistical distribution of the analyzed sample: masonry type

In Figure 2.4 the first label is related to the properties of masonry inside the wall thickness: if it is the same type for the whole thickness, if an internal filling layer is present or if it was not possible to survey the data (N.A.). The second label identifies the external layer and the last one the internal in-filled layer (for the most cases it was not possible to evaluate if the in-filled masonry layer properties). The last two types refer to double cross-section bell towers, the first description is related to the external barrel-face and the second to the internal one.

From the statistical analysis (Figure 2.4) it appears that the most common roof-types are characterized by two pitches (31%) or by tambour and dome (26%).

The final goal of this procedure is to obtain the seismic safety index from the values of flexural resistance and of bending moment; the difficulties connected to data gathering, in particular when the quickness and simplicity profile wants to be kept, is evident when dealing with aspects such as the drift (which is difficult to survey at a rough investigation level), the evaluation of the fundamental vibration period or the interaction with adjacent buildings are essential for the evaluation of the resistance, but not always easy to obtain. This is the reason why some operative tools are proposed in order to guarantee the effectiveness of results and preserving, at the same time, the territorial nature of the approach.

2.4.1 Assessment of the fundamental period

Considering the assumptions on which the model is based, hence a design bending moment depending evaluated from a linear distribution of forces, proportional to the first fundamental mode of vibration, it is clear that the correct assessment of the first fundamental period is a particularly important operation for the correct evaluation of the seismic load acting on the structure. Formulations provided by international codes and literature are several and they all provide a rough relation to quantify the first period of vibration of a slender structure, the most important are summarized in the following:

$T_1 = 0.0217H$ buildings and towers (H>50 m) [EN 1991 -1-4:2004] (1)

$T_1 = (0.015 - 0.018)\ H$ tall RC or mixed buildings [CNR-DT 207/2008] (2)

$T_1 = (0.020 - 0.024)\ H$ tall steel buildings [CNR-DT 207/2008] (3)

Using available data from the literature and from experimental dynamic investigations on masonry bell towers a good correlation between the height of the structure, with non cracked masonry, and the first fundamental period of vibration was found to be given by:

$T_1 = 0.0187\ H$

Which properly fits the experimental and literature data, as depicted in Figure 2.5

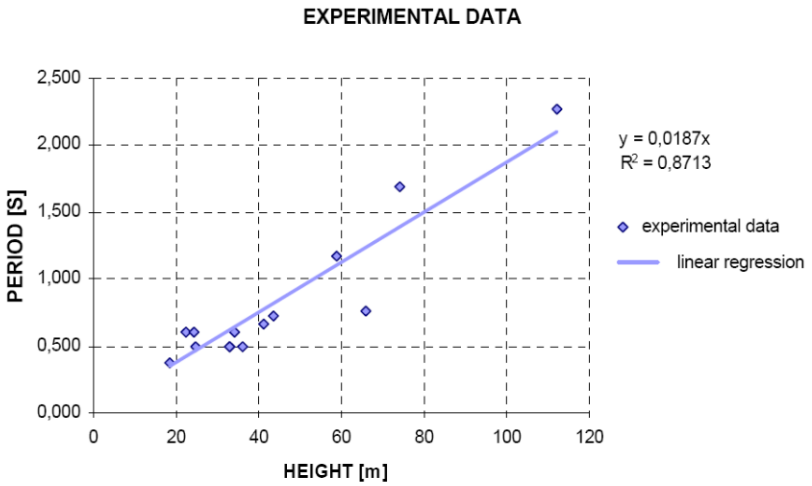

Figure 2.5 - Linear regression of the experimental data

2.4.2 Ultimate resistance and vertical eccentricity

The Guidelines suggest to consider the maximum flexural resistance valid for a rectangular single crossed section, assuming that the axial force acting on the section is lower than 0.85 f_d s a (f_d= masonry compressive strength, s = walls thickness, a = cross section dimension, perpendicular to the seismic action), then analytical formula were also developed for the case of double cross sections with random openings, as depicted in Figure 2.6 and Figure 2.7

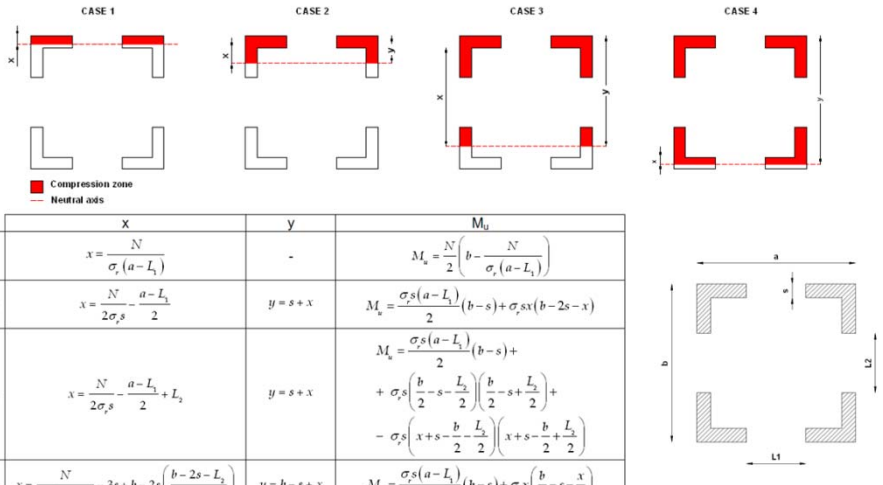

	x	y	M_u
CASE 1	$x = \frac{N}{\sigma_r (a - L_1)}$	-	$M_u = \frac{N}{2}\left(b - \frac{N}{\sigma_r (a - L_1)}\right)$
CASE 2	$x = \frac{N}{2\sigma_r s} - \frac{a - L_1}{2}$	$y = s + x$	$M_u = \frac{\sigma_r s (a - L_1)}{2}(b - s) + \sigma_r s x (b - 2s - x)$
CASE 3	$x = \frac{N}{2\sigma_r s} - \frac{a - L_1}{2} + L_2$	$y = s + x$	$M_u = \frac{\sigma_r s (a - L_1)}{2}(b - s) + + \sigma_r s \left(\frac{b}{2} - s - \frac{L_2}{2}\right)\left(\frac{b}{2} - s + \frac{L_2}{2}\right) + - \sigma_r s \left(x + s - \frac{b}{2} - \frac{L_2}{2}\right)\left(x + s - \frac{b}{2} + \frac{L_2}{2}\right)$
CASE 4	$x = \frac{N}{\sigma_r (a - L_1)} - 3s + b - 2s\left(\frac{b - 2s - L_2}{a - L_1}\right)$	$y = b - s + x$	$M_u = \frac{\sigma_r s (a - L_1)}{2}(b - s) + \sigma_r x \left(\frac{b}{2} - s - \frac{x}{2}\right)$

Figure 2.6 - Analytical formula for the evaluation of Mu for a single cross section

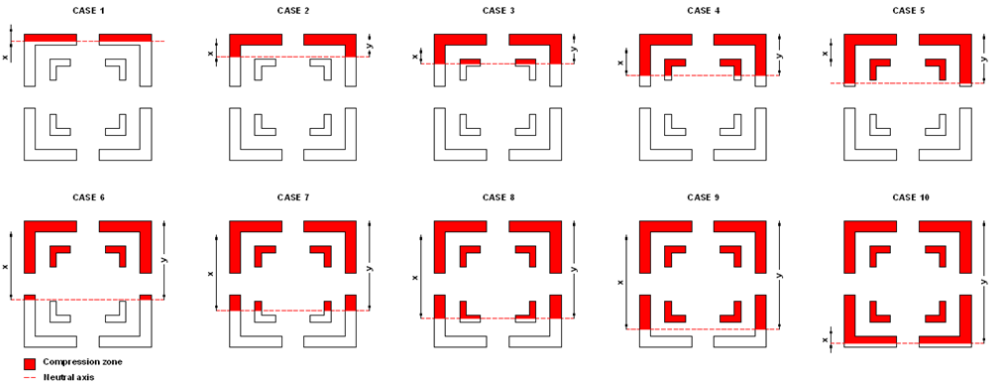

	x	y	M_u
CASE 1	$x=\frac{N}{\sigma_r(a-L_1)}$	-	$M_u=\frac{N}{2}\left(b-\frac{N}{\sigma_r(a-L_1)}\right)$
CASE 2	$x=\frac{N}{2\sigma_r s}-\frac{a-L_1}{2}$	$y=s+x$	$M_u=\frac{\sigma_r s(a-L_1)}{2}(b-s)+\sigma_r sx(b-2s-x)$
CASE 3	$x=\frac{N-\sigma_r s(a-L_1)+2\sigma_r cd_1}{2\sigma_r(s+d_1)}$	$y=s+x$	$M_u=\frac{\sigma_r s(a-L_1)}{2}(b-s)+$ $+\sigma_r sx(b-2s-x)+\sigma_r(x-c)d_1(b-2s-x-c)$
CASE 4	$x=\frac{N-\sigma_r s(a-L_1)-2\sigma_r s_1 d_1+2\sigma_r s_1 c+2\sigma_r s_1^2}{2\sigma_r(s+s_1)}$	$y=s+x$	$M_u=\frac{\sigma_r s(a-L_1)}{2}(b-s)+$ $+\sigma_r sx(b-2s-x)+\sigma_r d_1 s_1(b-2s-2c-s_1)+$ $+\sigma_r(x-c-s_1)s_1(b-2s-x-c-s_1)$
CASE 5	$x=\frac{N-\sigma_r s(a-L_1)-2\sigma_r s_1 d_1-2\sigma_r s_1 d+2\sigma_r s_1^2}{2\sigma_r s}$	$y=s+x$	$M_u=\frac{\sigma_r s(a-L_1)}{2}(b-s)+$ $+\sigma_r sx(b-2s-x)+\sigma_r d_1 s_1(b-2s-2c-s_1)+$ $+\sigma_r(d-s_1)s_1(b-2c-2s-d_1-s_1)$

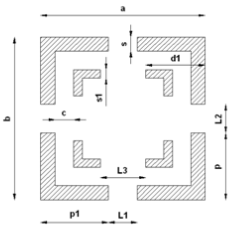

Figure 2.7 - Analytical formula for the evaluation of Mu for a double cross section

Another important aspect that affects the evaluation of the seismic safety index is the vertical eccentricity; the sample analyzed presents, in many cases, eccentricity in one or two directions that can sometimes be very high. For example the bell tower of San Martino in Burano island, has a measured maximum value of eccentricity on top that reaches 3.3 m, on a total height of 52 m.

Figure 2.8 - San Martino di Burano bell tower

The presence of vertical eccentricity, assuming a linear deformation, produces a secondary moment that reduces the maximum flexural resistance, this action comes out to have a great importance, in particular when considered that the absolute value of eccentricity can be noteworthy.

Figure 2.9 shows the statistical distribution of vertical eccentricity for the sample: the 37% of it has a measured value of eccentricity lower than 0.3°, but a great part of the sample has a medium value of eccentricity, between 0.3° and 2. Table 2.2 shows the effect of vertical eccentricity in terms of effect on the resisting moment of the structure.

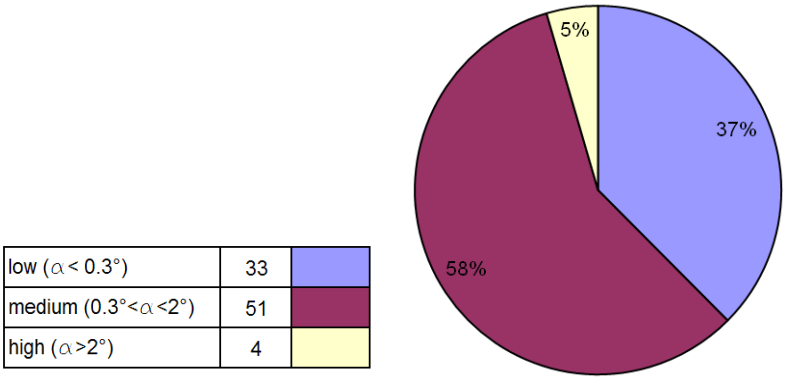

Figure 2.9 Statistical distribution of the analyzed sample: vertical eccentricity

Table 2.2 - Vertical eccentricity effect on ultimate bending moment

	Mu	Ms	Mres	Ms/Mu	vert. ecc.	Htot	vert. ecc /Htot
	[kN·m]	[kN·m]	[kN·m]	[-]	[m]	[m]	[-]
S. Martino di Burano	26399	15230	11169	58%	3.34	51.94	6.4%
S. Francesco Vigna	91081	14218	76863	16%	1.34	75.61	1.8%
S. Sofia	5174	842	4332	16%	0.733	19.3	3.8%
S. Stae	26120	7285	18835	28%	1.81	33.37	5.4%
S. Pietro Castello	56116	13240	42876	24%	1.342	46.26	2.9%
S.M. Carmini	29605	5318	24287	18%	0.907	45.9	2.0%
S. Giorgio Maggiore	53734	14341	39393	27%	0.974	67.18	1.4%

2.4.3 Interaction with adjacent buildings

Bell towers are not always isolated and free of restraint along their height, on the contrary, they are often bearing on other buildings that can belong to very different typologies, such as churches or houses. This interaction of course affects the dynamic response of the building, with in turn effects is the mechanical behavior. Thus, there additional layers of complexity for the definition of general and simple mechanical models, specifically considering that the restrain condition is neither the most dangerous nor it is permanent (it depends on the quality of the junction with the adjacent building). One first solution is to consider two different restraint conditions, the first one assuming the structure as isolated, as if there was no contact with other structures, and the second considering every form of interaction along each direction, as if the tower started from the level of restraint:

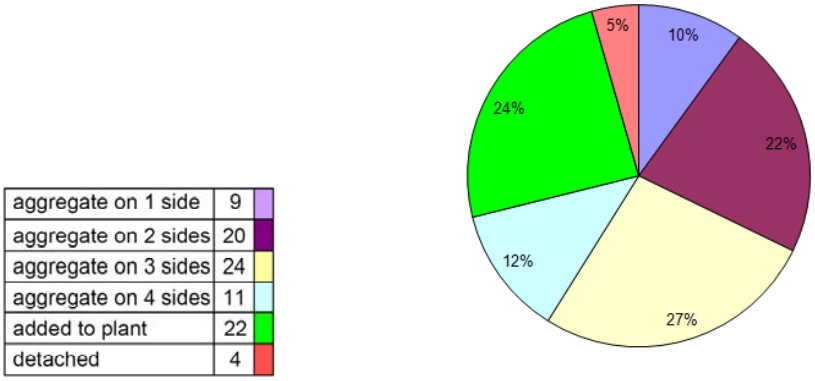

Figure 2.10 – Statistical distribution of the analyzed sample: interaction with adjacent building

Figure 2.10 shows the statistical distribution of the number of sides interacting with other structures for the sample. It is worth noting that, the verification as isolated is necessary even when the tower is restrained to another building because it represents the condition in which, during an earthquake, the connection is not enough resistant to provide an adequate level of restraint. Another aspect that is worth noting is that, when the bearing level is very high the experimental formula for the evaluation of the period might not fit the behavior of the upper part

2.4.4 Analysis results

According to the prescription given by the guidelines, two index for the evaluation of the seismic safety can be evaluated: the acceleration factor f_a and the safety index Is; they are respectively the ratio between the acceleration that leads to reach the ultimate limit state and the reference acceleration and which points out the lack of structural capacity, and the ratio between the return period of the action that leads to collapse and the return period of the reference action. Figure 2.11 shows both the values of f_a and I_s for the analyzed structures, within the hypothesis of isolated structure. The values follow the monotonic order of results.

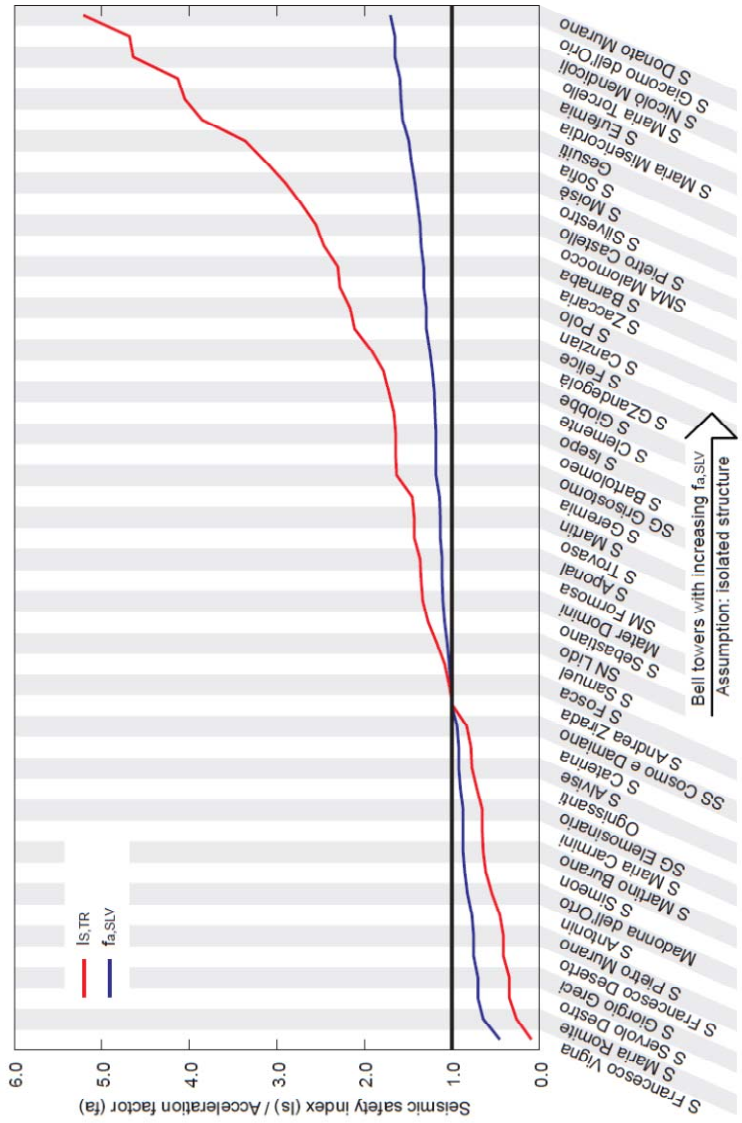

Figure 2.11 - Values of I_S and f_a for each analyzed bell towers

It is interesting noting that the two indexes provide the same global trend but on a completely different scale: the index evaluated with the return periods ratio. In the following results will be referred to the index evaluated from the accelerations ratio, since it gives a "quantitative" evaluation of the "resistance" lack of the structure. Concerning this in Figure 2.11 the only acceleration factor is depicted versus increasing slenderness (where the slenderness is calculated as the ratio between the bell tower height, from base to the center of mass of the roof, and the average base dimension). It is possible to underline an intrinsic vulnerability depending on the structural slenderness. This behavior, which was predictable on the basis of the model assumed, presents some differences mainly due to the following aspects:

it's found a lower peak of the safety index factor for those bell towers which have a high compression stress or a significant vertical eccentricity (i.e. S. Francesco della Vigna, Madonna dell'Orto, S. Antonin, S. Pietro Murano, etc.).

Higher values are found for the isolated towers, due to a higher behavior factor q (i.e. Torcello, S. Pietro di Castello, Misericordia, S. Donato Murano).

Figure 2.13 shows the results in terms of acceleration factor obtained from both the hypothesis of isolated structure and adjacent elements for a sample of 33 towers. It can be noted that the condition of isolated bell tower is the more cautionary; this points out that a smaller height, from one point of view, implies a higher frequency and hence higher

seismic forces, but on the other hand it reduces the vulnerability of the structure according with the characteristic of less slender structures to have a higher seismic safety index. It is worth noting that the cases in which the isolated and adjacent conditions concur are those in which the minimum value of the index is measured along a “free” direction, which can be resembled to the isolated condition.

Furthermore a study on the variability of the global response, according to a different level of knowledge, was performed. The vulnerability in terms of I_s was evaluated for different values of F_c (in the previous analyses it was assumed $F_c = 1.35$) considering the following scenarios:

$F_c = 1.18$, obtained considering $F_{c1} = 0.0$, $F_{c2} = 0.06$, $F_{c3} = 0.06$, $F_{c4} = 0.06$

$F_c = 1.00$, minimum value obtained assuming a very detailed geometrical and material survey

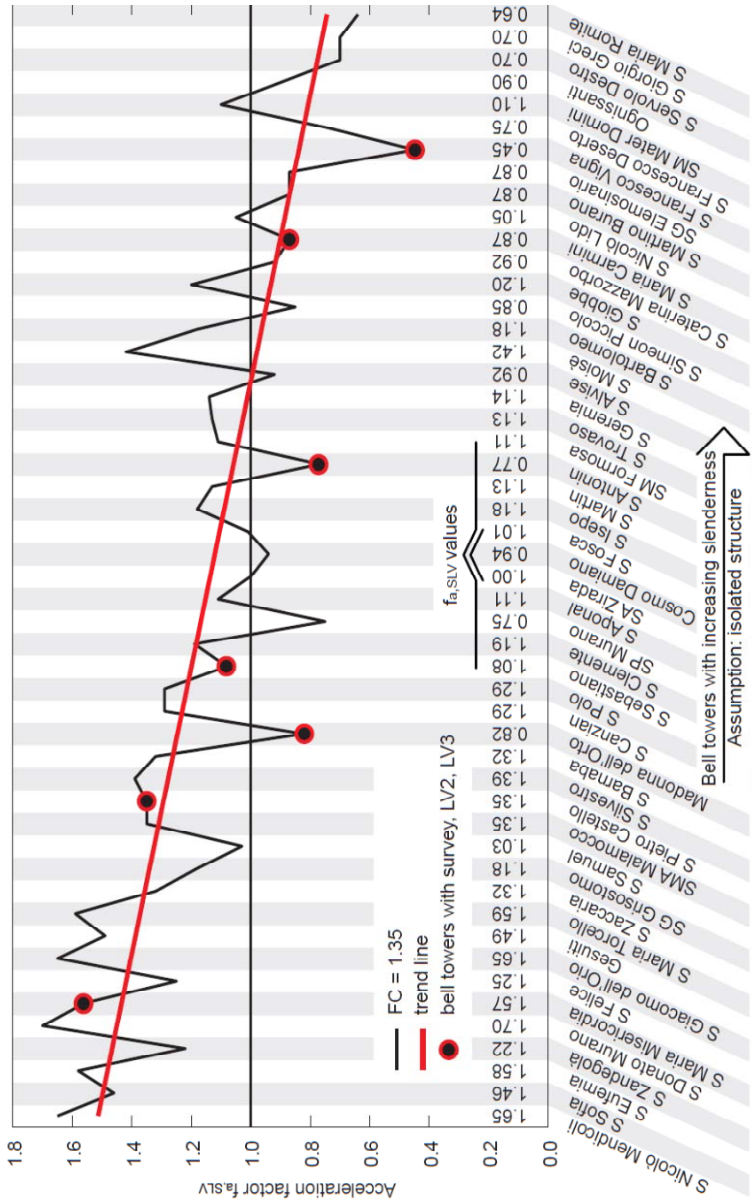

Figure 2.12 - Acceleration factor according to increasing height/base ratio

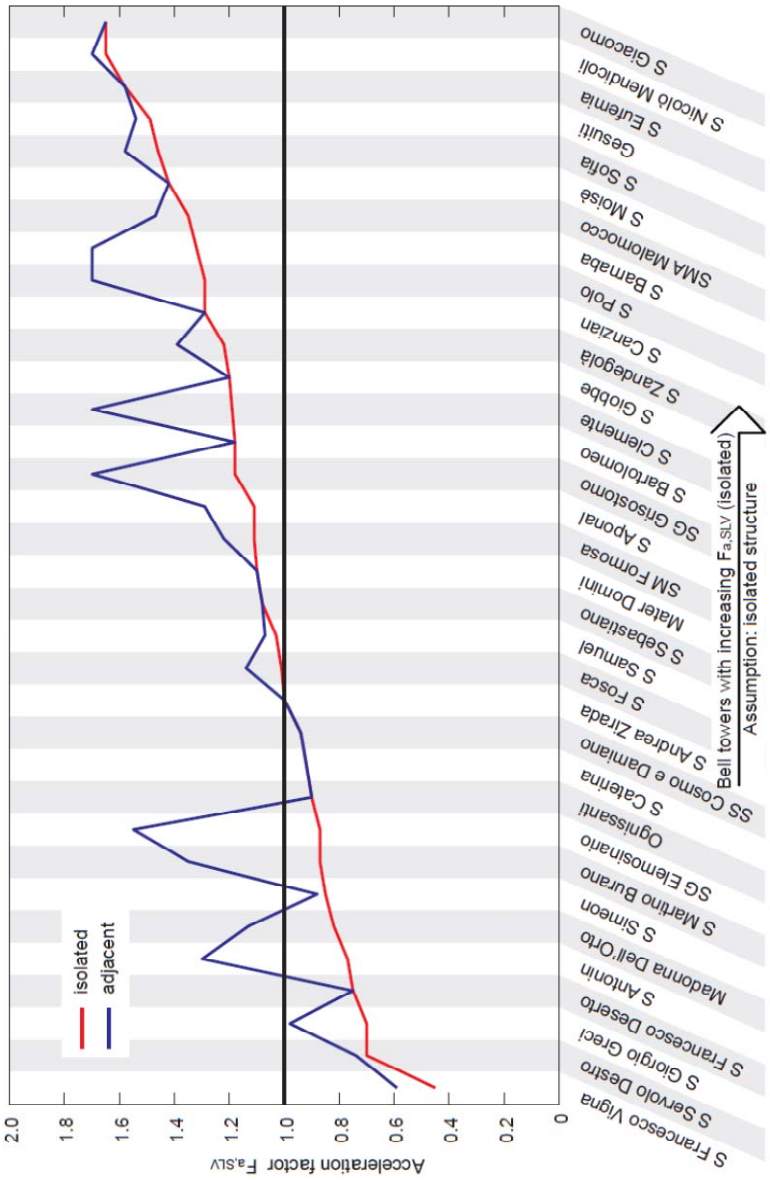

Figure 2.13 - Acceleration factor for bell tower as isolated and by considering adjacent elements

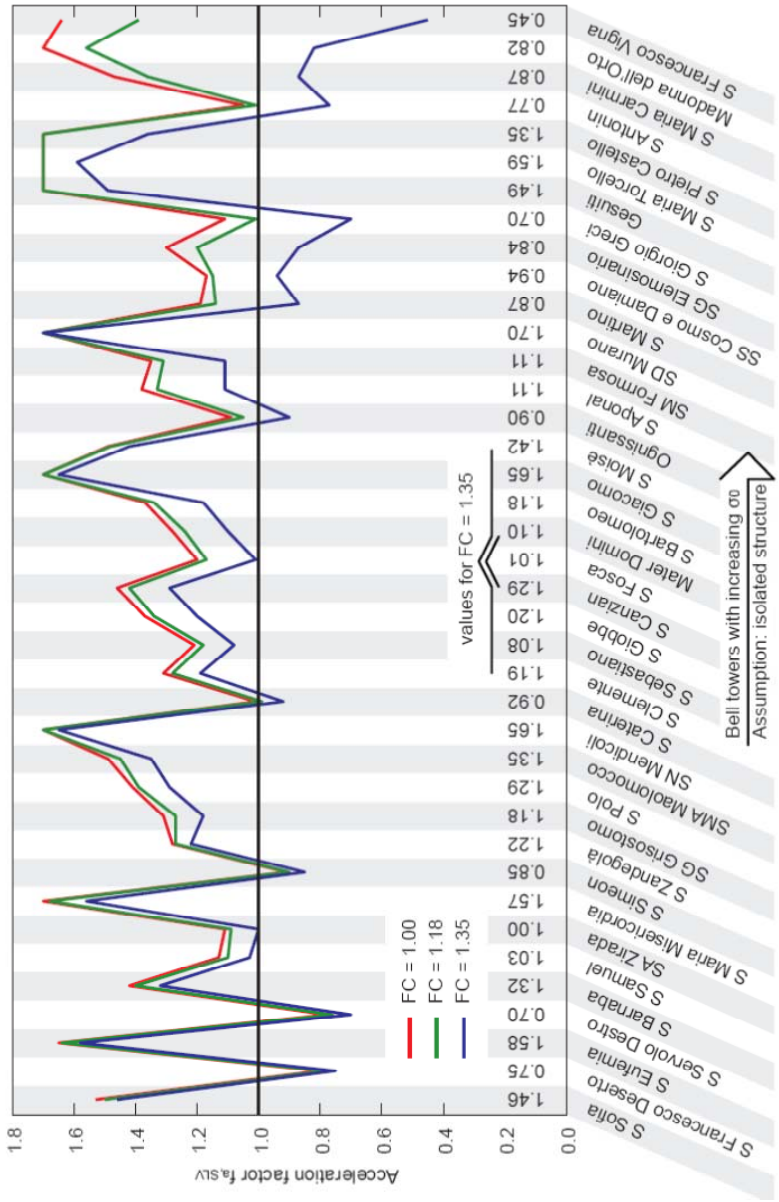

Figure 2.14 - Sensitivity to confidence factor Fc

Situations in which the variation of the value of F_c gives a noteworthy variation of the safety index are those in which the vertical load level is particularly high and provides a stress condition, due to vertical loads, close to the mechanical limit of the material; in these situation increasing the knowledge allows to assume a more resistant material; This means that, when the stress due to vertical loads is far below the mechanical limit, a deeper knowledge of the building does not give an effect as much visible as when the stress level is higher.

Finally some remarks can be made about this example: the methodology proposed by the guidelines seems to be efficient in terms of applicability, both for results reliability and for simplicity of application. It is also clear that a simplified approach is not always as easy as it seems in particular when dealing with problems with such a great level of contributions to uncertainty; the development and application of a simplified mechanical model is useful as much as dangerous when there is a high risk of sacrificing important features of the problem in order to obtain a method easy to handle. This approach, for instance, completely neglects any possibility of failure due to shear, or also does not consider

problems that can affect the belfry. On the other hand this approach demonstrates the effectiveness of a territorial approach with the purpose of drawing priority of intervention lists.

Since an overview of the application has just been given, the further step is to describe the application of these concepts, and of the other concepts proposed in the guidelines, to the case of art objects.

2.5 Extension of Guidelines Principles to art objects

As it was explained before the approach proposed in Guidelines was firstly defined for masonry structures hence the first draft and applications were addressed to this structural typology. Results were interesting and encouraging, and the Ministry for Artistic and Cultural Goods decided to study the possibility to extend the principles contained in this code to other structural and non structural types, such as reinforced concrete structures, archeological sites and art objects. This is exactly the niche where this work takes place. Indeed the main purpose of this dissertation is to propose an extension of the above described principles and criteria, contained in Guidelines, to the case of art objects. It is indeed worth to remind that Italy owns a considerable asset of artistic movable artifacts, which are exhibited and stored in museums and structures all over the national territory. These objects have very different characteristics and features that may make this a difficult task. It is nonetheless true that such a heritage needs to be properly protected from seismic risk, especially in a territory prone to earthquakes such as Italy. Recent examples demonstrated that the effects of an earthquake on movable objects can be strong and often irreversible (Figure 2.15 and Figure 2.16), and cause damages that can difficultly be quantified and restored, given the unique nature of the damaged objects.

Figure 2.15- loss of the art good due to earthquake

Figure 2.16 - loss of the art good due to earthquake

The extension of the Guidelines to art objects heritage requires an accurate analysis of the existing criteria that need to be modified to fit each different case of application. In this paragraph the extended procedure will be described and also compared with the classical definition of the chain of risk, trying to critically point out common aspects and differences between the different "reading keys" of the problem; afterwards, in the following chapters each aspect will be described and applied with attention to details. It is worth noting that, the Guidelines' approach and the risk chain's approach are just slightly different interpretations of a problem that, despite some differences, aim to achieve the same purpose.

In Figure 2.17 a graphical comparison between the three approaches is given, considering the general macro elements that constitute the different cases:

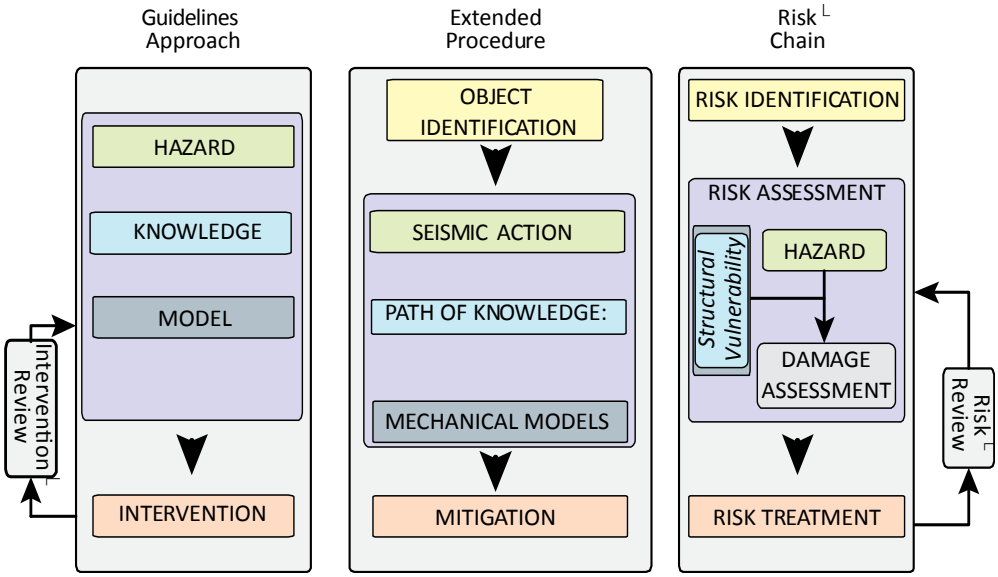

Figure 2.17 - approach frameworks

The description that will be provided in the immediate following has the purpose to give an overview of the main aspects of the "extended procedure" for art objects, in order to provide a "reading key" for the definition of the problem and to underline the basis of this work, which consists into a critical "adaptation" of an existing set of tools and indications to a different purpose.

Different aspects will be briefly listed, stressing main differences and similarities; a detailed description of each important point of the procedure is given in the following chapters.

As previously stated, the definition of seismic action can be treated as an independent block but its strong interdependencies with the knowledge phase and the model phase make it as a "procedure within the procedure" that needs to be handled with particular care for a correct evaluation of the condition of the object.

The second phase, on the left column of Figure 2.17, there is the group of knowledge: the path of knowledge requires a correct identification of both the object and the building in which it is contained, since the interaction between them can affect the assessment of the final level of safety, then, as much as it is important for masonry building, a reconstruction of the history of the artifact is fundamental for a more reliable evaluation of its health condition; according to the level of complexity that is required by the analyses, a geometrical and material survey needs to be performed pointing out all the aspects that can be useful for the analytical investigation. The aspects the attention of the surveys needs to be focused on (both geometrical and material) are of course different for the case of movable goods, indeed it is necessary to highlight those characteristics that, as it will be explained in the following, are necessary to define the mechanical model to chose (i.e. compact body or articulated body, presence of cracks and fissures, etc.); in particular, concerning the material survey, in this dissertation a framework for non destructive investigation on stone materials is proposed. It is worth noting that, in this case, it is important to underline the interaction between the object and the building that contains it.

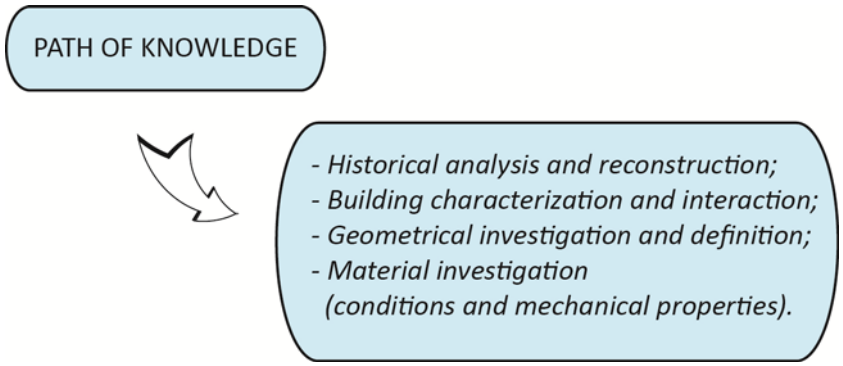

Figure 2.18 - path of knowledge for art objects

The choice for the mechanical model to apply depends both on the level of complexity of the required analysis and on the restraint conditions of the object, the possible approaches that are provided in this case are similar to those proposed for masonry structures, even though as it will be described in the assessment part, the levels of complexity adopted are not LV1, LV2 and LV3 as in the Guidelines but LS and LA, namely simplified level and accurate level; moreover the tools to use are different and designed "ad hoc".

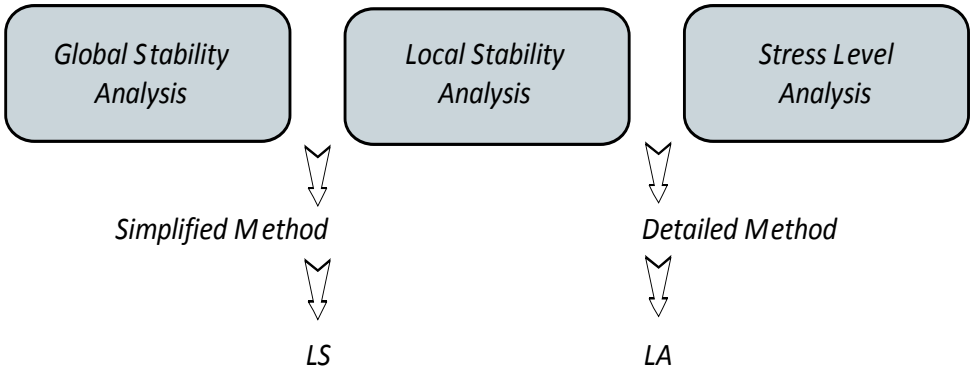

Figure 2.19 - levels of detail

The mechanical models proposed can deal with the object either as a rigid body or as a deformable body, according to its shape (compact or articulated), to the restrain conditions (unrestrained or restrained) and to the level of complexity adopted, even if the application seems to be easy, given the reduced dimensions of the objects (if compared to buildings), the variety of typologies that need to be assessed makes the definition of a reliable and flexible mechanical models mandatory. Figure 2.20 shows the framework to describe the different mechanical models available

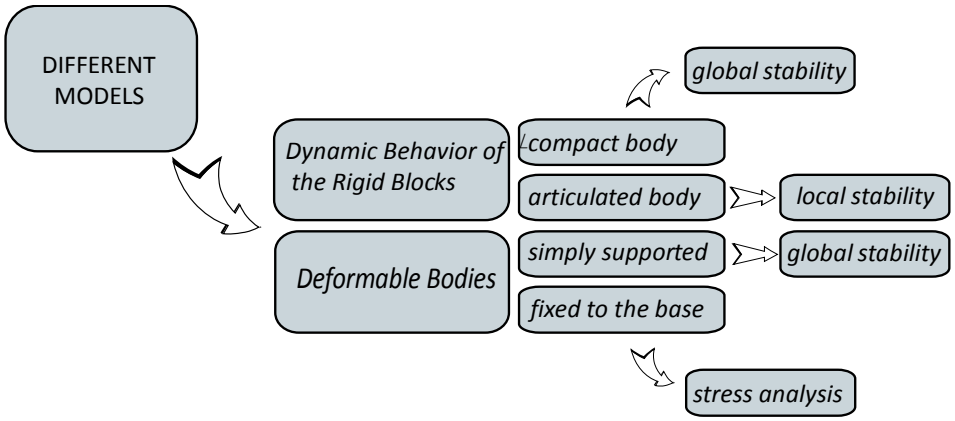

Figure 2.20 – models

The definition of the most suitable mechanical model to apply is necessary for an accurate assessment of vulnerability and consequently for decisions concerning the application of potential interventions. Figure 2.21 depicts the framework for the application of the proposed extension of the procedure, the different blocks of the general procedure are also pointed out.

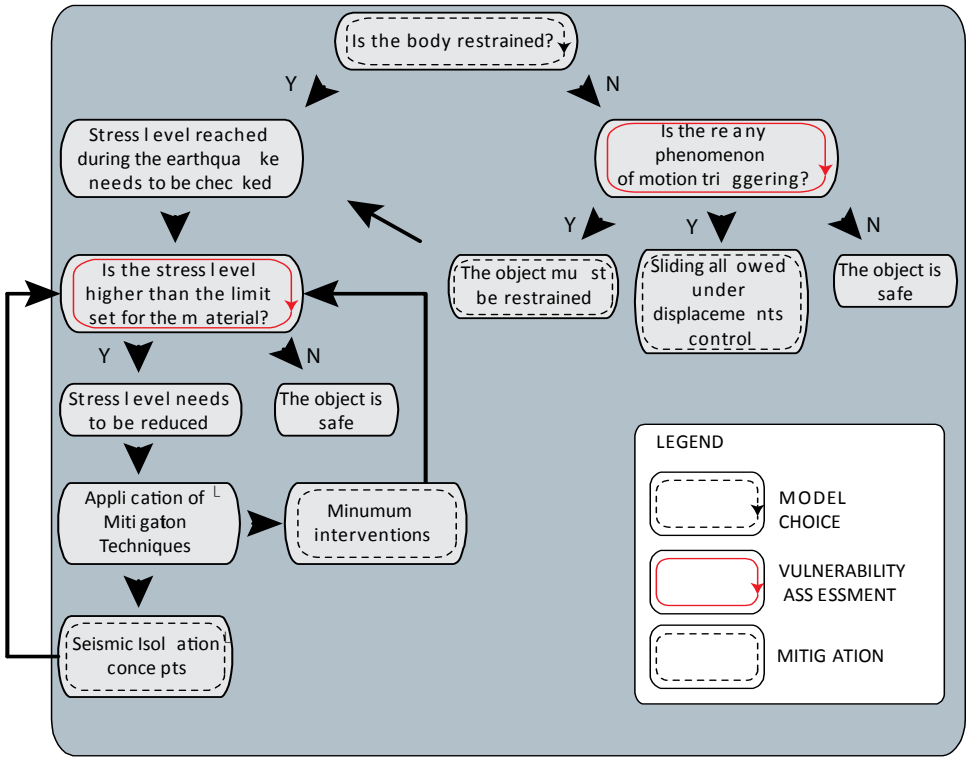

Figure 2.21 - framework for the application of the procedure

The framework starts from the observation of the restrain condition of the object, considering whether it is restrained or not. This aspect is actually a definition of the mechanical model to adopt. Once the mechanical model is chosen, also with the contribution of the data gathered in the knowledge phase and from the hazard analysis an evaluation of structural vulnerability is performed. Different scenarios are available according to the model chosen and to the results of the vulnerability analysis, but they all lead to a choice between two options: either the object can be considered safe or it is needed to mitigate the action of earthquake. After any application the effect of mitigation interventions needs to be checked, performing a further vulnerability analysis

After the assessment phase the mitigation phase is described, which has the same features for all the three approaches: techniques to reduce and mitigate the seismic risk for art objects will be widely discussed in a dedicated part of this dissertation, where a proposal for the application of innovative seismic isolation devices will be presented and discussed.

It is worth noting that many of the steps of the procedure need to be performed in the exact order in which they are listed, because they are often consequent one to the other and the quality of the result of one step depends on the information gathered from the previous one. However this is not always true: for instance, within the path of knowledge, the historical reconstruction is useful during the mechanical characterization, hence it would be reasonable to perform it before; on the other hand, the definition of the seismic action can be performed before the path of knowledge of the object or after that, without affecting the result. It is then reasonable to define that, within the same macro block the order of the steps should be in general kept as it is suggested, but it can be modified whenever it is justified by the situation.

Furthermore, if the proposed approach is compared to the procedure described by Olivato in (6), the affinity between the risk assessment framework and the methodology proposed in this dissertation is even more evident:

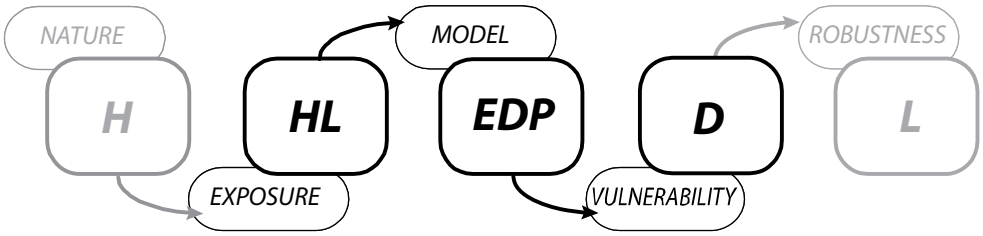

Figure 2.22 - Risk chain proposed by Olivato

The chain presented in Figure 2.22 allows the detailed calculation of the risk of a catastrophic event by means of a progressive definition of the rings of the chain with their interdependencies. The methodology proposed in this chapter focuses in particular on the rings that are highlighted. It proposes new tools for the vulnerability assessment of art objects, starting from a detailed overview of the state of the art of the artifacts and applying different models for to the elements at risk.

3. Assessment

3.1 Abstract

In order to assess the seismic vulnerability of an art object the path of knowledge needs to be applied and a proper mechanical model must be defined and chosen; according to the methodology proposed in the previous chapter different solutions can be adopted, considering different boundary conditions and different levels of detail, that could be available in each specific case of application of the proposed methodology. The main task of the following chapter is the description of the path of knowledge for art objects, the definition of adequate mechanical models to adopt and the application of the proposed procedure to the case of study of Galleria dell 'Accademia.

First of all the path of knowledge is presented, focusing the attention on its most relevant aspects: historical research, geometrical and material survey. For this last aspect an innovative approach to the non destructive survey of stone materials is also proposed.

Subsequently the mechanical models are introduced: as first static formulas for the study of the dynamic response of a rigid block are described, starting from a review of the well known equations given in literature (1) (2) for the description of sliding, rocking and overturning; as an improvement to these relations the possibility of investigating the response of a non symmetric rigid body with the presence of a vertical ground acceleration is also developed and described.

As a further level of detail in the analyses, and also as a feedback on the above mentioned relations, the governing equations of rocking phenomenon are solved by means of a computer program for time history integration. This tool considers the non linear solution of the equations, including the presence of vertical action and the possibility to study a non-symmetric body. Such a tool is then applied in several benchmarks in order to validate its applicability and results.

The "path of knowledge" and mechanical models that represent the dynamic response of the rigid body are then applied to the case study of Galleria dell'Accademia in Florence, both for big statues of "Galleria dei Prigioni" and for the busts of "Sala dell'Ottocento". Geometrical surveys are dealt with at different levels of detail for the objects of the case of study: three different levels for the statues of "Galleria dei Prigioni" and two different levels for the busts of "Sala dell'Ottocento". Next the materials were surveyed also by means of the application of the proposed procedure for non destructive assessment of mechanical properties: this method revealed some critical situations for the statues of the "Slaves".

Next the proposed mechanical models were employed for the effective assessment of the vulnerability of the objects under analysis; this application revealed that they may suffer problems of rocking and overturning, that can lead to damage to people or to the artifacts themselves. In particular the statues of the "Slaves" suffer of general diffused

problem of rocking and in some cases also of overturning. One of the possible solutions to this problem is to anchor them to the ground; according to the previously proposed methodology such a solution requires a study of the art object as it was deformable. Hence analyses with 3D finite element models are performed in order to assess the stress level induced in the statues by an earthquake input, in terms of maximum tensile stress and displacement.

3.2 Seismic action evaluation

One of the most important and difficult aspects of the assessment procedure is the definition of the reference seismic action. Indeed it allows identifying the seismic response of the building and a threshold action which will be the reference for all the further analyses performed.

3.2.1 General information

Unless the soil conditions require specific investigations about the local response, the elastic response spectrum given by the New Technical norms for Constructions (D.M. 14 Gennaio 2008, NTC in the following) can be used as a first approach for determining the seismic action. According to the NTC, seismic action on Italian territory is given by parameters that vary with the geographic location of the site, with reference to a grid 5 km by 5 km. These parameters are provided in each point of the grid for 9 return periods, from 30 to 2475 years. The response spectrum needs to be evaluated on the exact position of the building or of the city in which the site is located. Considering the peculiarity of the goods object of this study it is however suggested to investigate the seismicity of the site by means of historical researches and, whenever it is possible, of in situ examinations or of neighboring sites.

When dynamic time history analyses need to be preformed, in accordance with the standards, the seismic action must be characterized by an adequate number of properly chosen accelerograms, representing the three components of the seismic action: along two horizontal principal directions and along the vertical one. Different solutions are possible for the choice of seismic inputs: artificial inputs, generated inputs and natural inputs. Artificial earthquakes are generated to satisfy the compatibility to the response spectrum within an interval of periods defined in the norms. Generated earthquakes belonging to the second category are generated by algorithms that take into account the seismic features of the area; natural records are chosen within one or more database in order to fit the reference spectrum, in this case it is reasonable to set the compatibility around the main frequency of the structure.

Another important aspect is the presence of horizontal perpendicular actions at the same time. The choice for the natural accelerograms provides the opportunity to have at disposal two perpendicular recorded inputs. In case an analysis along the three main directions is required the natural inputs selection provides also the vertical component of the earthquake corresponding to the horizontal ones. The aspect of ground velocity is taken into account with reference to the norms, applying formulas for the correlation between the ground acceleration and the ground velocity. In particular paragraph 3.2.3.3 of NTC gives the formula:

$$v_g = 0.16 \cdot a_g \cdot S \cdot T_C \tag{3.1}$$

where:

- a_g is the maximum horizontal acceleration

- S is a coefficient that takes into account the characteristics of the soil

- T_c is the period corresponding to the beginning of the constant velocity branch of the response spectrum, which depends on the soil category as well

A similar expression is given by Chopra (7) for stiff soils:

$$v_g/ag = 48 \text{ in/sec/g} \tag{3.2}$$

Alternatively Bommer (8) proposed a relation for the evaluation of ground velocity:

$$v_g = 0.2\, a_g S\, T_c \tag{3.3}$$

The correct determination of the seismic action on an art object cannot neglect the filtering effect of the structure on the seismic signal: indeed the structure modifies the amplitude and the frequency of the applied motion. This effect is taken into account with an accurate analysis of the coupled system structure-object or also with the application of floor response spectra.

The amplification of the seismic action due to different heights of positioning, for example on shelves, can be considered by means of formulas provided by NTC at paragraph 7.2.3 for non structural elements; the increment of accelerations can be evaluated as:

$$S_a = \alpha \cdot S \cdot \left[\frac{3 \cdot (1 + \frac{Z}{H})}{1 + (1 - \frac{T_a}{T_1})^2} - 0.5 \right] \tag{3.4}$$

- α is the ratio between the maximum ground acceleration for type A soils for the considered limit state and the acceleration of gravity;
- T_a is the period of vibration of the nonstructural element;
- T_1 is the fundamental period of vibration of the structure along the considered direction ;
- Z is the height of the center of mass of the non structural element measured from the foundations ;
- H is the total height of the building from the foundations.

It is worth noting that similar formulas are provided also in different norms, such as the Greek seismic code or the American FEMA 273.

3.2.2 Evaluation of the critical action

As defined in paragraph 3.2.1, NTC standards define the local seismic action with a set of nine response spectra, each one characterized by a different return period, in the interval from 30 to 2475 years. They also require a definition of the critical seismic event that causes the exceeding of a particular limit state in terms of return period: after the evaluation of the critical value for acceleration or velocity, which causes respectively rocking and overturning, it is hence necessary to calculate the return period of the earthquake connected to this particular value. In practical terms it consist in calculating the return period of a response spectrum which for a given acceleration and a given period has a spectral value equal to the critical one. In this particular case the period of the structure, since rigid blocks are analyzed, can be set T = 0 s; the critical value is the one obtained as a result of the analysis considered. The recent standards, unlike the previous ones, do not easily allow to evaluate the return period from the value of critical acceleration, since characteristic values of the response spectrum $p\ (a_g, F_0, T_c^*)$, for the different return periods are connected by the expression:

$$\log p = \log p_1 + \log \frac{p_2}{p_1} \cdot \log \frac{T_r}{T_{r_1}} \cdot \left(\log \frac{T_{r_2}}{T_{r_1}} \right)^{-1} \tag{3.5}$$

T_{r_1} is the closest return period lower than T_r;

T_{r_2} is the closest return period higher than T_r;

p_1 is the value of the researched parameter corresponding to T_{r_1};

p_2 is the value of the researched parameter corresponding to T_{r_2};

When the upper and the lower limits T_{r_1} and T_{r_2} of the return period are set, with a reduced number of iterations, it is possible to obtain the characteristic parameters $p\ (a_g, F_0, T_c^*)$ of the response spectrum that give the required acceleration for the desired period of the structure. In order to perform this calculation a simple software tool was implemented for the application of the bisection method on the grid of seismic input. It is worth noting that the reference return period will be compared to two different return period obtained from the critical actions: one for the critical acceleration connected to the triggering of rocking (Artistic Limit State) and one for the critical velocity connected to the overturning phenomena

3.3 Safety and conservation

3.3.1 Definition of proper limit states

In order to evaluate the safety level and protection for art objects to seismic risk two main aspects must be considered: safeguard of life, and safeguard of objects themselves. These two principles can be considered as the introduction to two different limit states:

- the ULS (which is a Life-safeguard limit state) for the preservation of life: in case of seismic event the object must not experience failures or losses of global equilibrium that can compromise the safety of people surrounding it;

- the ALS (artistic limit state in the following): in case of seismic event the good is safe or it experiences damages that can be easily repaired without a significant loss of the cultural value.

It is worth noting that for art objects the artistic limit state, in most of the cases, must be checked according to the seismic action related to the ultimate limit state, because it considers a global loss of equilibrium, which would compromise, in any case, the preservation of the good. In these situations it must be checked whether the satisfaction of the ULS implies directly the satisfaction of the ALS and vice versa. Indeed there can be situations in which the two limit states have different thresholds even though they consider the same reference seismic action. Let's think about the analysis of the equilibrium conditions of an object that suffers triggering of motion of oscillation for the reference seismic input but that doesn't cause overturning. In this case the ALS is not satisfied, since rocking can damage the object, the absence of overturning, instead, suggests that the ULS is satisfied. Despite this fact there are situations in which different levels of seismic protection can be designed for the ALS that can be referred to less strong but more frequent earthquakes. In these situations partial damages to the art good can be accepted as long as they are restorable and a global conservation is provided.

3.3.2 Levels of evaluation and seismic safety levels

The assessment of seismic vulnerability of art object applies two different approaches with increasing levels of completeness:

- a simplified (LS) that allows the evaluation of the critical seismic actions for which the objects reach the ULS or the ALS limit level, by means of simplified methods. These methods use a reduced number of mechanical and geometrical parameters, sometimes they also apply qualitative pieces of information (such as visual and critical surveys). This level of complexity can be used for the assessment of seismic vulnerability of art objects on a territorial scale, for a large number of goods belonging to the same category. One of the possible application of this level is to draw up a list with a ranking of sensitivity to seismic action.

- a detailed level (LA) that allows more precise evaluations but, at the same time, requires a more detailed elaboration of the knowledge and the employment of more exhaustive evaluation methods.

3.4 The Path of knowledge

Proper knowledge of the artifact is a fundamental assumption both for obtaining a reliable evaluation of seismic safety of the "state of the art" and for the choice for effective intervention to protect and safeguard it. In accordance to the

Guidelines the data and information acquisition follows a logical path, called the "path of knowledge" which is articulated in different levels of examination, this involves:

analysis about the building where the object is located and its interaction with the artifact, with particular attention to the effect of the building on the seismic action. This aspect of the path of knowledge is peculiar and requires a deep study about the seismic behavior of the building in which the good is exhibited; if the building is classified as historical the reference norms are still the guidelines for the evaluation of seismic vulnerability.

identification of the good is a preliminary but fundamental phase in the path of knowledge to handle the problem of seismic vulnerability assessment, which requires the classification of the art object into a defined category;

historical research about the good, about the seismicity of the area and about possible interventions of restoration;

survey of geometry, **material** and state of conservation, both for the object and for the support, with particular attention to the interface between them;

mechanical characterization of the materials with non destructive diagnosis techniques;

monitoring: the periodical check about the conservation conditions of the art object is a fundamental tool that is warranty of the safeguard during years. In particular the definition of an accurate monitoring and maintenance program is fundamental, especially for those objects that are set in aggressive environments or outside . In these situations the monitoring allows to follow the evolution of degradation phenomena in time and also to check the validity of the mechanical models chosen.

In the following some of the aspects of the "path" on which this research focuses are described.

3.4.1 Knowledge of the building

In case the art object is exhibited outside, this phase of the path of knowledge is that described in the Direttiva at point 4.1.8, concerning geotechnical aspects.

When the analyzed objects are positioned inside a building, this phase of the path of knowledge is about collection of material to assess the seismic vulnerability of the building, to acquire data about geomorphological characteristic of the site and , in general about the dynamic response of the structure.

from a methodological point of view it is clear how a vulnerability assessment for any art object cannot be aside from the analysis of the building, from different points of view:

- the structure acts as a filter for the seismic action and this affects the input that acts on the contained object, structural type, materials, geometry, and position of the object (i.e. response floor spectra) must be considered, etc.;
- the evaluation of the maximum displacements for the object in order to avoid crashes and impacts against the building itself;
- the critical knowledge of the elements in direct relations with the good (e.g. structure of the floor).

This phase consists also in a first survey of the halls of the building, which can also be limited to quick techniques; it is aimed to point out and describe the goods contained and their interaction with the building itself. This operation can be summarized in forms in which the following details have to be listed:

- positioning of the hall within the architectural complex;
- photographic survey of the typologies of the supports that are present in the hall, with a graphic render of the most significant ones.

3.4.2 Identification of the good

The aim of this phase of the knowledge is to provide a first and quick evaluation of the possible critical situations and seismic vulnerabilities. At the same time, for each hall of the building, a quick survey of the goods is performed, in order

to obtain a typological divisions of the art objects in groups with common characteristic (i.e. material, support, etc.) for which a similar seismic response can be foreseen. A distinction based on geometric characteristics of the object can be made, considering the goods either as rigid bodies or as deformable bodies. The first group can be subdivided into compact bodies and articulate bodies (Figure 3.1).

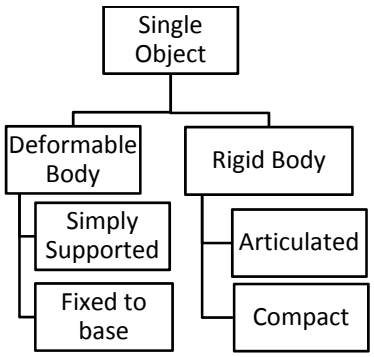

Figure 3.1 - schematic classification of single art objects

3.4.3 Historical analysis

This is a fundamental step for the "path of knowledge"; it consists of historical archive researches, gathering of details and information, such as drawings, photographic documentation, etc., with the aim of a complete reconstruction of good's history. It is indeed important to know the origins of the object but also to collect details about moving, locations of exhibition with particular attention to all those aspect that may have caused degradation phenomena, and obviously also to traumatic events (falls and collisions) and restoration interventions. At the same time, an important aspect that must not be ignored is the knowledge about the base such as pedestals, footings or shelves and the connection between it and the object. During the historical reconstruction phase information about the building must also be collected. This aspect aims to point out potential interaction between the container and the content in case of a seismic event. Since the assessment of the vulnerability of the object cannot be regardless towards the study of the seismic response of the building itself, it is necessary to find out the concerning documentation.

3.4.4 Object and material characterization

3.4.4.1 General consideration

The knowledge of the good needs an important phase of survey about geometry, material and state of conservation that can be carried out at different levels of detail. The geometric survey, which is necessary for the correct definition of the geometry of the good, it also aims to understand the relationship with the support and the environment. All details acquired from the survey will be used for the definition of the mechanical model to use for the assessment of seismic vulnerability. Moreover there must also be a detailed survey and render of the fractures and fissures pattern, the presence of iron pins or anchorages; similarly the presence of material alterations must be pointed out.

3.4.4.2 Geometrical survey

The geometrical survey consists in general in a graphic render that can be provided at different levels of detail according to the detail of the survey: from very rough and quick measurements taken with standard instruments (e.g.. a rule) to the application of innovative and accurate techniques such as the clouds of points obtained from the 3D laserscanner surveys. As it will be described in the following, level of approximation in the survey have significant effect to the results obtained from the application of mechanical models.

3.4.4.3 Material survey

The material survey must lead to a full characterization of the good, also including quality and conservation of materials, adopting different levels of investigation: from simple visual exams to indirect non destructive analyses. The peculiarity of the objects analyzed in this work and the need to develop references for materials characterization, it is considered useful presenting in the following some general notes about stone materials mostly used in the past for carving of statues; in particular the attention is focused on the possible influence of those characteristic that can affect the seismic vulnerability assessment.

The seismic vulnerability of a natural stone material depends mainly on:

- the structural characteristics, like shape, dimensions and mutual spatial correlation of the minerals/clasts/microfossils composing the rock;
- the textural characteristics, like stratification/layering, schistosity/foliation, brecciated/cataclastic fabric, fissuring/cracking, etc., intrinsic to the materials themselves;
- the physical-mechanical properties which again largely depend on the texture and the structure of the material.

The above-mentioned textural and structural characteristics may constitute elements of weakness in the materials, or in any case elements of anisotropic behavior which may increase the seismic vulnerability. It is in fact easy to understand how, for example, sussultatory earthquake shocks can dangerously reverberate on a statue carved from a not very compact and tectonic limestone, i.e. with many surfaces of minor cohesion, on which flow or sliding phenomena can occur. In the same way it is easy to understand how compact micro-granular rocks, for example micro-granites and fine grained marbles, offer a guarantee of optimum resistance to seismic damages while porous and mylonitic structures are without doubt weaker. As known, a stone material installed in a building, or a statue, once exposed to atmospheric elements, (thermal changes, action of freezing and thawing salt crystallization, atmospheric pollution, biodeterioration, etc.) is subject to chemical-physical decay phenomena (the stresscorrosion of the anglo-saxon authors) and biological deterioration, which mainly produce superficial degenerative morphologies. Such phenomena, in some cases, may cause an even more significant deterioration, (9),when it involves larger zones of the objects, causing a real structural weakening. It is thus easy to acknowledge that the marble or the stone of a sculpture after many years of outside exposure could be subject to a variation of its textural characteristics (e.g. broadening of sedimentary joints or schistosic planes, respectively in sedimentary and metamorphic rocks) and structural characteristics (e.g. increase of microporosity in sandstones, granites and marbles), as well as to a “weakening” of at least some of its physico-mechanical properties (e.g. increase of the “creep” due to loading stress in columns, pillars, caryatids and telamons). It should be also taken into account that possible damage occurring to stone materials during the quarrying and the subsequent shaping in the laboratory are not negligible; these are operations which may introduce superficial defects on which mechanical forces can concentrate with damaging effects (according to the theory of Griffith, (10), and Irwin, (11)), or also profound and latent defects, for example the case of what the Italian quarrymen of Carrara call “peli” produced by quarry extraction or during heavy mechanical workmanship. In case of artefacts subject to seismic action the determination of their evident state of conservation by macroscopic observations is thus of fundamental importance. Moreover some non-destructive tests, such as ultrasonic testing, could be very useful in evaluating the mechanical properties of the materials. Based on the above-mentioned considerations an attempt was made in this work to establish a possible standard procedure for petrographic evaluation of natural/artificial stone statues, (Figure 3.2) in order to obtain a more ample and articulated evaluation of their seismic vulnerability. This procedure must necessarily start with the correct identification of the stone material used both for statue and its base, defining, if possible, its origin (i.e. identification of the historical or modern quarries). This information can be obtained by autoptic means (12), or by micro-sampling from hidden or already deteriorated parts, which would allow the study of the mineralogic-petrographic/geochemical properties of the stone, (13). Moreover possible previous restorations and repairs have to be identified and classified, since they may also have a significant influence on the material characterization. Subsequently one must define, on the one hand, the physical-mechanical characteristics of the material– by comparison of the published data or through laboratory tests carried out on quarry samples of the rock used or of similar rocks – and on the other hand, the general condition of the sculpture under examination by detailed macroscopic observation, and possibly also by microscopic observation with a stereomicroscope, of the exposed surface. In this way one may evaluate the type of texture and grain of the material used, the presence of possible fractures, pins, forms of alteration and decay, patina’s and surface deposits, as well as the overall state of conservation. These observations can be summarized and transferred on a general card, accompanied by photographic documentation, which may be called “Summary card of the macroscopic evaluation. It should be pointed out that the state of preservation of the material constituting the artifact is one of the fundamental information necessary to perform reliable vulnerability analysis. In fact, a deterioration phenomenon, leading to a reduction of the mechanical characteristics of the material, has a direct consequence on the structural response of the element to the external actions.

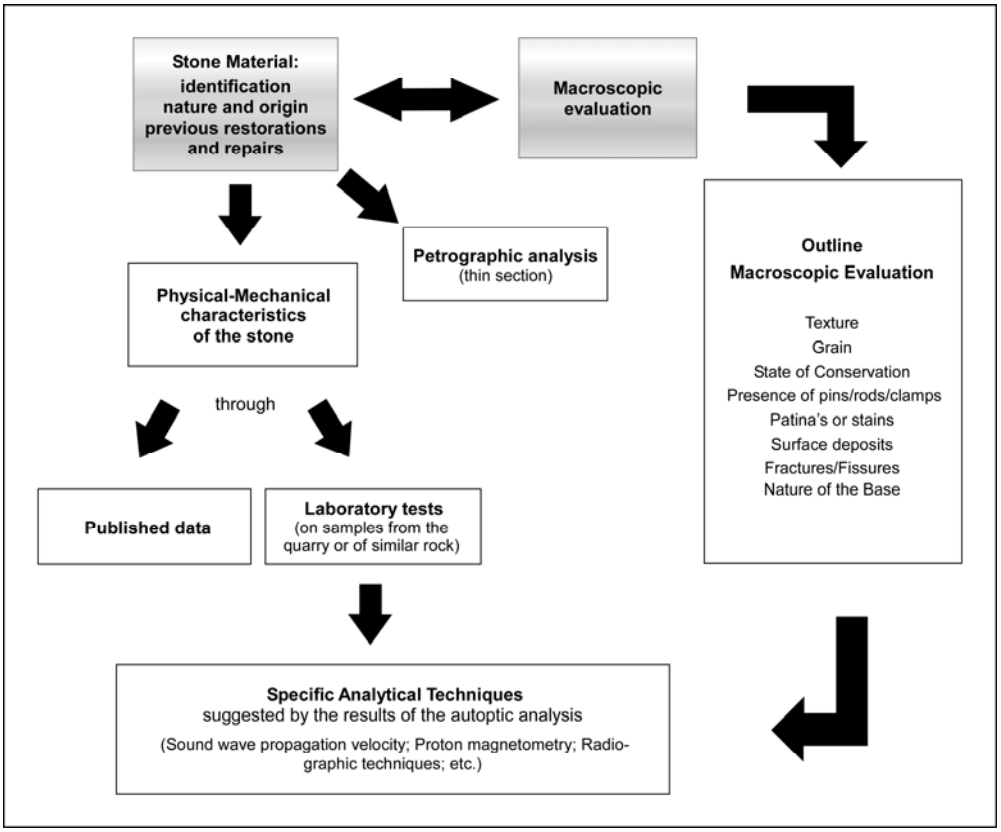

Figure 3.2 – operational procedure for the identification of the stone material

3.5 Levels of knowledge and confidence factors

Considering all the aspects and phases of the path of knowledge, such as the geometrical and material survey, the state of conservation, the correct identification of the relationship between the art good and its support and the interaction with the exhibition structure, it is possible to define a confidence factor F_c, greater than 1, in accordance to the Guidelines. This coefficient has the purpose to "pay" the knowledge about the object of study, in terms of reduction of the parameters that quantify the seismic vulnerability for the reached level of knowledge. The confidence factor is applied differently according to the models for the seismic vulnerability assessment that are considered:

- models that take into account the strength of materials and deformability of bodies;
- models that consider the limit equilibrium of the good or parts of it assuming the object as a rigid body.

In the first case the confidence factor is applied to materials properties, in particular as a reduction of the resistance; in the second case this factor is applied directly to the capacity of the structure, i.e. by means of a reduction of the acceleration or velocity value that leads to overcome the considered limit state. Values of the confidence factor can be defined from evaluations on the effects of different elements that concur to the final knowledge on the result.

One of the phases of knowledge that mostly affect the assessment of seismic vulnerability are the geometrical survey and the material survey. The first one has a great influence for the rigid body models, in terms of the position of the center of mass. It is clear that a rough survey, with a symmetric approximation of the object, for example with a rectangular body, causes an approximated evaluation on the seismic capacity of the object due to an inaccurate positioning of the center of mass. The second aspect that influences most the confidence factor is material and state of conservation survey: indeed the reliability and quality of the analyses on materials influence the evaluation of mechanical parameters that are going to be used in stress analyses.

3.6 Definition of mechanical models for the assessment of seismic vulnerability of art objects

For the assessment of seismic vulnerability of art goods models with different levels of complexity can be used, according to the available data and to the type of object under investigation, for example whether it can be considered as a rigid body or as a deformable body. However a global analysis which checks for possible losses of equilibrium, is always mandatory. For articulated bodies, also a local analysis is required: this is an analysis that considers the equilibrium of portions of the body, such as protruding parts connected, in case, with anchors or pins, or parts pin-pointed by cracks that show the possible development of a mechanism. For deformable bodies in addition to global equilibrium analyses, stress level and deformation analyses must be performed; these are aimed to verify that the stress induced in the object by the earthquake does not overcome the mechanical limit for the material. It is worth noting that these analyses must be carried out with particular attention to the difficulties connected to obtain a reliable model of the material. As a first step the application of linear elastic analyses is suggested to gather information about the order of magnitude and the pattern of the stress.

Application of the following methods is also available for these types of analyses:

- approximated methods, that apply symmetric rigid bodies analyses for evaluating the global equilibrium; these methods approximate the object with a parallelepiped with rectangular basis. Furthermore there can be simplified evaluations of the stress level in case of verifications about the resistance of the object. The results obtained with this method can be classified as LS level.
- detailed methods that apply more accurate models, considering also the presence of geometrical or material irregularities. Stress analyses are conducted with a higher level of detail. The results for the application of this method can be classified as LA level.

Another important aspect is the one concerning the restraint conditions, two limit situations can be considered: simply supported bodies (laid on a support such as the floor, a pedestal, a shelf) and fixed bodies (rigidly connected to the support). For the first group of objects global equilibrium analyses must be carried out, in order to investigate the possible triggering of dynamic phenomena such as sliding, rocking or overturning. Concerning the stress analyses, in this case the only force transferred to the body is the one correlated with the maximum friction at the interface “body – support”. For the second group, instead, once the forces acting on the entire system “body – support” are determined an evaluation of the resistance of the system must be performed: the entire seismic action will be considered as an input.

It is worth noting that sometimes a clear distinction between the two different restraint states is not possible and the case study cannot be identified as one of the two limit conditions; in these cases it can be useful to investigate both the restraint situations, with a careful interpretation of the results. At the same time a double verification on the restraint conditions can be used for preliminary decisions about interventions of seismic protection.

3.6.1 Rigid body models response – simplified static formulas approach (LS)

The response of an unanchored rigid body on a horizontal rigid floor to earthquake base excitations has been studied by several authors dealing with different features of this complex phenomenon (e.g. (7), (14), (15)). According to Lowry et. al. (16), six types of motion may be defined: (a) rest, when the rigid body moves firmly with the base during all the excitation; (b) sliding motion, when the body moves without losing the contact with the base; (c) rocking motion around one of the two bottom corners without sliding; (d), sliding-rocking, when a combination of rocking and sliding motions occurs; (e) free flight, when contact between body and floor is lost; (f) impact, when contact between body and floor is re-established. In some cases the rocking may lead to final overturning of the body. A more detailed description of such types of motions can be found in reference (15) and (17). This study focused on the criteria for triggering of rocking and overturning, which are two very dangerous conditions and could be respectively connected to the exceeding of the Artistic Limit State (ALS) and Ultimate Limit State (ULS). Actually, as previously stated, the triggering of oscillations could lead to uncontrollable damage of the object, thus causing the exceeding of the ALS, while when overturning occurs the safety of the persons which are near the object is not guaranteed anymore, exceeding the ULS. Concerning the sliding, in a preliminary phase it was assumed that the coefficient of friction between the block and the base is sufficient to prevent the occurrence of this phenomenon as the first critical event. Once the minimum values of PGA which cause rocking along the single directions are calculated (i.e. the values for which the ALS is reached) some considerations about coherent and reliable values of friction coefficients should be carried out. The configuration of non symmetric

body was also considered, with respect to the vertical central axis, in addition to the classical one of symmetric rectangular body, which has been studied in depth in literature (e.g. (18)) and which the stability analysis of art object is often referred to. Moreover the presence of vertical action was investigated, in order to better understand the interaction between horizontal and vertical actions, it is worth noting that the stability of small objects seems to be in general affected by the presence of a vertical action.

3.6.1.1 Symmetric bodies

The following paragraphs refer to Shenton's approach to the problem of the dynamic of a rectangular rigid body; the author also included a complete coverage of the motion phenomena that are not usually considered in other works. Since in this study it was assumed that the friction coefficient is always sufficient to prevent sliding as first critical event all the motion phenomena concerning it will be briefly described but not considered for the analyses. Shenton's approach is valid for rectangular rigid bodies, objects are not restrained and subjected only to horizontal actions, as shown in Figure 3.3. Block's features are mass m, weight W, moment of inertia I, base width 2B, height 2H; from these two parameters the ratio γ = H/B can be defined. Therefore the problem is plane, symmetric with respect to the vertical axis which divides the base into two equal halves of length B; B and H are hence the coordinates of the center of mass from the corner point O. f_x and f_y are respectively the horizontal and vertical reactions. Since as an assumption the interface body – surface is a Coulomb like friction relationship, the reaction f_x is the friction force between the block and the base, μ_s and μ_k are the values of the coefficients of friction, respectively the static and the dynamic one for the floor ($\mu_k \leq \mu_s$). Ground acceleration is given as $\ddot{x}_g = a_g g$, where a_g is the non dimensional peak ground acceleration and g is the value of acceleration of gravity. For further considerations about translation, roto-translation and rotation it is also assumed that at the initial instant the body is not moving, furthermore the acceleration is assumed constant in intervals.

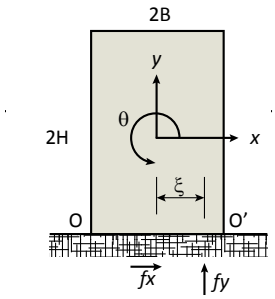

Figure 3.3 - rigid body model

3.6.1.1.1 Rest

Governing equations for this problem are:

$$f_x = m \cdot a_g g \qquad f_y - W = 0 \qquad f_x \cdot H + f_y \cdot \xi = 0$$

conditions for the body to move together with the ground are:

$$f_y > 0 \tag{3.6}$$

$$|f_x| \leq \mu_s \cdot |f_y|. \tag{3.7}$$

$$|\xi| \leq B \tag{3.8}$$

If the vertical component of the action is neglected, relation (3.6) is automatically verified, the conditions number reduces to two that, using the equilibrium equations can be written as:

$$a_g \leq \mu_s \tag{3.9}$$

$$a_g \leq \frac{B}{H} \tag{3.10}$$

also known as “West formula”

3.6.1.1.2 sliding/oscillation

Governing equations for this type of motion are:

$$-\mu_k \cdot S(\dot{x}_0) \cdot f_y = m \cdot (\ddot{x} + a_g g) \tag{3.11}$$

$$f_y - W = m \cdot \ddot{y} \tag{3.12}$$

$$-\mu_k \cdot S(\dot{x}_0) \cdot f_y \cdot H - f_y \cdot B = I \cdot \ddot{\theta} \tag{3.13}$$

since sliding is present the relative acceleration $\ddot{x}$ is given by a rotational and a translational component. Previous equations can also be written as follows:

$$f_y = \frac{m \cdot (\ddot{x} + a_g \cdot g)}{-\mu_k \cdot S(\dot{x}_0)} \tag{3.14}$$

$$f_y = m \cdot B \cdot \ddot{\theta} + W \tag{3.15}$$

$$-(\mu_k \cdot S(\dot{x}_0) \cdot f_y \cdot H + B) \cdot (m \cdot B \cdot \ddot{\theta} + W) = I \cdot \ddot{\theta} \tag{3.16}$$

From (3.14), (3.15) and (3.16), for a rectangular body, the following relation is obtained:

$$\ddot{\theta} = \frac{-3 \cdot g \cdot (\mu_k \cdot S(\dot{x}_0) \cdot \gamma + 1)}{B \cdot \left(4 + \gamma^2 + 3 \cdot \gamma \cdot \mu_k \cdot S(\dot{x}_0)\right)} \tag{3.17}$$

Conditions for the triggering of a sliding-rotation motion from a rest condition are:

$$\ddot{\theta} > 0$$

$$f_y > 0$$

In order to have $\ddot{\theta} > 0$ two conditions are available for $\ddot{\theta}$:

$$\mu_k \cdot S(\dot{x}_0) \cdot \gamma + 1 < 0 \text{ and } 4 + \gamma^2 + 3 \cdot \gamma \cdot \mu_k \cdot S(\dot{x}_0) > 0 \tag{3.18}$$

$$\mu_k \cdot S(\dot{x}_0) \cdot \gamma + 1 > 0 \text{and } 4 + \gamma^2 + 3 \cdot \gamma \cdot \mu_k \cdot S(\dot{x}_0) < 0 \tag{3.19}$$

When $S(\dot{x}_0) = 1$ none of (3.30) and (3.31) is satisfied. On the other hand, when $S(\dot{x}_0) = -1$, (3.19) leads to $\frac{1}{\gamma} > \mu_k > \frac{(4+\gamma^2)}{3 \cdot \gamma}$, which is not satisfied for any value of γ; relation (3.30) leads to $\frac{1}{\gamma} < \mu_k < \frac{(4+\gamma^2)}{3 \cdot \gamma}$. It can be shown that $\frac{(4+\gamma^2)}{3 \cdot \gamma} \geq 1,\overline{33}$, which is a trivial limit for the kinetic friction coefficient (always lower than 1). Hence $\ddot{\theta} > 0$ is satisfied when $\mu_k > \frac{1}{\gamma} = \frac{B}{H}$.

Considering the situation in which $S(\dot{x}_0) = -1$; from equation (3.16) the relation $\ddot{x}_0 = -a_g g - \mu_k \cdot S(\dot{x}_0) \cdot \left(B \cdot \ddot{\theta} + g\right) + H \cdot \ddot{\theta}$ is obtained. Assuming $S(\dot{x}_0) = -1$ and substituting $\ddot{\theta}$:

$$\ddot{x}_0 = -g \cdot \left[\frac{a_g \cdot (4 + \gamma^2 - 3 \cdot \mu_k \cdot \gamma) + 3 \cdot \gamma - (\mu_k + 4 \cdot \mu_k \cdot \gamma^2)}{4 + \gamma^2 - 3 \cdot \mu_k \cdot \gamma}\right] \tag{3.20}$$

which has to be less than zero. It has hence to be:

$$a_g > \frac{(1 + 4 \cdot \gamma^2) \cdot \mu_s - 3 \cdot \gamma}{(4 + \gamma^2) - 3 \cdot \gamma \cdot \mu_s} = a_g^* \tag{3.21}$$

in a different way:

$$\left|\frac{3\cdot\gamma+4\cdot a_g+\gamma^2\cdot a_g}{1+4\cdot\gamma^2+3\cdot\gamma\cdot a_g}\right|=\mu_s^*\geq\mu_s \tag{3.22}$$

3.6.1.1.3 sliding

Governing equations for this problem are:

$$-\mu_k\cdot S(\dot{x})\cdot f_y=m\cdot(\ddot{x}+a_g g) \tag{3.23}$$

$$f_y-W=0 \tag{3.24}$$

$$-\mu_k\cdot S(\dot{x})\cdot f_y\cdot H+f_y\cdot\xi=0 \tag{3.25}$$

where the sign function $S(\dot{x})$ is defined and it is equal to 1 when $\dot{x}>0$ and -1 when $\dot{x}<0$, so as to $-\mu_k\cdot S(\dot{x})\cdot f_y$ is the friction force on the floor, and it has always opposite direction of relative velocity $\dot{x}$. In the first equation the acceleration experienced by the body is the sum of the input acceleration on the floor $a_g g$ and the relative acceleration $\ddot{x}$: hence it is $\ddot{x}_{tot}=\ddot{x}+a_g g$.

Conditions for a motion of translation are:

$$f_y>0 \tag{3.26}$$

$$a_g>\mu_s \tag{3.27}$$

$$|\xi|\leq B \tag{3.28}$$

Since $|\xi|=\frac{\mu_k\cdot f_y\cdot H}{f_y}=\mu_k\cdot H$ the condition $\mu_k\leq\frac{B}{H}$.is obtained.

Assuming $\mu_k\cong\mu_s$, the afore stated condition becomes $\mu_s\leq\frac{B}{H}$. In this case the conditions become:

$$a_g>\mu_s \tag{3.29}$$

$$\mu_s\leq\frac{B}{H} \tag{3.30}$$

3.6.1.1.4 Oscillation

Assume that the body starts to rotate about the point O (rotation about point O' is the symmetric condition), without any relative displacement between the two surfaces. Immediately after the initial instant the block is in the situation depicted in Figure 3.4, with reactions f_x e f_y on the point O, which is the center of the rotation. Seismic acceleration causes an angular acceleration $\ddot{\theta}$.

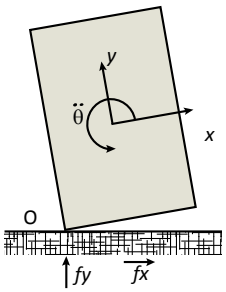

Figure 3.4 - rigid body model, rocking phase

The governing equations for the motion in this case are:

$$f_x = m \cdot (\ddot{x} + a_g g) \tag{3.31}$$

$$f_y - W = m \cdot \ddot{y} \tag{3.32}$$

$$f_x \cdot H - f_y \cdot B = I \cdot \ddot{\theta} \tag{3.33}$$

where I is the inertia moment of the body about the central axis.

Since it is a pure rotation motion the contribution of friction force does not appear, moreover it is: ha $\ddot{x} = -H \cdot \ddot{\theta}$ and $\ddot{y} = B \cdot \ddot{\theta}$. For the case of the rectangular body, for which the inertia moment is $I = \frac{m}{3} \cdot (H^2 + B^2)$, the three main equations can be written as follows:

$$f_x = \frac{W \cdot (3 \cdot \gamma + 4 \cdot a_g + \gamma^2 \cdot a_g)}{4 \cdot (1 + \gamma^2)} \tag{3.34}$$

$$f_y = \frac{W \cdot (1 + 4 \cdot \gamma^2 + 3 \cdot \gamma \cdot a_g)}{4 \cdot (1 + \gamma^2)} \tag{3.35}$$

$$\ddot{\theta} = \frac{3 \cdot g \cdot (\gamma \cdot a_g - 1)}{4 \cdot B \cdot (1 + \gamma^2)} \tag{3.36}$$

The assumptions for a pure rotation motion are:

$$\ddot{\theta} > 0 \tag{3.37}$$

$$f_y > 0 \tag{3.38}$$

$$|f_x| \leq \mu_s \cdot |f_y| \text{ (no sliding)} \tag{3.39}$$

For relation (3.37), since the denominator in the expression for $\ddot{\theta}$ is always greater than zero, it has to be $a_g > \frac{1}{\gamma} = \frac{B}{H}$ $(West\ formula)$. Condition (3.38) is always satisfied when $\ddot{\theta} > 0$, since $f_y = m \cdot B \cdot \ddot{\theta} + W > 0$. Concerning relation (3.39) it can be written as $\left|\frac{f_x}{f_y}\right| = \left|\frac{3 \cdot \gamma + 4 \cdot a_g + \gamma^2 \cdot a_g}{1 + 4 \cdot \gamma^2 + 3 \cdot \gamma \cdot a_g}\right| = \mu_s^* \leq \mu_s$ and so $a_g \leq \frac{(1 + 4 \cdot \gamma^2) \cdot \mu_s - 3 \cdot \gamma}{(4 + \gamma^2) - 3 \cdot \gamma \cdot \mu_s} = a_g^*$ giving in this way a definition for μ_s^* and a_g^*.

In this way conditions that need to be fulfilled for a pure rotation motion are two:

$$a_g > \frac{1}{\gamma} = \frac{B}{H} \ (West\ formula) \tag{3.40}$$

$$a_g \leq \frac{(1 + 4 \cdot \gamma^2) \cdot \mu_s - 3 \cdot \gamma}{(4 + \gamma^2) - 3 \cdot \gamma \cdot \mu_s} = a_g^* \tag{3.41}$$

A brief summary for the conditions of rigid body motion is given here for a symmetric rectangular body subjected to an horizontal acceleration input constant in intervals:

TYPE OF MOTION	CONDITION

Rest	$a_g \leq \mu_s$ and $a_g \leq B/H$
Traslation	$a_g > \mu_s$ and $\mu_s \leq B/H$
Rotation	$a_g > B/H$ and $a_g < a_g^*$
Rotation and traslation	$\mu_s > B/H$ and $a_g > a_g^*$

3.6.1.1.5 Overturning

One of the most detailed studies about the overturning phenomenon is the one carried out by Ishyiama, who, in 1984, published some criteria to define the condition of overturning for slender blocks (14) considering the accelerations , the velocities and displacements given as input. The displacement criterion is not interesting, since it appears to be less on the safe side than the other two; the criterion that limits the acceleration is, in facts, the afore mentioned "West formula" which is a necessary condition, but not sufficient, for the tilting of the body. It is indeed clear and experimentally confirmed, that the condition $a_g > B/H$ assures the rotation of the body but it does not represent a condition for the overturning. On the other hand it is physically clear that, for experiencing tilting, it is first of all necessary that it experiences oscillations. It is also clear that in order to have overturning a horizontal acceleration $a_g g$ that triggers oscillation is applied for a period long enough to reach a value of velocity high enough. Ishyiama developed a criterion regarding the critical velocity that induces overturning. In the following description figure (Figure 3.5) is taken as reference.

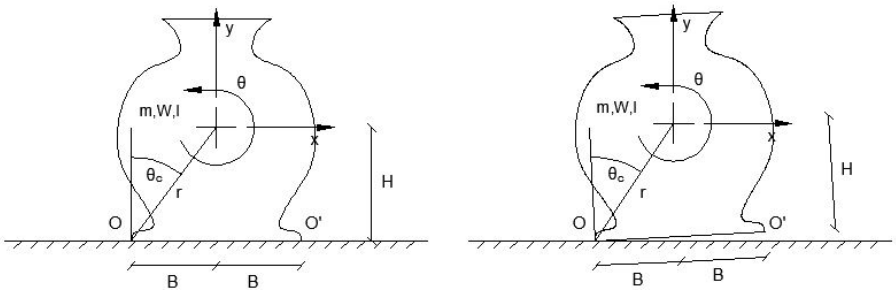

Figure 3.5 - rigid body model, overturning

In order to have overturning the body must rotate of an angle $\theta = \theta_c$, where $\theta_c = arctg\left(\frac{B}{H}\right) = arcos\left(\frac{H}{r}\right)$ over which the only self weight leads to overturning. An increment of potential energy $\Delta U = m \cdot g \cdot r \cdot (1 - \cos\theta_c)$ needs to be provided in order to obtain an uplift of the center of mass.

As clearly shown by Ciampoli (19), the kinetic energy of the body rotating about the rotation axis is given by the expression $T = \frac{1}{2} \cdot I_r \cdot \omega^2$, where $I_r = I_g + m \cdot r^2 = m \cdot (i^2 + r^2)$ is the inertia moment about the rotation axis, i=$\sqrt{\frac{I_g}{m}}$ is the inertia radius of the body in the rotation plan, and $r = \sqrt{B^2 + H^2}$ is the distance of center of mass from the rotation point. Comparing the two expressions:

$$\omega^2 = 2 \cdot g \cdot r \cdot \frac{m}{I_r} \cdot (1 - \cos\theta_c) \qquad (3.42)$$

Assuming that the body is rigidly moving with the ground, in a condition of fixed translation with critical velocity v_c and that it abruptly begins to rotate (i.e. the conditions that allow rotation are satisfied), the conservation of the linear momentum gives:

$$m \cdot V_c \cdot H = I_r \cdot \omega \text{ hence } \omega^2 = \frac{m^2 \cdot V_c^2 \cdot H^2}{I_r^2} \qquad (3.43)$$

Then from the comparison between the two expressions of ω^2 (3.42) and (3.43):

$$V_c^2 = 2 \cdot g \cdot r \cdot \frac{I_r}{m} \cdot (1 - \cos\theta_c) \cdot \frac{1}{H^2} = 2 \cdot g \cdot \frac{I_r}{m} \cdot (1 - \cos\theta_c) \cdot \frac{1}{H \cdot \cos\theta_c} \quad (3.44)$$

This velocity is hence the minimum required velocity for an overturning of the body. If rectangular bodies are considered the previous definition can be simplified:

assuming $\frac{I_r}{m} = \frac{4}{3} \cdot (H^2 + B^2) = \frac{4}{3} \cdot$

$$V_c^2 = \frac{8}{3} \cdot g \cdot r \frac{(1 - \cdot \theta_c)}{\cos^2 \theta_c} \quad (3.45)$$

In case of a rectangular slender body assuming $1 - \cos\theta_c \cong \frac{\theta_c^2}{2}$, $\cos\theta_c \cong 1$ and $\theta_c \cong tg\theta_c$ the result is:

the value of v_c is obtained:

$$V_c^2 = \frac{4\ g\ r\ B^2}{H}. \quad (3.46)$$

It is worth noting that a relation to evaluate the limit velocity was firstly proposed by Housner in the 60's as an energy balance, to evaluate the pseudo velocity necessary to predict a 50% of chance of overturning of rectangular bodies subjected to single horizontal shocks, as following:

$$v_c = \frac{1}{\cos\alpha} \sqrt{\left(\frac{8}{3}\ g\ r\ (1 - \cos\alpha)\right)} \quad (3.47)$$

By means of a series of numerical tests on rectangular bodies Ishyiama determined that, when the maximum velocity is lower than 0.4 V_c the stability of the object is almost given. The extension of the results to non rectangular generic bodies the criterion that gives the limit velocity for overturning that is:

$$V^* < 0.4 \cdot V_c \quad (3.48)$$

In the case of slender rectangular bodies the condition can be written as:

$$V^* < 14.46 \cdot \frac{B}{\sqrt{H}} \quad (3.49)$$

with V^* in cm/s e B and H in cm. This relation is often given as an approximation:

$$V^* < 10 \cdot \frac{B_{TOT}}{\sqrt{H_{TOT}}} \quad (3.50)$$

With B_{TOT}=2B and H_{TOT} =2H respectively equal to the total base width and total height expressed in cm.

It is worth noting that the previous description of the overturning phenomenon neglects the fact that the only horizontal acceleration is considered or also the vertical action is included, hence, as stated by Ishyiama (14),"the lower limits of acceleration and velocity to overturn the body are not affected much by B/H, size of the body, surface coefficient of friction and by the existence of vertical excitations".

3.6.1.2 Non symmetric bodies

3.6.1.2.1 Sliding/Oscillation

Concerning the dynamic phenomena of sliding ad rocking the above described formulation can be extended, obtaining results very similar to the symmetric ones, without conceptual difficulties. In particular the governing equations of motion are the same as long as the values of B and H represent the relative coordinates of the center of mass with respect of the rotation point that is considered, moreover the true inertia momentum must be considered; it is worth noting that in the only case of a symmetric body the values of B ad H correspond to the half-base and the half-height of the body.

For this reason, considering the oscillation motion two different conditions can be written: the first one about the rotation point O and the second one about the rotation point O'; these two equations consider respectively two values of B: B_{min} and B_{max}= B - B_{min}. This consideration allows to extend the afore described formulas for the symmetric body as long as it is considered B = B_{min}, hence the minimum distance between the projection of the center of mass on the base and the edge of the base itself. It must be underlined that Shenton's formulas are valid for rectangular bodies and they have to be properly re evaluated for non symmetric blocks taking into account the real inertia moment.

3.6.1.2.2 Overturning

In case of non symmetric bodies the definition of critical velocity V_c that governs the overturning, and as a consequence the limit velocity V*, must be reconsidered by taking into account the real inertia moment about the rotation point. A possible solution that allows to apply, at least from a theoretical point of view, that simple formulation to slender non symmetric bodies, is to assume an equivalent height of the body H' and refer to it as it is described in the following.

From the critical velocity $V_c^2 = \frac{g}{H} \cdot \frac{I_r}{m} \cdot \theta_c^2$ with $\theta_c = B/H$ it is set:

$$\frac{g}{H} \cdot \frac{I_r}{m} \cdot \theta_c^2 = \frac{4}{3} \cdot g \cdot B \cdot \theta_c' \tag{3.51}$$

where $\theta_c' = B/H'$

two equivalent expressions are obtained from this:

$$H' = \frac{4}{3} \cdot H^3 \cdot \frac{m}{I_r} \tag{3.52}$$

$$H' = \frac{4}{3} \cdot \frac{H^3}{(i^2 + r^2)} \tag{3.53}$$

$$V < V^* = 14.46 \cdot \frac{B}{\sqrt{H}} \tag{3.54}$$

considering the value of H' instead of H, the formula for critical velocity can be applied. It becomes:

$$V < V^* = 14.46 \cdot \frac{B}{\sqrt{H'}} \tag{3.55}$$

An important observation is that this equivalent height H' can be used only for the purpose of overturning evaluations, because a change of the height implies a change of the ratio B/H, which is fundamental for the definition of the oscillation phenomenon. Alternatively Boroschek (18) proposed to take into account eccentricity due to non symmetry, by means of a reduction of the coefficient introduced by Ishyiama. He suggested to evaluate critical velocity for bodies with eccentricity higher than 30% of the total base length:

$$V^* < 0.2 \cdot V_c \tag{3.56}$$

3.6.1.2.3 Presence of vertical action

One of the basic assumptions of what has been described so far in terms of dynamic of the rigid body is the absence of a vertical input acting at the same time as the horizontal one. The most of works available from literature take this same assumption and it can be considered reasonable also considering that several other assumptions are made in order to make this problem simpler for practical applications. However it is worth noting that a more detailed level of analyses is somehow possible, including in the theoretical study the presence of the vertical action. An example was given by Tung (20) who included the vertical action in Shenton's work.

Assumptions taken for this extension are the same for the description of Shenton's model, the object is once again a rectangular and symmetric rigid body, as depicted in Figure 3.6:

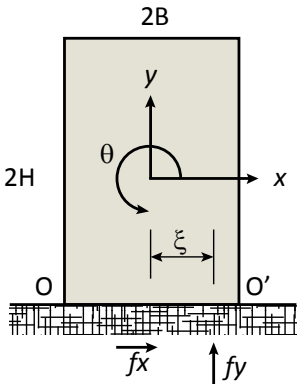

Figure 3.6 - Rigid body model, rocking

The horizontal force between the block and the floor f_x is governed by Coulomb's friction law, the value of the static and dynamic friction coefficients can be assumed the same and equal to μ. The vertical reaction f_y, acts at distance ξ from the vertical projection of the center of mass on the base. The acceleration induced by the earthquake is defined as $\ddot{x}_g$along the x direction, and as $\ddot{y}_g$ along the y direction, which is assumed positive when directed upwards.

3.6.1.2.4 Rest

The equation that describes the rest condition along the horizontal direction is the same as for the case of absence of vertical acceleration:

$$\mathrm{m} \cdot \ddot{\mathrm{x}}_{\mathrm{g}} = \mathrm{f}_{\mathrm{x}} \tag{3.57}$$

instead along the vertical direction the term including the vertical ground acceleration is included $m \cdot \ddot{y}_g$:

$$\mathrm{m} \cdot \ddot{\mathrm{y}}_{\mathrm{g}} = \mathrm{f}_{\mathrm{y}} - \mathrm{m} \cdot \mathrm{g} \tag{3.58}$$

the conditions that must be satisfied for a rest situation are:

$$\mathrm{f}_{\mathrm{y}} > 0 \text{ to avoid any uplift;} \tag{3.59}$$

the condition

$$\mathrm{f}_{\mathrm{y}} = \mathrm{m} \cdot (\ddot{\mathrm{y}}_{\mathrm{b}} + \mathrm{g}) = \mathrm{m} \cdot \mathrm{Y} > 0 \tag{3.60}$$

where Y is introduced. It is worth noting that $Y > 0$ means $\ddot{y}_b > -g$: as long as the value of the vertical acceleration does not exceed that of the gravity there can't be any uplift phenomenon.

$|\xi| \leq B$ in order to have the sum of the reactions is within the base; since $|\xi| = \left|\frac{f_x \cdot H}{f_y}\right| = \left|\frac{\ddot{x}_g}{g+\ddot{y}_g}\right| \cdot H$, from the definition of

$$\left|\frac{\ddot{x}_g}{g+\ddot{y}_g}\right| = \left|\frac{X}{Y}\right| = |Z|, \tag{3.61}$$

the condition

$$|Z| \leq \frac{B}{H} = \frac{1}{\gamma} \tag{3.62}$$

results.

$$|f_x| \leq \mu \cdot |f_y| \tag{3.63}$$

To assure that the friction coefficient is high enough to avoid sliding; from this limit the condition $|Z| \leq \mu$ is obtained.

3.6.1.2.5 Sliding

The governing equations for the motion are:

$$-\mu \cdot S(\dot{x}) \cdot f_y = \pm \mu \cdot f_y = f_x = m \cdot (\ddot{x} + \ddot{x}_g) \quad (3.64)$$

$$m \cdot \ddot{y}_g = f_y - m \cdot g \quad (3.65)$$

Conditions for a motion of translation are:

$$f_y > 0 \quad (3.66)$$

from which $Y > 0$ results.

$$|\xi| \leq B \quad (3.67)$$

Since $|\xi| = \left|\frac{\pm\mu \cdot f_y}{f_y}\right| \cdot H = \mu \cdot H$, the condition:

$$\mu \leq \frac{B}{H} = \frac{1}{\gamma} \text{ is obtained.} \quad (3.68)$$

Moreover, from a rest condition the following situations are possible :

$$f_x = \mu \cdot f_y > 0 \text{ (when } \dot{x} < 0 \text{ and hence } \ddot{x} < 0) \quad (3.69)$$

therefore, since $\mu \cdot m \cdot (\ddot{y}_g + g) = m \cdot (\ddot{x} + \ddot{x}_g)$ as well as $\ddot{x} = \mu \cdot Y - X = Y \cdot (\mu - Z)$, from $\ddot{x} < 0$ the condition $Z \geq \mu$,

which is valid when $Z > 0$ is derived;

$$f_x = -\mu \cdot f_y < 0 \text{ (when } \dot{x} > 0 \text{ and hence } \ddot{x} > 0) \quad (3.70)$$

therefore since $\ddot{x} = -\mu \cdot Y - X = -Y \cdot (\mu + Z)$, from $\ddot{x} > 0$ the condition $Z \leq -\mu$ is obtained, which is valid when $Z < 0$. Indeed Z can be negative, although $Y > 0$, this happens when $X < 0$.

3.6.1.2.6 Oscillation

Since the motion of rotation and oscillation in general is not restrained to the assumption of Y > 0 it is useful to divide the case in which Y > 0 from that in which Y < 0. Since the problem is still symmetric all the consideration will be referred to the rotation point O, but they can easily be extended to the rocking point O', in the following considerations will be referred to the case Y > 0 and rocking about point O., the governing equations are:

along x: $$m \cdot (\ddot{x} + \ddot{x}_g) = f_x \quad (3.71)$$

where the relative acceleration $\ddot{x} = -H \cdot \ddot{\theta}$ is given only by the rotation (of the center of mass), since it is a pure rotation situation.

along y: $$m \cdot (\ddot{y} + \ddot{y}_g) = f_y - m \cdot g \quad (3.72)$$

where the vertical relative acceleration $\ddot{y} = B \cdot \ddot{\theta}$ is given only by the rotation (of the center of mass), and the vertical component of the seismic acceleration $\ddot{y}_g$ is the only difference from Shenton's work.

along z: $$f_x \cdot H - f_y \cdot B = I \cdot \ddot{\theta} \quad (3.73)$$

where I is the inertia moment of the rectangle about the central axis $I = \frac{m}{3} \cdot (H^2 + B^2)$.

For the case of a rectangular body previous equation can be written as:

along x: $$f_x = \frac{m \cdot (a \cdot X + b \cdot Y)}{4 \cdot (1 + \gamma^2)} = \frac{m \cdot Y \cdot (a \cdot Z + b)}{4 \cdot (1 + \gamma^2)} \quad (3.74)$$

along y: $$f_y = \frac{m \cdot (b \cdot X + d \cdot Y)}{4 \cdot (1 + \gamma^2)} = \frac{m \cdot Y \cdot (b \cdot Z + d)}{4 \cdot (1 + \gamma^2)} \quad (3.75)$$

along z: $$\ddot{\theta} = \frac{3 \cdot (\gamma \cdot X - Y)}{4 \cdot B \cdot (1 + \gamma^2)} = \frac{3 \cdot Y \cdot (\gamma \cdot Z - 1)}{4 \cdot B \cdot (1 + \gamma^2)} \quad (3.76)$$

where the usual ratio $\gamma = H/B$ is used and $a = 4 + \gamma^2$, $b = 3 \cdot \gamma$ and $d = 1 + 4 \cdot \gamma^2$are defined.

The conditions for a rocking motion about the point O, with $Y > 0$, are:

$$\ddot{\theta} > 0 \quad (3.77)$$

then it has to be $\gamma \cdot Z - 1 \geq 0$, from which $Z \geq \frac{1}{\gamma}$ then once again $Z = \frac{1}{\gamma}$;it is worth noting that, in order to fulfill this condition it has to be $Z > 0$.

$$f_y > 0 \quad (3.78)$$

then it has to be $b \cdot Z + d > 0$, from which $Z > -\frac{d}{b}$; despite this, since it has to be $Z > 0$ this latest condition is not relevant.

$$|f_x| \leq \mu \cdot |f_y| \quad (3.79)$$

this condition assures that sliding and rocking do not happen at the same time;

From (3.92), that is $\left|\frac{m \cdot Y \cdot (a \cdot Z + b)}{4 \cdot (1+\gamma^2)} \cdot \frac{4 \cdot (1+\gamma^2)}{m \cdot Y \cdot (b \cdot Z + d)}\right| \leq \mu$, the result $\mu \geq \frac{a \cdot Z + b}{b \cdot Z + d} = \mu^*$is obtained;

value of $\mu^*$is : $1/\gamma$ when $Z = 1/\gamma$;

- goes to a/b when Z goes to $+\infty$;
- 0 when $Z = -b/a$;
- goes to $-\infty$ when $Z = -d/$.

In case of rotation about O' similar results can be found, the conditions for rocking about the point O', with Y > 0 become:

$$Z < 1/\gamma; \quad (3.80)$$

$$\mu \geq \frac{-a \cdot Z + b}{-b \cdot Z + d} = \mu^* \quad (3.81)$$

The description of rocking phenomenon in presence of vertical action can be applied also for application to bodies with non symmetric features; indeed it can be considered the difference between the distance from the center of mass to each rocking point. Furthermore, in terms of the application of static formulas the studied condition is, in general, the worst of the two.

Conditions governing sliding-rocking motion can be found in Tung (20). The case describing Y < 0 is not presented in this dissertation, the reader is referred to Tung (20) for all the details.

3.6.2 Rigid body models response – time history integration approach (check on LS results and LA approach)

3.6.2.1 General Considerations

A different and more precise approach for evaluating the dynamic response of rigid bodies is the integration of the equations of motion, to describe the behavior of a block under the action of a ground movement. This approach can be used both as a feedback for the results obtained with the simplified formulas of the LS level and as a tool for further and more refined analyses on single specific rigid blocks or for probabilistic evaluations. In particular attention was focused on the two main phenomena of rocking and overturning which are related, as stated before, with two important limit states, the Artistic Limit State and the Ultimate Limit State. In line with these first considerations this paragraph aims to present the general theoretical approach to the integration of the equations of rocking motion, keeping focus on different steps of detail that can be included in the formulation and to their effects on the general outcome.

It is worth noting that the problem of oscillation of rigid bodies was widely discussed during years, with the application of different approaches: deterministic, probabilistic and stochastic. The interest on this topic has always been high also considering the wide choice of possible applications it has; this work does not aim to investigate different solutions or to find out new approaches to the numerical solution of the equations of rocking but instead it aims to develop a numerical tool to deal with the problem of seismic vulnerability assessment on art objects when considering them as rigid non anchored blocks.

As stated before, the different levels of evaluation and complexity that are used in this methodology, need to include in the calculations features of the object and of the input that must be considered with particular attention in the dynamic approach to the solution. In particular these features concern the non symmetry of the body and the presence of vertical accelerations. Considering the fact that, from a detailed literature review, a wide number of works dealing with this topic were found, and considering also that only some of them give a theoretical description of the problem with both non symmetry and vertical action acting at the same time (21), an important aspect of this study is the integration of the equations of motion including effects non symmetry and vertical acceleration together.

3.6.2.2 Equations of motion: rocking formulation

The mathematical model presented in this dissertation is aimed in particular to calculate the rocking dynamic response, including the possibility of overturning, of a rigid body under the effect of a seismic (or generic) base input. The presented description refers to the work of Purvance (22). Who considered rocking phenomenon for a non symmetric body; vertical action effect, which was not considered in the afore mentioned work is then introduced in this dissertation. This model corresponds to the physical model depicted in Figure 3.7 which represents a rectangular 2-D block.

Figure 3.7 - rocking body

The assumptions made for the solution include: non symmetric block, block and floor rigidity, perfectly inelastic impact (no bouncing is allowed), sufficiently high friction to inhibit sliding, momentum conservation impact, horizontal base, the block never loses contact with the base. The following description refers to the general case of a non symmetric rigid body.

The first step towards an investigation of the overturning response is to derive the equations of motion that govern the problem. All the following consideration will be referred to the 2 - D model depicted in Figure 3.7 .

W is the weight vector;

R_i is the vector connecting the center of mass to the rocking point;

α_i is the angle between the vectors W and R_i, when the body is in its rest condition;

θ is the rotation angle around the rocking point.

Assuming also that there are only two different rocking points RP_1 and RP_2 the sign convention $\theta > 0$ when rocking about RP_1 and $\theta < 0$ when rocking about RP_2 is taken. When the body is rotated to the angle θ about RP_1 by the force F acting horizontally through the center of mass, the restoring moment is M = W R_1 sin(α_1-θ). The equation of free rocking about RP_1 is:

$$I_1\ddot{\theta} = -WR_1 sin(\alpha_1 - \theta) = -mgR_1 sin(\alpha_1 - \theta), with\ \theta > 0 \quad (3.82)$$

where I_1 is the moment of inertia about RP_1. Similarly free rocking around RP_2 is given by

$$I_2\ddot{\theta} = -WR_2 sin(-\alpha_2 - \theta) = -mgR_2 sin(-\alpha_2 - \theta), with\ \theta < 0 \quad (3.83)$$

It is worth noting that none of these two equations is applicable when the rotation $\theta = 0$, which is the instant of impact. This is a critical point of the problem and it will be given proper importance in the following. So far only a condition of free oscillation has been described: when a horizontal acceleration is provided to the system, by means of a ground motion (assume $a_g^x(t) < 0$), rocking initiates about RP_1. Considering the contribution of this horizontal acceleration leads to the equation of motion subjected to an input:

$$\ddot{\theta}\, I_1 + mg\, R_1\ sin(\alpha_1 - \theta) = -m\ddot{u}_g R_1 cos(\alpha_1 - \theta) \quad (3.84)$$

$$\ddot{\theta}\, I_2 + mg\, R_2\, sin(-\alpha_2 - \theta) = -m\ddot{u}_g R_2 cos(-\alpha_2 - \theta) \quad (3.85)$$

Initiation of rocking motion begins from a quiescent condition, with $\theta = 0\ and\ \ddot{\theta} = 0$ yielding to the definition of a criterion for individuating the initiation of rocking. Indeed, as it was mentioned before, the governing equations are not valid when the rotation angle is zero. The two criteria applied in this study are:

$$a_g{}^x(t) \leq -g\ tan\ (\alpha_1) \quad (3.86)$$

$$a_g{}^x(t) \geq g\ tan\ (\alpha_2) \quad (3.87)$$

it is interesting noting that these two criteria reduce to West's formula in case of a symmetric body.

Once the equations are defined in case of non symmetric body, the further step of generalization is the inclusion of the vertical action $\ddot{y}_g$ (vertical action is considered positive when oriented upwards); in order to generalize the governing equation a further assumption needs to be made, about the vertical action: the vertical acceleration must not exceed the acceleration of gravity for keeping the object in contact to the ground, avoiding the "free flight " condition. The governing equations then become:

$$\ddot{\theta}\, I_1 + m(g + \ddot{y}_g)\, R_1\ sin(\alpha_1 - \theta) = -m\ddot{u}_g R_1 cos(\alpha_1 - \theta) \quad (3.88)$$

$$\ddot{\theta}\, I_2 + m(g + \ddot{y}_g)\, R_2\, sin(-\alpha_2 - \theta) = -m\ddot{u}_g R_2 cos(-\alpha_2 - \theta) \quad (3.89)$$

The vertical acceleration appears as a variation on the gravity acceleration, which has effect (stabilizing or unstabilzing, according to its sign) on the restoring moment from which the condition of equilibrium is evaluated from. Furthermore it affects the triggering conditions of rocking which become:

$$a_g{}^x(t) \leq -(g + \ddot{y}_g)\tan(\alpha_1) \quad (3.90)$$

$$a_g{}^x(t) \geq (g + \ddot{y}_g)\tan(\alpha_2) \quad (3.91)$$

Which correspond to the relation proposed by Tung (20)

3.6.2.3 Inelastic impact and restitution coefficient

As it was just described, the problem is governed by two independent equations that define two different phases of motion, for positive and for negative rotation angles. This means that the problem is discontinuous and, one of the most significant aspects of the solution, is how to deal with the switching between the first equation and the second and vice versa. The most diffused method is the one that applies conservation of angular momentum, to provide connection between equation (3.84) and equation (3.85) when θ = 0; the velocities before and after the impact are defined as $\dot{\theta}(t_0 - \delta t)$ and $\dot{\theta}(t_0 + \delta t)$. Several authors worked on this point and proposed numerous different approaches for the evaluation of a coefficient, capable to describe the behavior of the body around the instant of impact, namely "coefficient of restitution". A general definition of this coefficient, independent from the shape of the object, is defined in the work of Purvance (22), who gives the following relation for the ratio between the velocities at two in instants immediately before and after the impact:

$$\dot{\theta}(t_0 - \delta t)(I_1 - mR_1\sin(\alpha_1)(R_1\sin\alpha_1 + R_2\sin\alpha_2) = I_2\,\dot{\theta}(t_0 + \delta t) \quad (3.92)$$

For the case of impact about RP_2 this ratio is given by:

$$e_2 = \frac{\dot{\theta}(t_0 + \delta t)}{\dot{\theta}(t_0 - \delta t)} = 1/I_2[(I_1 - mR_1\sin(\alpha_1)(R_1\sin\alpha_1 + R_2\sin\alpha_2)] \quad (3.93)$$

Housner (15) and Chopra (7) assumed that the transition from one rocking point to the other happens smoothly , i.e. inelastically, and with angular momentum conservation, they proposed the following definition of the "coefficient of restitution" for rectangular bodies:

$$e = 1 - \frac{3}{2}sin^2\alpha \quad (3.94)$$

Both the authors evaluated the energy lost in the impact by means of the ratio between the kinetic energy after and before the impact. Hence the energy loss due to impact is 1-r = 1-e^2. The higher is the coefficient of restitution the smaller the inelastic energy loss.

The relation (3.78) considering a rectangular body, gives as a result (3.80). It is worth noting that r_i depends only on geometrical parameters of the block. In the graph (Figure 3.8) the behavior of the restitution coefficient is given for rectangular bodies with different slenderness coefficients (Chopra, (7)).

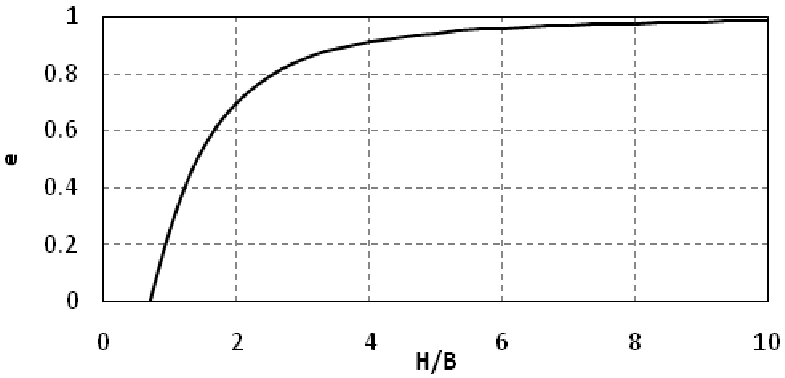

Figure 3.8 - variation of the coefficient of restitution

For slenderness values higher than 4 (which is close, as it will be shown in the following, to those concerning the case study) the value of the coefficient is higher than 0.9 and it increases up to 1 (elastic impact) with the increasing slenderness of the considered object. In this dissertation the relation (3.93) is used to evaluate the energy dissipated in the impact.

It is worth noting that this aspect of the integration of the equations of motion is particularly delicate and it opens up a wide topic which is still argument of discussion among the scientific community; it is hence beyond the purpose of this work to discuss this aspect in detail but it is important to understand how it affects the results of the analyses tool developed and used in this work.

3.6.2.4 Numerical solution to the equations:

Equations (3.78) and (3.79) are non linear and discontinuous so they require the use of numerical integration techniques; the solution was sought via the 4th order Runge Kutta method, implemented in the Matlab ODE solver (23): the solution initiates when either the condition (3.86) or (3.87) is satisfied; assuming the rocking phenomenon initiates about the point RP_1, the response before the instant t_i is characterized by $\theta = 0$; solution is calculated until either tilting or impact occurs. In case impact occurs the velocity needs to be reduced of the value of the restitution coefficient and the governing equation is switched. The process of rocking, restitution and switching is calculated as long as the phenomenon ceases or overturning is experienced. Furthermore a criterion for the definition of the overturning must be set: in this work the limit $|\theta| \geq |\alpha_C|$ is chosen.

Different assumptions and choices need to be taken in the solution of this problem; the first choice that was made was about the level of approximation: the governing equations indeed can be considered with different levels of approximation of the nonlinear part; trigonometric functions can be approximated either linearly or with a properly stopped expansion in series, or they can also be treated as non linear. Linearization is possible when the body is slender enough to approximate the sine of the critical angle with the angle itself and also when the rotation angle keeps in the small displacements field. Two levels of approximation were tested and compared with the non linear solution. The first approximation, named "linear" in the following, is described in (3.95) and (3.96):

$$\ddot{\theta}\, I_1 + mg\, R_1(\alpha_1 - \theta) = -m\ddot{u}_g R_1 \tag{3.95}$$

$$\ddot{\theta}\, I_2 + mg\, R_2(-\alpha_2 - \theta) = -m\ddot{u}_g R_2 \tag{3.96}$$

The second level of approximation , named "approximated" in the following, handles the trigonometric part of the governing equation with their series expansions, arrested at the second order, as it is shown in (3.97) and (3.98).

$$\ddot{\theta}\, I_1 + mg\, R_1(\alpha_1 - \theta) = -m\ddot{u}_g R_1\left(1 - \frac{(\alpha_1 - \theta)^2}{2}\right) \tag{3.97}$$

$$\ddot{\theta}\, I_2 + mg\, R_2(-\alpha_2 - \theta) = -mgR_2\left(1 - \frac{(-\alpha_2 - \theta)^2}{2}\right) \tag{3.98}$$

The graphs depicted in Figure 3.9 show the behavior of rectangular bodies under the effect of a sinusoidal input, applying the three different levels of approximation described above. The following charts represent the response of the six different rectangular bodies to the same horizontal input , the horizontal axis shows the time, while vertical axis shows the ratio between the value of the rotation angle θ and the critical angle α , which is the threshold over which the body can be considered tilted. When the ratio reaches the value of 1 the body experienced overturning.

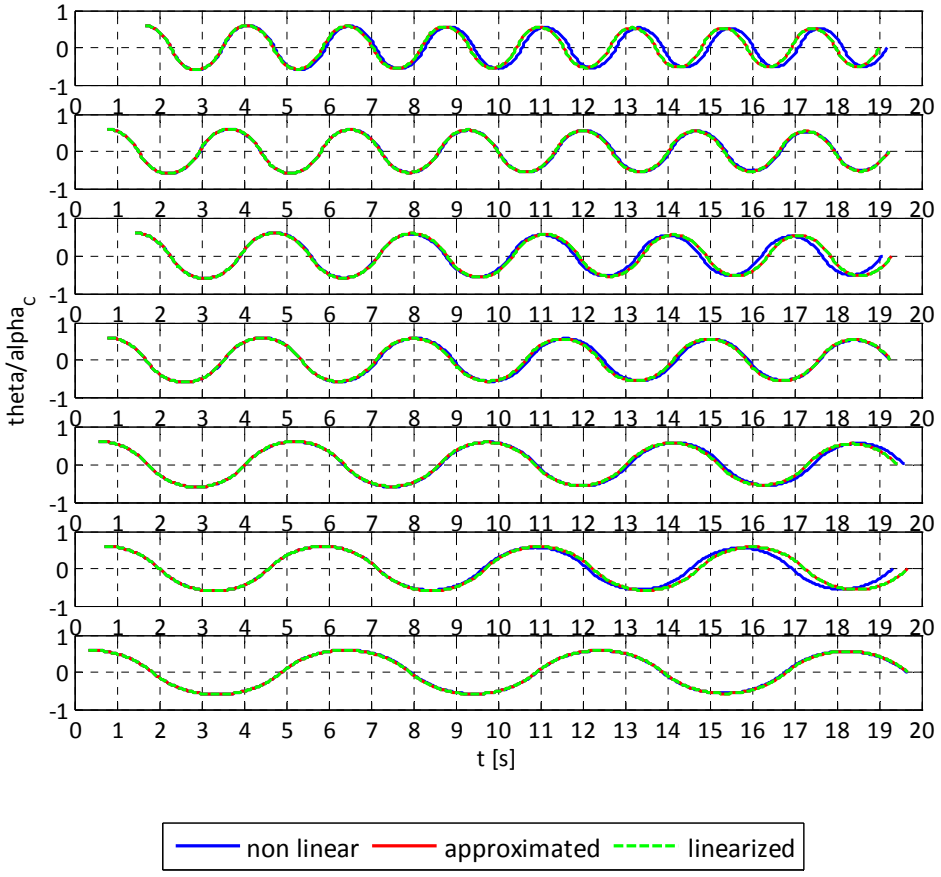

Figure 3.9 - comparison between different levels of approximation

The graphs depicted above describe the free oscillation motion of rectangular rigid bodies with increasing slenderness, λ =2, 3, 4, 5, 8, 10 and 14, evaluated with the different levels of approximation described before; it is worth noting that, the difference between the three solutions decreases when the slenderness increases, this means that, as long as the body is slender the different approximations give reliable results. However when an horizontal earthquake input is applied the difference is more evident, as shown in Figure 3.10

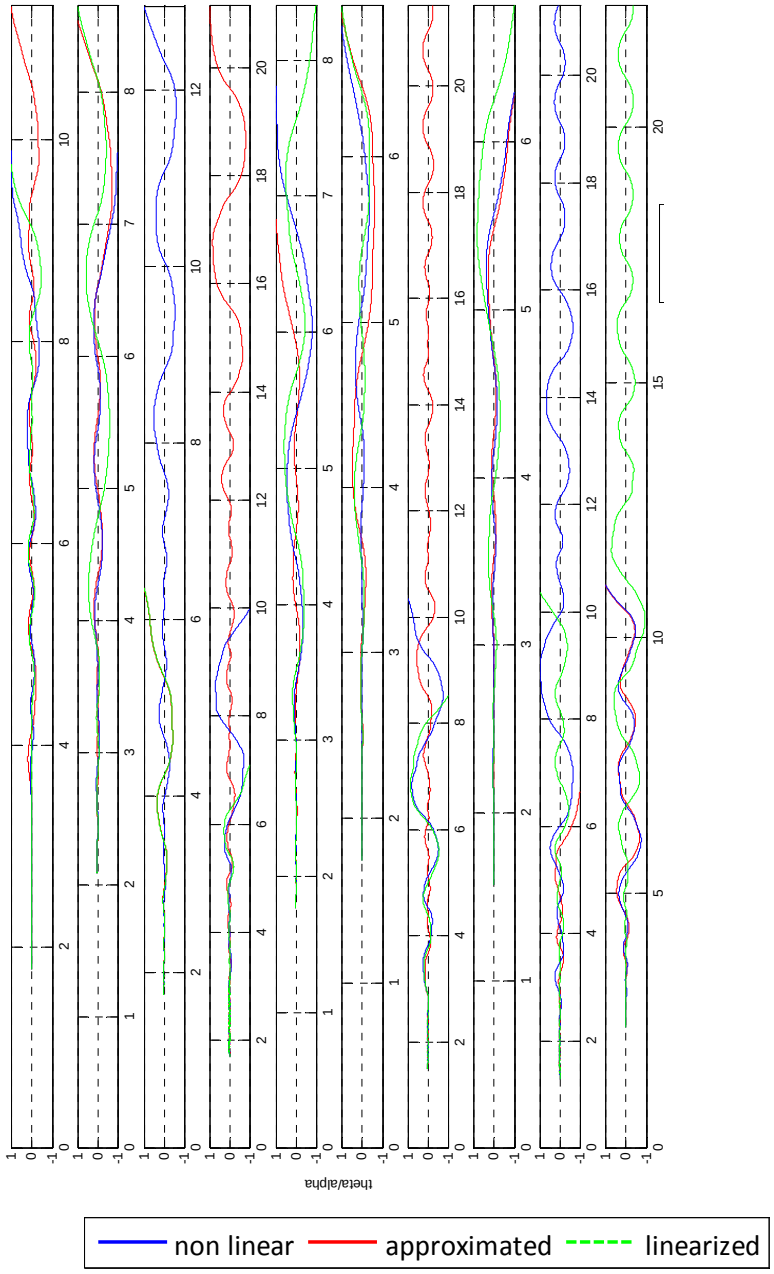

Figure 3.10 - symmetric rigid body response to earthquake input

More analyses were carried out to study the different approaches to the solution, considering also different inputs. Indeed in Figure 3.10 the response of a rigid body of given slenderness to different generated earthquakes is given: the ten time histories presented describe the behavior of the same rectangular body under the effect of ten different earthquakes, the assumption of elastic behavior was also made, so there is no dissipation of energy in the impact (e = 1). This case is more complicated by the type of input : it is not a free oscillation problem anymore, but a problem that applies as a forcing function a seismic signal; it can be pointed out that the increasing of the precision of the approach from the linear to the quadratic one does not generally imply a behavior closer to the non linear approach.

After a series of sensitivity analyses to compare the different outcomes of these three possible solutions to the problem, according to the slenderness of the body and to the calculation time, the conclusion was to use the fully non linear equations, since they give more precise results also for small slenderness ratios, moreover since overturning phenomenon is going to be analyzed it cannot be assumed a small rotations regime, therefore the choice for the non linear approach seemed to be the most proper.

Concerning the numerical solution different numerical schemes were also tested in order to understand the best approach for a reliable and reasonably quick solution of the problem. The comparison was carried out for the linearized equations between the method of Newmark and a Runge – Kutta of the fourth order with constant time step, and the variable time step Runge Kutta method available in Matlab. The choice, comparing the quality of the results and the time of calculation was for variable timestep Runge – Kutta method of the IV order, which is implemented in Matlab, in the built-in function for the solution of ordinary differential equations, *ODE45* (23). It is also worth noting that several previous works reviewed in literature ((7), (22)) about this topic were developed with the same numerical tool.

3.6.2.5 Numerical issues in the integration

3.6.2.5.1 Accuracy in the determination of the impact instant

The accuracy in the determination of dynamic conditions around the instant of impact are a fundamental aspect for the quality of the result; indeed the phenomenon of impact with the related energy dissipation that is connected to it, can seriously affect the response. As it was mentioned before the energy dissipation is taken into account by means of the coefficient of restitution, applied to the angular velocity for the conservation of the angular momentum. The numerical procedure is implemented to research the time instant in which the rotation is lower than a fixed tolerance, then it evaluates the angular velocity at the same instant, by means of a linear interpolation between the immediately after and immediately before the solution with elastic impact. After this the evaluated velocity is multiplied by the coefficient of restitution and taken as the initial condition for the equation for rotations about the opposite rocking point, it is also assumed that the initial rotation is zero.

The value of the tolerance assumed was chosen considering some sensitivity analyses, performed by varying the numerical value of the tolerance. Tests presented in Figure 3.11 represent the integration of the free oscillations for a rigid body with dimensions B = 0.3 m and H = 1.36 m, that are the dimensions of the symmetric equivalent block for the statue of San Matteo. The values of tolerance tested are *toll* = 10^{-5}, *toll* = 10^{-10}, *toll* = 10^{-15}, *toll* = 10^{-20}.

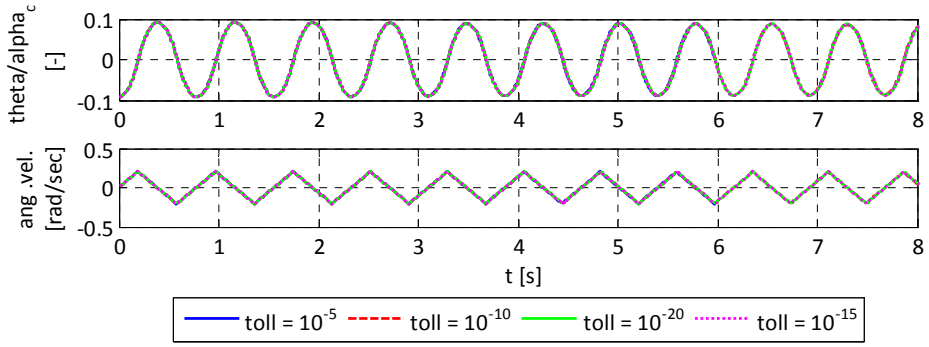

Figure 3.11 - sensitivity for tolerance, rotations and angular velocity

Results show that with tolerance lower than *toll* = 10^{-5} the response does not show differences neither from the point of view of the rotation nor from the point of view of angular velocity. A value of tolerance *toll* = 10^{-10} is assumed for the analyses.

3.6.2.5.2 Damping

Numerical integration is always conditioned by effects of numerical damping; moreover, the discontinuity of the problem, given by the two different equations that govern the rocking around the two points, and the inclusion of the impact phenomenon (even when the restitution coefficient is set equal to 1) can introduce some phenomena of dissipation that can affect the results. The following benchmark shows the results of free oscillations for a rigid rectangular body with B = 0.3 m and H = 1.36 m, with a restitution coefficient e = 1, which represents a perfectly elastic impact and tolerance *toll* = 10^{-10}.

The amplitude of the response is underlined in Figure 3.13 and a small reduction over time is visible, but when its variation is considered (in percentage), as depicted in Figure 3.14, it is confirmed that the difference of each peak (when compared to the initial condition on rotation, θ_0 =-0.02 rad) varies between 0.0 % and 0.6 %. This means that the effect of numerical damping can be neglected in the application of this tool. As a further confirmation of this concept also the period of the response is investigated: Figure 3.15 shows the half period measured between two following

peaks (positive and negative) , the average value is T/2 = 0.774 s without any visible variation from it. The conclusion of this brief but important benchmark is that, although a numerical damping is present, its presence has no relevant effects on the dynamic response of the system.

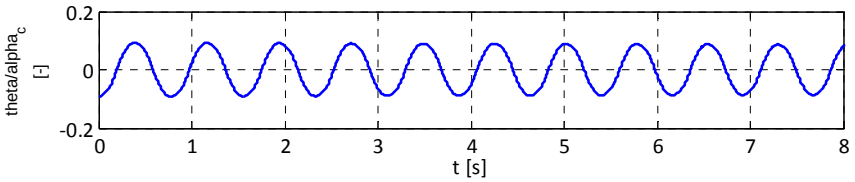

Figure 3.12 - free oscillations for a rectangular body

The graph depicted in Figure 3.12 does not show an evident presence of damping connected to numerical problems:

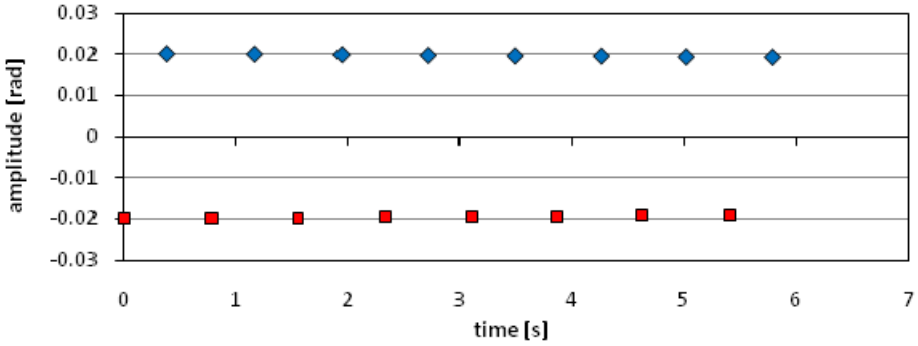

Figure 3.13 - amplitude of oscillation peaks

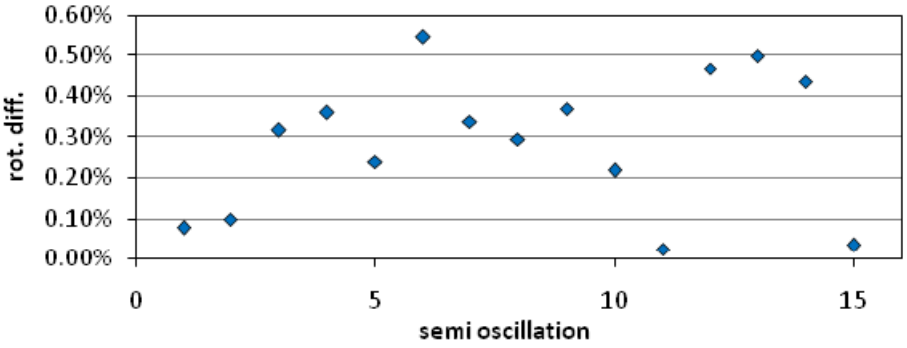

Figure 3.14 - variation in rotations

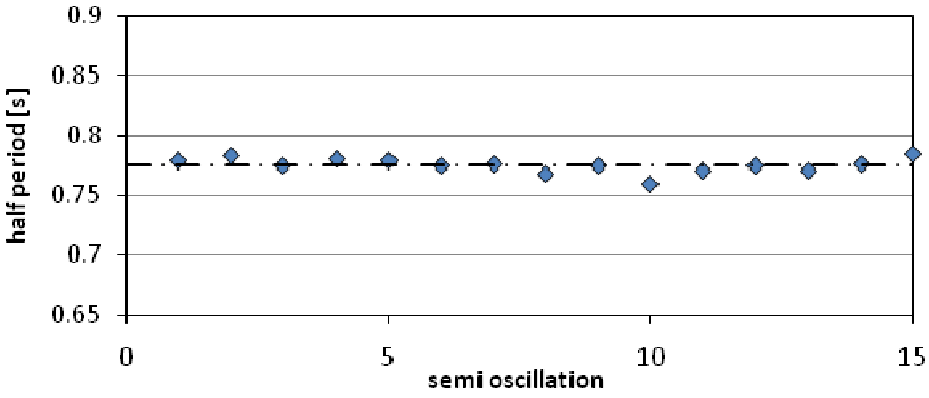

Figure 3.15 - period of the response

3.6.2.6 Validation Tests

A first application of the program was aimed to reproduce some of the examples reported by literature, in order to obtain a feedback about the results that come out from the application of this method. It must be taken into account though, that the number of variables that are involved is very high and it is not always possible to obtain the same exact condition of the reference that is used as comparison; hence the target of these first analyses is to obtain a result in accordance with it and to pinpoint the cause of the possible differences.

3.6.2.6.1 Benchmark 1

Firstly numerical tests perfomed by Chopra (7) in a work about dynamic response of rigid bodies were reproduced with the Matlab Code. This benchmark aims to validate the developed program, and also to show how the above mentioned levels of approximation for the governing equations can affect the results.

In this work a series of rigid rectangular blocks were studied under the action of a simple ground acceleration of one and half cycle of triangular shape (Figure 3.16). Geometrical features of the blocks were selected to obtain increasing slenderness, keeping constant the value of the distance between the center of mass and the rocking points (R). The bodies are considered symmetric and the coefficient of restitution e is assumed constant e =0.925.

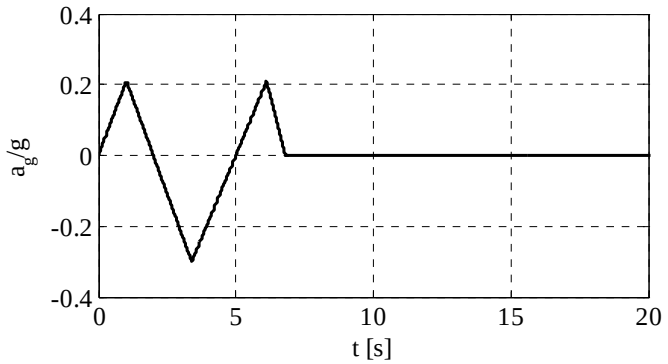

Figure 3.16 - input ground motion

The problem is solved applying three different levels of approximation for the solution of the two equations as already mentioned before. The two equations were linearized at two different levels of detail: the first one considers the rotation angle θ small enough to approximate the cosine and the sine function with the value 1, the second one instead, uses an approximation considering the Taylor series of the cosine up to the term of second order (3.97) and (3.98); the third takes into account the fully non linear equations. It is clear that the approximation is more precise the higher is the slenderness of the body is high. Characteristics of the bodies considered in the example are summarized in Table 3.1

H/B	H [ft]	B [ft]	R [ft]	H [m]	B [m]	R [m]	b [m]	H_g [m]
4	19.402	4.850	10	5.913	1.478	3.048	0.739	2.956
4.2	19.456	4.632	10	5.930	1.411	3.048	0.705	2.965
4.3	19.480	4.530	10	5.937	1.380	3.048	0.690	2.968
4.31	19.482	4.520	10	5.938	1.377	3.048	0.688	2.969
4.33	19.487	4.500	10	5.939	1.371	3.048	0.685	2.969
4.5	19.523	4.338	10	5.950	1.322	3.048	0.661	2.975
5	19.611	3.922	10	5.977	1.195	3.048	0.597	2.988

Table 3.1 – characteristic of the bodies studied in the benchmark

This consideration can also be interpreted from a limit state point of view: when a rocking phenomenon is pointed out then the Artistic Limit State was exceeded, instead when the check parameter θ/α reaches the value of 1 the Ultimate Limit State is exceeded.

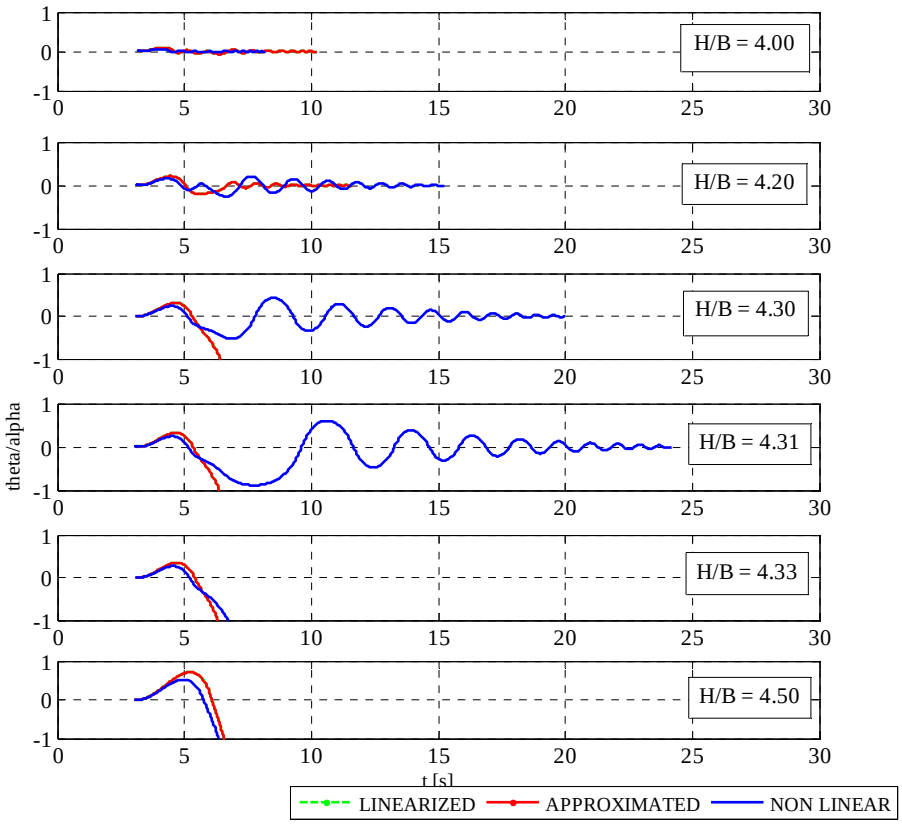

Figure 3.17 - dynamic responses of symmetric rectangular rigid bodies with increasing slenderness

It can be observed that the two levels of approximation give results that are perfectly overlapped, the detail level of the results is the same; this means that choosing one criterion above the other is not worth. On the other hand it is interesting to note that the gap between the non linear solution and the two approximated ones is important, because when the amplitude of oscillations is low (H/B = 4 and H/B = 4.2) the different solutions give slightly different responses in terms of amplitude of rotation: in H/B = 4.20, for instance, the dashed line shows a wide second oscillation, while the solid line has a quick change of rocking point this observation is important if connected with the concept that rocking, as ALS exceeding, causes a damage to the object; when the oscillations become wider the approximated solutions show overturning from slenderness H/B = 4.3 on, while the non linear solution describes fully developed rocking motions, without overturning until H/B = 4.31. The two events that produce overturning for both solutions give slightly different results as well. These results also show, as expected, that the non linear approach gives more “resistance storage”.

If the results of non linear solution are compared to those provided by Chopra a good accordance is found; this result agrees with the expectations:

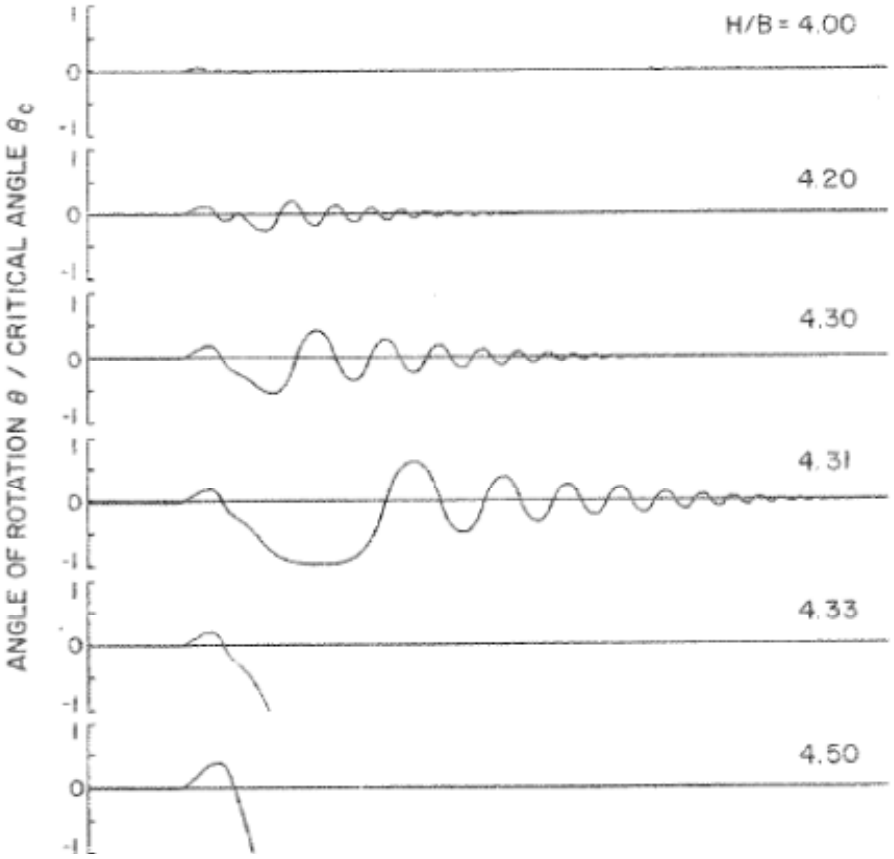

Figure 3.18 - - dynamic responses presented by Yim and Chopra in (7)

3.6.2.6.2 Benchmark 2

The numerical approach to the solution of the rocking equations was also tested with a further example from literature: Makris et al. (24) in 2006, in the context of a wider study on historical goods, considered a multidrum classical column under the effect of a seismic action. One of the parts of this work considered the column, which is actually made of more drums overlapped, as a whole rigid body in order to study its dynamic response under different recorded earthquakes. The governing equations are the same as described above 3.6.2.2, the reference problem is solved considering the two non linear equations, one for each rocking point, merged in one single equation containing the "sign" function: this is one of the possible solutions to this problem which makes the two approaches slightly different, this means that the expected results cannot always perfectly fit the reference example. The object tested by Makris is sketched in Figure 3.19 it is worth noting that several assumptions were made for the solution of this problem: first of all the shape of the body is considered planar with average section equal to the maximum transversal section of the column, which in reality is circular.

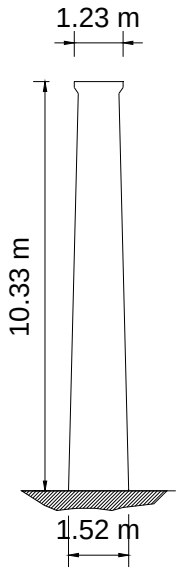

Volume [m^3]	18.681
Volume centroid [m]	0.76, 0.76, 4.707
Volume moments of inertia about world coordinate axes	
I_x:	590.659
I_y:	590.659
I_z:	27.343
Radii of gyration about world coordinate axes	
R_x:	5.622
R_y:	5.622
R_z:	1.209
Moments of inertia about centroid coordinate axes	
I_x:	165.879
I_y:	165.879
I_z:	5.7633
Radii of gyration about centroid coordinate axes	
R_x:	2.979
R_y:	2.979
$R_{z:}$	0.555

Figure 3.19 - Column object of study

Details given in table of Figure 3.19 summarize the geometrical characteristics of the maximum transverse section of the column that are used as input to simulate the dynamic response.

The column was tested considering five different recorded inputs :

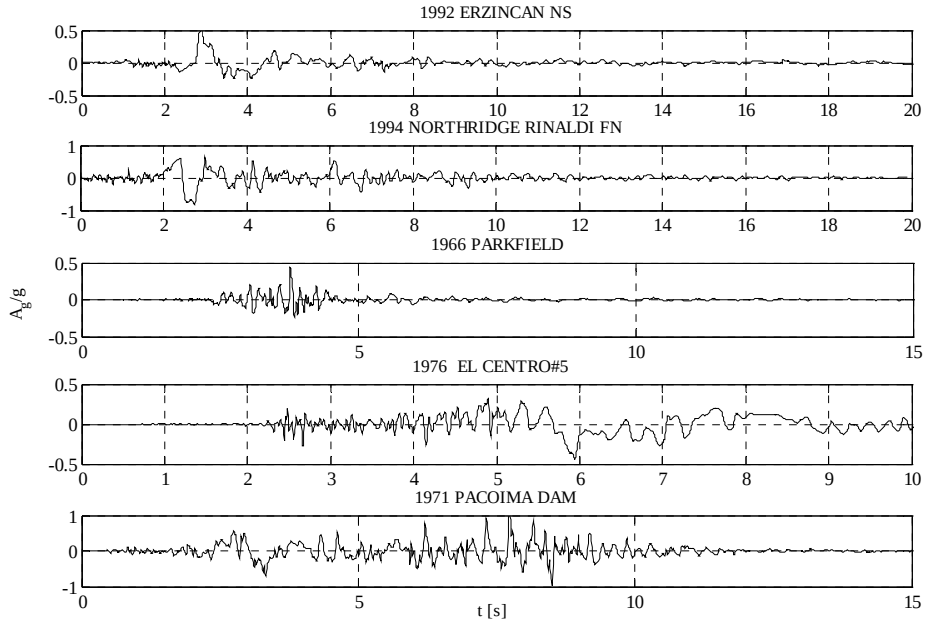

Figure 3.20 - recorded earthquakes used as inputs

The response was then evaluated by means of the Matlab tool described above, in Figure 3.21 the time history responses are depicted; the column experiences two situations of early overturning that occurs after small rocking.

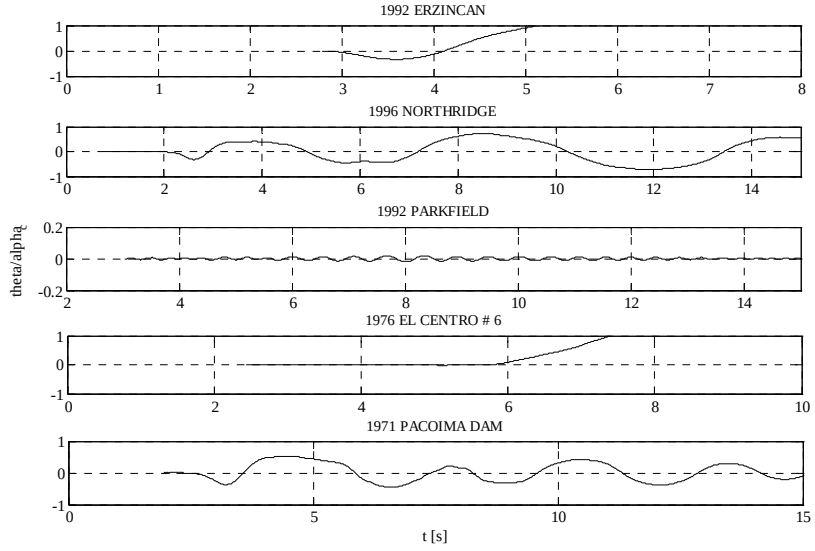

Figure 3.21 - evaluated responses

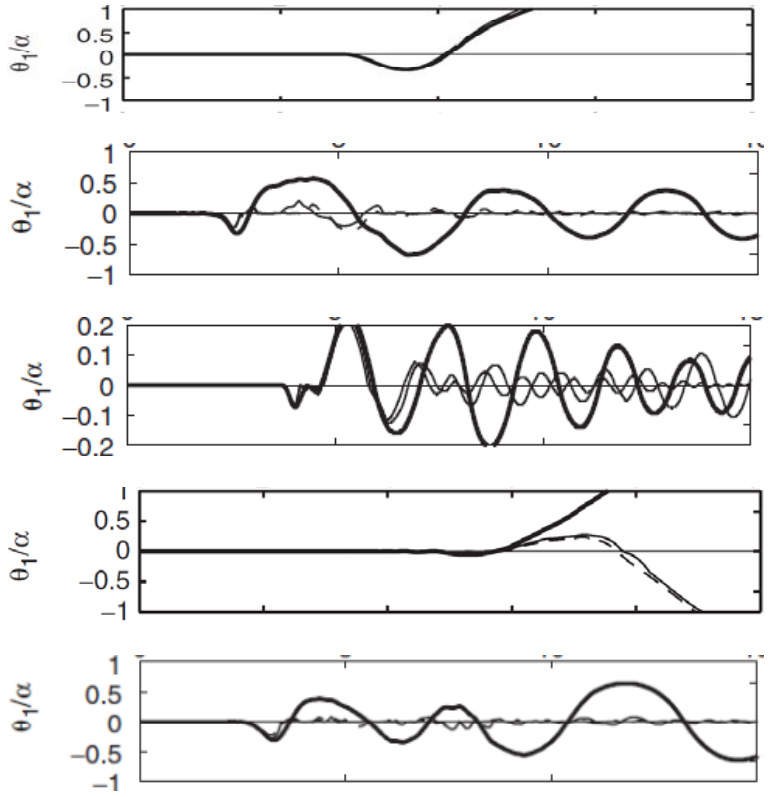

Figure 3.22 - Dynamic responses presented in Makris et al, (24)

It can be observed that the results obtained are comparable to those given by the literature reference for the two cases of overturning, overturn occurs at the same time instant and on the same side; despite the fact overturning response is reliable, results in terms of rocking are not perfectly the same: in fact the response number 3, to Parkfield earthquake, even though it begins rocking at the same time in the two cases, has slightly different results in terms of amplitude; the test number five, that uses as an input the Pacoima dam record, shows a difference in the number of oscillations in the same time interval. This observation points out that this method is very sensitive to the numerical choices, in particular those connected to the number of equations to solve. When an approach with two merged equations is chosen the integration is carried out with less detail around the rocking point.

3.6.2.6.3 Benchmark 3

The investigation of the response of a single body is not the only possible application of such an approach; it can be also applied for investigations on a large scale in order to perform sensitivity analyses of the model to input parameters, such as the geometry of the body or the intensity of the input, both in terms of peak ground acceleration and in terms of peak ground velocity. This can be very useful as a feedback for the simplified formulas described in the previous part. A first comparison can be made between the two approaches in case of 28 symmetric bodies, with different values of slenderness, under the action of 130 different earthquake records, similarly to the analyses carried out by Boroschek (18).

The accelerograms used as inputs were generated with the software Simqke (25) according to the Italian Standards. The records give an increasing peak ground acceleration obtained by increasing the return period of the reference spectrum, and for each one the peak ground velocity is computed. The chart in Figure 3.23 summarizes the values of these two parameters for each record.

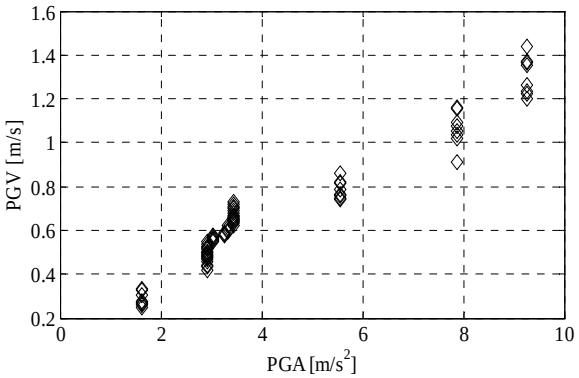

Figure 3.23- PGA-PGV for the generated earthquake

Figure 3.24 shows the extreme response of the symmetric rigid bodies subjected to the impulse of the set of earthquakes previously described. Each chart describes the behavior of bodies with different slenderness ratio characterized by the same height of the centre of gravity, h, and different values of b. In particular, the value of PGV obtained from the solution of the non linear equations of motions is reported: the red markers identify the analyses in which overturning occurred, while the black markers identify those analyses in which the body did not tilt. The solid lines drawn in the four charts represent the Ishyiama overturning criterion.

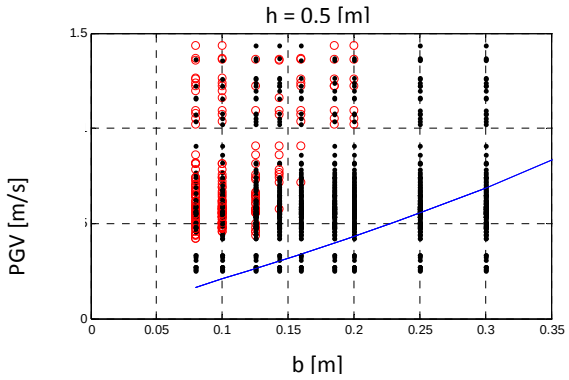

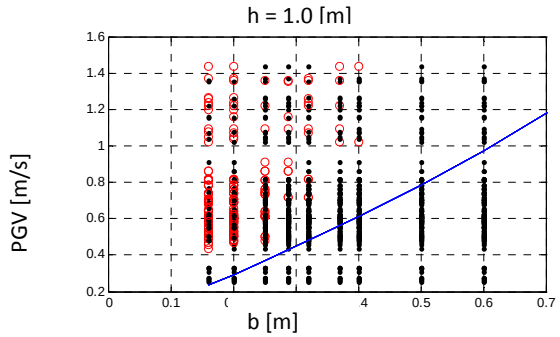

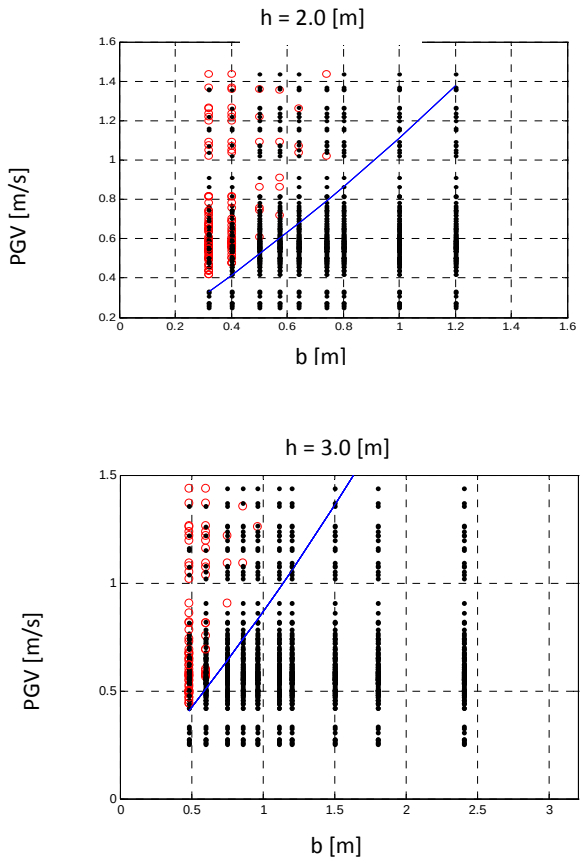

Figure 3.24 -response of symmetric bodies for different slenderness ratio

It is worth noting that the overturning limit provided by Ishyiama criterion is always on the safe side with respect to the results obtained from the numerical integration with Matlab code.

Probability of overturning:

The application of this method allows an interpretation of the results also in terms of percentage of overturning events, over the number of tests, which can improve the understanding of this phenomenon in relations with the parameters governing the problem, for a better interpretation of the results the following parameters will be then introduced:

R_T = n° overturnings /n° tests;

R_{RA} = n° overturnings /n° tests in cui $B/H > a_g/g$;

R_{RV} = n° overturnings/ n° tests in cui $v > v_{cr}$;

These parameters allow to understand the general trends in the analyses; the first one (R_T) is the most general one and it is given as the number of occurred overturnings out of the number of performed tests; the second one (R_{RA}) is the number of overturnings out of the number of tests in which there is the triggering of a motion phenomenon, hence all the tests in which the West formula is satisfied. The third one (R_{RV}), instead, accounts the total number of overturnings out of the analyses that have maximum input velocity bigger than the critical velocity calculated with the Ishyiama formula, these results are useful to understand the reliability of the formula given for the evaluation of the critical velocity.

From Figure 3.25 to Figure 3.27 results are summarized in terms of the percentage of overturning, expressed as R_T, R_{RA}, R_{RV}, according to the peak ground velocity. From Figure 3.28 to Figure 3.30 result are depicted according to the slenderness.

Results are shown for different vertical position of the center of mass (H = 0.5, H = 1.0, H = 2 and H = 3) and also for decreasing slenderness ratio (assuming $\lambda = H/B$, they are $\lambda = 6.25$, $\lambda = 5$, $\lambda = 4$ and $\lambda = 3.57$); since the objects studied

are rectangular the value of x_g corresponds to half of the dimension of the base (x_g = B). It is interesting to compare the results with Housner (3.47) and Ishyiama (3.48) formulas. The comparison is given in Table 3.2:

Table 3.2- Summary of critical velocities evaluated with different methods

H [m]	**0.5**			**1**			**2**		
B [m]	0.08	0.1	0.125	0.16	0.2	0.25	0.32	0.4	0.5
λ	6.25	5	4	6.25	5	4	6.25	5	4
$v_{ishiyama}$ [m/s]	0.16	0.20	0.26	0.23	0.29	0.36	0.33	0.41	0.51
$v_{housner}$ [m/s]	0.41	0.51	0.64	0.58	0.72	0.90	0.82	1.02	1.28
proablility $v_{ishiyama}$	0%	0%	0%	0%	0%	0%	0%	2%	2%
proablility $v_{housner}$	5%	15%	18%	30%	40%	20%	42%	45%	20%

The comparison between results obtained from the performed analyses and Ishyiama's and Housners's criteria shows that, for velocities lower than the velocity evaluated with Ishyiama relation (hence $v<0.4\ v_{lim}$), the probability of overturning obtained from the analyses is averagely zero; this means that this relation provides a criterion that can be considered very conservative. The comparison between the result and Housners's shows that the calculated probability of overturning is between 20% and 45% which is inferior than the 50% expected from the analytical relation. This difference can be justified with the fact that the above mentioned criterion is referred to rectangular bodies subjected to a single horizontal shock.

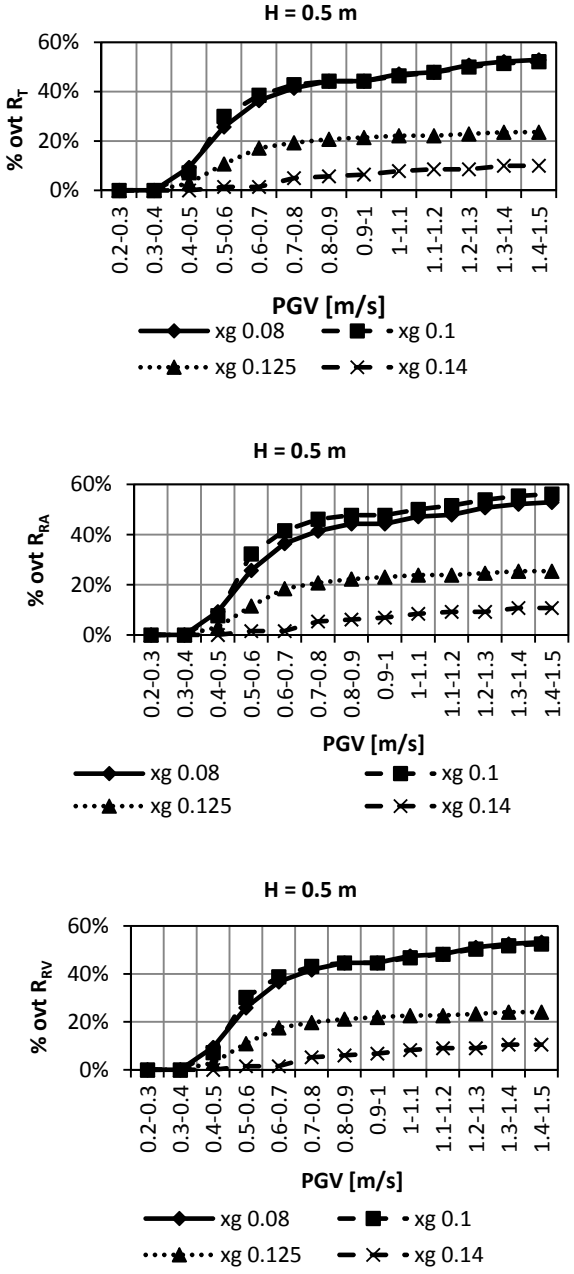

Figure 3.25 - overturning probability with decreasing slenderness hg = 0.5 m, a) total overturnings, b) overturnings relative to rocking triggering, c) overturnings relative to critical velocity

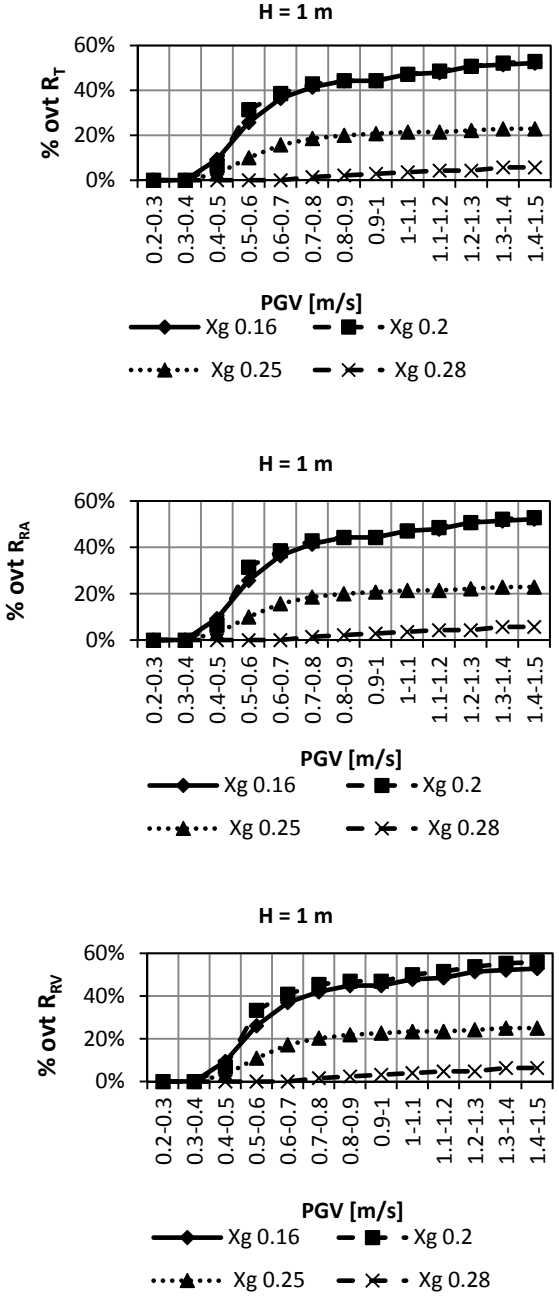

Figure 3.26 - overturning probability with decreasing slenderness hg = 1 m, a) total overturnings, b) overturnings relative to rocking triggering, c) overturnings relative to critical velocity

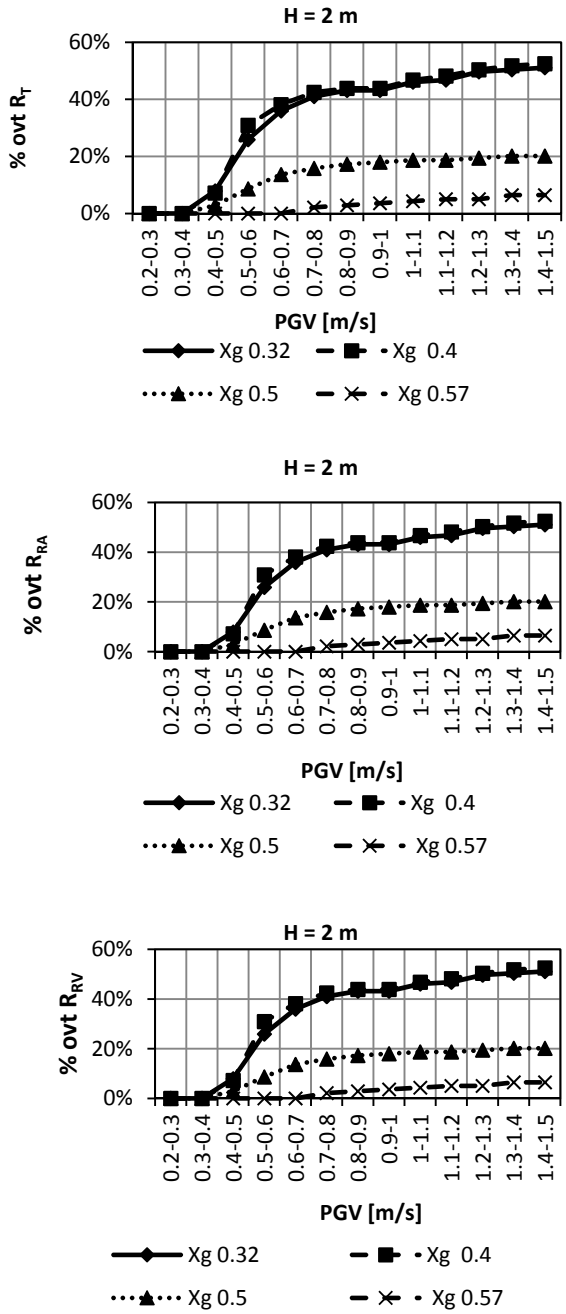

Figure 3.27 - overturning probability with decreasing slenderness hg = 1 m, a) total overturnings, b) overturnings relative to rocking triggering, c) overturnings relative to critical velocity

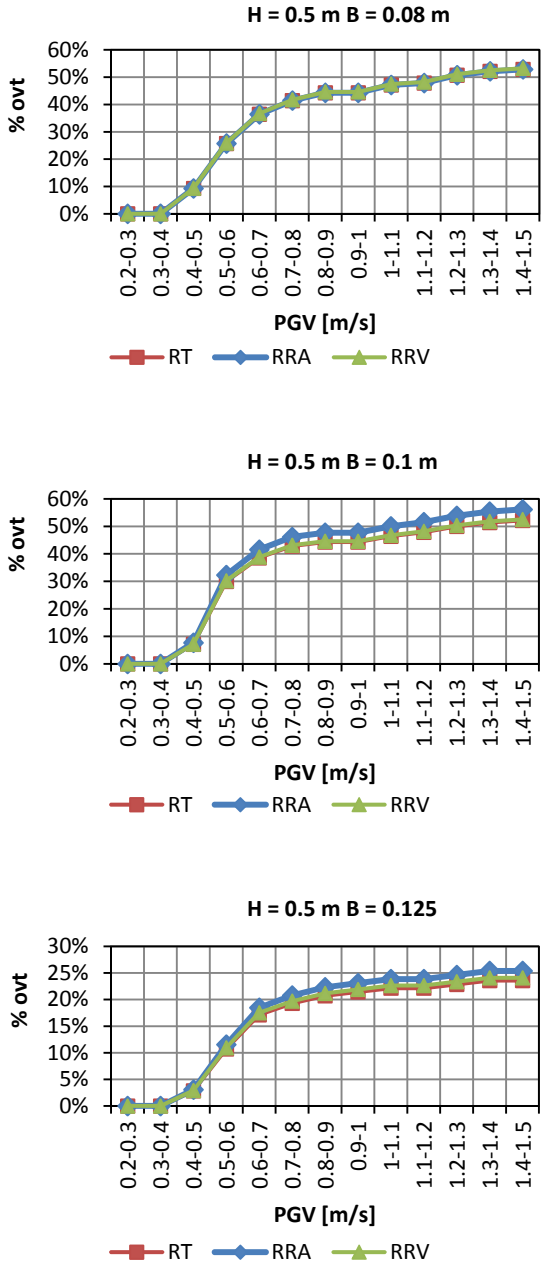

Figure 3.28 - overturning probability for the same slenderness, a) λ =6.25 ,b)λ= 5,c)λ=4

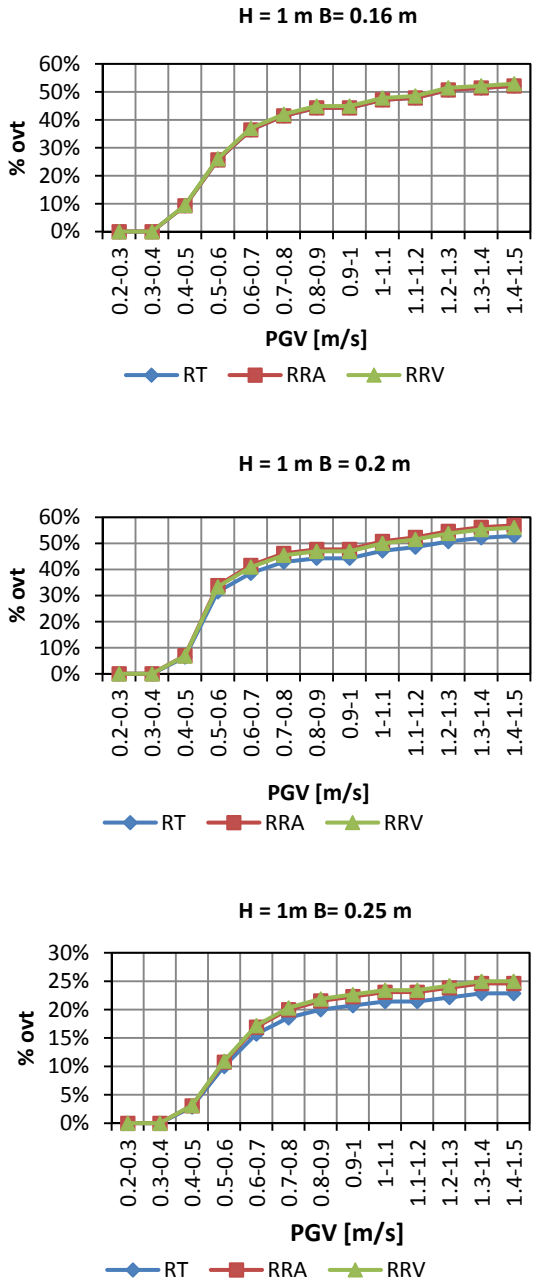

Figure 3.29- overturning probability for the same slenderness, a) λ =6.25 ,b) λ= 5 ,c) λ= 4

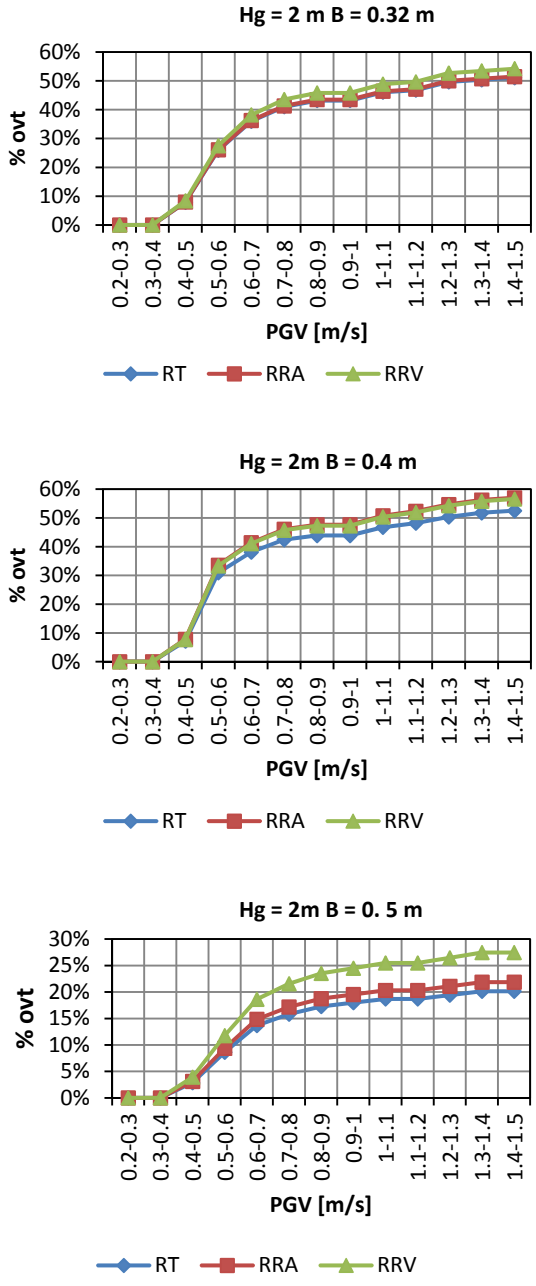

Figure 3.30 - overturning probability for the same slenderness, a) λ =6.25 ,b) λ= 5,c) λ= 4

3.6.3 Detailed modeling of deformable bodies (LA)

3.6.3.1.1 General description

Finite element method can be applied whenever further investigations, with a more detailed level of complexity, are required; these models can be applied for stress or deformation analyses under either static or dynamic load conditions. In this type of analyses an accurate evaluation of mechanical characteristics of materials must be done, since these parameters have a relevant effect on results. In this case the average values of mechanical resistance and elasticity modulus must be used, also considering a proper confidence factor, conveniently chosen according to the level of knowledge reached in the knowledge phase. According to the category of the object analyzed, of the knowledge reached and of the type of the possible intervention of mitigation, the choice for the type of analysis can be very different: linear static analyses, modal analyses to catch the vibration modes or linear and non linear dynamic analyses with application of earthquake records. It is worth noting that, when an intervention of mitigation by means of seismic isolation is prescribed, it is mandatory to assess the safety level by means of linear or non linear dynamic analyses, when the isolation system cannot be described by an equivalent linear model.

3.6.3.1.2 Presence of vertical action

An important aspect considered in this work is the effect of the vertical component of the seismic input: as described by Priestley (26) *"recent near field accelerograms of shallow earthquakes have indicated vertical accelerations that have in many cases exceeded the peak horizontal acceleration"* seismic events have shown the presence of vertical action that is often as dangerous as the horizontal ones; in particular when dealing with such art objects with a number of possible dynamic behaviors involved. As it was described and commented for the rigid body approach, the vertical action can affect the response of such light weight objects, leading to an increase of the seismic vulnerability, which needs to be investigated in detail; similarly stress analyses must take into account the presence of the vertical action because it can induce variations into the stress pattern that can be dangerous for the objects, for instance in those situations in which the problem of an articulated body is investigated: prominent parts can be considered similar to cantilever beams and variations of vertical acceleration can seriously influence the stress pattern in these parts that, moreover, usually have reduced cross sections.

3.7 Case study

The case study we are considering is the "*Galleria dell'Accademia*" in Florence; after a preliminary analysis of the building and of its contents and after some meetings with the director of the Museum and the Architect from ministry of architectural goods it was decided to focus attention on two different aspects:

Big statues.

For this typology it was decided to study the "*Galleria dei Prigioni*" that houses the four "*Prigioni*", the "*Pietà da Palestrina*" and the "*San Matteo*", six marble statues carved by Michelangelo.

Busts and small statues. For this typology it was decided to focus attention on the "*Sala dell'Ottocento*", in which more than 300 gypsum busts are exhibited on supports and shelves.

These two choices were made considering both the potentially critical situation of seismic vulnerability in which the objects are and also the aim of this research of the development of a methodological approach to apply to specific type of objects. The "Sala dell'Ottocento" shows a remarkable critical level, in terms of seismic vulnerability, and it is particularly suitable to a methodological approach; indeed most of the works contained in it are gypsum busts of the average height of 60 cm, they are stored on shelves which are located at height from 2 to 6.5 meters from the ground; at the moment they do not have any form of restraint nor protection. In Figure 3.31 (a) an example of wall I is shown. In case of an earthquake of low intensity, and hence with a smaller return period, the objects can collide each other or fall and there might be the risk of damaging the object or injuring visitors of the exhibition.

Figure 3.31 - Galleria dell'accademia (a) sala dell'ottocento (b) galleria dei prigioni

With reference to figure (Figure 3.31 (b)) the "*Galleria dei Prigioni*", located at the ground floor of the Accademia in Florence houses six important Michelangelo's statues thus creating a suggestive path leading the visitor to the center of the tribune where the famous David stands. The Gallery takes its name from the four big unfinished statues known as the Slave Prisoners: "*Prigione che si Sveglia*", "*Prigione il Giovane", "Prigione Barbuto"* and *"Prigione Atlante"*; besides them in the room the sculpture of "San Matteo" and "Pietà" are displayed. The sample that is studied in this work is made of the above mentioned statues that can be considered slender (three of the Prigioni and the san Matteo); one statue, the Prigione Barbuto, slender as well, which is also characterized by an evident fissure and the Pietà da Palestrina, which has different geometrical features and background.

In Figure 3.32 images of the statues of the Galleria dei Prigioni are shown, also including some first details about their geometry, as given in the archive of "Polo Museale". A global study of the condition of seismic vulnerability of the entire sample was carried out, with particular attention to those aspect that cause dangerous situations. As it will be described in the following, the application of the proposed procedure showed that, among the six statues, the "Schiavo Barbuto" and the "San Matteo" needed further analyses because of different reasons that increase their level of vulnerability, therefore more detailed analyses were performed on these two statues.

"Che si sveglia" 282x108

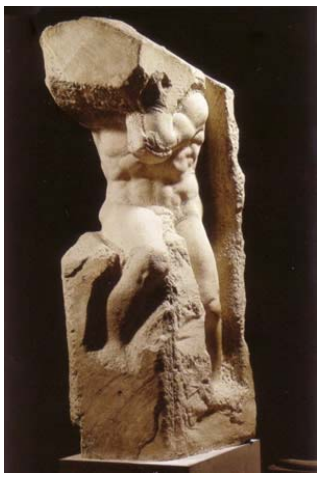

"Atlante" 277x102

"Barbuto" 258.5x94

"Il giovane" 256x80

"San Matteo" 271.5x75

"La Pietà di Palestrina" 253xn.d.

Figure 3.32 - statues exhibited in Galleria dei Prigioni

3.7.1 Definition of the seismic action

The evaluation of the characteristic parameters of the seismic action for the site in which Galleria dell'Accademia is located, takes as references , as stated before, the studied carried out by INGV (Istituto Nazionale di Geofisica e Vulcanologia) as suggested by the recent Italian building code (NTC) and also the seismic micro-zoning of Professor Vannucchi. The object of this study is the Tuscan area of "Pretola-Castello", but according to the author results of his investigations can be extended to a much wider area, including urban centers of Firenze, Sesto Fiorentino and Prato.

The institute INGV provides the spectral accelerations for different return periods on the hazard gridpoints. Results are given 16^{th} , 50^{th} and 84^{th} percentiles of all possible results obtained from the application of the Cornell probabilistic method. The seismic actions parameter can be calculated for each town by knowing the geographical coordinates and interpolating the values from the gridpoints.

The position of the Museum is:

- Long: 11.258°
- Lat: 43.776°

For the seismic action evaluation the nominal life was set at 50 years with a coefficient c_u = 1.5, according to the fact that the building, as a museum, belongs to the III Class (ref. Circolare applicativa "*As an example, belonging to the Class III, we remind schools theaters, museums, as buildings subjected to crowding*").

According to the aforementioned assumptions the reference period is:

$$V_R = V_N \cdot C_U = 75 \text{ years}$$

3.7.1.1 Characterization of the seismic action in terms of response spectrum

Given the reference period set, a complete definition of the seismic action it is possible in terms of response spectrum for the reference limit state. In Table 3.3 characteristic parameters for an elastic response spectrum, evaluated for the site of study, considering a type A soil and a reference period V_r = 75 years are summarized in Table 3.3, where SLO and SLD belong to the Serviceability limit states, while SLV and SLC belong to Ultimate limit states. They are defined as:

SLO: as a consequence of an earthquake the building and its structural and non structural elements do not suffer severe damage or interruption;

SLD: as a consequence of an earthquake the building and its structural and non structural elements do not suffer damage that produce risk situations for people and do not compromise resistance and stiffness for vertical loads;

SLV: as a consequence of an earthquake the building suffers damage and collapse of non structural elements and severe damage to structural elements which is associated to a loss of stiffness and resistance towards horizontal actions; the building preserves part of its stiffness and resistance for vertical action and an adequate margin of safety towards collapse due to horizontal actions;

SLC: as a consequence of earthquake the building suffers damage and collapse to non structural elements and severe damage to structural components; the structure has a margin of safety for vertical action and a reduced margin of safety towards collapse due to horizontal action.

Table 3.3 - characteristic seismic action parameters

LIMIT STATE		T_R [years]	a_g [g]	F_0 [-]	T^*_c [s]
SLE	**SLO**	45	0,054	2,581	0,264
	SLD	75	0,065	2,598	0,277
SLU	**SLV**	712	0,150	2,396	0,307
	SLC	1462	0,188	2,399	0,314

The type of soil is considered by means of the introduction of coefficient S, given as:

$$S = S_S \cdot S_T$$

where S_S is the value of the coefficient of stratigraphic amplification and S_T is the value of topographic amplification. For the Galleria dell'Accademia the coefficient of topographic amplification $S_T = 1$, while, for the type of soil evidenced by the investigations (which can vary from B to D) the stratigraphic coefficient can assume a value between 1.2 and 1.8, consequently the value of S is :

$$1.2 \leq S \leq 1.8$$

This allows to calculate the values of the peak ground acceleration (PGA) as:

$$PGA = \mathrm{S} \cdot \mathrm{a_g}$$

Values of PGA corresponding to each limit state are summarized in Table 3.4

Table 3.4 - peak ground accelerations for the reference limit states

LIMIT STATE	T_R [years]	PGA [g]
SLO	45	0.0648 - 0.0972
SLD	75	0.0780 - 0.117
SLV	712	0.180 - 0.270
SLC	1462	0.2256 - 0.3384

In the following the seismic action corresponding to a type D soil is assumed; the investigations gave as a result an uncertain category of the soil, for this reason a category D was assumed, for keeping calculations on the safe side.

The value of maximum horizontal ground velocity was evaluated by means of the relation 3.2.3.3 of the NTC (3.2); for the case of big statues the alternative relation proposed by Bommer (3.3) was applied as a critical comparison between results.

3.7.1.2 Selection of compatible accelerograms

The selection of proper accelerograms to apply as inputs for dynamic analyses was made according to the NTC norms and to the afore mentioned (par. 3.7.1) report by Vannucchi. In this work two different methods for earthquake selection were used: the first one is the application of the software Rexel (27), for the selection of recorded earthquakes from available database, the second method consists of the application of the software Simqke (25) that allows generation of seismic inputs compatible with a reference spectrum. Since any further investigation is not available it is reasonable to assume that the geotechnical and geological characteristics of the soil for the Galleria dell'Accademia are similar to those given for the "Pretola – Castello" area and to use them for the determination of the seismic inputs for the site. In Vannucchi's work 19 areas were pointed out and described as potential sources for the area of "Pretola – Castello". In particular the seismic activity in a squared zone 300 km by 300 km with the center on the city of Florence was studied. The upper limit for the expected magnitude and the relationships between the magnitude and frequency of events was defined for each area. The next step was the evaluation, by means of proper attenuation laws, (for example the Sabetta-Pugliese law, based on an Italian dataset, or Ambraseys et al., who use a European dataset), of the perceived intensity on the study site of an earthquake that has its origin from a source area. Attenuation laws depend on several factors, such as the type of soil, the hypocenter depth, the distance from the source , the fracture model, etc. The last step is the calculation of the probability for a given parameter (such as the acceleration) to overcome the reference value for the considered return period.

Lower limit M_0 and upper limit M_u values for the magnitude are:

M_0 = 3.5 and M_u = (max of history) + 0.5, according with the use of neglecting seismic events with magnitude lower than 3-4. The value of magnitude from the work by Vannucchi is: $M_{u,max}$ = 6.8.

Referring to NTC, for the acceleration parameter, the value of acceleration with a probability of overcoming of 10% in 50 years (Tr = 475 years) is 0.133 g for the 50th percentile. This value is aligned with the results given by the above mentioned work, which provides a result of maximum expected acceleration of 0.14 g. The disaggregation graph of the ag value for the closest grid point to the Accademia with return period 475 years is depicted in Figure 3.33. this graph allows to deduce the magnitude interval M and the distance R to be used for the research of natural accelerograms.

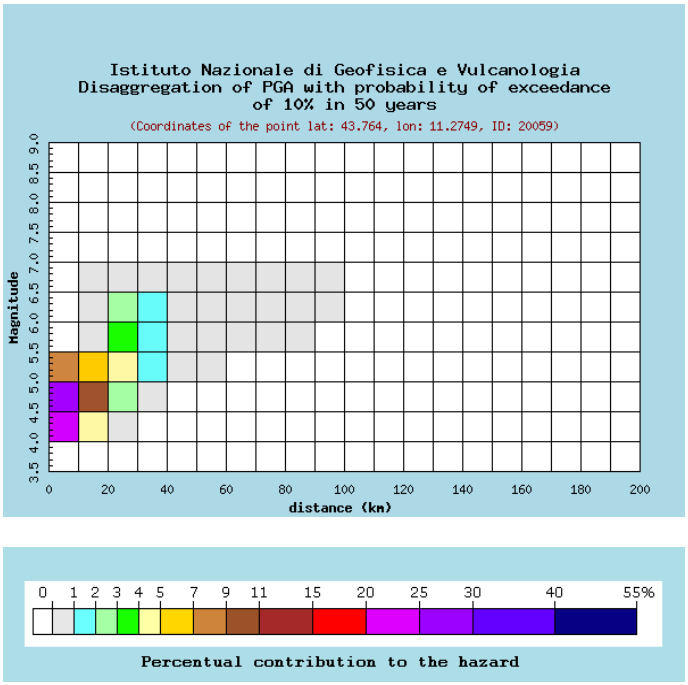

Figure 3.33 - disagregation curves for Tr=475 years

When considering a higher return period of 975 years. with 5% of probability of overcoming in 50 years, the acceleration value is 0.167 g and the corresponding disaggregation graph is given in Figure 3.34.

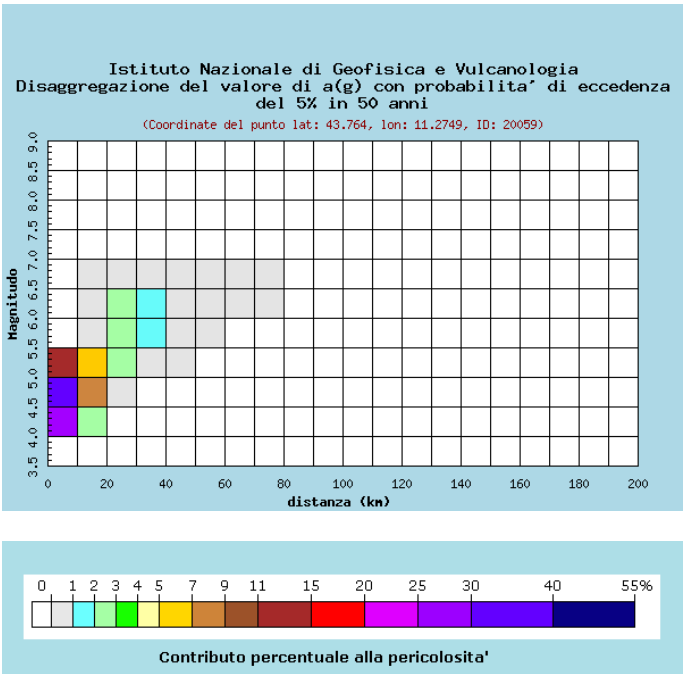

Figure 3.34 - disagregation curves fir Tr =975 years

Consequently, considering also the return period assumed as a reference in this work is 712 years, the selection of accelerograms was performed using the following parameters:

- M = 4 – 7
- R = 0 – 40 km

As it was stated above the selection was made by means of the software REXEL, considering the European database ESD and setting the compatibility around the interest period. Three groups of three accelerograms were obtained, each group is characterized by three perpendicular components of the motion, two horizontal and one vertical.

3.7.2 Application of the path of knowledge to the case study

3.7.2.1 Knowledge of the building

A deep and accurate study of the structural features of the building and of its response in case of an earthquake is a fundamental aspect for a reliable assessment of the seismic risk of the art objects contained in the museum. As such, even though one of the goals of this work is to assess the vulnerability of the objects (and not that of the building) it is nevertheless clear that neglecting the interaction with the structure can lead to wrong evaluations. For this reason an identification of the structure, with particular attention to the two halls that host the objects studied in this work, was made by means of geometrical surveys of the floor plans and of the elevations of the rooms, also collecting data about the location of the objects in their context.

The first exhibition room is at the first floor of the building , while the second one is placed on a mezzanine with a 60 cm rise. The investigations pointed out, under the Sala dell'Ottocento, the presence of a basement belonging to the Accademia di Belle Arti and to the Faculty of Architecture; this hollow space has a rectangular floor plan with an average height between 2.40 and 2.80 meters. the ceiling is made of brick cross vaults which bear on perimeter stone walls and brick pillars as it is shown in Figure 3.35. The geometrical survey and a photographic reconstruction of this room were found through archivial research, Figure 3.36 and Figure 3.37.

Figure 3.35 - basement under Sala dell'Ottocento

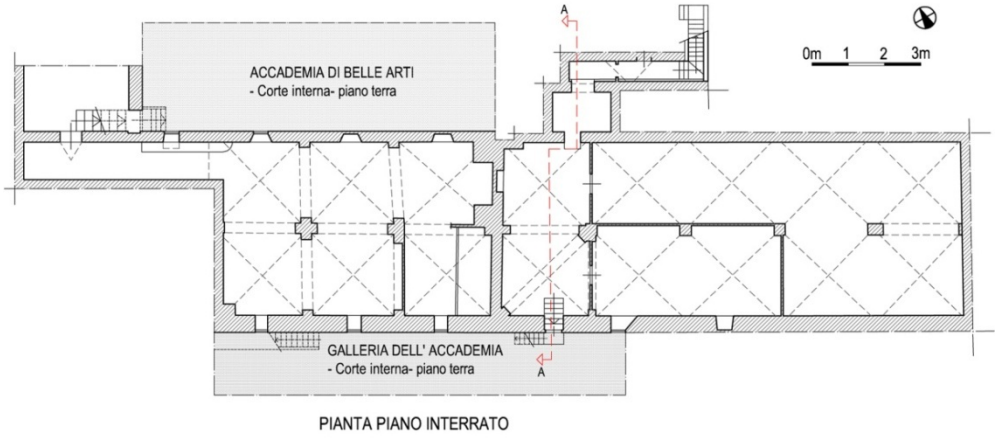

Figure 3.36 - basement under Sala dell'Ottocento: plan view

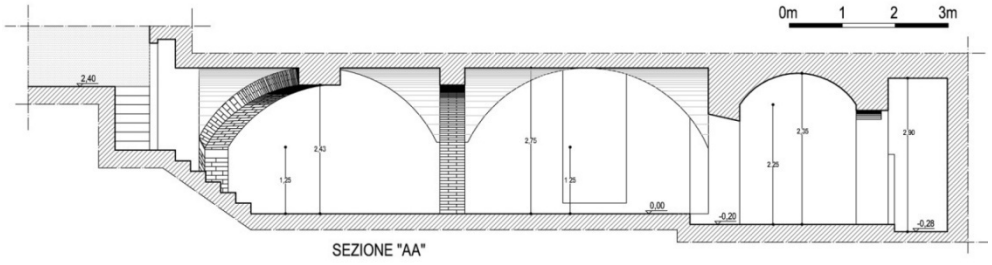

Figure 3.37 - basement under Sala dell'Ottocento: elevation view

Meanwhile, for the rooms containing the object of study historical research was carried out, with the collection of all drawings, plans and pictures available, given by the authority of the museum. This type of investigation gathers a very important role in the methodology in particular when there is the chance to improve the condition of the objects with interventions that may involve structural or architectural changes; from this investigation, for instance, it was learnt that the original floor of the Galleria dei Prigioni was demolished and re built in the beginning of the 80s, and since it is not an artistic value element it could be possible to apply an isolation system under the floor level of this room.

3.7.3 Application of the path of knowledge to busts and small objects

In Sala dell'Ottocento more than 300 gypsum busts are exhibited, they were carved during IXX century and they are attributed to the Tuscan sculptor Lorenzo Bartolini. The exhibition of the hall was set in the 80's and the works are placed on shelves at different height and very close to each other (the average distance between two busts is 4-5 cm). The objects are very different in shape, geometrical features and characteristics. In order to verify the proposed approach a sample of ten busts was considered, selecting them according to the main morphological features (with or without pedestal, figure with or without shoulders, hollow or filled) and for each morphological typology it was considered either hollow or filled inside. The selection procedure is summarized in Figure 3.38

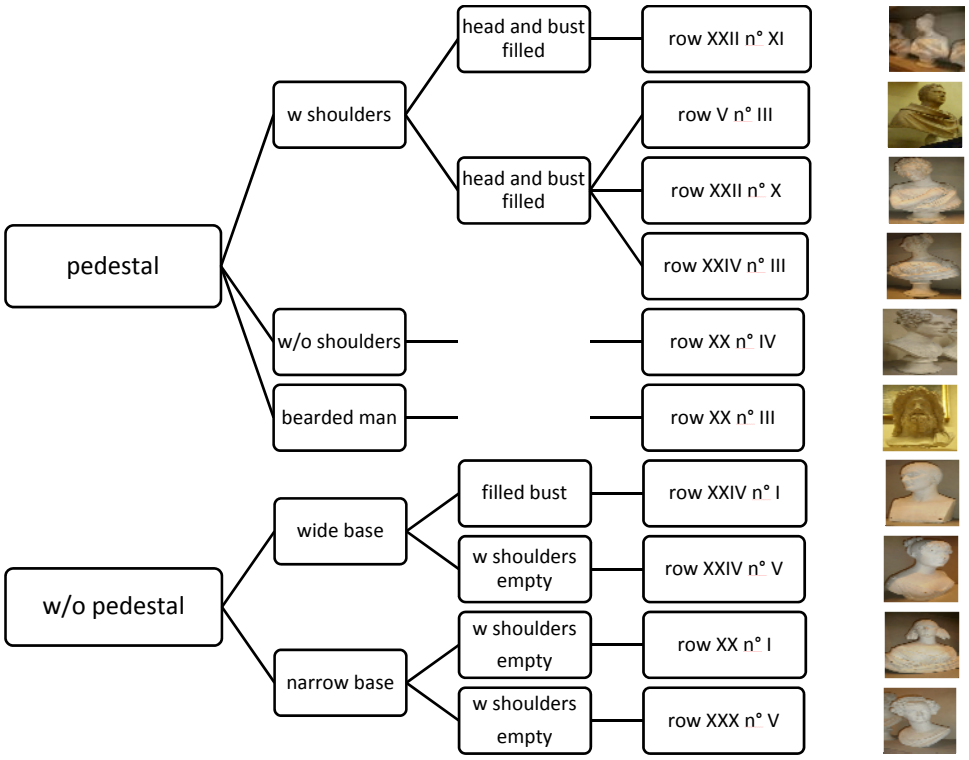

Figure 3.38 - definition of the sample according to morphological characteristics

3.7.3.1 Historical research

The first documentation about the "*Gipsoteca Bartoliniana*" is given by the sculptor himself in 1846: 500 busts, 36 pieces such as sculptures, groups and low-relieves. After the author was dead, in 1850, his fellow Romanelli collected all his works and put them into the atelier of borgo San Frediano. From a picture of the atelier taken in 1850 a superficial dark patina is visible. In 1881 inheritors entered into negotiation with Napoleon III for selling the "*Gipsoteca*" but an article published by Saltini on "la *Nazione*" denounced the bad condition of neglect of the works, encouraging contacts between inheritors and direction of "*Gallerie Fiorentine*". The busts collection have a background full of movements and changes of settings. The collection was divided in smaller groups since it was not possible (given the high number of object) to find a proper exhibition space that could host them all. Probably the most important event for their history was the flooding of 1966, during which some of them (those stored in the basement of the cenacolo di San Salvi) were covered with water and mud and significantly damaged; they were cleaned and restored with proper interventions.

3.7.3.2 Cases study

In order to describe the principles of this methodology to the case of small objects, two busts were chosen among the ten that were actually surveyed. Details about survey and geometry will be given for two selected samples, and also a general overview of the results for all the ten objects will be provided.

The two selected objects both belong to the category of “busts with pedestal” that is considered the most sensitive to the seismic action. In particular attention was focused on one bust from the category “without shoulders” (in the following identified as female bust) and one from the category “with shoulders” (in the following male bust). In the analyses they are considered as compact bodies for the application of rigid body models for the evaluations about global equilibrium. It is worth noting that the assumption of flat and regular interface between the object and the shelf is taken so there is perfect contact between the two surfaces, on the contrary, all the results given may become more meaningless the more the surface is rough.

Since the objects are placed on shelves located at different heights from the floor, the reference seismic action will be amplified according to the relation (3.4) that considers the increment of acceleration with the height of the control point. It was also assumed that, for the evaluation of the height of the shelves, the reference level is the ground floor. Indeed the basement located under the Sala dell’Ottocento has structural features (i.e. thick walls, stable vault system) that easily allow to assume it perfectly rigid and able to transfer the entire ground acceleration without any amplification or filter effect. A further assumption is that of considering the busts as rigid bodies and hence the ratio $T_a/T_1 = 0$.

Moreover, since the coefficient of friction μ is not known “a priori” it is considered not useful to study the motions of sliding and rocking-sliding combined. In the following only the single phenomena of rocking and overturning will be considered. For this reason it is interesting to consider that, for this case study, it is reasonable to assume $\mu_s > B/H$ since in this type of works the ratio B/H is in general small enough to be considered lower than the friction coefficient. If it wasn’t it would be desirable to provide an adequate interface in order to establish a condition in which $\mu_s > B/H$. Indeed the possibility of relative motion between busts and support can be very dangerous, given the very dense exhibition layout: movements could easily end up in falls or, at least, collisions between the objects.

3.7.3.2.1 Female bust

The first object studied in this part is the bust number 4 of the row XXX. It is a female portrait of princess of Saxony Luisa Carlotta di Borbone made in 1852 by the sculptor Lorenzo Bartolini, Figure 3.39. The bust is made out of gypsum and it seems to be filled, it is provided with a pedestal of 17 cm diameter; the total height is 63 cm. The bust is simply supported on a shelf at 3.00 m from the floor level.

Figure 3.39 -bust n.4 row XXX

3.7.3.2.2 Male bust

The second bust studied is the number 3 of row V. It is the portrait of a man made in the period between 1815-1830 by the Tuscan sculptor Lorenzo Bartolini, and restored in 1971. The bust is made out of gypsum, the head seems to be hollow, even though an accurate identification of the right thickness was difficult. It is provided with a pedestal with 23 cm of diameter, the total height is 81 cm. the object is simply supported on a shelf at 2.40 m from the floor level.

Figure 3.40 -bust n.3 row V

3.7.3.2.3 Geometrical survey

Two levels of detail were adopted for the render of the geometry of the objects, a simplified one and a detailed one. The simplified one consists of an approximation with symmetric rectangular areas in order to determine the height of the center of mass and then the equivalent block to assume for verifications. At this level frontal and lateral prospects are separately considered and eccentricity in the perpendicular plan is neglected. Examples of this survey level are given in Figure 3.41 and Figure 3.42:

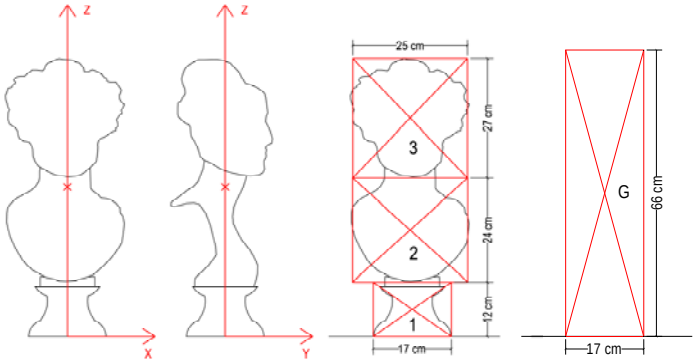

Figure 3.41 - female bust, equivalent block

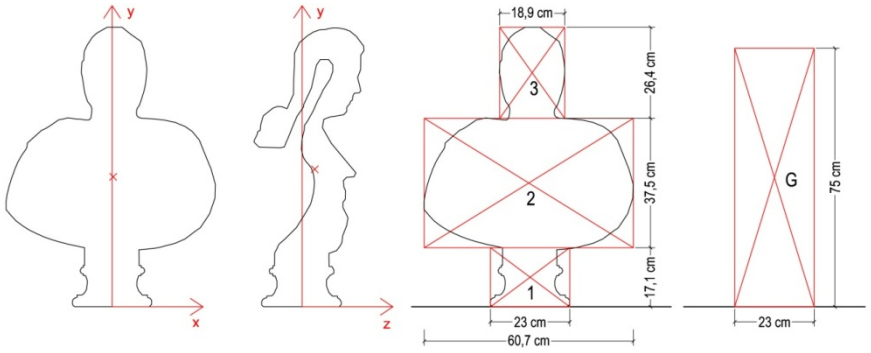

Figure 3.42 - male bust, equivalent block

For more detailed analyses of vulnerability it is necessary to consider surveys and renders with higher level of detail in the determination of the center of mass, also considering the asymmetries that are present. The three dimensional development of the body must be also taken into account, but since 3D surveys were not available the details from the two 2D surveys were joined. In particular busts were subdivided into different regions in the frontal view and in the side

view; for busts with cavity in the head two possible solutions were considered: the first one that best renders the survey (named TC) was considered in its worse condition of full head (named TP). Moreover, for the typology of busts with pedestal (from TI to TIV), since surveys revealed the presence of a cavity of dimensions that are not easily determinable, two conditions were considered as well: the first one assuming the full pedestal (PP) and the second one assuming a half empty pedestal (PSP).

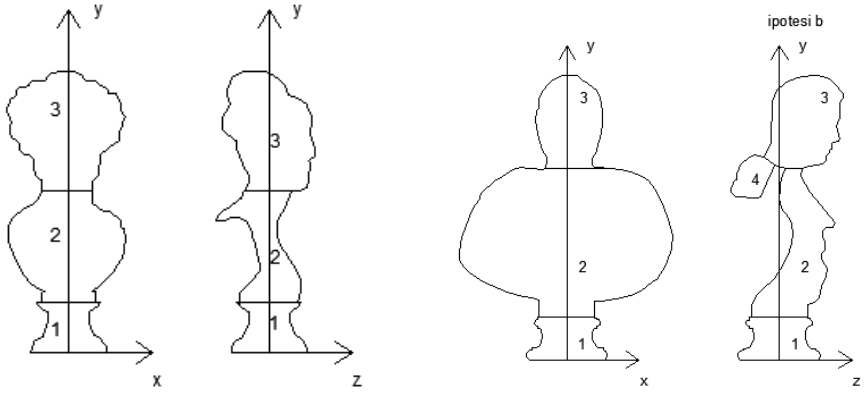

Figure 3.43 - detailed determination of geometry

3.7.4 Application of the simplified method to the case study of Sala dell'Ottocento

In the vulnerability analyses the objects will be considered as compact so the method for the assessment of vulnerability of rigid bodies, for evaluation of global equilibrium will be applied. In this phase of the investigation the conditions that cause rocking and overturning are taken into account , assuming that friction coefficient is high enough to prevent sliding; moreover a flat contact surface is assumed; the model and the relations applied are those described in (15) (14) (19) (17) (28).

As already mentioned the procedure will be developed and described in detail, for the case study of the Sala dell'Ottocento, only for the selected examples "Male Bust", in order to show the main aspects and details of the proposed procedure. Then a general overview of the results for all the ten selected objects will be reported and commented, underlining the important aspects emerged from the investigation.

3.7.4.1 Male Bust

This bust belongs to the category TII, and it is placed on a shelf 2.3 meters high from the ground level. The head seems to be empty but a precise evaluation of thickness is difficult. Table summarizes the results in terms of critical values of acceleration and velocity, with the corresponding returning periods for two significant cases: 1) full head and pedestal (TPPP); 2) empty head and full empty pedestal (TCPSP) which is the most probable condition. It is worth noting that the return period for overturning is lower than the one for rocking, which means that, once rocking is triggered the probability of overturning is very high. Despite this object is placed on a shelf at low level from the floor the Safeguard of life and the Artistic limit state are not satisfied; moreover, along direction y the critical overturning action is Tr = 104 years.

Table 3.5- results summary for the male bust

	Hp	**plane x-z**		**plane y-z**	
		$a_{g,c}/g$	**T_r (years)**	**$a_{g,c}/g$**	**T_r (years)**
rocking	TPPP	0.283	445	0.197	180
	TCPSP	0.252	326	0.163	104
		v_c(m/s)	**T_r (years)**	**v_c(m/s)**	**T_r (years)**

overturning	TPPP	0.251	281→445	0.181	132→180
	TCPSP	0.221	104→326	0.155	84→104

General results for the sample of study

Results obtained from the above described procedure extended to all the ten objects studied for this part of the research are summarized in Figure 3.43 and Figure 3.44; for each bust the critical overturning ground acceleration is given (S a_g), calculated with different techniques for the determination of the center of mass and also considering the amplification due to height. It can be remarked that the samples show diffused and high vulnerability, except for the bust belonging to category V, which is characterized by a very low slenderness ratio (h/b<0.33), and has a critical return period higher than the reference value (Tr =712 years). The case of "*Giove da Orticoli*", viceversa, is in the opposite condition, in fact for this example overturning occurs for a return period smaller than 100 years, this is due in particular to the high eccentricity of the object.

In general it can be pointed out that the simplified 2D analysis is not on the safe side and it is much more reliable the result obtained with the tridimensional approach. It is worth noting that the group of busts with base give results that are more scattered.

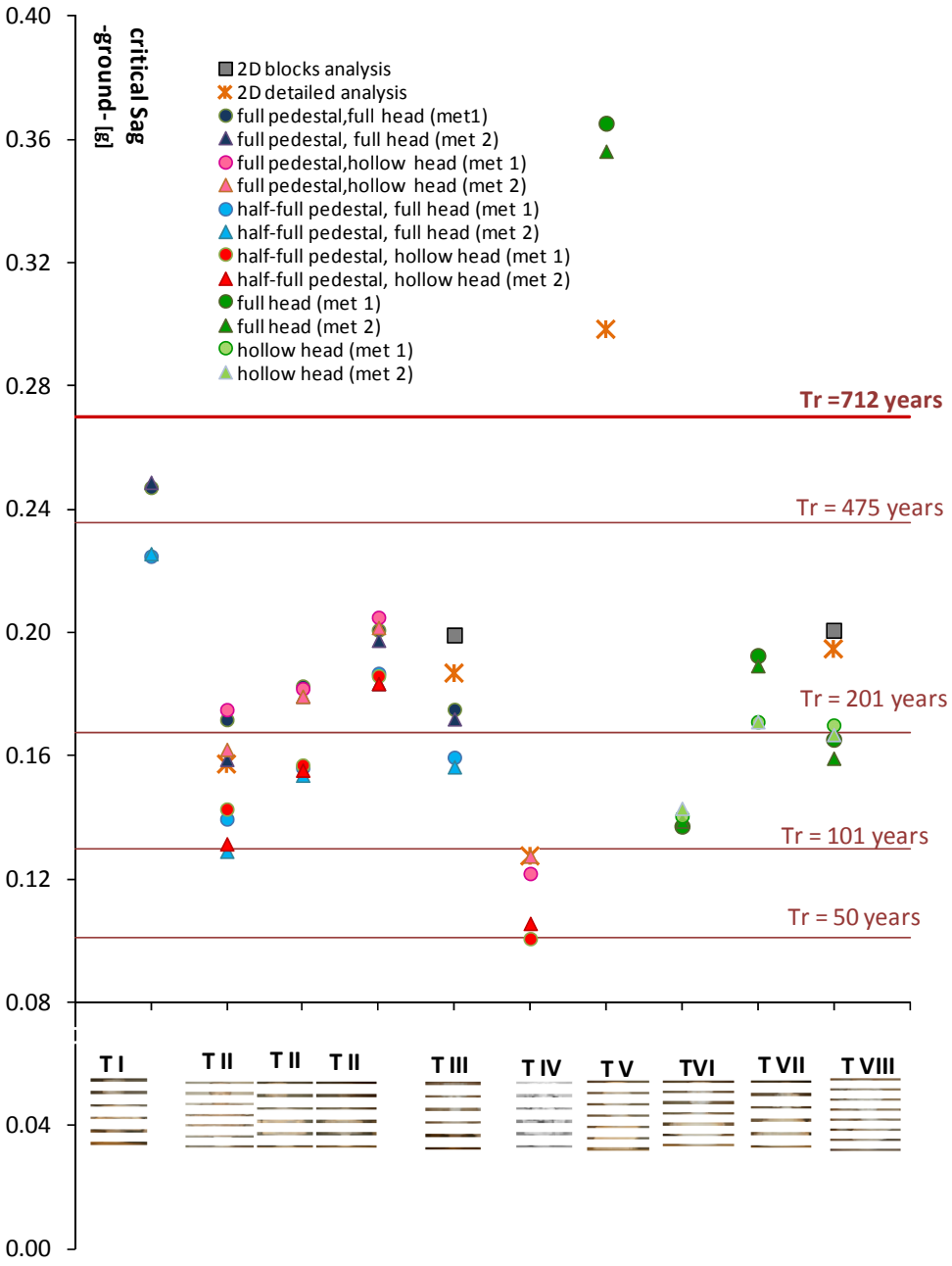

Figure 3.44- Limit ground acceleration corresponding to triggering of the oscillation/overturning for different morphological types with variation of the method for determining the center of mass position

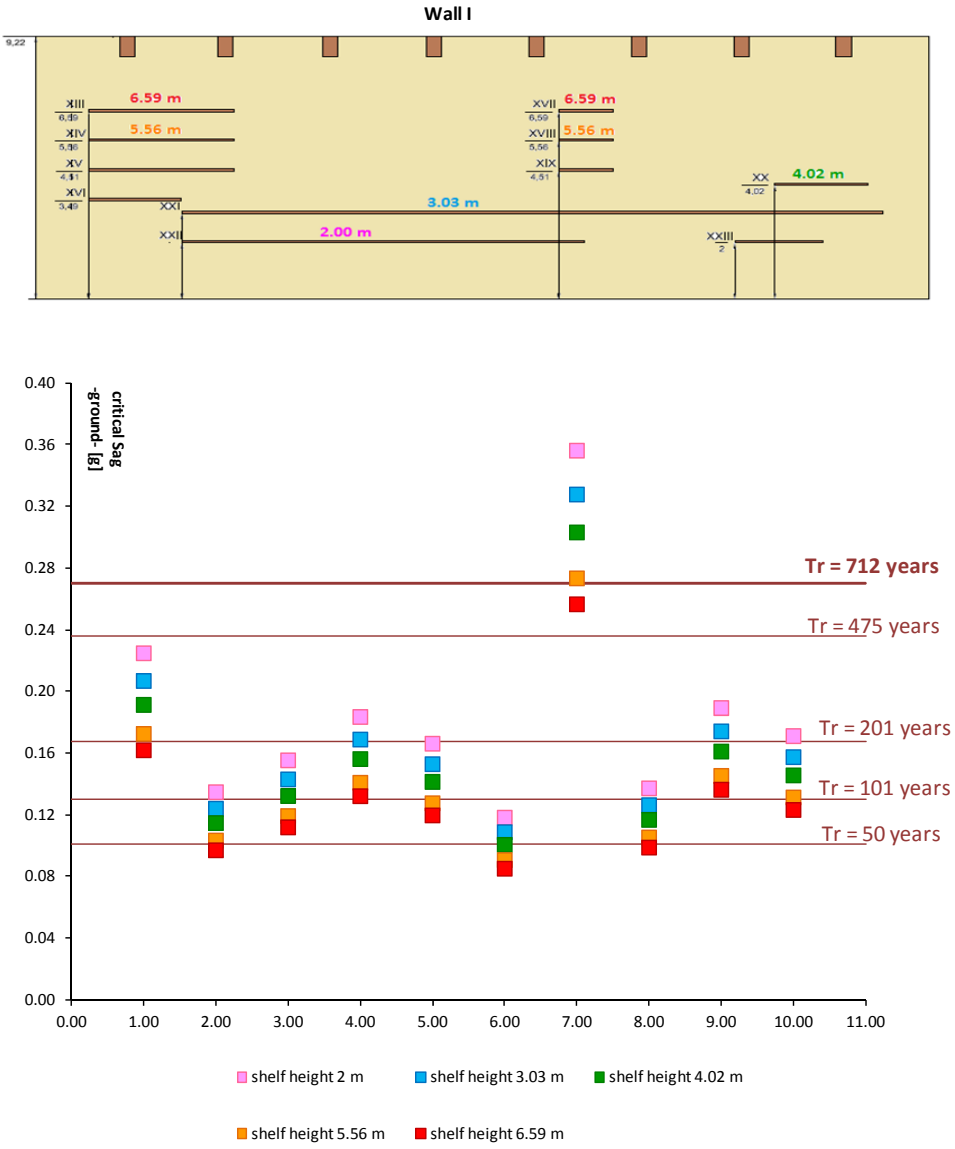

Figure 3.45 - Limit ground acceleration for triggering of rocking/overturning for different morphologies changing support height

3.7.4.2 Presence of vertical action

Triggering of oscillation can be affected by the presence of vertical action, that can cause a reduction of the return period of the critical event. The definition of vertical action is referred to in paragraph 3.2.3.2.2 of the NTC standards that identifies the value of the vertical action $\ddot{y}_g$ (m/s^2) for bodies with period of free vibration equal to zero as:

$$\ddot{y}_g = a_g \cdot S \cdot \frac{F_V}{F_O}$$

where Fv is the coefficient that describes the vertical spectral amplification on a rigid soil as:

$$F_V = 1{,}35 \cdot F_O \cdot \left(\frac{a_g}{g}\right)^{0{,}5}$$

Technically this operation requires the assessment of the values of $\ddot{x}_g$ and $\ddot{y}_g$that , combined and at the height of the supporting shelf, give the critical value Z = Z_{lim} = B/H. For the detailed analyses of the busts an evaluation of the critical return period in case of vertical action is conducted always referring to the principal plans (x-y and z-y). The return period is evaluated by means of the application of the method described above.

Male Bust

- plane x-y:

including $\ddot{y}_g$: $T_r = 346\ years$

neglecting $\ddot{y}_g$: $T_r = 445\ years$

with a variation around 22% of the highest value calculated

- plane z-y:

including $\ddot{y}_g$: $T_r = 157\ years$

neglecting $\ddot{y}_g$: $T_r = 180\ years$

with a variation around 13% of the highest value calculated

It can be observed that, as expected, the inclusion of the vertical action leads to results more on the safe side; from the results obtained it can be remarked that the higher is the return period Tr the more significant is the error, or better the approximation, made because of this choice.

3.7.5 Application of the path of knowledge to big statues

With reference to the "*Galleria dei Prigioni*" the available graphic material was organized according to a geometrical survey of the spaces, of the hall and of the exhibition path. Furthermore dimensions of the existing protection system were measured (glass rail) also considering the application of seismic protection systems under the statues.

In the first phase of the study researches about the historical background of the sculptures were made to collect useful details about their movements and past locations, to point out possible degradation phenomena that may affect the statues and traumatic events or interventions of restoration. Specifications about pedestals and foundations were similarly sought. Concerning the characterization of the six sculptures, different levels of geometrical survey were applied: the first, simple and quick, was an in situ survey made with basic tools, a second level considering the bodies as multiblock systems and a third level using of the detailed clouds of points obtained with 3D laserscanner techniques

3.7.5.1 Historical research

The Slaves were carved by Michelangelo between 1530 and 1536 and were intended for the tomb of Pope Julius II. After the death of Michelangelo they were given as a gift to Cosimo I, the Grand Duke of Tuscany, and then placed in the "Grotta del Buontalenti" in the Boboli Gardens in Florence, where they remained up to 1909 when they were moved to the Accademia Gallery. In the same year Michelangelo's statue of "San Matteo", sculpted in 1505-1506, was transferred from the court to the inside of the Gallery. Such a sculpture was the only one finished of the series of twelve Apostles commissioned for the Cathedral of Florence. It stood inside the Opera of Santa Maria del Fiore until 1834, when it was moved outside to the court of the Gallery where it has remained for 75 years. Regarding the "Pietà da Palestrina", discovered in the Barberini chapel in Palestrina and purchased by the Accademia in 1939, it was long attributed to Michelangelo though experts now consider such an attribution to be dubious. All the sculptures, with a possible exception of the "Pietà da Palestrina" for which there is no precise information, are simply supported by bases lying on masonry footings built in 1909 below the gallery floor. The original timber pedestals of the four Slaves' sculptures were replaced in 2000 with new bases made of "Pietra Serena" (a litharenite pertaining to the Langhian Marly-Arenaceous Formation of the northern Tuscan Apennine quarried very near the town of Florence (29)) on which the sculptures were simply leant on lead sheets. The new bases are made of three parts: the lower one is a solid compact block 20 cm height over which a hollow parallelepiped of 8 cm thick and 40 to 45 cm high is superimposed, braced with some steel ties; a cover 15-20 cm thick is used as upper closure.

3.7.5.2 Geometrical survey

The geometrical survey is fundamental for defining the model to be used in the analysis phase; the level of accuracy required by the survey has to be related to the adopted methods of analysis and to the aims of the analysis itself. In this work data obtained by three different geometrical surveys, with highly different detail level, were used: 1) a rough

survey based on the measurement of the most significant geometrical dimensions (i.e. maximum depth, width, and height of the object) was performed in order to obtain the necessary data for a preliminary stability analysis; 2) an intermediate multi-block level of survey was used: an approximation by means of different rectangular blocks was defined 3) the high accurate 3D digital representation of each sculpture obtained with laser scanner technology by the Visual Computing Laboratory, ISTI-CNR. Results of the survey allowed to accurate computation of some fundamental geometrical properties, such as the volume of the statues, their detailed dimensions, and the position of the centre of gravity. Examples of the three levels of detail are depicted in Figure 3.46, Figure 3.47 and Figure 3.48.

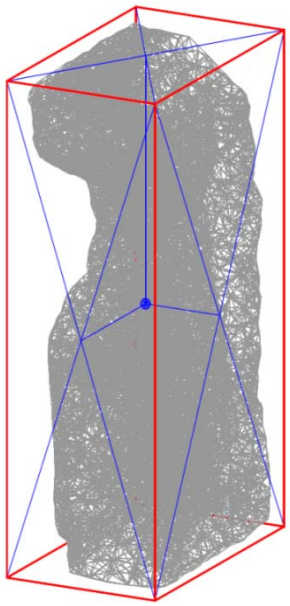

Figure 3.46 - "Prigione Atlante" approximated block

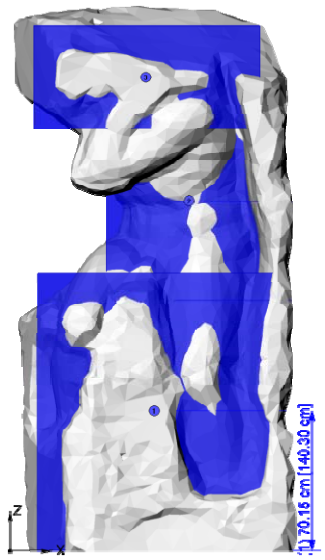

Figure 3.47 - "Prigione Atlante" multi block approach

Figure 3.48 - "Prigione Atlante" 3D laserscan survey

It is worth mentioning that, for the scope of this work, the original 3D laserscanner survey precision was reduced and a surface with around 50k faces was chosen. With this resolution it is possible to obtain reliable results with an acceptable computational time. A range of resolutions, between 500k and 30k, were considered and tested in order to assure accuracy of the results. With this resolution it is possible to obtain reliable results with an acceptable computational time.

3.7.5.3 Stone characterization

All the “Galleria dei Prigioni” statues are made of white Carrara marble. As far as the marble provenance is concerned, there is not direct historical documentation, but it is worth mentioning that archaeometric studies and multimethod techniques based on spectroscopic, isotopic and petrographic measurements on the marble of David (29)and of the Crouching Boy (“Adolescente”) at the Hermitage (30) confirmed that Michelangelo used marble blocks coming from the quarries of Fantiscritti (Val di Miseglia) and of Polvaccio (Val di Torano) respectively. In the next paragraph physical and mechanical properties of Carrara Marble are given and the procedure to evaluate the state of conservation and the petrographic characterization of ancient statues, described in paragraph 3.4.4.3 is applied to the six statues.

Physical and mechanical properties of Carrara Marble

According to the reader is referred to some notes on Carrara Marble; the main physico-mechanical properties of the best quality Carrara Marble now on the market (the variety named “Bianco Acquabianca”, very likely equivalent to the statuario quarried in antiquity), reported in the most updated literature, (31), (32) are summarized in the following paragraph either in terms of the main average values along with standard deviation (st.dev.), if relevant (measured according to the European Norms UNI EN), or in terms of range of values:

- Apparent density (UNI EN 1936-07): 27,1 kN/m^3;

- Open porosity (UNI EN 1936-07): 0.4 %;

- Water absorption at atmospheric pressure (UNI EN 13755-08): 0.19 w%;

- Uniaxial compressive strength (UNI EN 1926-07): 103.5 MPa (st. dev. 20.7);

- Flexural strength in natural conditions (UNI EN 12372-07): 12.6 MPa (st. dev. 1.3);

- Flexural strength after 48 frost cycles (UNI EN 12371-03): 7.9 MPA (st. dev. 0.8);

- Young's modulus (UNI EN 14580): 60000-75000 MPa.

As far as the tensile strength is concerned, little data is available in literature due to the difficulties in the testing methods. As reference an optimal range 4-9 MPa could be assumed, e.g. (32).

Autoptic examination of the external surface of the Michelangelo's sculptures

The result of the macroscopic observation carried out on the six marble sculptures by Michelangelo is summarized in

Table 3.6 - Sum up of the information obtained through the macroscopic study of the case study

STATUE	TEXTURES	GRAIN SIZE	STATE OF CONSERVATION	EXPOSED SURFACE	PINS/RODS/CLAMPS SURFACE PATINA SURFACE DEPOSITS
San Matteo	Anisotropic Compacted Foliated	Fine (<2mm)	Mediocre	Smooth, partially washed out, locally not cohesive, scaled and corroded	No Patinas due to biological actions (oxalate) Black crusts and algal deposits
	***NOTES**: small open compound fissure, approximately 22 cm, starting from the inguinal area and ending in the area of contact between left and right thigh. Dimensions < mm*				
Pietà da Palestrina	Anisotropic Compacted Foliated	Fine (<2mm)	Good	Smooth	Yes Biological localized patinas Traces of concrete and mortar
	***NOTES**: open compound fissure of dimensions around mm, up to the chest along a foliation plan, latent microfissure in the left ankle of the left figure. Mediocre quality of the marble block.*				
Prigione Che Si Sveglia	Isotropic Massive Compacted	Fine (<2mm)	Good	Partially washed out, low damage level	Yes Coloured patinas No deposits
	***NOTES**:*				
Prigione il Giovane	Isotropic Massive Compacted	Fine (<2mm)	Excellent	Not damaged	Yes Pinkish patinas likely of biologic origin No deposits
	***NOTES**:*				
Prigione Barbuto	Isotropic Massive Compacted	Fine (<2mm)	Good	Smooth, with scales, low level of damage	No Pink -reddish patinas likely from biological actions No deposits
	***NOTES**: Open compound fissure from side to side, plastered over in the central area, dimensions cm*				
Prigione Atlante	Isotropic Massive Foliated	Fine (<2mm)	Mediocre-good	Partially washed out, weakly scaled, corroded	Yes Pink - reddish patinas No deposits
	***NOTES**: Latent foliation along the left side of the block*				

Following the organization of the cards adopted for the macroscopic evaluation, the detailed observation of the sculptures shows, on average, a good state of conservation except for the "San Matteo" and the "Prigione Atlante", with mediocre conservation, because they display several zones affected by rain washing processes due to weather exposure. Nevertheless, a significant presence of iron pins and millimetric or sub-millimetric fractures, was evidenced in most statues together with a moderate phenomenon of marblescaling, which can be mainly related to mechanical workmanship. Moreover, natural foliation of the rock of mediocre quality used to carve the statues "Prigione Atlante" and "Pietà di Palestrina" was evident as can be seen in Figure 3.49 where the manifest foliation affecting the left side of the *Atlante's* block is shown: i.e. the marble is subdivided in pluri-centimetric layers and tends to scale. Furthermore, Figure 3.50 shows the iron pins set in the "*Prigione Atlante*" statue, along with micro-scaling of the marble. The presence of reddish surface stains (probably due to iron or/and lead oxidation) is also evident. It is worth noting that in case of sculptures with large iron pins and rings, an evaluation of their penetration depth in the marble through proton magnetometry or, alternatively, through specific radiographic techniques, may be useful to fully comprehend the local state of conservation. Finally, in the specific case of the "*Prigione Barbuto",* a through-going fracture, filled up with stucco, marks the central part of the sculpture, constituting a possible weak plane in case of seismic events (Figure 3.51). Such fracture probably dates back to the time when the sculpture was staying in the Boboli Gardens in Florence. The fact that the fracture is visible all around the surface of the sculpture indicates that it is almost certainly through-

going, as hypothesized by the scientists who have recently performed a monitoring study (29) and confirmed by the direct examination of the statue. Moreover such a monitoring study showed a relatively stable trend of the fracture.

Figure 3.49 -Foliation fo Atlante

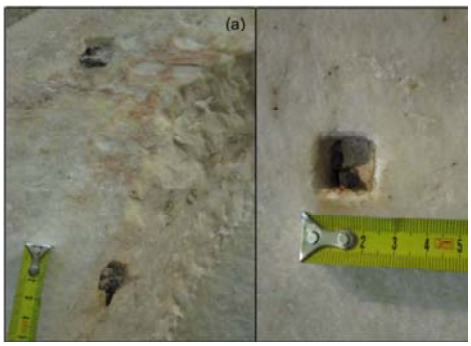

Figure 3.50 - pin holes in the Barbuto

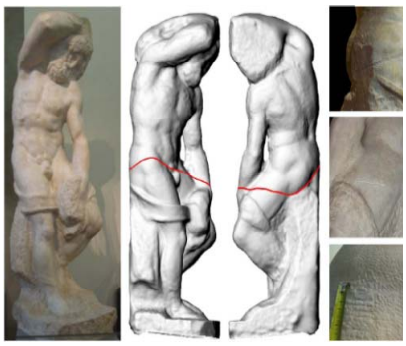

Figure 3.51 -fracture of the Barbuto

3.7.6 Application of mechanical models to big statues

3.7.6.1 Application of the simplified models to the case study of big statues

The purpose of this part of the work is the application of the methods described in the previous section, to assess the seismic vulnerability of the objects of the case study by means of simplified methods and criteria, in particular the study of the conditions of global equilibrium. The application of these relations is useful in case of a quick approach for analyses on a territorial scale, that can involve a high number of objects to study, with the purpose to draw a "ranking" or a priority list. Since different levels of detail in the survey are available, the influence of a different level of approximation needs to be taken into account. As stated before the Guidelines associate different confidence factors to different levels of detail, but in this first phase of analysis it is assumed equal to 1 for each survey level. Such a choice allows emphasizing the different results obtained with the different approaches. In the following the significance of the introduction of a proper confidence factor will be studied for each case.

3.7.6.1.1 Results from the application of the low detail survey

The low detail survey basically consists of an on-site measurement with common precision tools (such as a rule), followed by an approximation of the body with parallelepiped volume, as depicted in Figure 3.52 for the case of San Matteo:

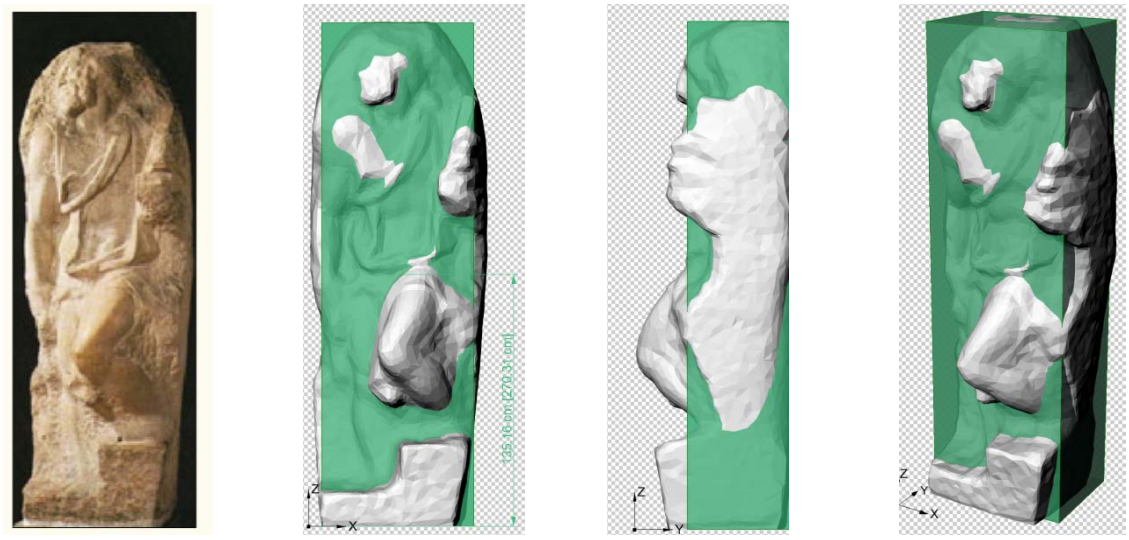

Figure 3.52 - equivalent block for San Matteo

The equivalent block closely resembles the object's shape and it facilitates to a quick application of the simplified formulas. Geometrical characteristic for the six statues are summarized in Table 3.7

Table 3.7 - simplified approach, geometrical features

	Bx [m]	By [m]	H [m]
"San Matteo"	0.76	0.60	2.72
"Pietà da Palestrina"	1.36	0.78	2.52
"Prigione Che Si Sveglia"	1.18	0.64	2.82
"Prigione il Giovane"	0.82	0.72	2.56
"Prigione Barbuto"	0.92	0.74	2.58
"Prigione Atlante"	1.16	0.90	2.78

Where B_x and B_y are the total dimensions of the base and H is the total height of the equivalent block; the following part is a detailed example of the application of the classical formulas to the case of the San Matteo, for brevity only results for the other statues of the case study will be given.

The position for the center of mass can be obtained as

$$h = \frac{2.720}{2} = 1.360\ m \tag{3.99}$$

$$b_x = \frac{0.76}{2} = 0.380\ m \tag{3.100}$$

$$b_y = \frac{0.60}{2} = 0.300\ m \tag{3.101}$$

By applying the formulas (3.9) the threshold values for the accelerations that limit the rocking phenomenon can be calculated along the two principal directions:

Directon x

Rest condition:

$$\frac{a_g}{g} < \frac{B}{H} = \frac{0.380}{1.360} = 0.279 \tag{3.102}$$

$$\frac{a_g}{g} < \mu_s \tag{3.103}$$

Sliding condition

$$\frac{a_g}{g} < \frac{B}{H} = 0.279 \tag{3.104}$$

$$\frac{a_g}{g} > \mu_s \tag{3.105}$$

Pure rocking condition

$$\frac{a_g}{g} > \frac{B}{H} = 0.279 \tag{3.106}$$

$$\frac{a_g}{g} \leq f(\mu_s) = \frac{(1+4\gamma^2)\mu_s - 3\gamma}{(4+\gamma^2) - 3\gamma\mu_s} = \frac{(1+4\cdot 3.623^2)\mu_s - 3\cdot 3.623}{4+3.623^2 - 3\cdot 3.623\cdot \mu_s} \quad (3.107)$$

$$\frac{a_g}{g} > \frac{B}{H} = 0.276 \quad (3.108)$$

$$\frac{a_g}{g} > f(\mu_s) = \frac{(1+4\gamma^2)\mu_s - 3\gamma}{(4+\gamma^2) - 3\gamma\mu_s} \quad (3.109)$$

Velocity of potential overturning (simplified formula)

$$V = 10\frac{2B_{TOT}}{\sqrt{2H_{TOT}}} = 10\cdot\frac{2\cdot 38.0}{\sqrt{2\cdot 136.0}} = 45.52\ \frac{cm}{s} = 0.455\ \frac{m}{s} \quad (3.110)$$

Direction y

Rest condition

$$\frac{a_g}{g} < \frac{b}{H} = \frac{0.30}{1.360} = 0.221 \quad (3.111)$$

$$\frac{a_g}{g} < \mu_s \quad (3.112)$$

Sliding condition

$$\frac{a_g}{g} < \frac{b}{H} = 0.221 \quad (3.113)$$

$$\frac{a_g}{g} > \mu_s \quad (3.114)$$

Pure rocking

$$\frac{a_g}{g} > \frac{B}{H} = 0.221 \quad (3.115)$$

$$\frac{a_g}{g} \leq f(\mu_s) = \frac{(1+4\gamma^2)\mu_s - 3\gamma}{(4+\gamma^2) - 3\gamma\mu_s} = \frac{(1+4\cdot 4.525^2)\mu_s - 3\cdot 4.525}{4+4.525^2 - 3\cdot 4.525\cdot \mu_s} \quad (3.116)$$

$$\frac{a_g}{g} > \frac{b}{H} = 0.221 \quad (3.117)$$

$$\frac{a_g}{g} > f(\mu_s) = \frac{(1+4\gamma^2)\mu_s - 3\gamma}{(4+\gamma^2) - 3\gamma\mu_s} \quad (3.118)$$

Velocity of potential overturning (simplified formula)

$$V = 10\frac{2b_{TOT}}{\sqrt{2H_{TOT}}} = 10\cdot\frac{2\cdot 30}{\sqrt{2\cdot 136.0}} = 36.41\ \frac{cm}{s} = 0.364\ \frac{m}{s} \quad (3.119)$$

Values of acceleration and velocity obtained this way have now to be compared to reference values of the seismic action, which for the return period of 712 years chosen for this case are: PGA = 0.27 g and PGV = 0.29 m/s. Results are summarized in Table 3.1

Tabella 3.1-critical actions and return periods for rocking, simplified model

	Rocking $a_{g,c}$[g]		Rocking Tr [years]	
	x	y	x	y
"San Matteo"	0.279	0.221	795.6	399
"Pietà da Palestrina"	0.540	0.310	>2475	1083
"Prigione Che Si Sveglia"	0.418	0.226	>2475	423
"Prigione il Giovane"	0.320	0.281	1379	791
"Prigione Barbuto"	0.357	0.287	>2475	860
"Prigione Atlante"	0.417	0.324	>2475	1509

Table 3.8 - critical actions and return periods for overturning, simplified model

	Overturning v_c[m/s]		Overturning Tr [years]	
	x	y	x	y
"San Matteo"	0.461	0.364	>2475	1600
"Pietà da Palestrina"	0.856	0.491	>2475	>2475
"Prigione Che Si Sveglia"	0.702	0.381	>2475	2136
"Prigione il Giovane"	0.513	0.45	>2475	>2475
"Prigione Barbuto"	0.573	0.461	>2475	>2475
"Prigione Atlante"	0.696	0.541	>2475	>2475

The equivalent body approach describes a situation of general safety for the statues, indeed the actions that lead to rocking phenomena are higher than the reference action except for the case of "*San Matteo*" and "*Prigione che si sveglia*" which may experience rocking even for events of lower intensity than the reference one. Overturning instead occurs for actions that are safely higher than the reference action.

3.7.6.2 Results from the application of the multi block approach

A possible definition of the object can be given by means of a multi block approach: the geometry can be approximated with a finite number of parallelepipeds that best fit the different parts of the body. The center of mass position and the dimensions to assume for the verifications are easily determined from the sum of the single blocks. It is reasonable to expect that the higher is the number of blocks the higher is the precision that can be obtained for the geometrical fitting; a good compromise between quality of the result and simplicity of the survey can be set from time to time, keeping in mind that this is still an approach for territorial analyses.

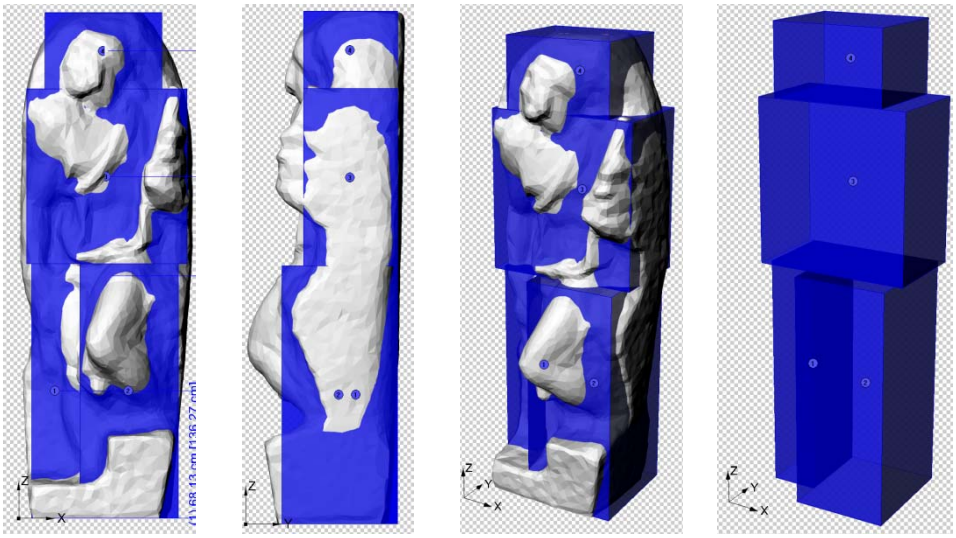

Figure 3.53 - multi block approximation for San Matteo

Some preliminary observations and remarks about the choice of the best approximation will be presented in the following:

A first application of this method is given for San Matteo statue, which was approximated by means of three different blocks as depicted in Figure 3.53. This first approximation was obtained with the objective to keep a good accordance between the real volumes, the characteristics of inertia and the absolute position of the center of mass. The comparison between the three accuracy levels, simplified, multi-block (MBlockHyp 1) and detailed, shows that, despite the fact that a higher geometrical precision (in terms of inertia , of the ratio between the inertia momentum and the mass I_r/m, of which the value for the weak direction is presented in Table 3.9) the multi-block approach can provide slightly less accurate results for overturning , for instance Figure 3.54 b), shows how the first multi-block approach for San Matteo statue does not provide a visible improving of the results in terms of rocking as regard to the simplified approach, but it even provides a less conservative level of critical velocity in terms of overturning .

According to this remark a different multi-block solution was tested: the second approximation was designed adding a block at the level of the base, with the purpose of keeping the same “base print” of the simplified block (0.76mx0.60m), in order to better describe the relative position of the center of mass with respect of the “base print”, maintaining at the same time a reasonable accordance between the inertial values and the detailed model (Table 3.9).

Results obtained with this approach are closer to the those obtained for the detailed model (if compared to the simplified model) with the second approximation hypothesis 2 (MBlockHyp2) .

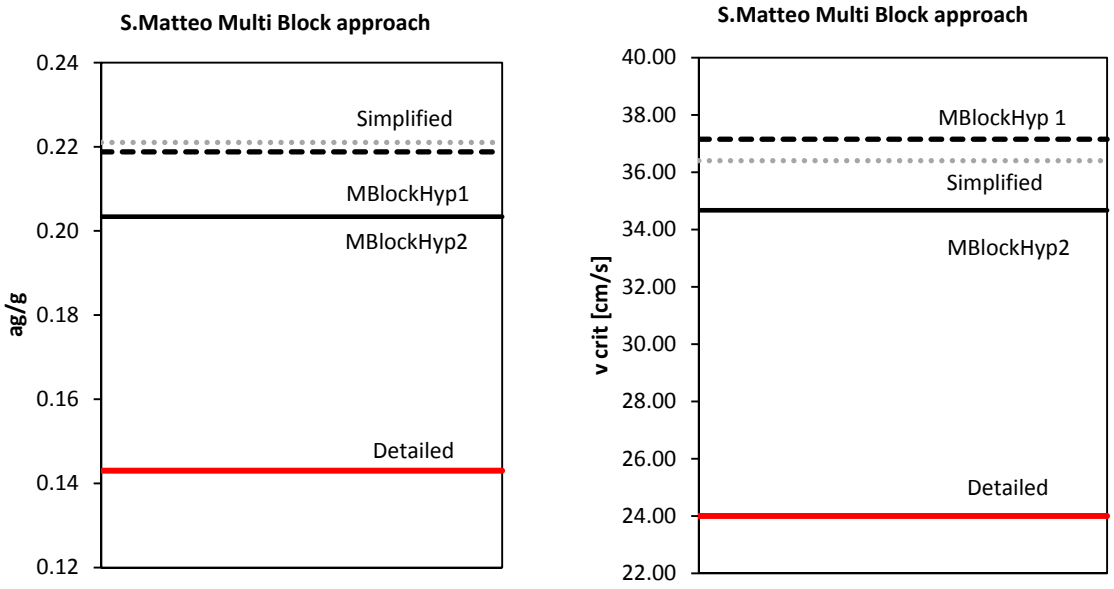

Figure 3.54 - comparison between different levels of accuracy: a) rocking; b) overturning.

Table 3.9 - comparison between different geometrical approaches for San Matteo statue

San Matteo	H [m]	by_2 [m]	Ir/m	v_{crit} [m/s]
Simplified	1.36	0.3	2.586	0.36
Hp 1	1.317	0.288	2.422	0.37
Hp 2	1.349	0.274	2.501	0.34
Detailed	1.325	0.189	2.380	0.240

Some preliminary remarks can be done considering the above presented results:

First of all it is worth noting that the application of more complex geometrical models (e.g. approximation with 3 blocks instead of a single element) does not necessarily lead to a more accurate evaluation of the safety conditions of the target object, but it can even lead to less conservative results. Furthermore the improving in the quality of the results obtained with a more accurate description, given by a higher number of blocks (for instance: switching from a single block to a three blocks approach) provides a variation of the critical velocity of only the 2%. Obviously a more accurate geometrical description leads to a better interpretation of the problem, but it could not justify the greater computational costs, as in the case of switching from a single block to a three blocks approach.

A correct evaluation of the relevant parameters involved in the problem is hence fundamental. The most meaningful features that need to be fitted are: inertia of the object, height and relative position of the center of mass as regard to the “base print”. It is interesting to highlight that, in the description of rocking phenomena, height and position of the center of mass are involved as a ratio, and it is hence necessary to assess their “coupled” variation. It becomes a hard task to define if and when a model can be considered “more detailed” than another or in other terms when a survey has to be considered actually more detailed than another.

On the basis of these first observations it can be stated that, in this type of analyses, the application of apparently more detailed models is not warranty of a result closer to reality. It is hence not correct to assume the confidence factors that correspond to the higher level of knowledge assumed since they would lead to a further and not justified reduction of the safety level.

3.7.6.3 Results from the application of the 3D laserscanner survey

The most detailed level available for the survey is the one obtained from the application of the innovative laser scanning technology. Such a survey allows to determine all the geometrical and inertial features of the object, with a much higher level of accuracy, close to the millimeter; such a detailed survey, though, is not always available and, in most of the cases in which a quick and wide scale analysis is required, it is even unaffordable. It is however interesting to apply this technique, as a measure of the sensitivity of the method to the quality of the measurements. An example of its application is given for the statue of San Matteo, whose render of the detailed survey is given in Figure 3.55.

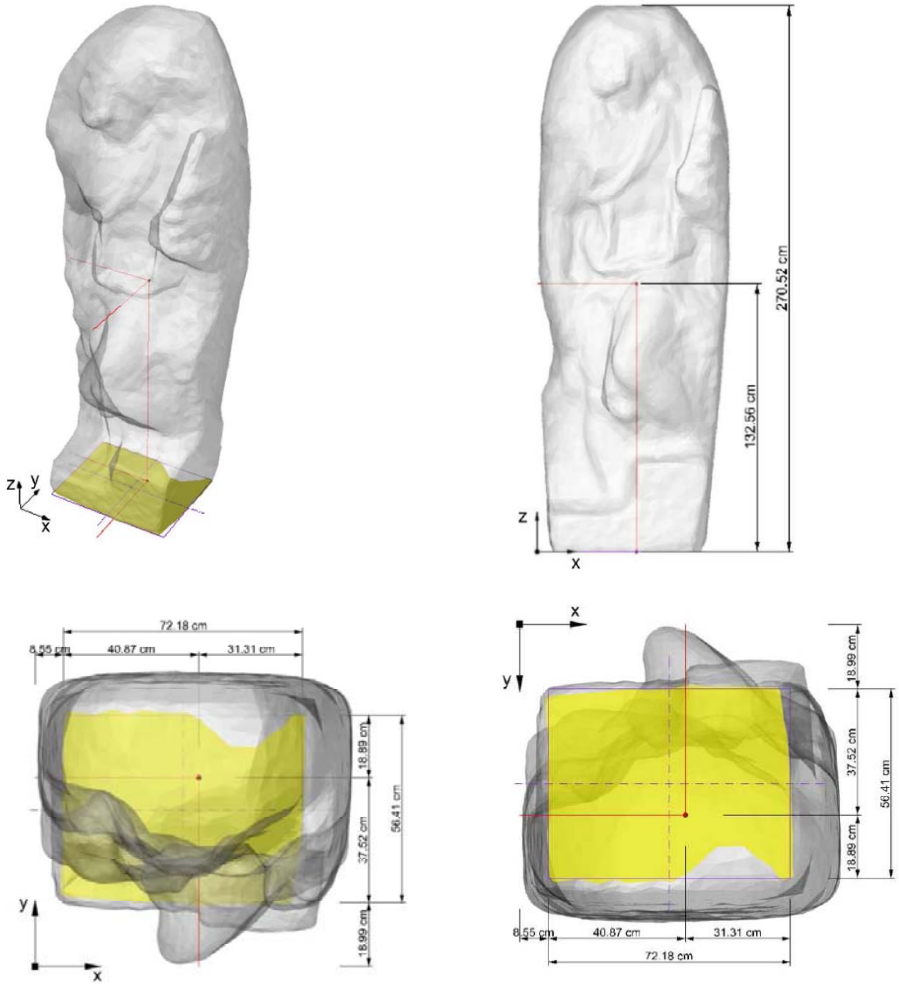

Figure 3.55 - San Matteo render of the 3D laserscanner survey

Considering the detailed survey the geometrical features of the statue are summarized in Table 3.10, where b_x and b_x' denote the horizontal projection along x direction of the distance between the center of mass and the base corner.

Table 3.10 - geometrical features from the detailed survey

	bx [*m*]	**bx'** [*m*]	**by** [*m*]	**by'** [*m*]	**h** [*m*]
"San Matteo"	0.409	0.313	0.375	0.189	1.326
"Pietà da Palestrina"	0.448	0.575	0.409	0.255	1.163

	bx [*m*]	bx' [*m*]	by [*m*]	by' [*m*]	h [*m*]
"Prigione Che Si Sveglia"	0.500	0.496	0.426	0.295	1.175
"Prigione il Giovane"	0.348	0.341	0.547	0.296	1.096
"Prigione Barbuto"	0.358	0.264	0.532	0.294	1.290
"Prigione Atlante"	0.557	0.567	0.404	0.260	1.290

The expressions used above for the evaluation of the critical acceleration that causes rocking can be applied in this case as well. Since in this case two verifications are needed for each side four total critical values of acceleration can be obtained. For reasons of brevity only the worst condition for each side is given in Table 3.11

Table 3.11 - critical accelerations for the detailed model

ROCKING	$a_{gc,x}$ [*g*]	$a_{gc,y}$ [*g*]	Tr x [years]	Tr y [years]
"San Matteo"	0.236	0.143	500	131
"Pietà da Palestrina"	0.385	0.219	>2475	388
"Prigione Che Si Sveglia"	0.422	0.251	>2475	568
"Prigione il Giovane"	0.311	0.270	1147	697
"Prigione Barbuto"	0.205	0.228	330	432
"Prigione Atlante"	0.437	0.202	>2475	313

For the evaluation of overturning critical events the afore mentioned formulas need, as it is mentioned in 3.6.1.2.2,to be modified with the introduction of the inertia moments about the rocking axes of each side – namely *x*, *x*', *y*, *y*' – from these values the equivalent heights for the evaluation of the limit velocity $V^* = V_{lim}$ were calculated : important features are summarized in Table 3.12:

Table 3.12 - equivalent height for detailed models

OVERTURNING	**h' [m]**			
	x	**x'**	**y**	**y'**
"San Matteo"	1.224	1.259	1.249	1.302
"Pietà da Palestrina"	1.024	0.963	1.077	1.136
"Prigione Che Si Sveglia"	0.947	0.949	0.859	0.958
"Prigione il Giovane"	0.949	0.951	1.003	1.048
"Prigione Barbuto"	1.180	1.209	1.100	1.190
"Prigione Atlante"	1.065	1.068	1.142	1.181

Table 3.13 - overturning critical velocities and return periods

OVERTURNING	v_c [m/s]					Tr [years]
	x	x'	y	y'	min	min
"San Matteo"	0.53	0.40	0.49	0.24	0.24	450
"Pietà da Palestrina"	0.64	0.85	0.57	0.35	0.35	1353
"Prigione Che Si Sveglia"	0.51	0.51	0.85	0.44	0.44	>2475
"Prigione il Giovane"	0.74	0.74	0.62	0.42	0.42	>2475
"Prigione Barbuto"	0.48	0.35	0.73	0.39	0.35	1353
"Prigione Atlante"	0.79	0.78	0.55	0.37	0.37	1752

The application of this level of detail shows diffused problems of rocking. Each object has at least one direction along which the triggering of oscillations begins for an action characterized by a return period lower than the reference one, according to the Artistic Limit State set (Tr = 712 years). Overturning, on the other hand, occurs only in the case of San Matteo, along the y direction, this means that the Ultimate Limit State is exceeded in only one situation.

3.7.6.4 Presence of vertical action

This paragraph shows how the effect of a vertical motion, combined with the horizontal one, can influence the response of the object in terms of critical action that leads to rocking. The formulas in section 3.6.1.2.3 were applied assuming the direction of the vertical action is that it depicts the worst scenario for the object, iterations with the method described in 3.2.2 are then performed in order to obtain the return period of the critical action. Results for the detailed model are summarized in the following.

Table 3.14 - effects of vertical action on rocking, detailed model

ROCKING	Horizontal action		Horizontal + Vertical action	
	Tr x [years]	Tr y [years]	Tr x [years]	Tr y [years]
"San Matteo"	500	131	368	117.7
"Pietà da Palestrina"	>2475	388	1272	313
"Prigione Che Si Sveglia"	>2475	568	1830	420.8
"Prigione il Giovane"	1147	697	699.6	494
"Prigione Barbuto"	330	432	269	341
"Prigione Atlante"	>2475	313	2009	260

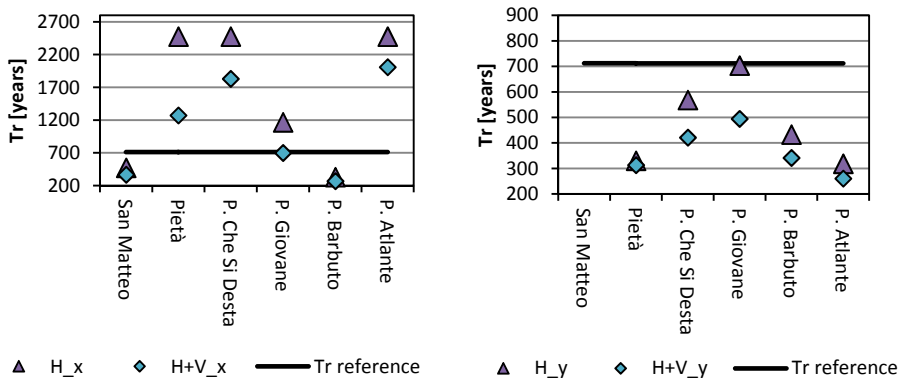

Figure 3.56 effect of vertical action in rocking, detailed model, a) x direction, b) y direction

Figure 3.56 shows the effect of the presence of vertical action; the limit of 2475 was assumed for the cases in which the threshold is overcome, the contribution of vertical acceleration, for the detailed model shows a general worse condition, in general attention should be focused for all those situations in which considering or not the presence of the vertical acceleration gives a either a safe condition or a critical condition.

3.7.6.5 Results comparison

A first interesting comparison between the two opposite methods is the one about the increasing of the critical events when a more detailed method of survey is used: the quick survey indeed, shows potential rocking problems for the statues of "*San Matteo*" and for the "*Prigione che si sveglia*", and none of them shows to have possible overturning problems. On the contrary results given by the application of the detailed survey, show that the statues can suffer potential rocking problems in every single situation and overturning only for the case of "*San Matteo*". However the choice for a more detailed level of survey does not imply in general a worse condition of safety: the different response is indeed ruled by the distribution of mass of the object. For instance a more detailed survey leads to a worse condition (i.e. lower critical return period) when the body is tapered with narrow base and wide top, but, on the contrary, in the case in which the body is tapered with a wide base and narrow top the passage from rough to detailed survey can lead to a safer condition (i.e. higher critical return period). This is visible for the case of "*Schiavo Giovane*" whose critical events for rocking are characterized by a return period of 405 years and 568 years respectively using the equivalent block and the detailed survey. This is an important aspect to be considered, because the choice for the approach relevantly affects the reliability of the results, but it is also true that the target of the analyses cannot be forgotten at all: it is clear that the laserscanner survey allows a very high precision in the definition of the geometry that reflects in a higher precision of the seismic safety assessment, but it is also unaffordable to adopt this technique for a large number of analyses such as for a territorial approach (which is the target of LV1 level). On the other hand results just shown underline that an approach with the equivalent block introduces such a high number of uncertainties that it is inapplicable unless results are not reduced with a proper confidence factor. It is also worth noting that the equivalent block approach is very sensitive to the "user": different surveyors can come out with very different results in terms of equivalent blocks of the same object.

3.7.6.6 Comparison between the simplified method and the reference norm

As this research aims to extend the principles and criteria of the Guidelines developed for masonry structures, it is interesting to compare the simplified formulas described in the previous part and the criteria given by the standards, about global equilibrium analyses for masonry structures.

The approaches proposed by the standards are two. The first one is a linear approach that aims to obtain the critical acceleration that leads to the definition and activation of a labile mechanism on a masonry structure, the so called "*linear kinematic analysis*".

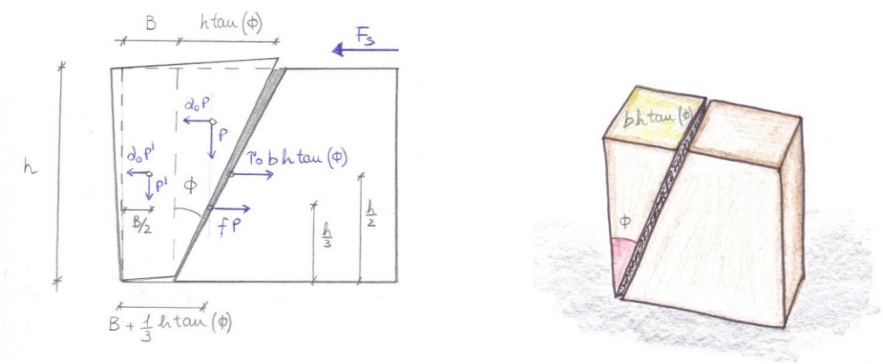

Figure 3.57 - forces involved in the linear kinematic analysis

The object of the "linear kinematic analysis" is to identify the critical multiplier for the seismic action that provides the triggering of motion in a part of it. By means of equilibrium relations the multiplier of the horizontal action α_0 is defined for the three main different phases of the phenomenon:

triggering: $$\alpha_{0i} M_s + M_{est} = M_{rc} + M_{ra} \quad (3.120)$$

cracking: $$\alpha_{0f} M_s + M_{est} = M_{ra} \quad (3.121)$$

collapse: $$\alpha_{0c} M_s + M_{est} = M_{rf} \quad (3.122)$$

With reference to Figure 3.57 M_s is the moment due to the seismic action (α times the vertical loads P, P'), M_{est} is the moment due to external forces, M_{rc} is the resisting moment due to cohesive forces (depending on the stress τ_{0d}), M_{ra} is the resisting moment due to friction and M_{rf} is the resisting moment due to the actual shape of the mechanism.

The critical multiplier for overturning is assumed to be the maximum between the triggering one and the collapse one, since that referred to cracking is always lower than the triggering one; the evaluation of the capacity of the mechanism can also be reached with the application of the virtual works principle. However, since the aim of this work is not to give an overview of the standards' approaches, it will be not described in detail.

Once the capacity is evaluated the demand must be defined as well, in order to compare them and obtain the assessment of the condition of the object. The standards give the definition of both a serviceability limit state and an ultimate limit state defined as:

$$a_0^* \geq a_g(P_{V_r}) S \quad (3.123)$$

with a probability of exceeding of 63% during the reference life, for an object placed on the ground level; this first method, sets the triggering of a mechanism and its equivalent to the West formula applied before, which also comes from an equilibrium condition of the system for the rotation about a point. On the other hand the possibility to use this approach to describe other critical phenomena, such as overturning, are given by means of the coefficient q;

$$a_0^* \geq \frac{a_g(P_{V_r}) S}{q} \quad (3.124)$$

with a probability of exceeding of 10% during the reference life, for an object placed on the ground level; q represents the behavior factor, which takes into account the "reserves" of the object in the non linear field, before the global equilibrium is lost; hence the introduction of the coefficient q is a way to define an overturning limit from the condition of triggering of rocking. This coefficient is very important because it accounts the reserves that an object with triggered rocking has, before reaching the limit point. It can then be compared to the approach that was mentioned so far as "Ishyiama's"; it is worth noting that its definition is as much important as delicate and further considerations will be given in the following.

The second approach, that can be compared to the afore presented method concerns the considerations about overturning. It is the so called "*non linear kinematic analysis*", which considers the evolution of the mechanism after the

triggering until the loss of global equilibrium. The two limiting situations for this method are the triggering of the mechanism and the loss of global equilibrium. The behavior of a control point, in terms of displacements, is given from the initial configuration (triggering) to the deformed limit configuration (ultimate displacement); the behavior is characterized by the increasing of the displacements and, at the same time, by the reduction of the multiplier of the seismic action (3.70).

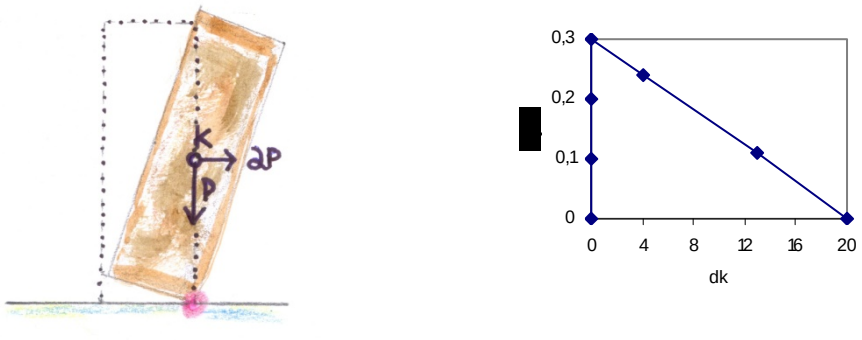

Figure 3.58 - non linear kinematic analysis, sketch

The critical action needs to be evaluated, the evolution of the mechanism can be depicted in a chart (d_k,α) (Figure 3.58), where d is the displacement of the check point and a is the seismic load multiplier. The reference changes from α to α*, so that a verification can be carried out on the plane (d*,α*) for an equivalent single degree of freedom system. After this the ultimate displacement is calculated as well as the period T_s; once the system is defined the real verification can be carried out with the comparison between the seismic demand and the capacity of the structure. In order to give a clearer overview of the procedure it will be summarized in the following:

- Evaluation of the activation multiplier α_0;
- Definition of the check point: in general it is the center of the system of acting forces;
- Evaluation of the displacement $d_{k,0}$:

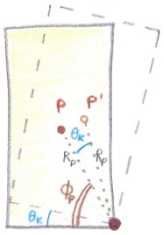

Figure 3.59 - evaluation of displacement dk

it is the displacement obtained from the virtual works principle assuming a = 0 and then solving for the incognita $q_{k,0}$;

- Conversion of $d_{k,0}$ into d_0* and a_0 into a_0*:

$$d^* = d_k \frac{\sum_{i=1}^{n+m} P_i \delta_{X,i}^2}{\delta_{X,K} P_i \delta_{X,i}} \tag{3.125}$$

$$a^* = \frac{a_g}{e^* FC} \tag{3.126}$$

- Definition of the capacity curve a*-d*:

$$a^* = a_0\left(1 - \frac{d^*}{d_0^*}\right) \quad (3.127)$$

- Evaluation of the ultimate displacement du*: du* is the minimum displacement between 40% of d_0* and a limit set in the design phase by the designer.
- Evaluation of the period Ts: this requires to evaluate $d_s^* = 0.4\, d_u^*$, $a_s^* = a_0^*\left(1 - \frac{d_s^*}{d_0^*}\right)$ then $T_s = 2\pi\sqrt{d_s^*/a_s^*}$
- Comparison between demand and capacity: verification, as in this case, at ground level $d_u^* \geq S_{D_e}(T_s)$, and $S_{D_e}(T) = S_e(T)\left(\frac{T}{2\pi}\right)^2$

Since this work proposes the extension of an existing standard to the case of art objects the results obtained with the methods used in the norms need to be compared to those here proposed, in order to understand the effective correlation and accordance between the two. Indeed, since the problems are different but with many common points, the results are expected to be similar. Figure 3.62 shows the results for the *non linear kinematic analysis* obtained from a comparison between the results of the *linear kinematic analysis* proposed by NTC and the results obtained with the application of Ishyiama formulas. Concerning these relations, in particular, it was assumed as reference velocity for the seismic action both the relation (3.2) from NTC standards and relation (3.3) proposed by Bommer. Moreover, for the *linear kinematic analysis* a value of q = 2 was assumed. Particular attention needs to be given to the comparison between the proposed method for overturning evaluation, which in fact gives as a result a critical value of velocity, and the *non linear kinematic analyses*.

A comparison between the results obtained from the different methods is presented in the following as charts:

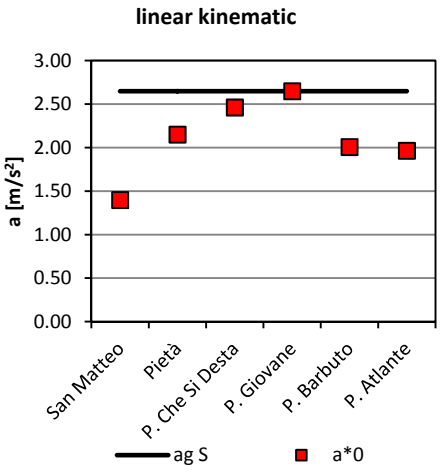

Figure 3.60 - Oscillations triggering with linear kinematic analysis

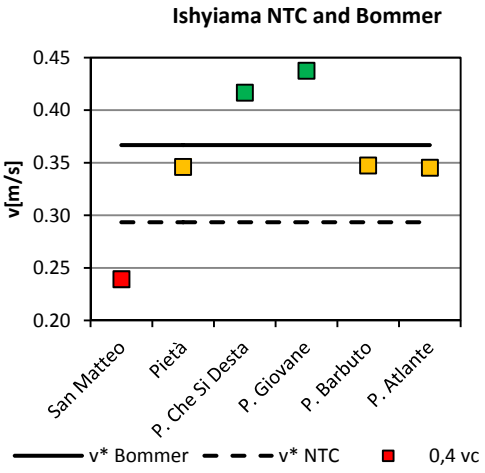

Figure 3.61 - Overturning results , NTC vs Bommer

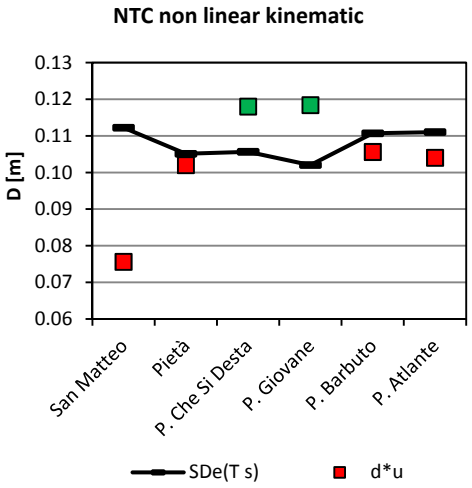

Figure 3.62 - Overturning results, non linear kinematic approach

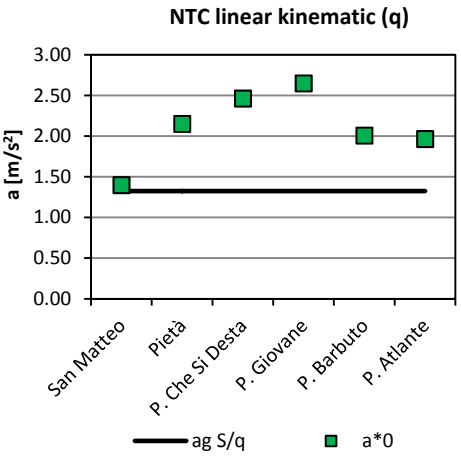

Figure 3.63 - Overturning results, linear kinematic approach with factor q

From the comparison of the two approaches of overturning, as shown by the graph of Figure 3.61, slightly different results were obtained. The comparison between the two reference values, the NTC one and Bommer's one, show that the choice for a more cautionary action can, as expected, give more critical results. There are three cases in which the choice for one reference action or the other makes the difference between a critical situation and a safe situation.

There is instead good accordance between the Ishyiama approach with Bommer reference velocity and the "*non linear kinematic analyses*" (Figure 3.61 and Figure 3.62): the objects satisfy at the same time both the criteria, while great differences appear when the "linear kinematic" approach is considered for ultimate limit state. Indeed from Figure 3.63 it can be remarked that none of the statues seems to suffer problems of overturning. Even for the case of San Matteo, which was found to be in an unsafe situation with all the other approaches applied, the result is very close to the limit but still positive.

This macroscopic difference is mainly due to the coefficient q that in this phase was applied in accordance to the NTC standards for masonry (33) which assumes for it the general value of q = 2, as a result of experimental tests conducted on masonry walls. The obtained results suggest that the behavior factor q for this type of objects should be suitably evaluated. Before introducing the proposal for the evaluation of the coefficient q more considerations about the differences between the above described methods could be made. The different relationships that describe the overturning criteria can be written in the form:

non linear kinematic analysis :

$$\frac{B}{\sqrt{H}} \geq 0.416\, a_g S\, T_c/\sqrt{g} \qquad (3.128)$$

Ishyiama method (NTC reference action) :

$$\frac{B}{\sqrt{H'}} \geq 0.346\, a_g S\, T_c/\sqrt{g} \qquad (3.129)$$

Ishyiama method (Bommer reference action) :

$$\frac{B}{\sqrt{H'}} \geq 0.433\, a_g S \frac{T_c}{\sqrt{g}} \qquad (3.130)$$

With H'=H in case of slender symmetric rectangular blocks.

Figure 3.64 shows for the statues of the case study, with the simplified approach: the lines represent the threshold of the criteria (3.128)-(3.130) in the plane $B - \sqrt{H}$. The markers show the different conditions of the statues: according to their position with respect of the limits it can be stated whether they satisfy or not the verification.

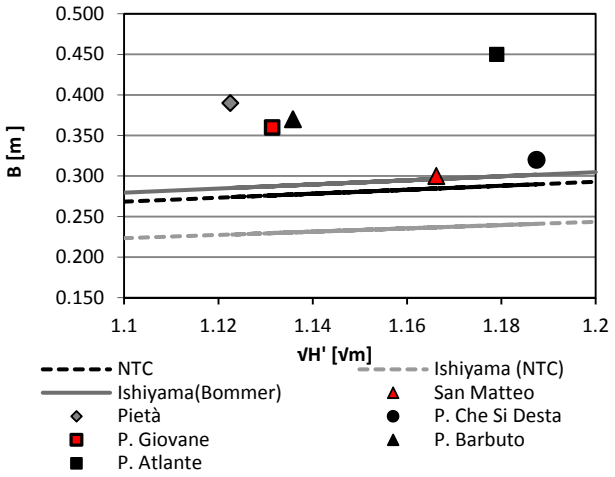

Figure 3.64 - overturning: comparison between approaches, simplified survey

The graph confirms that for rectangular bodies results obtained with NTC non linear kinematic are in good accordance with those obtained with Ishyiama-Bommer velocity criterion. Furthermore it can be remarked that Ishyiama-NTC velocity criterion is less conservative.

It is worth noting that, in case of non symmetric bodies, relation (3.128) takes into account only the position of the center of mass and not the inertia (and consequently the shape) of the object, while the (3.129) and (3.130) include the effect of inertia by means of effective height H'.

3.7.6.7 The behavior factor q in the linear kinematic approach

It was previously pointed out that the linear kinematic approach provides results for overturning that in general do not fit the other approaches; this is due to the behavior factor *q* which comes from experimental results on masonry walls. It is also clear from the results summarized in this part, that an application of a behavior factor of 2 does not assure results on the safe side. It is hence necessary to investigate the possible values to give to q in order to obtain reasonable results. The best value of q was researched in order to obtain, from the linear kinematic analysis, results in accordance with the other methods for each statue:

- San Matteo : $\mathbf{q_{lim}}$ = 1.85;

- Pietà : $\mathbf{q_{lim}}$ = 1.23;

- P. Barbuto : $\mathbf{q_{lim}}$ = 1.32;

- P. Atlante : $\mathbf{q_{lim}}$ = 1.35;

In order to obtain results comparable to the "*non linear kinematic*" analyses, for the statues that do not satisfy the verifications, it is necessary to assume $q < q_{lim,gl}$, where $q_{lim,gl} = \min(q_{lim}) = 1.23$. The same procedure applied for the two statues that satisfied the verifications with both methods allows to calculate the lower limit for the coefficient *q* in particular the P. Giovane was considered which requires $q = 1$ for setting the accordance between the two methods .

The coefficient q has then to be :

$q_{inf} = 1 < q < 1.23 = q_{lim,gl}$

A further possible way to determine the best behavior factor for the accordance between linear and non linear kinematic approach is a "minimum difference" method. It consists in evaluating the behavior factor that is necessary to keep the same level of safety between the two methods, by writing the expression

$$\frac{a_g S}{q a_0^*} = \frac{S_{D_e}(T)}{d_u^*} \tag{3.131}$$

calculating the value of q from it as

$$q_{marg} = \frac{d_u^*}{S_{D_e}(T)} \frac{a_g S}{q a_0^*} \tag{3.132}$$

Results obtained are summarized in Table 3.14 and Figure 3.65

Table 3.15 - minimum difference q factors

	q_{marg}
San Matteo	1.28
Pietà	1.19
P. Che Si Desta	1.20
P. Giovane	1.16
P. Barbuto	1.26
P. Atlante	1.26

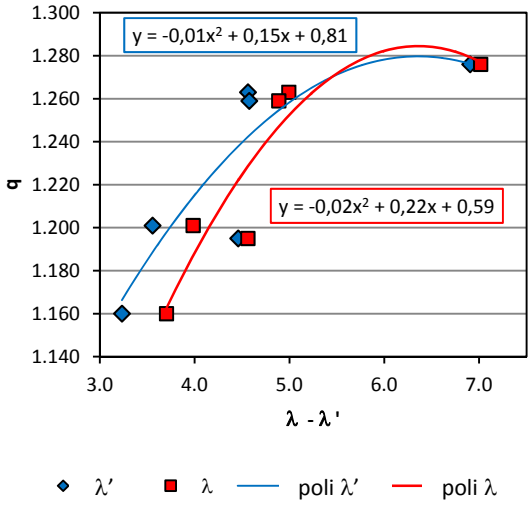

Figure 3.65 - q factor versus slenderness, detailed model

Figure 3.65 shows the general trend of the behavior factor q_{marg} for the different statues according to their slenderness $\lambda = H/B$. As it can be observed from the graph, factor q varies between 1.16 and 1.28, following the proposed interpolating functions. Figure 3.65 also depicts the results according to the value of $\lambda' = H'/B$ in order to consider the possible non symmetry of the object. Also in this case a proposal of interpolating function is presented.

3.7.6.8 Effects of errors in measurements and survey

As it was already pointed out the quality of measurements is a very important aspect for the assessment of the vulnerability, in particular when simplified methods are applied; it was just shown how different approaches and levels of detail affect the critical values of the action and as a consequence the safety of the object; nonetheless surveys can be affected by numerous types of errors: measurements errors, rendering errors and errors, or better effects, due to different choices in the assumption of the geometric model (e.g. equivalent block). The "human component" is important as well: different operators can measure different values of the same feature.

For these reasons some sensitivity analyses were performed for investigating the effects of errors in the model. These analyses are a first preliminary approach to the issue of the confidence factor.

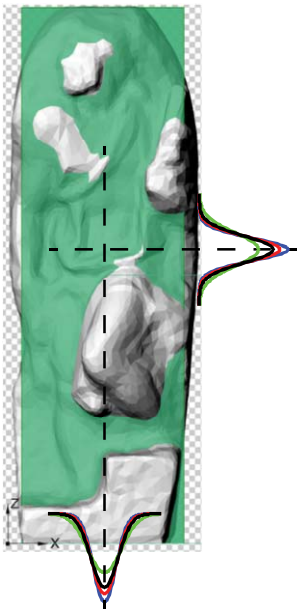

Figure 3.66 - San Matteo equivalent block, errors

In this paragraph this aspect is investigated with particular attention to the equivalent blocks that, for the characteristic of the survey, can suffer more of errors. Some analyses were carried out assuming a systematic variation of the dimensions B and H of the rectangular block. The assumed levels of variability are 1%, 2% and 5% of the dimensions, in order to define a worse scenario, i.e. reduction of the base dimension and increment of the height were assumed.

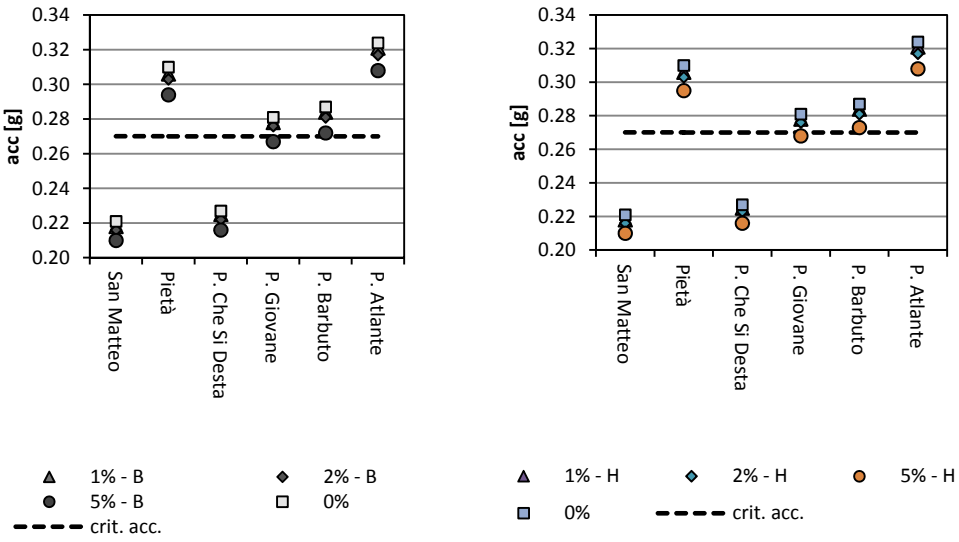

Figure 3.67 - Effects of dimensions variation on rocking and comparison with the critical velocity

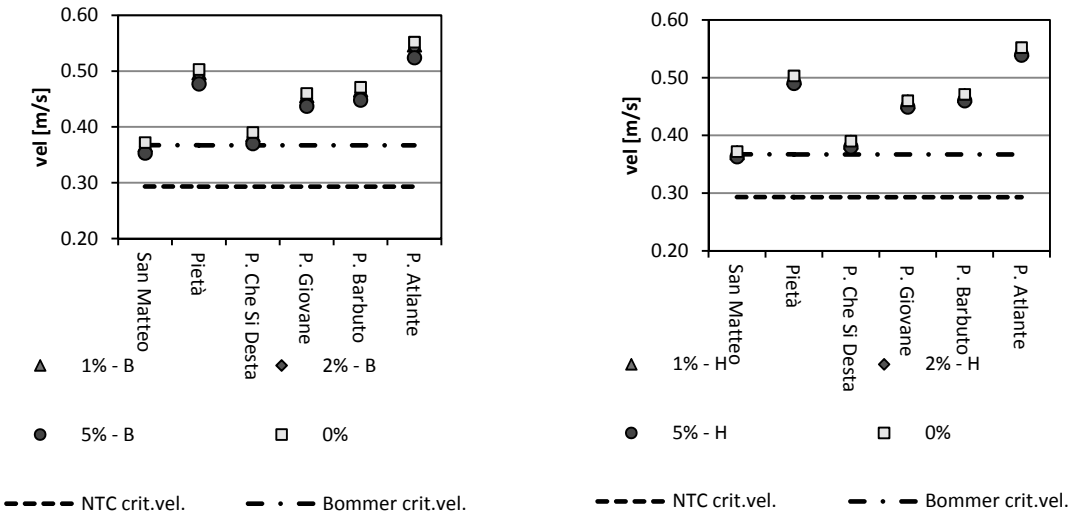

Figure 3.68 - effects of dimensions variations on overturning (NTC)

Graphs depicted in Figure 3.67 and Figure 3.68 show the different conditions of the statues, described with their equivalent blocks, in respect to variations of dimensions, in terms of rocking (Figure 3.67) and overturning (Figure 3.68). The dashed lines mark the threshold between the "safe" and "unsafe" condition. It is worth noting that a variation of 1 %, both for width and height, does not give significant variations in the response, as well as the 2% difference; first remarkable effects can be pointed out for the 5% variation, in particular for the rocking phenomenon, and only in the situations in which the condition is close to the threshold.

3.7.7 Application of the numerical integration to the case study

The tool developed for the direct integration described of the equations of rocking in the previous part was used to investigate the response of the single statues under the effect of different earthquakes. This is a purpose that goes further than the LV1's one of a territorial approach; moreover an application of the same method can be used for a large scale approach.

3.7.7.1 Application for the dynamic response of a single body

The method of the direct integration can be used, as previously stated, for determining the dynamic response of a single body for a given seismic input, this allows not only to understand whether a dynamic phenomenon will occur or not, but also to have information about the intensity of oscillations, their frequency and amplitude. This interpretation can be useful if the relation between rocking motion and the exceeding of the Artistic Limit State is reminded; indeed it was already mentioned that oscillations may induce damage on the object. It is hence clear that the more this phenomenon is intense the higher is the potential damage.

3.7.7.1.1 Numerical integration for the San Matteo:

Since the statue of San Matteo came out to be the one with the most critical situation, in terms of rigid body phenomena, it was used as first example for the application of the direct integration method: set of seven earthquake records was generated by SIMQKE (25), compatible with the response spectrum of the site of the case study for a return period of 1600 years, which, as obtained by the simplified analysis, may cause overturning of the body assumed as the equivalent symmetric body. In Figure 3.69 the results for this first analyses are plotted: each graph represents the time response due to a single earthquake input in terms of ratio between the rotation angle θ and the critical angle α_c, over which the body is considered tilted; the two lines (red and blue) are obtained from the application of the same input in the two possible directions, since it is not possible to decide "a priori" which will be the direction of the earthquake, it is taken into account as an envelope. It is worth noting that, since the body is symmetric, the responses in the two directions are symmetric as well. Results are in general of diffused rocking with two events of overturning. The possible interpretation, from the limit state point of view, is that, whenever rocking is experienced the Artistic Limit State is exceeded, and when the ratio θ/α_c reaches the value of 1 then the Ultimate Limit State is exceeded.

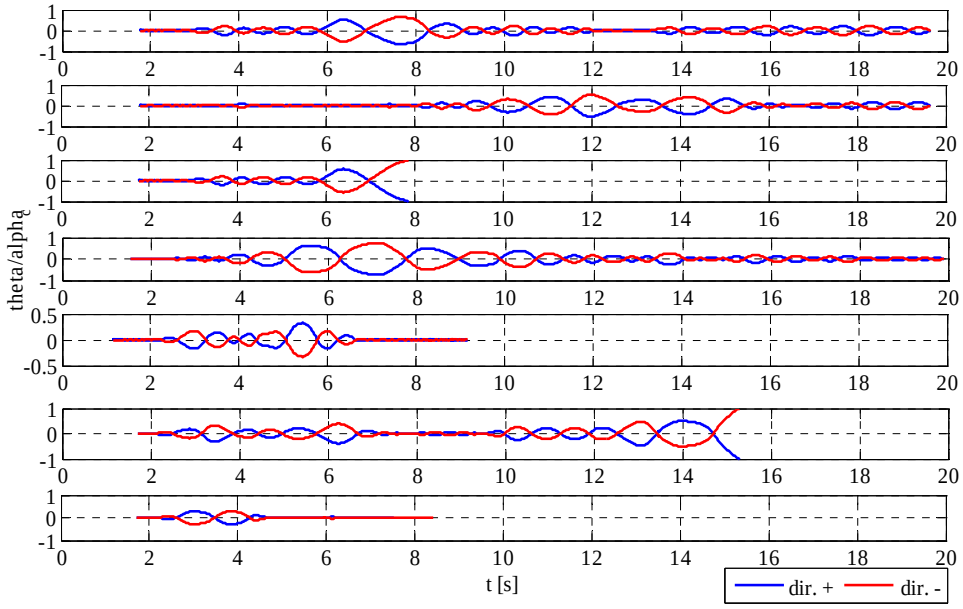

Figure 3.69 - time history response for the San Matteo equivalent block, Tr = 1600 years

Let consider the same set of accelerograms, always compatible with a response spectrum with return period of 1600 years, but this time the object to study is the San Matteo, statue considered as non symmetric. Results are given in Figure 3.70:

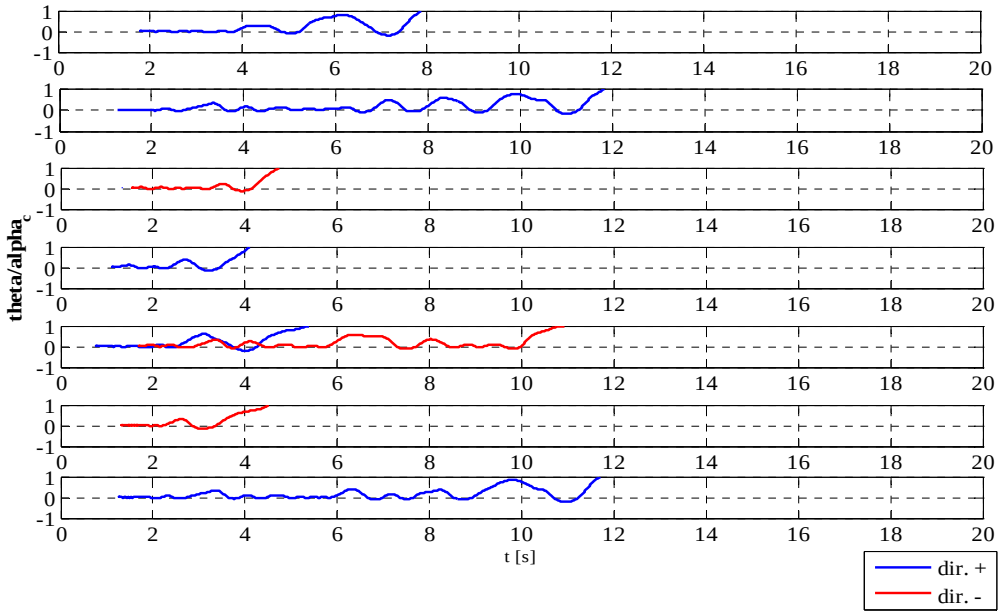

Figure 3.70 - time history response for the non symmetric San Matteo, Tr = 1600 years

In this case results show the occurrence of overturning for every single envelope of the events, as it was expected. In fact the application of the detailed survey to simplified formulas gave as a result for the overturning period of the statue of San Matteo a value of 450 years. As in the previous case the two lines, blue and red, represent the application of the same input with opposite direction; it is interesting noting that there is not a preferential direction for the application of the input that points out a worse scenario, but a remark can be made about the direction of overturning: the ratio θ/α_c always reaches the value of 1 (i.e. the Ultimate Limit State) in the same half plane, in this case the positive one. This means that the object overturns always on the same side, which is the weakest one. It is also interesting noting how, in response number 5 the same earthquake can induce overturning if applied in both directions

but with a much longer oscillation phenomenon in one of the two directions. For the other six inputs only one response is shown, because the opposite direction of application does not produce any relevant dynamic phenomenon.

Some other results are presented, keeping the focus on the more detailed level of survey, for a set of accelerograms compatible with a spectrum with 475 years of return period. This level of action is the one that came out to be the critical one for the non symmetric approach for the San Matteo; the procedure of analysis is the same described above and the responses for the seven accelerograms are depicted in Figure 3.71:

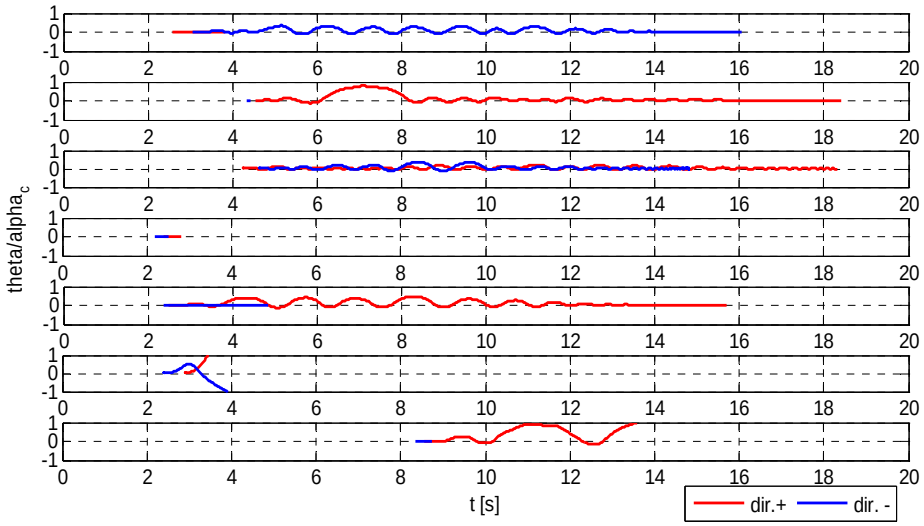

Figure 3.71 - time history response for the non symmetric San Matteo, Tr = 475 years

The responses of Figure 3.71 show diffused phenomena of rocking with wide amplitude of oscillations, response number 2, for instance, shows a wide oscillation in the beginning phases of motion which almost reaches the rotation necessary for tilting the body. Although the Ultimate Limit State is not exceeded such a situation can cause serious damage to the object which falls back and impacts with the ground, with a potential high level of damage. It is worth noting that while exceeding the Ultimate Limit State is, from a point of view, the overcoming of a limit, exceeding the Artistic Limit State and its definition for this particular case, can assume a wider meaning, connecting the amplitude of the oscillation to the level of damage for the object. Other remarkable situations are represented in the above mentioned graph: for instance for two events the object experiences overturning and, in one of the two, tilt happens along both directions. These result well fit the expectations in terms of response prediction.

After this first series of analyses, which only included horizontal acceleration as input, a further series of analyses including vertical action were performed. As it was already mentioned in this work, the influence of the vertical action on rigid bodies, in particular when they are non symmetric, can be significant and it has not been widely studied in technical literature. The importance of the vertical action becomes even greater if considered that, records of recent earthquakes happened all over the world, showed vertical components often bigger than the reference actions given by the codes. The dynamic behavior of rigid bodies subjected to both horizontal and vertical acceleration input was already studied in literature (7) but the studies did not underline any general trend in the response change.

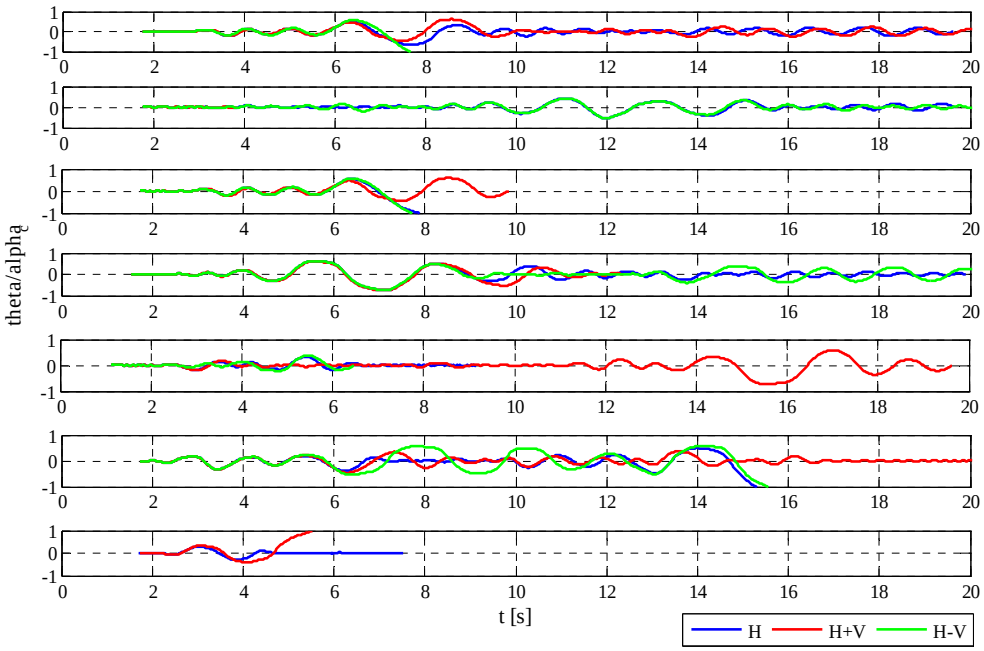

Figure 3.72 - time history response with vertical action for the non symmetric San Matteo, Tr = 1600 years

The graphs depicted in Figure 3.72 give the responses for the equivalent block of the San Matteo subjected to an input with the same characteristics of the one used for the example of Figure 3.69, but including also a vertical component, compatible with a vertical response spectrum with the same return period of the horizontal. Since the body is symmetric the horizontal action is considered only in one direction, while the vertical action is considered as an envelope. The blue line in the graphs is the response to the only horizontal component, while the red and green lines represent respectively the response to the combined actions horizontal plus vertical and horizontal minus vertical. From the results it can be observed that the envelope of the responses with the vertical actions often defines a worse scenario for the seismic response of the body, but this cannot be taken as a general trend. Indeed there are situations in which the vertical action causes overturning, where the horizontal one only caused rocking, for instance the responses 1 and 7; in other cases the effect of the vertical action does not induce directly the overturning but just makes it occur earlier (i.e. response 3). Furthermore in other events the vertical action does not affect the overturning response but it only increases the amplitude of rocking oscillations, as it is visible from response 2, 3 and 4. Despite the fact that a precise trend is not pointed out from this example it is anyway important to properly consider the presence of the vertical action because it can induce worsening conditions in the object.

If the detailed survey for the statue of San Matteo is considered, with the same set of accelerograms used for the rough model (1600 years), as well as the presence of vertical acceleration and in the case of non symmetric body a wider set of situations has to be taken into account. The dynamic response needs to be studied assuming the seismic input acting along both the main directions of the object. It can be remarked that, the presence of a vertical action also in this case, as it was previously stated, leads to a worsening condition for the stability of the object; in Figure 3.73 and Figure 3.74 the results of analyses with compatible vertical actions are presented: the vertical accelerogram adopted is the same for all the analyses set, all the horizontal actions were considered acting in the two possible directions. In many cases the results presented represent only one direction, this means that the result along the other one was not interesting for these considerations. The blue lines depict the response of the body subjected to the horizontal action only, the green and red lines, instead, depict the response of the body subjected to the horizontal action and the vertical action taken, respectively with the positive and the negative sign.

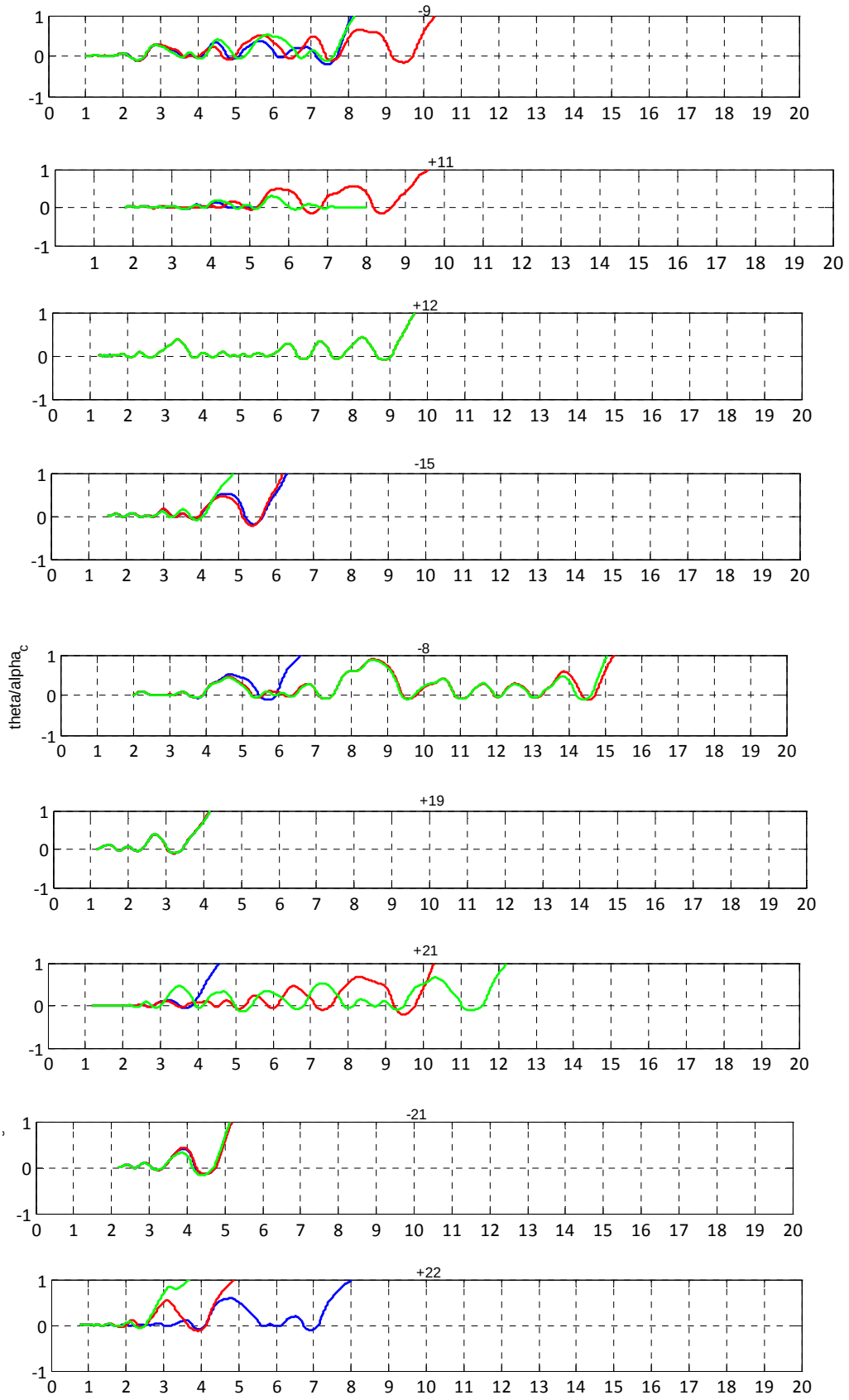
-9
+11
+12
-15
theta/alpha$_c$
-8
+19
+21
-21
+22

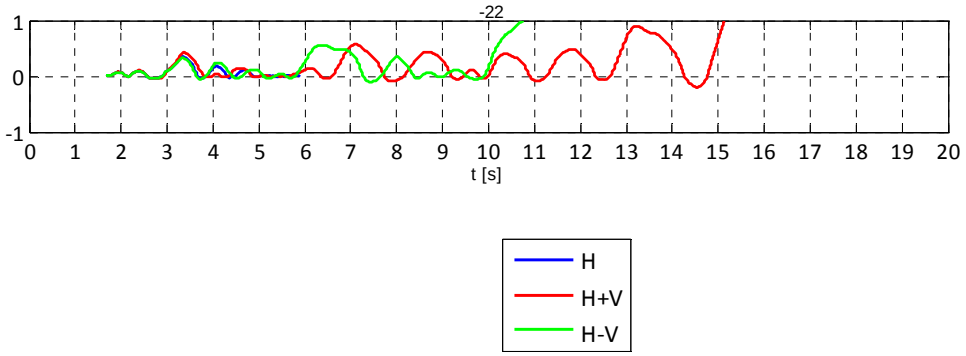

Figure 3.73 - Tr 1600 + vertical action, non symmetric model

The presence of a vertical action, even though of reduced intensity (it is worth noting that recent experiences proved that the amplitude of a compatible vertical accelerogram often underestimates the real vertical action recorded during seismic events), provides in general a worsening effect in the dynamic response of the object. As seen in Figure 3.73 when the horizontal ground motion leads to overturning, the inclusion of vertical action induces an earlier overturning; the effect on rocking, instead, is an amplification of the amplitude of oscillations that, as it was stated above, increases the damage connected to the artistic limit state. It is important to underline that, since the body is non symmetric both directions of action are considered in order to take into account the worst scenario possible, but, for brevity, only relevant results are shown.

The application of static formulas to the detailed model gave as a result a return period for the action that leads to overturning equal to 450 years. As it was previously stated the results obtained from static analysis are on the safe side, hence the effective return period for overturning is higher than the one obtained with such an approach. This concept was already proved in Figure 3.71, where a set of 7 accelerogram with return period equal to the one of the critical action was used, and overturning was reached in two situations. It is interesting noting how the presence of vertical action influences the response of the body, as it is depicted in Figure 3.74.

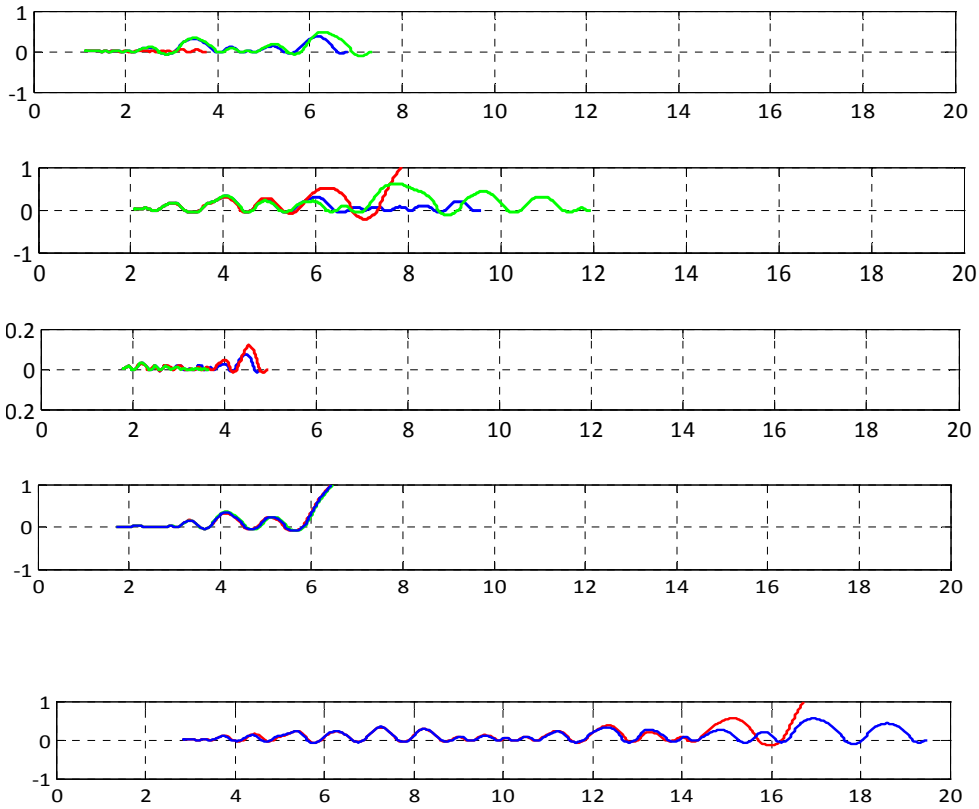

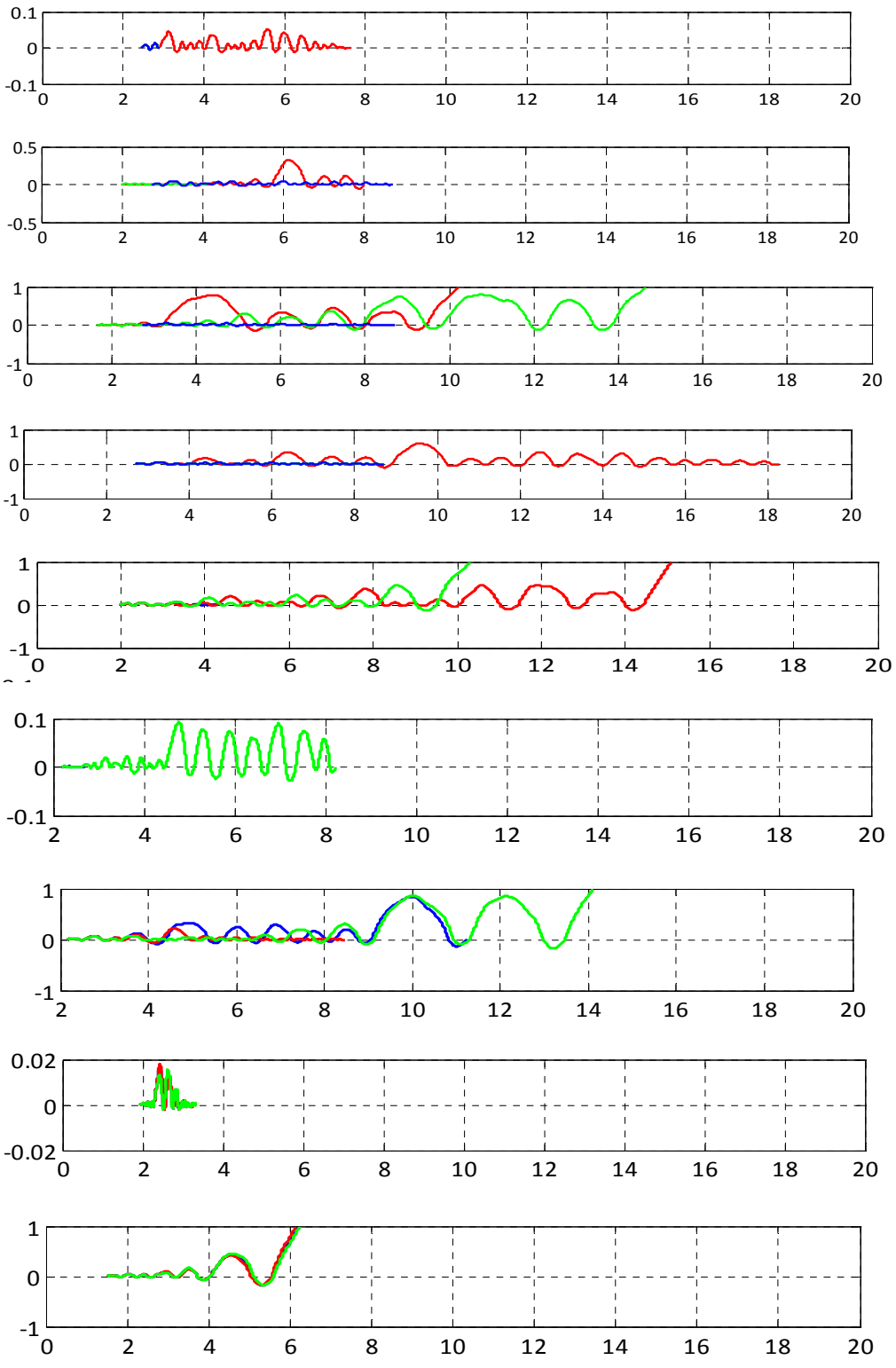

Figure 3.74 -S Matteo non symmetric block + vertical, Tr=475 years input

The presence of vertical action leads to different responses, the object can either experience a higher amplitude of oscillations, without necessarily concluding its motion with tilting, or it can also experience an earlier overturning, in the situations in which overturning was present also with the only horizontal action, but above all it is interesting noting that in some cases, overturning can occur when the horizontal action was only able to produce a rocking response; this is the worst scenario possible and it proves the fact that the presence of a vertical input needs to be properly taken into account otherwise results may not be on the safe side.

3.7.7.1.2 An Application to San Matteo Statue

As it was already mentioned the San Matteo statue has the most critical situation, among the statues of the case study, in terms of rocking and overturning predicted with the simplified formulas approach. Therefore it is interesting to study the behavior of this object with the numerical tool developed, in order to study the response of the statue with this detailed level of analysis and compare it with the other approaches adopted so far.

For the following evaluations the statue was described with its detailed model. It was chosen to apply a set of one hundred generated accelerograms divided into five groups for five defined return periods, with increasing peak ground acceleration; a summary of the features of the dataset is given in Table 3.16

Table 3.16 - details for the reference inputs

Vr [years]	Tr [years]	PGA/g
25	237	0.179
50	475	0.236
75	712	0.271
103	974	0.301
260	MCE	0.353

The considered seismic input acts along the direction in which the rocking phenomenon triggers first (i.e. y direction), the two dimensions used in this case are hence B_1 = 0.189 m and B_2 = 0.375 m. The two conditions for the direction of the action are considered. A summary of peak ground accelerations and peak ground velocities is given in Figure 3.75, it can be observed that the variability of the velocity is always small, except for the last group of accelerograms.

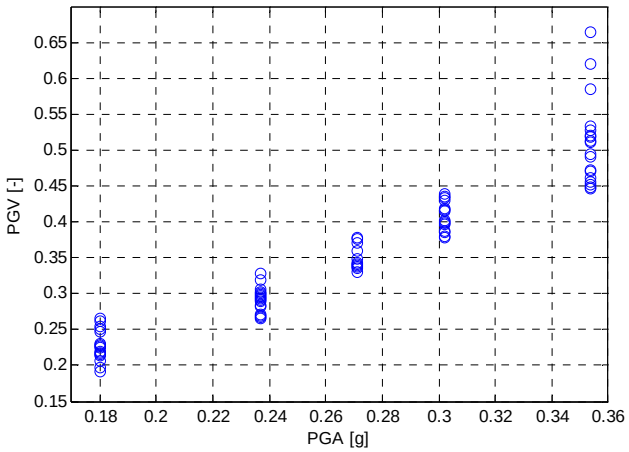

Figure 3.75 - PGA and PGV for the input dataset

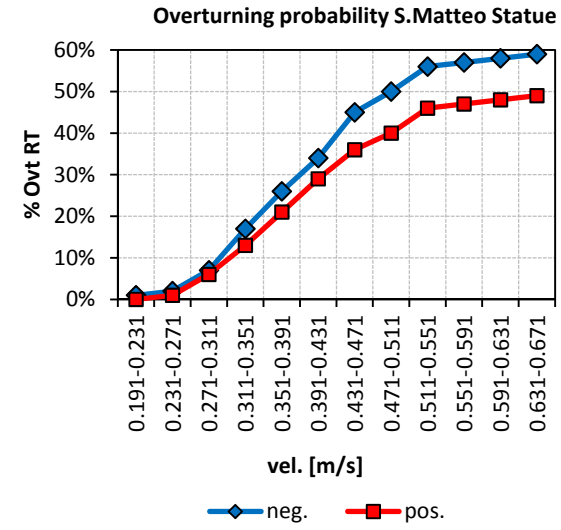

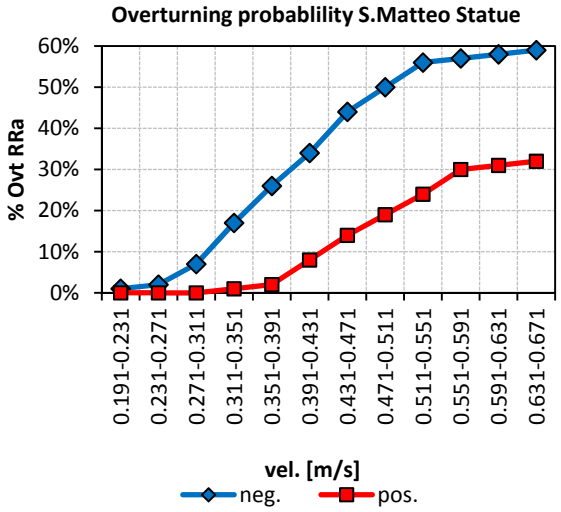

Figure 3.76 - overturning probability for san Matteo a) Rt, b) RRa

Table 3.17- Cumulative overturning probability Rt

Vel. [m/s]	Neg. Cum.	Cum. Pos.	Neg.Perc.	Pos.Perc.
0.191-0.231	1	0	1.0%	0.0%
0.231-0.271	1	1	2.0%	1.0%
0.271-0.311	5	5	7.0%	6.0%
0.311-0.351	10	7	17.0%	13.0%
0.351-0.391	9	8	26.0%	21.0%
0.391-0.431	8	8	34.0%	29.0%
0.431-0.471	11	7	45.0%	36.0%
0.471-0.511	5	4	50.0%	40.0%
0.511-0.551	6	6	56.0%	46.0%
0.551-0.591	1	1	57.0%	47.0%

Vel. [m/s]	Neg. Cum.	Cum. Pos.	Neg.Perc.	Pos.Perc.
0.591-0.631	1	1	58.0%	48.0%
0.631-0.671	1	1	59.0%	49.0%

Table 3.18 - Cumulative overturning probability RRa

Vel. [m/s]	Neg. Cum.	Cum. Pos.	Neg.Perc.	Pos.Perc.
0.191-0.231	1	0	1%	0%
0.231-0.271	2	0	2%	0%
0.271-0.311	7	0	7%	0%
0.311-0.351	17	1	17%	1%
0.351-0.391	26	2	26%	2%
0.391-0.431	34	8	34%	8%
0.431-0.471	44	14	44%	14%
0.471-0.511	50	19	50%	19%
0.511-0.551	56	24	56%	24%
0.551-0.591	57	30	57%	30%
0.591-0.631	58	31	58%	31%
0.631-0.671	59	32	59%	32%

The cumulative probability of overturning is presented in Figure 3.76, the two curves in each graph represent the two opposite directions of action; the parameters considered are R_t and RR_a, which is more significant for the comparisons about the overturning criteria. As it was expected the statue experiences more tilts along the weakest direction. Graph b) shows a lower percentage of overturnings considering the RR_a parameter, due to the higher value of acceleration needed for triggering a motion of rocking.

It is interesting to compare these results with the limits calculated with Housner's (3.47) and Ishyiama's (3.49) criteria, that respectively give:

$$v_{HOUSNER} = 0.598\ m/s;$$

$$v_{ISHIYAMA} = 0.239\ m/s;$$

The numerical curves predict, for the Ishyiama velocity, an overturning probability of 2% for the positive direction and 0% for the negative direction. Concerning Housner's critical velocity, considering the R_T parameter, the results obtained from the numerical tests provide a probability of overturning of 48% along the positive direction and 55% along the negative direction; instead, when the RR_a is considered, the probability of overturning for Ishyiama's criterion is again 0% in the positive direction and 2 % in the negative direction, while a difference is evident in the comparison with Housner's criterion: indeed the numerical predicted probability of overturning is 31% along the positive direction and 58 % along the negative direction. This confirms the results obtained in section 3.6.2.It is worth noting that, Housner relation was proposed for rectangular bodies subjected to a single shock horizontal input, while the presented results refer to seismic inputs. These graphs also allow to compare results obtained with different levels of detail and to evaluate their reliability in terms of probability of overturning.

The minimum critical velocity of overturning evaluated with the simplified model (3.49) is v_c = 0.364 m/s and it corresponds to a probability of overturning calculated as 28 % . With the detailed model the critical velocity is v_c = 0.24 m/s that corresponds to a probability of overturning of 2%.

3.7.7.2 Application of the detailed modeling of deformable bodies (LA) to the case study of big statues

Since analyses with simplified formulas revealed the tendency for some of the objects to rigid motion problems, one of the possible choices available to handle this problem is to fix them to the surface on which they are laid. This choice gives positive results from one side, because the anchorage prevents any potential motion due to motions of the ground. On the other hand it requires a series of further analyses aimed to check the stress level caused by the ground motion: in fact the entire action given by the earthquake is transmitted directly to the body with a consequent stress level that needs to be monitored. For the case study of the "Prigioni" the condition of restraint between the body and the base is considered. This solution is certainly on the safe side considering the state of the art of the objects, because the real connection between the two parts is not known "a priori" and the rate of seismic force acting on the objects is unknown as well. With this assumption the maximum level of seismic force is considered. The real situation in which the statues are is reasonably an "in between" of the two extreme conditions: the afore mentioned one and the condition of simple support over a low friction material layer.

However the analysis with a totally restrained body also describes the situation of an intervention of mitigation limited to anchorages or pins to fix it to the ground and to avoid rigid motion phenomena.

3.7.7.2.1 General considerations

Finite elements analyses were carried out by means of the general purpose software "Midas Gen" and "SAP2000". It is reasonable to begin the investigations with 3D linear elastic time history analyses, since this level of approach has a good accordance with the unique geometry of the objects under study and, on the other hand, the high uncertainty about materials characteristic make a linear solution the best choice for an overview of the stress pattern, before investigating the details with more refined non linear mechanical models. Moreover, it is also worth noting that, in the perspective of an intervention with anti seismic devices further non linear dynamic analyses will be required.

For these analyses three dimensional models were implemented from the detailed laserscanner survey, converting them into numerical meshes composed by thetraedric elements with four nodes. The solution was researched using Newmark's integration scheme, with constant accelerations. The models were restrained to the base. Since no direct experimental investigations about the marble characteristics are available, the reference values were assumed. Mechanical characteristics assumed are the following:

Density : γ = 2700 kg/m^3;

Young Modulus : E = 50-70 GPa;

Maximum compression strength: R_c = 85-125 MPa;

Maximum tensile strength: R_t = 5 – 15 MPa;

Values given above refer to material without cracks or deteriorations of any sort, they are failure values. As a consequence these values should be reduced, in those cases in which, a deterioration of the marble is pointed out, due for instance to a long period outside exhibition that affected the quality of material with weathering (e.g. San Matteo) or due to a lower quality of the marble block out of which the statue was carved. These resistance values should then be reduced, for the purpose of the assessment of the seismic vulnerability, by means of the application of a coefficient of safety similar to γ_m, used for construction materials; in this dissertation a value of γ_m = 2 was assumed; moreover a reduction of 20 % was considered when the survey on the material underlines possible deterioration effects

For the statues of the case study the following values were hence assumed:

San Matteo, Pietà di Palestrina, Atlante (clearly detriorated marble)

Maximum uniaxial compressive strength: f_{cd} = 25-58 MPa;

Maximum tensile strength: f_{td} = 1.6 – 3.6 MPa;

Che si desta, Barbuto, Giovane

Maximum compression strength: f_{cd} = 31-72 MPa;

Maximum tensile strength: f_{td} = 2 – 4.5 MPa;

Moreover, considering the elasticity modulus, analyses of sensitivity were carried out, in order to understand the effects of the variation of this parameter among the limit values given in table (from 50 to 70 GPa). This investigation pointed out that the worst condition is when the lowest value of Young modulus is assumed. The following results assume a value on the safe side (E = 50 GPa) in order to describe the worst scenario for the objects. The dynamic analyses were carried out considering three couples of contemporary accelerograms as shown in section 3.2.2; each couple was applied along the two main directions of the base, also considering a rotation of 90 degrees, therefore six load cases were analyzed, hence three couples of earthquakes acting along two different orientations (*xy* and *yx*).

The results of the analyses in terms of distribution of principal tensile stress for the worst load case are shown and commented in the following; as expected, due to the massive proportions of the statues , the results of the dynamic analyses showed a low stress level, which in most of the cases was safely far from the tensile threshold assumed for the material. Despite the fact that some of the statues showed conditions that deserve more attention.

"San Matteo"

number of nodes	5844
number of tethraedric elements	19108
total volume	1.1984 m^3

This is the object in the most critical condition: the level of stress shown in the pattern of Figure 3.77 shows a tensile stress of about 1 MPa reached around the ankle area, which is the weakest one, due to the sharp reduction of the cross section. The values reached are very close to the limit of the material and they surely deserve further investigations. The stress level must be taken into particular consideration because of the quality of the material and its state of conservation, as underlined both from the historical analysis and from the petrographic inspections. The first one, indeed, pointed out the potential reductions of the mechanical parameters due to weathering and outside exhibition, while the second one stressed the attention on some areas that show evident deterioration.

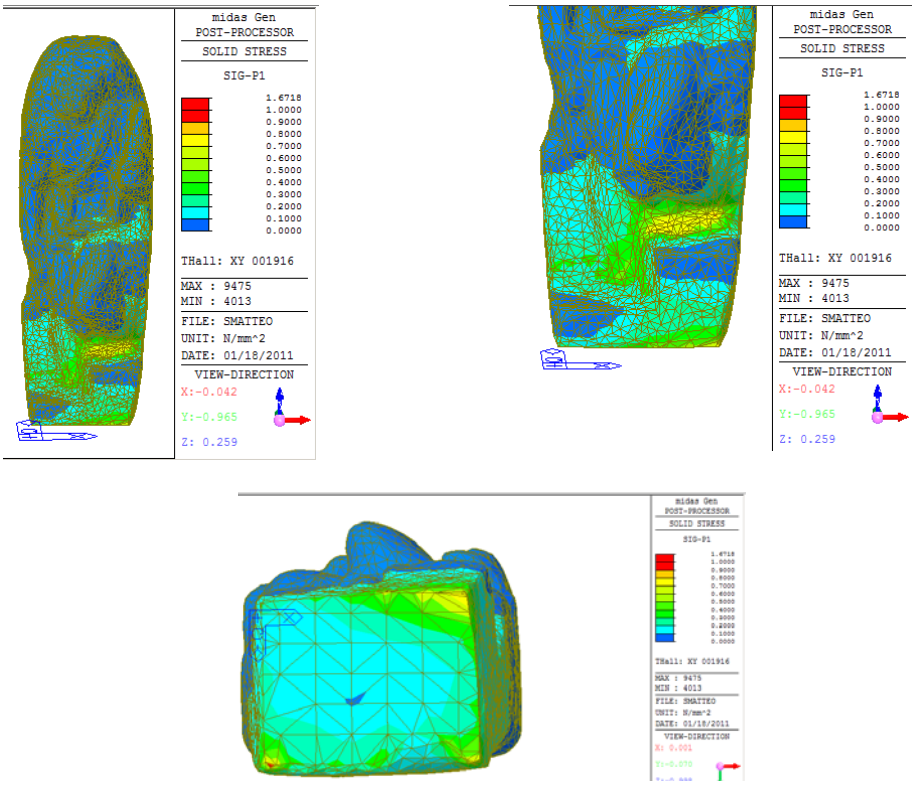

Figure 3.77 – San Matteo stress level

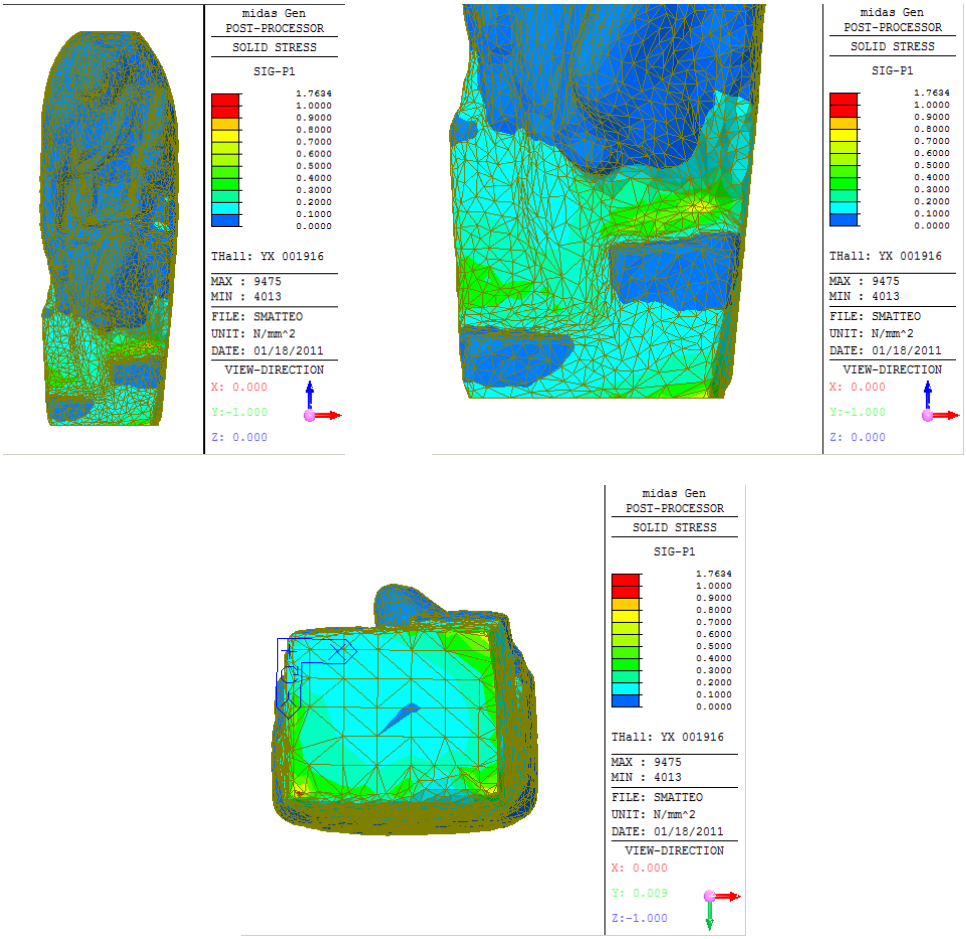

Figure 3.78 – San Matteo stress level

“Prigione Barbuto”

number of nodes	3410
number of tethraedric elements	10371
total volume	0.8421 m^3

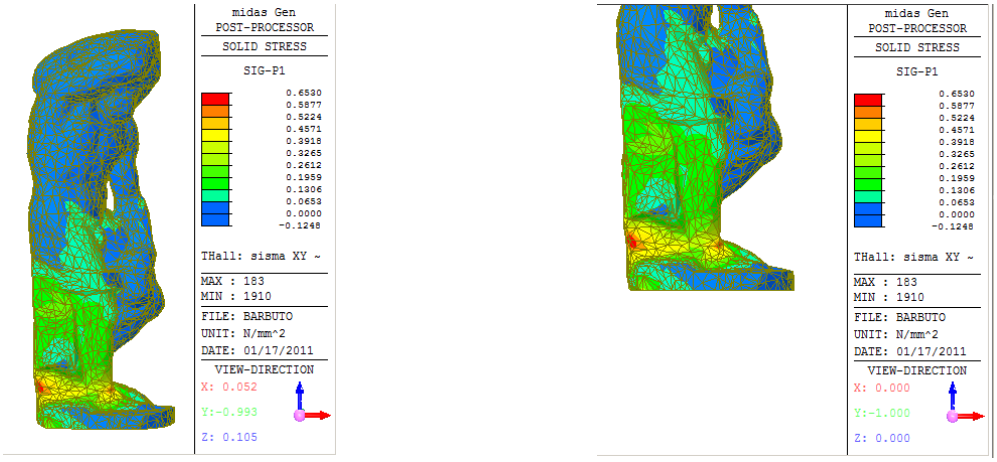

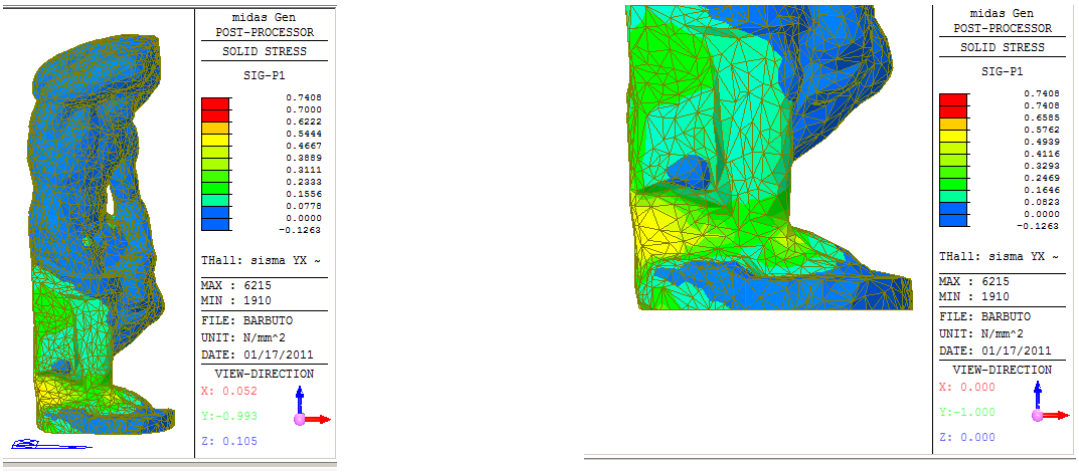

Figure 3.79 - Schiavo Barbuto stress level

The results of the linear analyses for the *"Schiavo Barbuto"* do not show an extremely high level of stress. Indeed the value of 0.7 MPa is reached in the ankles area, in particular, on the right ankle where the cross section reduces to half, as happened for San Matteo. Although this level of stress is far from the limit it is fundamental to recall the result of the surveys on this object. The object is characterized by a through going fracture that can be potentially dangerous for the stability in case of an earthquake. Even though the stress pattern do not show dangerous levels of tensile stress across the fracture further investigation, for example with non linear analyses, would be required for a more precise description of the problem and a more reliable evaluation of the seismic vulnerability.

"Pietà da Palestrina"

number of nodes	5855
number of tethraedric elements	19244
total volume	1.4368 m^3

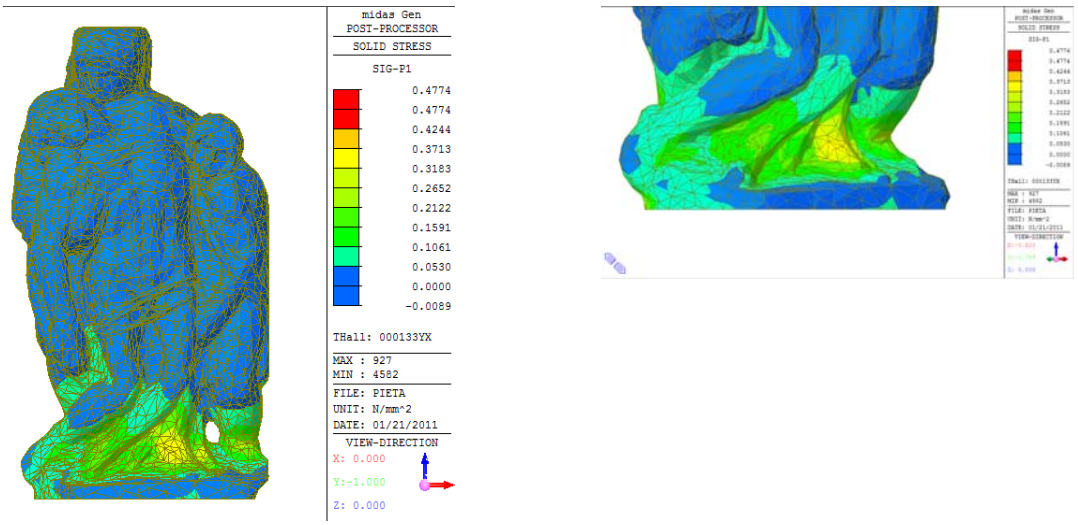

Figure 3.80 – Pietà stress level

Despite this work is one of the most massive of the case study, the analyses pointed out different critical situations, in particular two are worth to note: the first one is located in the ankles area of the left figure, the other one is in the bottom part of the Madonna. Stresses of 0.5 MPa result from the analyses. Once again the values of stress obtained from the analyses are lower than the resistance limits set, but since the petrographic survey on the materials pin

pointed for this statue diffused foliation and a possible microfractures on the area that results the most stressed from the analyses.

“Prigione che si desta”

number of nodes 3316

number of tethraedric elements 10455

total volume 1.6032 m^3

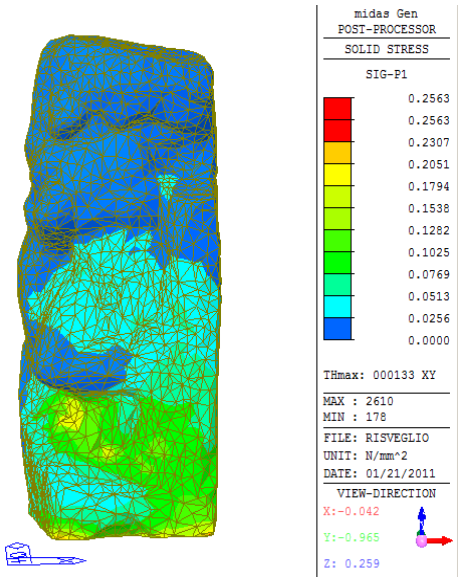

Figure 3.81 - Schiavo che si desta stress level

Concerning the “Prigione che si desta” the stress pattern is shown in Figure 3.81; principal stresses never exceed 0.3 MPa which is far from the mechanical limit. This object doesn’t show any particular weakness or critical point in case of an intervention of reduction of seismic vulnerability with anchorages

“Prigione giovane”

number of nodes 3909

number of tethraedric elements 12109

total volume 0.8876 m^3

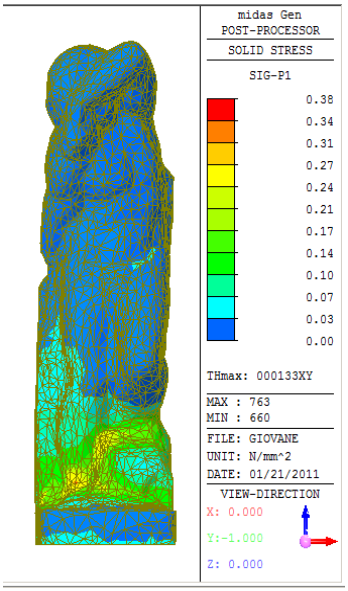

Figure 3.82 -Prigione Giovane stress level

The stress pattern for this object is not dangerously high, the highest level reached is about 0.4 MPa for the event 000133xy; as it was expected the weakest zone is the ankles area in correspondence of the reduction of the cross section.

"Prigione Atlante"

number of nodes	3810
number of tethraedric elements	12175
total volume	1.7096 m^3

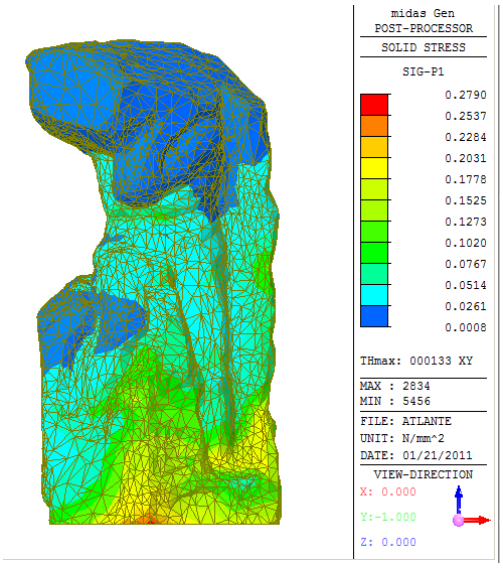

Figure 3.83 – Prigione Atlante stress level

The "Atlante" is the most massive among the four Prigioni and, as a consequence it does not suffer of any particular stress problem. The maximum stress level reached sets around 0.3 MPa and it affects the area of the restrained nodes so it is not that important. Despite that, the conclusions of the petrographic analysis points out a slight level of deterioration which deserves further analyses.

Presence of vertical action

As described in section (3.2.2) seismic events have recently shown the presence of a vertical component of the action that is often as dangerous as the horizontal ones, it is furthermore stated by Priestley (26) that *"recent near field accelerograms of shallow earthquakes have indicated vertical accelerations that have in many cases exceeded the peak horizontal acceleration"*. As it was described and commented for the rigid body approach the vertical action can affect the response of light weight objects, as those targeted in this dissertation, leading to a possible increase of the seismic vulnerability which needs to be investigated in detail; similarly stress analyses must take into account the presence of the vertical action because it can induce variations into the stress pattern that can be dangerous for the objects, in particular in those situations in which the problem of an articulated body is investigated: prominent parts can be compared to cantilever beams and variations of vertical acceleration can seriously influence the stress pattern of these elements.

In the context of this work some preliminary time history analyses were performed in order to get general information about the influence of the vertical action on the response of the structure. These first analyses have as a object of study the statue of San Matteo, because of its potentially dangerous health condition; they were carried out with a different set of natural accelerograms than the one presented before. This set was obtained with the same procedure described above, by means of the software REXEL (27). Also in this case earthquake records were selected considering the seismic characteristics of the case study site: return period 712 years, M = 4 – 7 and R = 0 – 40 km . The following images depict the stress pattern measured in the statue of San Matteo :

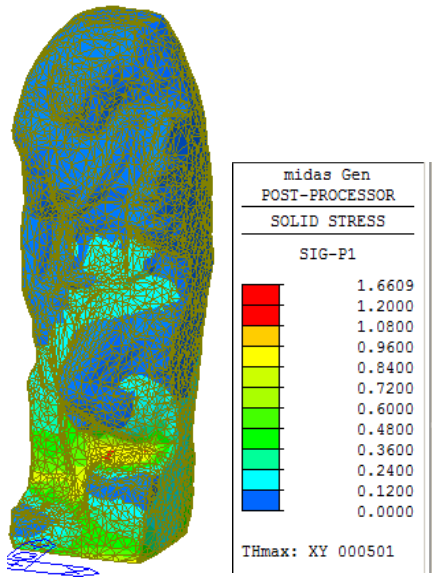

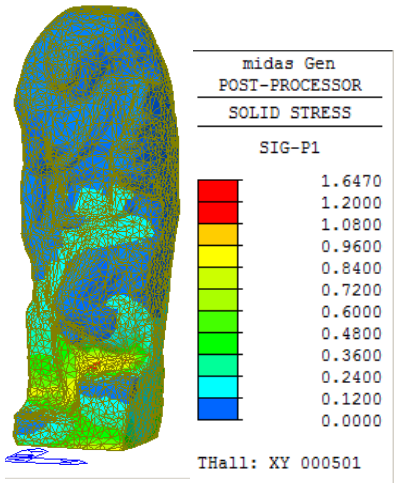

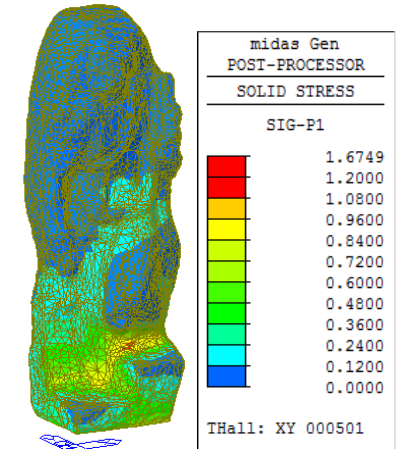

Figure 3.84 - san Matteo stress pattern a) horizontal XY b) XY+z c) XY-z

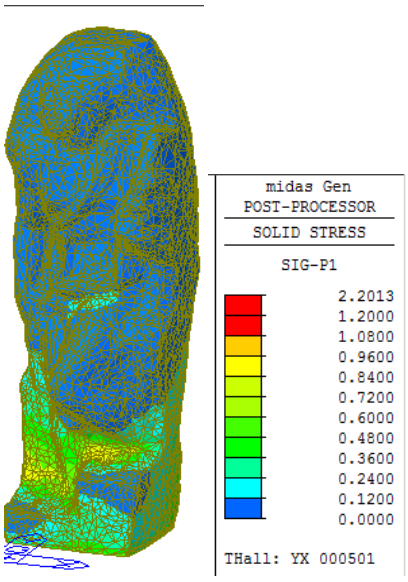

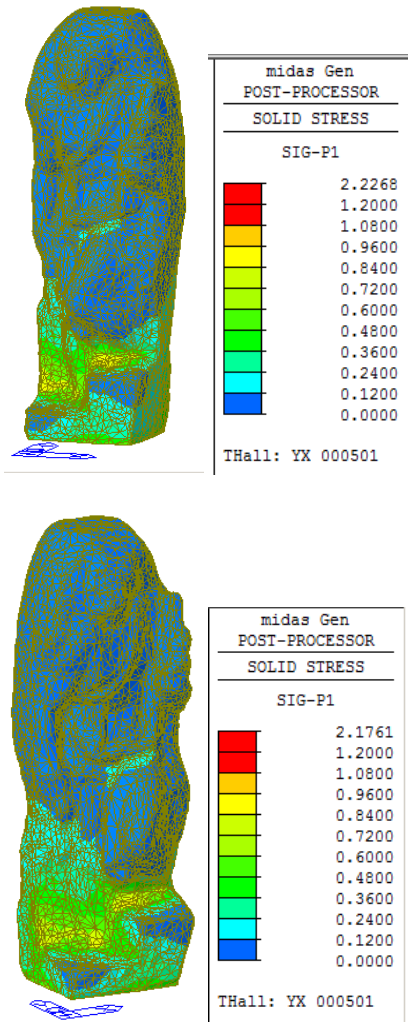

Figure 3.85- san Matteo stress pattern a) horizontal YX b) YX+z c) YX-z

Figure 3.84 and Figure 3.85 highlight the fact that, when a vertical action is present, effects can be both of amplification and of reduction of the stress level in the object. For example, considering the presence of a vertical action assumed with positive direction provides a higher level of stress in the object, while considering it with vertical direction provides a reduction of the stress level.

The stress pattern depends on several parameters such as the horizontal inputs chosen, their direction of application and the direction of the vertical action. According to this remark it is necessary to underline the importance of carrying out specific analyses to assess the effects of the vertical earthquake on the dynamic response of the system, because it cannot be stated “a priori” whether this condition provides a worse scenario for the targeted object.

4. Mitigation

4.1 Abstract

The procedure of assessment described so far allows to identify all situations that, in a museum environment, are potentially dangerous, and in some way allows also to classify and quantify the seismic vulnerability of these situations. This aspect is fundamental for the further step of the procedure: the reduction of the vulnerabilities pointed out; it is worth to remind that the Guidelines give great importance to the mitigation aspect and they propose techniques and methods for vulnerability reduction. It is nonetheless true that the choice for interventions of mitigation is not simple because it must take into account different aspects of the problem: the results of the assessment phase, the intensity of the reference action which the object should be protected from, the importance of the object itself (which is a delicate aspect, since the "importance" of work of art is difficult to quantify) and last but not least the costs of intervention. Despite the fact that superposition of all these aspects, that need to be considered at the same time, makes it a really hard task to deal with, the target of conservation cannot be forgotten, hence different approaches are developed in order to cover the highest number of situations; for instance with quick and low cost interventions that can be applied for a large number of objects that need to be protected, or with more specific and precise measures on single objects:

- increasing the stability of the body by means of modifications of the ratio between base and height adopting, for instance, pedestals or bases that with their dimensions or with their weight, modify the above mentioned ratio. An extreme interpretation of this concept is to connect together on a single base element several objects;

- anchoring the objects to their pedestals or to their supports with proper systems. It is clear that such a solution is subordinated to the condition that the seismic action on the fixed system does not overcome the mechanical characteristic of the material;

- decoupling the dynamic response of the object from the dynamic of the ground by means of specific seismic isolation systems;

In the following interventions will be divided into two main categories: minimum interventions, cheaper and of more simple applications, and interventions with specific devices, that require the employment of isolators or dampers to reduce the seismic vulnerability of the object. The target of this part of the chapter is a general overview of the state of the art in the field of seismic protection of art objects by means of isolation devices, hence a summary and a critical review of some of the most famous interventions is proposed.

4.2 Minimum interventions

Exhibitions in general include such a different variety of typologies of art objects and goods that it is unaffordable to think about an approach with specific design for each one of them; for this reason it is necessary to classify and divide them into categories, in order to obtain an easier way to assess and mitigate the seismic vulnerability according to the general response to earthquake of each category, and not of the single object. In the following some general considerations about the reduction of seismic vulnerability are given, also considering the interventions already studied and applied by technicians and mountmakers of the J.P. Getty Villa museum in Malibu, which is the most important institute dealing with this peculiar problem at the moment (16). The procedures and techniques described in the following are very simple and sometimes more similar to rules of thumb, but it must be kept in mind that they represent the easiest, cheapest and quickest choice that can be applied in order to obtain a large scale vulnerability reduction.

A first and very quick intervention, applicable in general for objects on a flat surface, such as a shelf or a floor, is to improve the quality of the interface between the support and the object, allowing a better and more uniform distribution of the vertical load, and improving also the equilibrium and adhesion condition. A technique which is very diffused is the application of thixotropic resins, to cover the bottom surface of the object and fill possible gaps, always having care of applying, between the resin and the object, a thin film to prevent damages due to the interaction.

Further interventions to prevent from or to reduce the probability of rocking and overturning are:

- increasing the weight of the bottom part of the object, for instance vases can be filled with sand bags, Figure 4.1;
- increasing the dimensions of the base joining, for example, more object onto the same support, Figure 4.2;
- anchoring the objects to the support by means of proper systems, Figure 4.3.

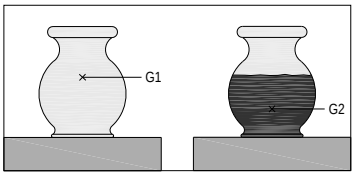

Figure 4.1 - stabilizing by lowering the center of mass

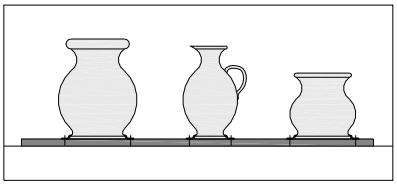

Figure 4.2 - stabilizing by base widening

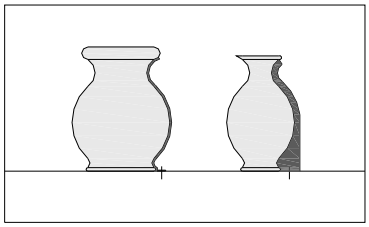

Figure 4.3 - stabilizing by anchorages

The most suitable solution is the design of a specific support and it allows to obtain the best fitting possible according to the object itself (shape, material, state of conservation), to the material of the support and to the interaction object-support in case of a seismic event. However it must be taken into account that the support must be able to withstand forces due to a seismic event, the material must also be chemically compatible with the object and, moreover, the aesthetical aspect of the support must be taken into proper account.

The choice to fix the object to the floor is a good solution from the point of view of the reduction of the rocking and overturning phenomena, but it makes necessary to investigate the stress level induced by the seismic action into the connection elements and also into the good itself, because it can induce problems of cracking that can lead to damage the object and also, in the worst scenario, to lose it. The anchorage solution must take into account the shape of the object avoiding to put the restraint in those sections that are intrinsically weak, for instance for standing human-shaped figures they are ankles, feet and neck. Whenever pre existing holes or cavities are available they can be used for the application of pins and pivots, taking care to provide the best adherence between the supporting element and the walls of the hole, by means of a layer of properly shaped ductile material, Figure 4.4.

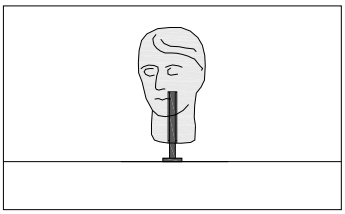

Figure 4.4 - example of anchorage

Specific mount makings of different materials, designed for each situation can also be installed; a support that follows the shape of the object gives the positive contribution of a good distribution of the actions, reducing the level of stress induced by external actions (if it is compared to the same action on a smaller contact area), on the other hand this type of intervention often has a high visual impact and it does not result suitable for situations in which the external appearance of the good needs to be kept unaltered. Another proficient technique of protection of art goods is to let the body slide in case of horizontal action, allowing the energy given by the earthquake to be dissipated by means of friction; in this case displacements must be carefully evaluated because a free sliding can produce impact with other bodies or with supports and it can also cause the falling of the object from the support plane, causing both damages to the artwork and potential injuries to people. However this condition can be put in practice by means of the application of low friction material layers; it is worth noting that this solution, even if ideally very easy, hides a great number of problems; indeed the dynamics of a motion governed by friction are difficult to predict, because of the high number of uncertainties that characterize the problem; then a significant knowledge of the characteristics of the expected earthquake is required, moreover the presence of a vertical component of the seismic input affects the value of the coefficient of friction and it makes the behavior even more difficult to be described.

4.3 Case study: proposals of minimum interventions

In this paragraph some proposals of application of minimum intervention techniques are presented and briefly discussed, they are mainly application of the above mentioned concepts to case study of Sala dell'Ottocento; from the assessment section 3 it was evident that the situation of that particular exhibition is extremely critical, both for number and layout conditions of the objects. A possible solution needs hence to be proficient in terms of reduction of the seismic vulnerability and also in terms of feasibility.

The solutions proposed basically suggest to fix the objects to the shelves by means of two different methods: the first is to provide them with metallic anchorages on the back side, the second one is to "bound" them with a net of transparent nylon chords; the interventions are described by sketches from Figure 4.5 to Figure 4.7. It is clear that, despite the fact that the description refers to busts it can easily be applied to different typologies of objects.

As it was mentioned before, fixing the objects implies that the stress level must be monitored and carefully considered, to avoid damages and fractures to the object. A reasonable stress level, that is not dangerously high, can be obtained with simple design details such as avoiding to set the connection elements on weak sections or also increasing the number of chords and setting them up to have the best stress distribution. It is worth noting that in such interventions nylon chords should be prestressed, in order to prevent the objects from any possible motion and to keep their initial position during the seismic event, avoiding dangerous relative movements. Although the afore described intervention needs to be specifically tailored in each situation, it is constituted by modular elements that can be easily produced on industrial scale, moreover they are suitable for exhibitions that can be subjected to variation in the layout or for temporary exhibitions; the following summary is a proposal for some possible interventions:

- application of metallic anchorages;
- application of nylon chords;
- application of plexiglas elements anchored to the supports;
- application of metallic anchorages. Small regular objects (such as vases or sculptures with pedestal) can be fixed by means of metallic elements (in the minimum number of three), with an interposed layer of padding, to prevent potential damages in the points where there is a concentration of stress;
- application of nylon strings;
- nylon chords keep the object in the initial position, fixed to the support, with configurations that depend on the object's shape. Strings can be fixed to the support in different ways:
    - with eye-bolts fixed to the shelves, or in case of low resistance of the shelves' material, to metal plates that can re distribute the stress; a useful prescription is to use at least three chords for each object.
    - connected to plexiglas plates properly connected to the wall; chords pass through eye bolts anchored to two Plexiglas plates that allow to apply the anchorages at different levels to obtain a better distribution of the stress. Plexiglas should provide the lowest visual impact;
    - connected to plexiglas plates anchored by means of metal frames to the shelf;
    - connected to metal bars departing from the shelf.

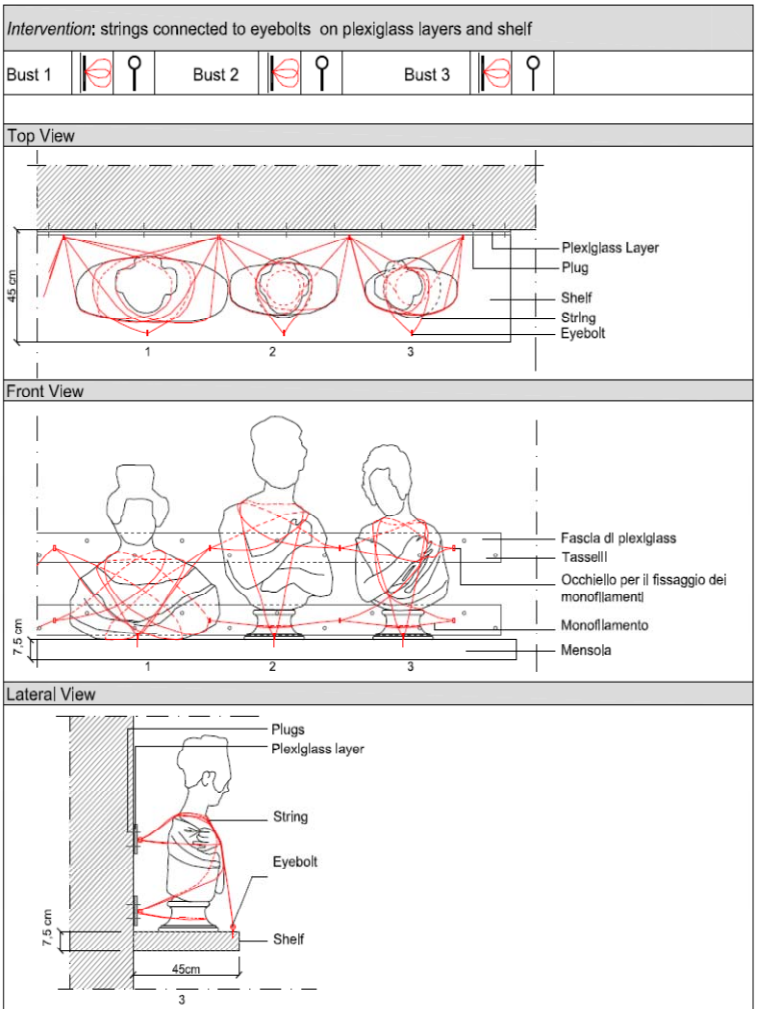

Figure 4.5 - intervention of mitigation 1

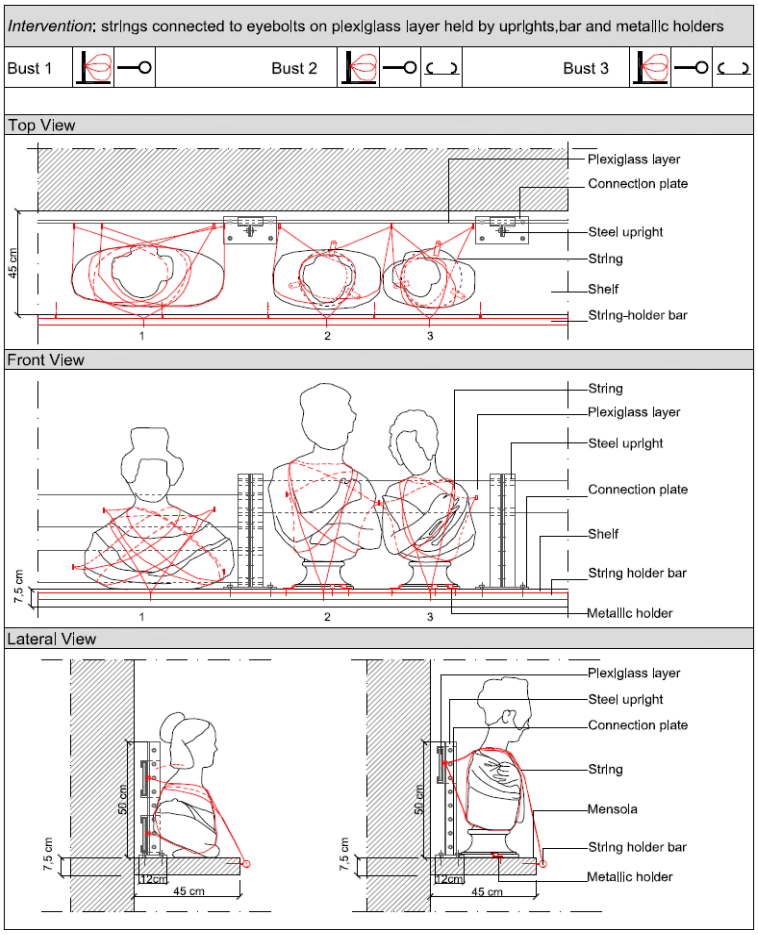

Figure 4.6 - intervention of mitigation 2

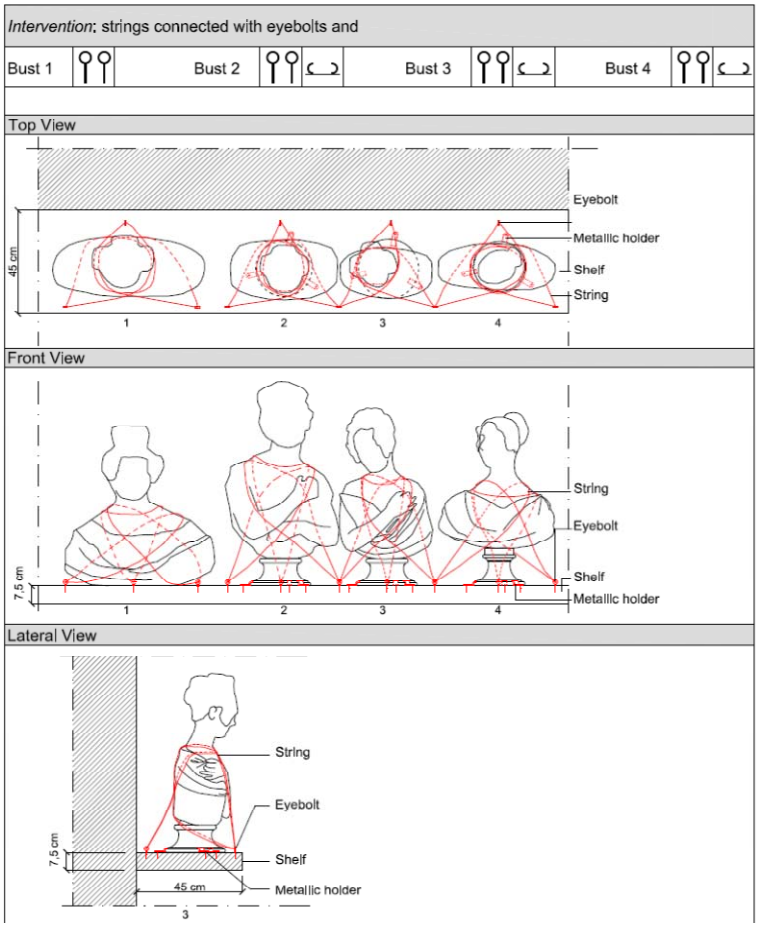

Figure 4.7 - intervention of mitigation 3

4.4 Interventions with base isolation

4.4.1 Introduction

The application of mitigation techniques can also involve more refined and specific technical solutions to protect the objects and prevent them from damages; the examples that were presented so far concern only low impact and low cost solution which are useful for large scale approaches and are not applicable in more specific and peculiar situations. This is the main reason why, for artworks of high interest, solutions often apply seismic isolation concepts.

4.4.2 Seismic isolation concepts

Even though it is not the purpose of this work to discuss about basics and theoretical concepts of seismic isolation it is interesting and worth to summarize main principles before moving to the following part, in which both famous applications and the case study of this dissertation will be described.

Seismic isolation for structures and infrastructures is a simple concept that has began to spread more than hundred years ago, with several proposals, made by scientists from all over the world, of different types of devices designed to reduce the severity of the earthquake action on buildings. These ideas were developed through years and the concept of seismic isolation has become reality in the last forty years. The main purpose of isolation is to mitigate or reduce earthquake damage potential, and it applies a quite simple idea, as described by Kelly (34):" *the system decouples the building or structure from the horizontal component of ground motion by interposing structural elements with low horizontal stiffness between the structure and the foundation*", the isolation system gives the structure a fundamental frequency lower than both the fixed base frequency (the main one of the structure) and the main one of the ground. This means that the isolation system does not absorb the energy of the system but it rather changes the dynamic of the system in order to "isolate" it from the earthquake and shifts its period in a range where the energy content of the earthquake is lower. As a consequence it can be said that isolation does not depend on damping, even though a certain

level of damping is positive to avoid resonance phenomena and also to help reducing the oscillations in time, and it also provides a certain amount of energy dissipation. Considering a generic design spectrum (the one we would use for designing the structure against seismic loads), seismic isolations acts in two different ways to mitigate the effect of the seismic action: first it sets a fundamental frequency for the structure which is defined in the design phase, shifting it in the range where the energy content of the earthquake is reduced, then, by means of damping, it helps reducing the energy transferred by the earthquake (Figure 4.9).

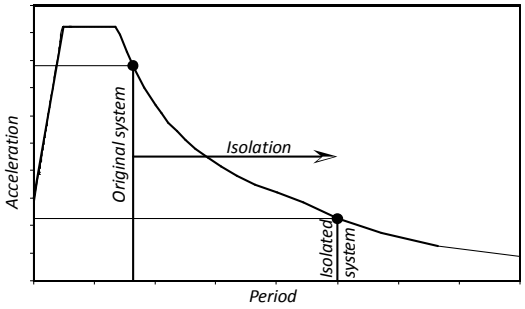

Figure 4.8 - isolation effect

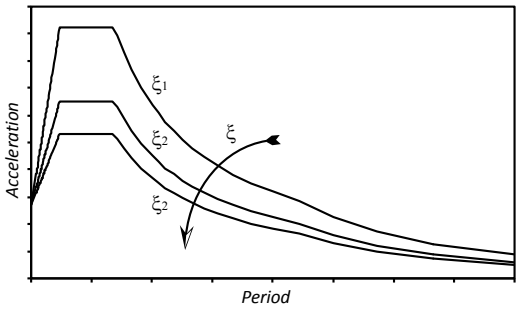

Figure 4.9 - damping effect

4.4.3 Applications to seismic isolation concepts to statues, state of the art

Isolation is an excellent solution to mitigate the seismic risk on structures, because it helps reducing the construction costs limiting the action on the structure; it is also important to remember that there are other categories of objects, different from structures, that need to be protected from earthquakes as well and that cannot withstand even low levels of seismic action; they are in general secondary elements contained into buildings such as medical devices or art objects. Even though the basic concepts and theories that govern the problem are the same for civil structures and small objects, the application of usual isolation techniques to this second category is much more problematic for a series of issues: art objects, for example, involve masses that are orders of magnitude smaller than usual, moreover they are much smaller than civil structures and they are often placed in museums or buildings that cannot be isolated because they are considered monuments as well. Indeed retrofitting an art object means to deal not only with the object itself, but also with the container, finding a solution that needs to find agreement of experts of different branches: from engineers to architects and museum curators. Application of isolating devices must actually reduce the seismic risk for the object, it needs to be either “invisible” or, at least, it shouldn’t affect the “visual equilibrium” of the exhibition. For these reasons the application of anti seismic devices for art objects may result more difficult.

There are many examples of protection of art objects, they involve different techniques, applied for assembling different devices, but with the same main general purpose: reduce the effect of the earthquake on the isolated good and on visitors of the exhibition. One of the most active institution in this field is the “Getty Conservation Institute” which has provided the first examples of anti seismic devices specifically designed for art objects, basically showcases and big statues, in particular exhibited in Getty Villa, in Malibu. The area in which Getty Villa is set is prone to seismic damage, it was hence mandatory to protect the collections from any possible damage and also to provide an acceptable level for visitors’ safety. The Getty Conservation Institute adopts different techniques to protect art objects, mountmakers work both on the side of rough and low impact techniques, such as mount makings, and on the side of seismic isolation. Isolators they assemble in their laboratory, in Malibu, are sliding bearings, realized as multiple layers of unidirectional sliders , made as small carts moving on lubricated spheres along a restrained direction . Characteristics of devices are tailored for each art object and they perfectly fit the environment of the museum, with subtle and almost invisible set ups.

Figure 4.10 - Getty isolation device, application

One of the most famous examples of seismic isolation in the Getty Villa is the one concerning the statue of a Kouros (the Agrigento Youth), on a loan from "*Museo Archeologico Regionale*" of Agrigento, which was equipped with a custom seismic isolated base and pedestal (Figure 4.10) based on the technology described above.

Figure 4.11 - Example of isolation application for a statue at Getty Villa, Malibu (source www.getty.edu)

Areas particularly prone to earthquake damage are obviously those in which the choice of isolation is mostly taken, another famous example is the retrofitting work on the "*Gates of Hell*" by Rodin, a massive bronze sculpture standing in the front garden of the National Museum of Western Art in Tokyo. In 1998 it was decided to retrofit it with seismic isolation base in order to prevent it from falling over in case of a major earthquake; the sculpture is 5.4 meters tall and 3.9 meters wide, its approximate weight is 7 tons. The intervention isolated the base on which the sculpture is set and it comprises five circular roller bearings in which rollers can move on curved surfaces; by combining two bearings oriented along two main directions the object can freely move in every horizontal direction.

Figure 4.12 - Rodin "Gates of Hell"

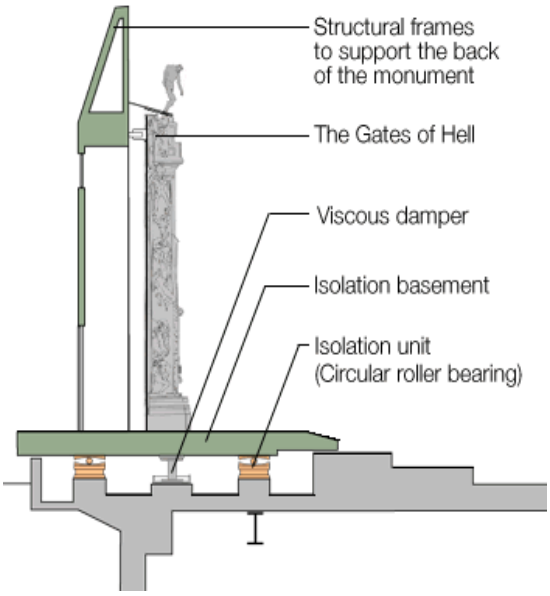

Figure 4.13 - "Gates of Hell" , isolation system sketch (source www.takenaka.co.jp)

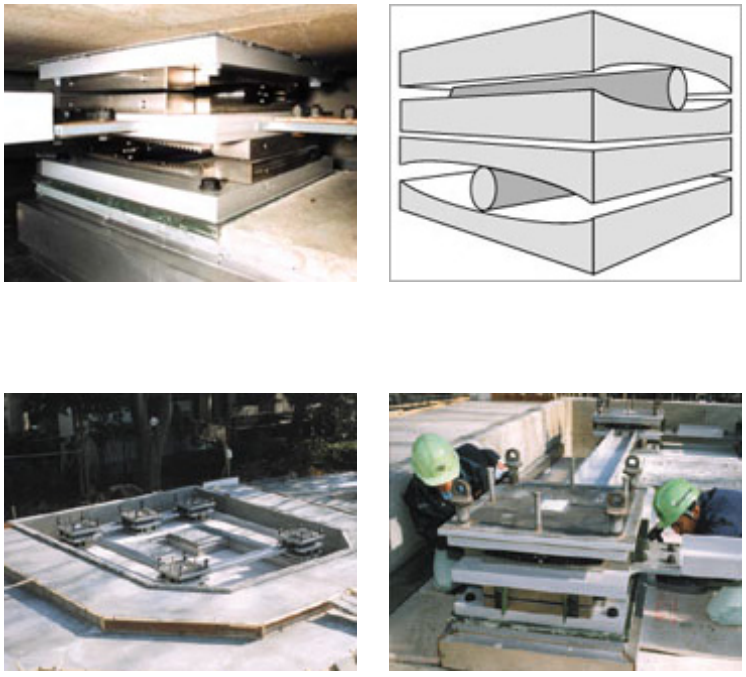

Figure 4.14 - "Gates of Hell" isolation system details (source www.takenaka.co.jp)

This solution applies also a viscous damper to reduce the oscillations. In this case the application is simpler because the object is placed outside. It is worth noting that the choice of this type of device requires a wide area for the application and, because of the fact that overlapped bearings are used, the intervention requires also to develop in the vertical

direction; hence this is an example of effective and reliable isolation solution but it is also exclusive for this particular art piece.

Italy has to face this problem as well, indeed on Italian territory two key factors are present and cannot be neglected: first the medium high level of seismic risk, which is spread on all the territory, in particular on the southern area, then the high concentration of art objects and goods that characterizes Italy; for these reasons some important examples of application of mitigation techniques by means of isolation were used in the recent past. One of the most famous examples of isolation is the retrofitting of the statue of Nettuno and Scilla in Messina.

Another important intervention, which had very recent development is the one for the mitigation of the two famous "*Bronzi di Riace*"; the two statues were isolated with a system of sliding isolation. The isolation system of the "*Bronzi*" was replaced with a new device made out of marble; it consists in a base (made out of marble as well), rigidly anchored to the ground, with four circular areas shaped for allowing the sliding of four marble spheres, the system is topped with another element, similar to the bearing base, on which the statue is restrained (Figure 4.15)

Figure 4.15 - "Bronzi di Riace" isolation system (source titano.sede.enea.it)

Figure 4.16 - "Bronzi di Riace", application of the isolation system (source titano.sede.enea.it)

This system applies sliding concepts in a new shape, joining both the technical and the aesthetical point of view, it was proved by experimental tests on a full scale model of the statues (Figure 4.15) that the application fulfills the expected objectives. Although the results are encouraging it has to be noticed that there are some aspects that can be problematic. First of all such a system has to be specifically designed and shaped for each single application: this means that it can be a good choice for all those statues and objects that are extremely famous and considered masterpieces (for example the "*David*" , or the "*Bronzi di Riace*"); but this can be a problem if we consider that the amount of goods in need for protection is huge. Another aspect that can't be forgotten is that such an isolation system does not provide any vertical action resistance for traction, hence the effect of vertical action of earthquake must be considered, moreover rocking effects due to the position of the center of mass can influence the dynamic behavior in case of earthquake.

As a further example it is worth mentioning the case of Praxiteles's statue of Hermes (Figure 4.17) at the Olympia museum in Greece, which was isolated with four friction pendulum devices produced by EPS (Vallejo, California) and tested at University of Buffalo earthquake engineering laboratory.

4.4.4 Application of traditional devices to art objects

Applications described in the previous paragraph concern art objects isolated by means of devices that were specifically studied and designed for the situation in which they needed to be applied; the idea proposed in this work is to apply traditional devices that need to be properly re designed in order to fit the situation. An example of application of traditional devices is the one of Praxitele's Hermes, in The Olympia Museum.

The statue of Hermes carrying Dionysos (Figure 4.17) is the only known surviving work of the sculptor Praxiteles. It is made from a white Parian marble and has a height of 2.13 m. When the statue was found in 1877 some parts of the body were missing but they were replaced by gypsum plaster restorations.

This is an example of base isolated art object: the isolation system was designed to protect it from overturning and to provide adequate stability and strength in case of a strong ground motion. A large pit below the museum area was constructed (approximately 4 m by 4m, Figure 4.18) in which four isolators were placed. The devices, manufactured by EPS, are four single concave friction pendulum that can accommodate a maximum displacement of 32 cm.

Figure 4.17 - Praxitele's Hermes

Figure 4.18 - Hermes Isolation system set up

Figure 4.19 - Hermes Isolated platform

The devices were tested at Earthquake laboratory of the University of New York at Buffalo. A stereolitographic model of the statue was then constructed and, from that, a finite element model with solid tetrahedral elements was built. This model was used to evaluate the stress level in the two conditions , of rigidly anchored body and of the isolated system. The results obtained from the finite elements analyses showed that the solution of isolating the statue was effective in terms of reduction of the stress level, in particular in the restored areas, which were in a condition closer to the mechanical threshold of the material. It is worth noting that, when dealing with art objects and their stress analyses the mechanical limits of the material are not clear and defined, indeed the material has experienced different conditions through centuries, which have influenced its mechanical characteristics.

5. Proposal for an isolation system

5.1 Abstract

According to the results obtained from analyses presented in chapter 3, the statues displayed in “Galleria dei Prigioni” do not experience a stress level dangerously high; although this result is encouraging, one must remind the numerous uncertainties that affect, and that may reduce, the mechanical characteristics of the material. In the following chapter the specific aspect of mitigation of seismic vulnerability by means of anti seismic devices will be presented and discussed; the innovative solution proposed in this chapter regards the application of double concave friction pendulum devices, specifically designed to fit the peculiar case of art objects. Indeed, even though the technical background behind these devices is consistent, the application of this technology in such a context involves several issues that make this task not as easy as it seems.

First of all the traditional devices are presented in applications to civil structures and infrastructures, afterwards the traditional model that describes their mechanical behavior is also described and commented.

As it was just mentioned the application to art objects requires an accurate design phase in order to develop a device capable to fit the different functioning conditions: light weight of the targeted isolated body, reduced space of application and high position of

the center of mass (when compared to base dimensions); these problems made necessary a re-design phase, that was carried out in cooperation with “FIP industriale”; the result of this phase is a specific double concave friction pendulum, with reduced dimensions (diameter of the device 270 mm and equivalent curvature radius 3000 mm), which is presented in this chapter. Four prototypes were then built, in order to carry out a series of experimental tests, that were aimed to a reliable characterization of the mechanical properties of the devices, in particular stiffness and friction. The first series of tests presented in this dissertation were carried out at FIP facility in Padova, in this chapter some results for the first assessment of the values of the mechanical parameters are presented. Basically the most important parameter to assess in this first phase is the coefficient of friction which depends on the diameter of the slider and on vertical load acting on it: it was evaluated about 5%.

Subsequently to these experimental tests a further series of experiments was carried out at SRMD facility of the University of San Diego. This second group of tests was aimed to study the dynamic response of a system constituted of four isolators and an object with mass and inertia features similar to those of the case of study of the “Galleria dei Prigioni”, but also adjustable in order to highlight potential different behavioral aspects of the system. First of all the physical model was designed and built out of four reinforced concrete blocks that can be assembled in different configurations to best fit the statues of the case of study. Afterwards different tests were performed in order to investigate those aspect that could particularly affect the response of the system: rocking phenomena, presence of bidirectional and vertical input, low vertical load. The first tests aimed also to validate the mechanical parameters

assessed during the first experimental phase: it emerged that the first evaluation of the coefficient of friction was inaccurate and that the effective value sets about 2%, even if it has a light variability.

In general, first results on unidirectional tests highlighted an encouraging behavior with a good reduction of the transferred acceleration, which becomes more effective as the peak ground acceleration of the input increases (the peak ground levels tested were 0.04 g, 0.07g, 0.15g and 0.35g). Good results were also obtained in terms of correspondence between the experimental results and the theoretical mechanical model proposed in literature (1). Tests with bidirectional inputs were also performed but, although the reduction of the transferred action recorded in these tests confirmed the results obtained from the unidirectional ones, the response in terms of force displacement cycles was different from what it was expected. Furthermore several unexpected phenomena, that were evident also in the unidirectional tests, appear more evidently and pushed to a deeper investigation about the actual behavior of these re scaled devices.

Part of this chapter is spent to present and justify the numerous problems and unexpected phenomena that were highlighted during the tests. Particular attention is paid to the amplification of displacements in bidirectional tests, to local oscillations that largely affect the force displacement cycles and to those aspects of the behavior of the devices that make not satisfy the initial assumptions of the traditional mechanical model. The outcome of these analyses are general considerations that need to be taken into account during the design phase because the effects of all these phenomena, that in general occur together, can influence the response of all the system and they can cause a reduction of the maximum allowed displacement, an increment of the eccentricity, a loss of the vertical alignment that, for over determined systems, can generate a dangerous amplification of the oscillations.

The last part of the chapter concerns the modeling phase: the proposed methodology indeed requires analyses aimed to the assessment of the effects of the application of mitigation techniques. In this case 3D finite element analyses of the isolated system were performed and results compared to those of the fixed base object; numerical models were implemented with “all purpose” software Midas and SAP 2000, that contain the traditional mechanical model for friction pendulum devices. The first set of analyses were performed in order to understand whether the traditional mechanical model can be applied in case of the innovative devices proposed in this work. With this purpose an initial phase of calibration and validation of the most relevant mechanical parameters was performed; the most relevant input parameters considered were friction coefficient, initial stiffness and numerical damping. Friction coefficient was set considering the results of the experimental tests carried out at SRMD, numerical damping was set 0.5% or 5% respectively when the numerical model of the statues or of the experimental blocks was considered. This choice is justified by the fact that the concrete blocks of the experimental model can experience relative displacements that cause an increasing of dissipation which, on the other hand, is not possible when the statues are considered. The third parameter, i.e. initial stiffness, was calibrated performing sensitivity analyses in which different values proposed in literature were considered. Numerical results were then compared to those obtained from the experimental tests: a good accordance was found but it is worth noting that, despite this general good result, the implemented model is not able to describe all those unexpected phenomena highlighted in the experimental tests.

After this phase of calibration of the model analyses of the statue of the case of study were carried out. Results pointed out a good reduction of the transferred actions and a reduction of the stress pattern measured on the objects.

5.2 Friction Pendulum devices

5.2.1 Examples of applications of friction pendulum to civil structures

The friction pendulum system has been widely used through years because of its simplicity of application for retrofitting existing structures, in particular bridges. Its first application was in 1986, to retrofit a four–storey apartment building in San Francisco, after this the system was applied in several other situations and it was also developed and improved during years; another significant example of retrofitting with friction pendulum , in this case of a bridge, is the Benicia Martinez bridge, a over 6000 ft long bridge with ten steel truss spans supported by concrete piers; it was retrofitted applying friction pendulum bearings between the piers and the deck, the devices have a diameter of 13 feet (3.9 m) and a displacement capacity of 53 inches (1.34 m) (Figure 5.1,Figure 5.2).

Figure 5.1 - Benicia Martinez Bridge, (CA) (source www.earthquakeprotection.com)

Figure 5.2 - Benicia Martinez friction pendulum (source www.earthquakeprotection.com)

Another interesting example of the application of friction pendulum devices, as tools for retrofitting existing structures, is Pasadena City Hall (Figure 5.3), where friction pendulum bearings were installed between the foundations and the concrete floor slab (Figure 5.4)

Figure 5.3 - Pasadena City Hall (source www.earthquakeprotection.com)

Figure 5.4 - Detail of concrete slab and isolation system (source www.earthquakeprotection.com)

One of the most important improvements to the friction pendulum was the introduction of a second spherical sliding surface that connects the structure above to the device; as we will see in the following part, this technical solution allows a reduction of the total displacement of the structure. Some examples can also be found on Italian territory, such as the isolation of tanks (Figure 5.5, Figure 5.6) in 2008 or the big intervention, after the seismic events of l'Aquila, in the "progetto C.A.S.E." in which a large number of buildings were built and protected with FPD.

Figure 5.5 - Example of application of friction pendulum devices to a water tank

Figure 5.6 - Detail of application of friction pendulum to a water tank

Figure 5.7 - Project "C.A.S.E." , L'Aquila source (www.fip-group.it)

Finally, San Francisco international airport terminal is a building designed by Skidmore, Owings and Merrill to resist a magnitude 8 earthquake occurring on San Andreas fault. It is isolated by means of 267 Friction Pendulum bearings, provided by EPS, which make the over 22 million cubic feet of interior space, the largest isolated building in the world. The bearings provide an isolated period of 3 seconds, reducing the force demand by 70%.

Figure 5.8 - San Francisco Airport, details of the isolation system (source www.earthquakeprotection.com)

Figure 5.9 - San Francisco Airport, details of the isolation system (source www.earthquakeprotection.com)

Figure 5.10 - San Francisco airport (source www.earthquakeprotection.com)

5.2.2 Friction pendulum and double concave friction pendulum device

Isolating devices are mainly of two different types: elastomeric bearings and sliding bearings; sliding devices assume that a low value of friction between the contact surfaces of the devices will reduce the transfer of acceleration from the ground to the structure. Using sliders allows the arrangement of isolated systems (with system we mean structure and devices) with very long periods, and hence with very low shear transfer. But also these devices have their drawbacks.

One of the most relevant problems is providing the adequate restoring force to allow a reduction of displacements: indeed if no restoring force is provided the diameter of the bearing plates would be extremely large; several solutions to this issue have been proposed, one of them is to use a curve sliding surface: the weight of the structure is carried on a spherical sliding surface that slides when the motion exceeds a fixed level and then goes back to the initial position taking advantage of the restoring force due to the curvature (Figure 5.11); this solution gave origin to the friction pendulum device.

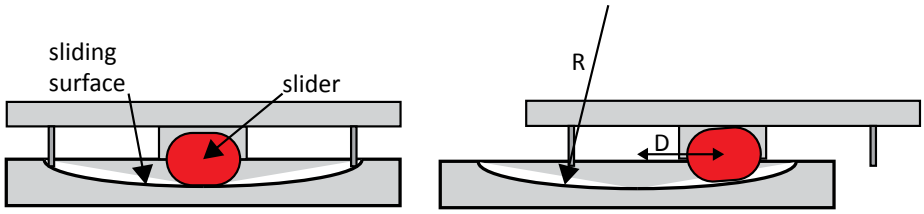

Figure 5.11 - Friction pendulum device, sketch

Several manufacturers put on the market their version of this technology, proposing the same basic concept, with differences on technical choices: such as materials, sliders' shapes and other more. Many improvements to the friction pendulum were proposed as well, one of the most important is the introduction of a second curve surface, which substantially allows to accommodate larger displacements in the identical plane dimension of a single concave device; moreover there is the capability to use different friction coefficients or curvature radii for the two surfaces in order to obtain more flexibility for designer to optimize performances as described in (35), even though, as it will be discussed further on, adding such mechanical variation leads to a more uncertain dynamic response of the device. Friction pendulum system and the double concave version theoretically provides many benefits: the capacity of self re-centering, the independence of the period of the system from the carried mass and the reduced vertical dimension. These characteristics helped this technology to spread even though the real behavior of these devices is far from theory, as it will be shown in the following.

5.2.3 Mechanical behavior of SCCSS and DCCS

Mechanical behavior of concave surface slider devices is characterized by a small number of geometrical and material parameters. If W is the load on the bearing, D the horizontal displacement and μ the coefficient of friction, the resisting force F is given by:

$$F = \frac{W}{R} D + \mu(sgn\dot{D}) \tag{5.1}$$

R is the radius curvature of the sliding surface. The first term in equation (5.1) represents the restoring force due to rise of mass, this provides the horizontal stiffness

$$K_h = \frac{W}{R} \tag{5.2}$$

The period of the isolated structure T is given by

$$T = 2\pi\sqrt{R/g} \tag{5.3}$$

as it can be noted from equation (5.3) the period of the isolated system is independent from the mass of the carried structure. The second term in (5.1) is the friction force between the slider and the sliding surface. It is well known from literature (36) that the friction coefficient depends on both the pressure and the relative velocity of sliding between the surfaces; the coefficient decreases with the increasing pressure and becomes independent of velocity above 51 mm/s (at a pressure greater than 14 MPa), this behavior is the result of experimental tests conducted on friction based devices (also friction pendulums) with spherical surfaces in stainless steel and Teflon sliders. It is worth noting that the frictional force at initiation of sliding (breakaway force, Figure 5.12) is characterized by a static coefficient of friction μs which is substantially larger than the value recorded after the initiation of sliding μd; the coefficient of sliding friction at sliding velocity $\dot{D}$ was approximated by the following equation (36):

$$\mu_s = f_{max} - \delta f \exp(-\alpha \dot{D}) \quad (5.4)$$

Where f_{max} is the maximum coefficient of friction and δf is the difference between maximum friction and friction at very low velocity, α is a constant given for the material. The theoretical hysteresis loop for a friction pendulum is depicted in Figure 5.13

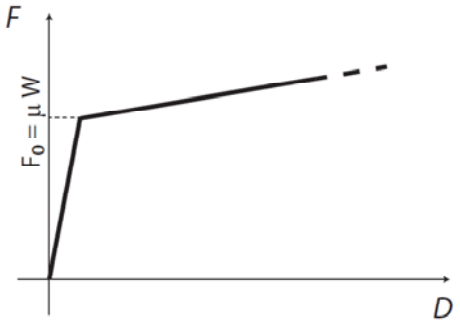

Figure 5.12 - breakaway force

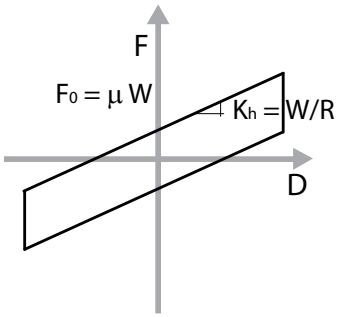

Figure 5.13- Friction pendulum force displacement law

The figure shows clearly the strong linear nature of the restoring force, the high stiffness before sliding occurs and the energy dissipation due to friction. Double concave friction pendulum behavior is not much different from the single concave one; the modeling of this specific device was described by Constantinou (35):

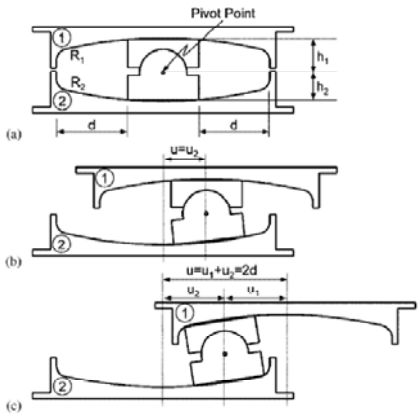

Figure 5.14 - Double concave friction pendulum sketch (36)

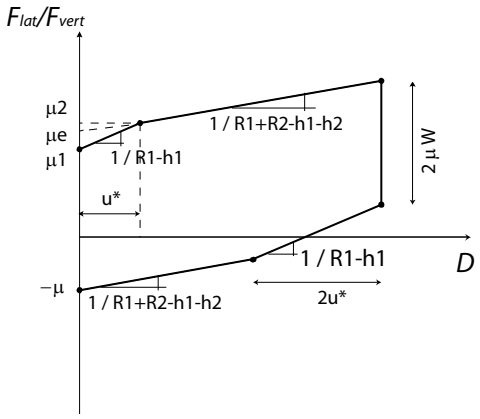

Figure 5.15 - double concave friction pendulum mechanical model

There are different options available for modeling double concave friction pendulum in time history analyses; in the simplest one, describing the situation in which R1-h1 = R2-h2, the bearing can be modeled as the single concave friction pendulum with a nominal radius of curvature R* = R1+R2-h1-h2 and a friction coefficient determined by experiments. The dependence of coefficient of friction from the velocity is described, as for the single friction pendulum, by (36).

Situations in which the coefficients of friction and the curvature radii are unequal can be modeled as two friction pendulum, with different characteristics, placed in series.

5.3 FIP Double Concave Curved Surface Slider for small objects

The application of traditional seismic isolation systems to art objects, with particular attention to big monolithic statues, is a challenging task which requires to take into account, apart from the usual design issues, further aspects associated with the peculiarity of the objects dealt with. First of all, art goods are in general light weight, hence the interaction with the bearing is slightly different from the usual one; moreover it's often difficult to handle the problem of the applicability of the devices in the context of the containing building. The issue of space is also connected to another aspect, which is the maximum design displacement of the system: it is related both to the level of protection we want to set and to the availability of room in the exhibition area.

These considerations lead the choice for the isolating device towards the concave surface slider, in particular its version with two sliding surfaces. This seems to be a worthwhile choice since this device has a reduced application space (in particular in vertical direction), in addition, considering that double concave devices were chosen, they can accommodate double displacements if compared to the single concave ones. Once the type of device is chosen according to its characteristics, it needs to be redesigned in order to obtain its best performance. In collaboration with an Italian firm, FIP industrial from Padova, a leader in the production of anti seismic devices, the redesign of the double concave friction pendulum and their applicability for art objects was carried out. Special attention was paid to the statues of the case study, but also to other light weight objects such as computer servers or medical devices.

The first step of this work on isolation devices was the initial redesign phase: indeed a simple scaling of the standard devices was not sufficient to provide a reliable solution and it was necessary to perform a complete re configuration of the mechanical parts of the devices, also considering different materials and constructive technologies. Devices resulting from such a re disegn phase can be characterized by unexpected behaviors that are not typical of the applications with traditional dimension. For this reason adequate analyses need to be carried out. Results presented in the following part of this work describe the outcomes of the analyses on the resized prototypes of DCCSS, which are different from those with traditional dimensions.

The design parameters of the isolators are the results of a simple iterative procedure based on the actions summarized in the response spectrum for the considered site and a proper return period:

h = 75 mm;
Φ = 270 mm;
$\mathbf{D_{max}}$ = ± 160 mm;
R* = 3000 mm;
N = 10 kN;
μ = value to find;

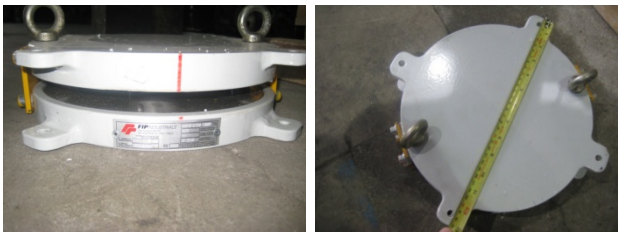

Figure 5.16 - Double concave friction pendulum for the case study

Where h is the height of the device, Φ is its diameter, D_{max} is the maximum displacement the device can accommodate, R* is the effective curvature radius and will be defined in the next paragraph, N is the vertical load acting and μ is the value of the friction coefficient. Of note the value of the coefficient of friction is fundamental for the description of the mechanical behavior of the object and it is strictly linked to energy dissipations. This aspect must be investigated with care because we expect to find very different values of it, much lower than what usually given for traditional DCCSS. The evaluation of friction coefficient will be discussed in the next paragraphs in which results of experimental tests are

presented. An important aspect that characterizes this specific application in terms of friction coefficient is the choice to apply a layer of lubricant on the spherical sliding surfaces. This choice allows to reach very low levels of friction that can be useful in case of a very delicate structure to protect; indeed the limit force to trigger the activation of the device (breakaway force) can set a stress condition that overcomes the mechanical limit of material and damage it even if isolated, this is the reason why lubricating the sliding surfaces was chosen. It is worth noting that, from the point of view of maintenance, the use of lubricant does not require any further control during the life of the isolator more than those prescribed for the un-lubricated conditions; in fact the standards concerning this aspect specify that it is not necessary to re-apply it.

5.4 Experimental tests at FIP

5.4.1 Description of the test set up

In the following paragraph results of experimental tests on resized double concave friction pendulum will be presented and discussed. The first target of this series of experiments is to investigate the general behavior and the dynamic response of these resized devices. Considering that some objects to be isolated are much lighter than other more common ones, it becomes clear that a total prediction of the response is not possible as the response is strictly linked to the operating pressure and to the interaction between physical characteristics of the system. This first series of experiments were conducted at FIP, the Italian firm that cooperated on the design and construction of the devices. Figure 5.17 to Figure 5.21 depict the set up of tests:

Figure 5.17 - test setup

Figure 5.18 - Detail of the displacements recording system

Figure 5.19 – Overview test set up

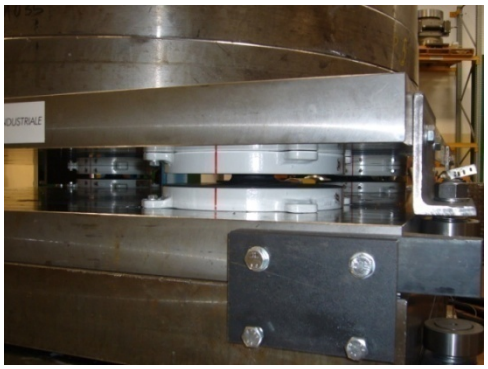

Figure 5.20 - Isolators position

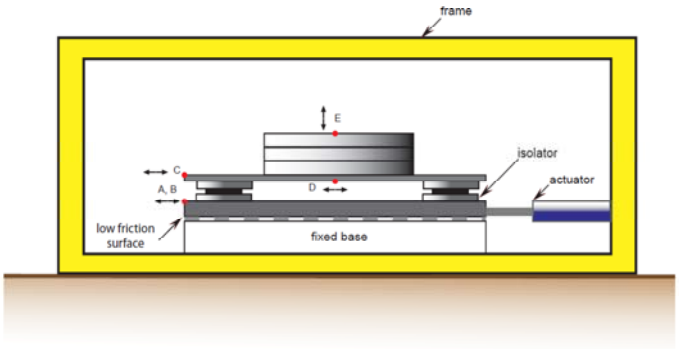

Figure 5.21 - Sketch of test setup

In Figure 5.21 sensors for data acquisition are pointed out, the following list explains the function of each sensor:

- Sensor for moving base acceleration;
- Sensor for base displacements;
- Sensor for isolated mass acceleration;
- Sensor for isolated mass differential displacements;
- Sensor for vertical acceleration.

The specimen consists of three steel plates assembled to obtain a low center of mass configuration with similar total mass to the case study and geometrical characteristic of the isolators set up, similar to the case study as well. Isolators are fixed to a steel plate which is moved by the actuator, and slides on a very low friction surface; the specimen is forced to move only along one direction by means of rails that restrain it from any lateral displacement. The upper plane of the isolator is then fixed to the part of the specimen representing the isolated object. Two groups of tests were performed, one without lubrication of isolators' surfaces and another group with a layer of lubricant to reduce the friction coefficient of the devices and to minimize the level of forces transmitted to the isolated system; indeed the lower is the value of friction coefficient the lower is, consequently, the value of the breakaway force that the isolated object suffers.

The main target of these investigations was to understand the mechanical behavior of the devices and their response in case of an horizontal input. A summary of the tests that were carried out is given in Table 5.1 and Table 5.2

Table 5.1 – un-lubricated device tests

test	x0	f_0	T	v	acc.	acc./g
	[mm]	[Hz]	[s]	[mm/s]	[mm/s^2]	[N/A]
p3	100	0.3136	3.1888	197	388	0.040
p2	100	0.4000	2.5000	251	632	0.064
p4	100	0.4464	2.2401	280	787	0.080
p5	100	0.4880	2.0492	307	940	0.096
p6	100	0.5263	1.9001	331	1094	0.111
p13	125	0.4464	2.2401	351	983	0.100
p7	100	0.5620	1.7794	353	1247	0.127
p8	100	0.5955	1.6793	374	1400	0.143
p14	150	0.4464	2.2401	421	1180	0.120
p12	125	0.5955	1.6793	468	1750	0.178
p17	175	0.4464	2.2401	491	1377	0.140
p18	200	0.4464	2.2401	561	1573	0.160

Table 5.2- lubricated device tests

test	x0	f_0	T	v	acc.	acc./g
	[mm]	[Hz]	[s]	[mm/s]	[mm/s^2]	[N/A]
p2	50	0.3136	3.1888	99	194	0.020
p4	50	0.4464	2.2401	140	393	0.040
p12	75	0.3136	3.1888	148	291	0.030
p6	50	0.5620	1.7794	177	623	0.064
p8	50	0.5955	1.6793	187	700	0.071
p5	75	0.4464	2.2401	210	590	0.060
p10	50	0.7410	1.3495	233	1084	0.110
p7	75	0.5620	1.7794	265	935	0.095
p9	75	0.5955	1.6793	281	1050	0.107
p11	75	0.7410	1.3495	349	1626	0.166

Inputs are sinusoidal functions applied as displacements; the maximum displacement is set equal to x_0 and, after that, frequency is changed to obtain different levels of velocity and acceleration. Each input is applied with an entrance and an exit half loop to avoid discontinuities and peaks in the response, after that a proper number of cycles is applied, to investigate the steady phase of the motion.

5.4.2 Significant results

For brevity in this paragraph only some significant results of the tests will be presented, in order to provide a general overview of the dynamic response of the devices and of their behavior, compared with the theoretical reference model (35).

5.4.2.1 Displacements and accelerations

First of all the tests with no lubrication will be discussed; this condition represents the normal application of DCCSS, with a governing coefficient of friction given by the interaction between the stainless steel of the surfaces and the slider, the layout of the results shows for each test described an overview of the relative displacements of the isolated mass (difference between the displacement of the ground and of the isolated mass); the acceleration of the isolated mass compared to the input ground acceleration and two typical cycles "force versus displacement" referred to the average behavior of one device (obtained considering the part of vertical load that acts on each isolator); in the hysteresis loops graphs two other straight lines are depicted: the red dash-dotted line represents the best fitting line for the constant stiffness part of the loop; the black dashed line, instead, represents the straight line, with slope equal to the expected theoretical value (W/R^*) and having the same value of force of the experimental tests when the displacements are zero.

Test 6 Non Lubricated

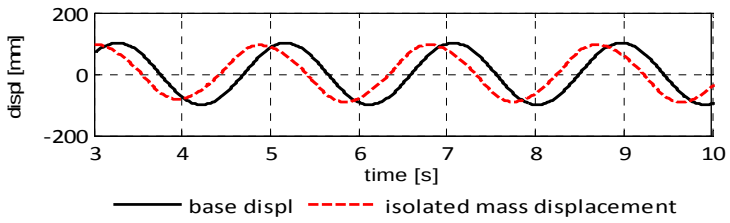

Figure 5.22 - test 6 NL displacements

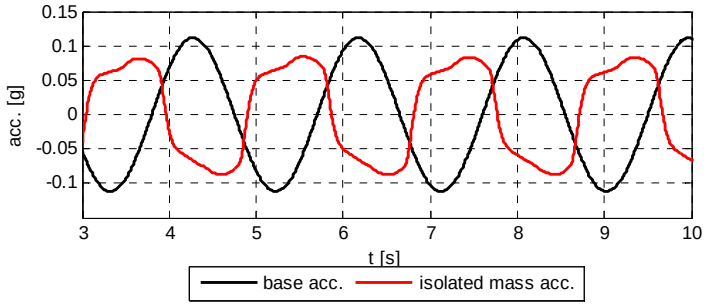

Figure 5.23 - test 6 NL accelerations

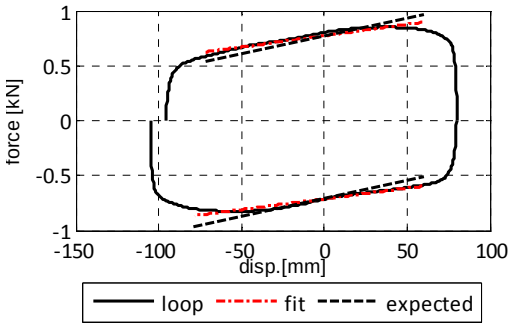

Figure 5.24 - test 6 NL cycle 2

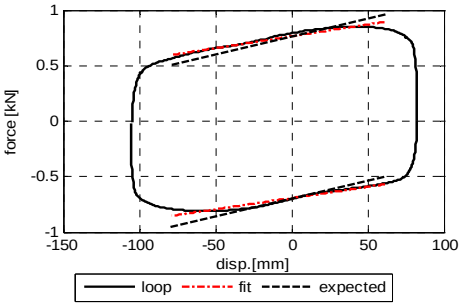

Figure 5.25 - test 6 NL cycle 5

The relative displacement of the mass (Figure 5.22) has a maximum value as wide as the base displacement which means that the system is providing a proficient level of isolation; the acceleration response (Figure 5.23) reaches the value of 0.08 g, it is worth noting that the profile of the response is very close to what was expected, with an almost vertical part corresponding to the change of the acceleration sign. Figure 5.24 and Figure 5.25 are two typical force-displacement cycles, that follows a behavior which is very close to the one expected from the theoretical model.

Test 7 Non Lubricated

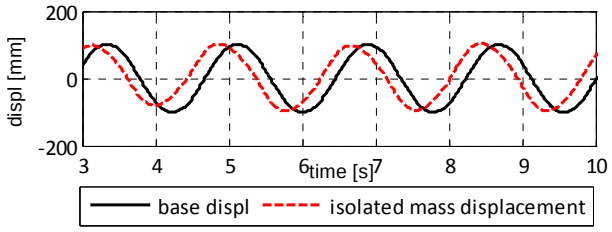

Figure 5.26 - test 7 NL displacements

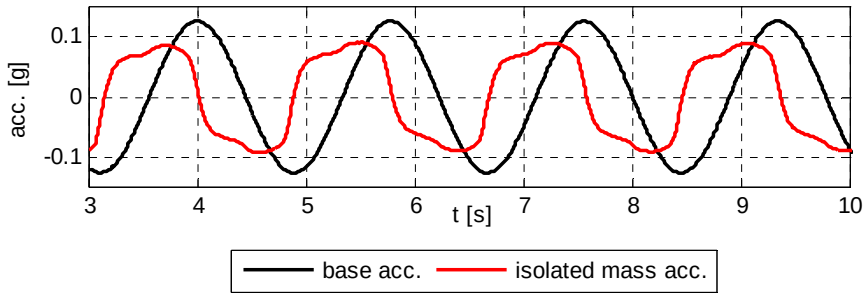

Figure 5.27 - test 7 NL accelerations

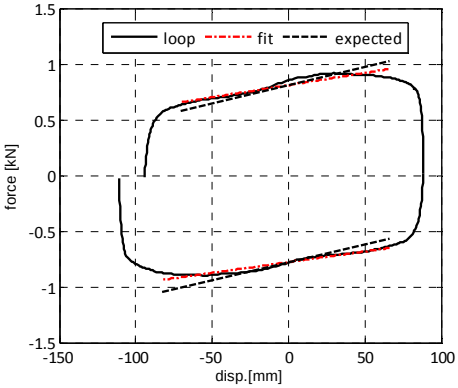

Figure 5.28 - test 7 NL cycle 2

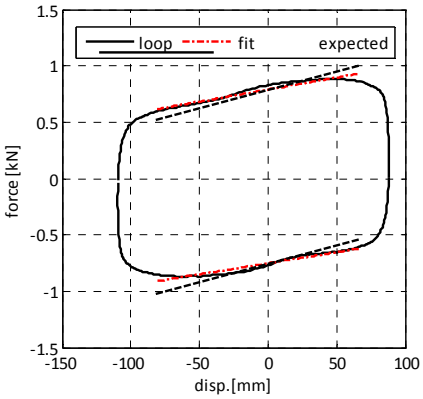

Figure 5.29 - test 7 NL cycle 2

Test 8 Non Lubricated

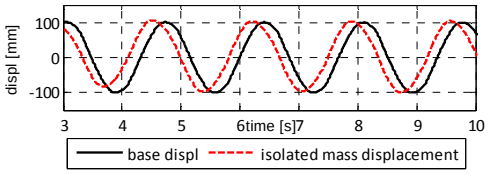

Figure 5.30 - test 8 NL displacements

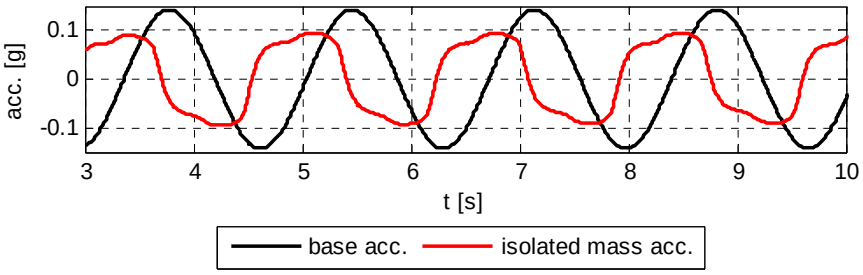

Figure 5.31 - test 8 NL accelerations

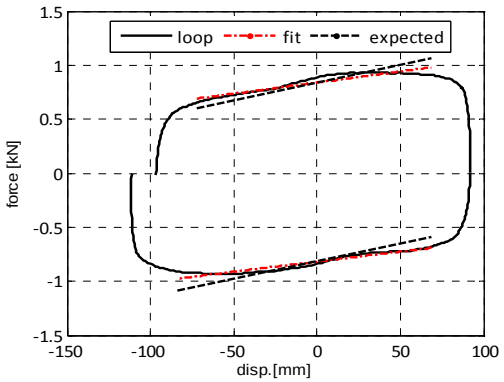

Figure 5.32 - test 8 NL cycle 2

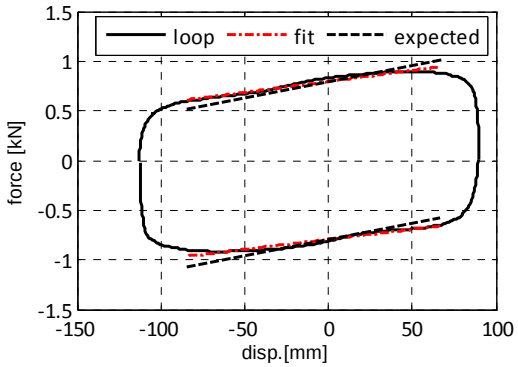

Figure 5.33 - test 8 NL cycle 5

Test p9 Lubricated

The second group of tests were performed with lubricated surfaces, i.e. with the application of a layer of lubricant between the slider and the sliding surfaces, that during the motion spreads it on the sliding surfaces. This choice allows to reduce the value of the friction coefficient between the mechanical components of the devices and it consequently helps to set a lower value of the "breakaway force" transmitted to the isolated object.

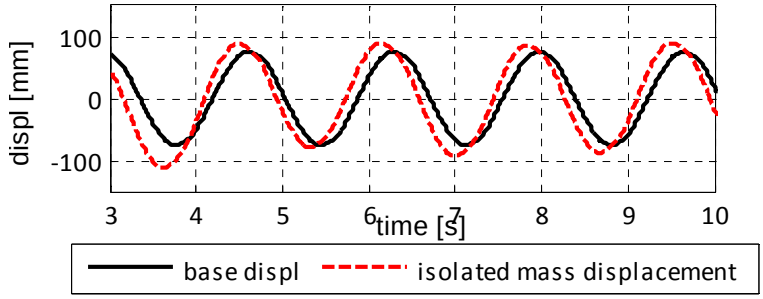

Figure 5.34 - test 9 L displacements

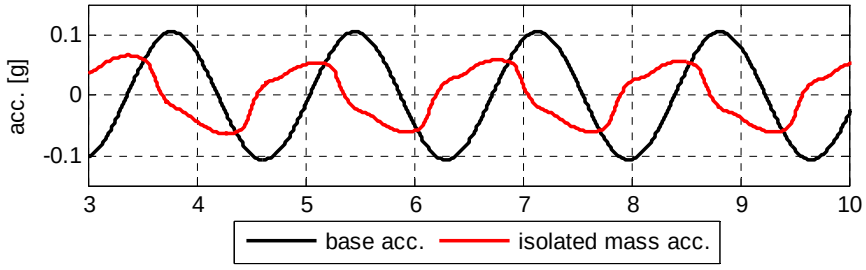

Figure 5.35 - test 9 L accelerations

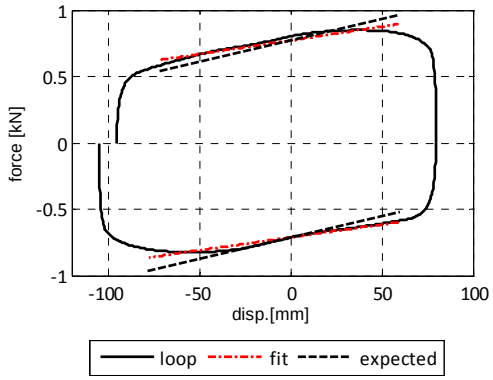

Figure 5.36 - test 9 L cycle 2

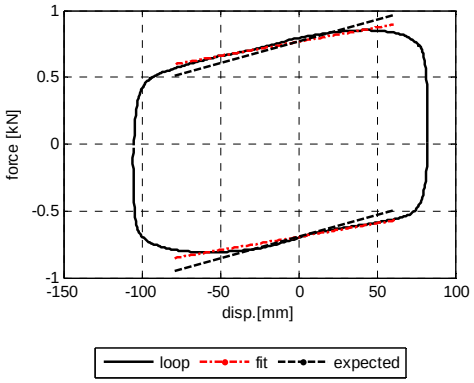

Figure 5.37 - test 9 L cycle 5

Test 10 Lubricated

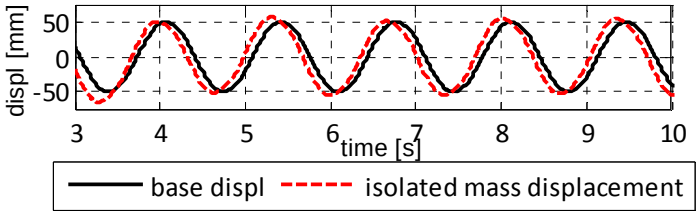

Figure 5.38 - test 10 L displacements

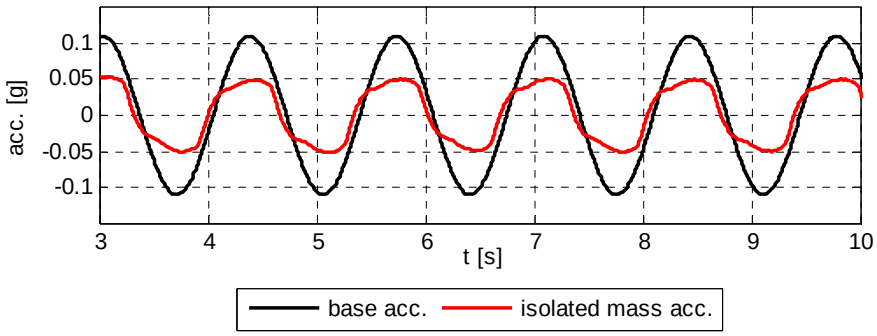

Figure 5.39 - test 10 L accelerations

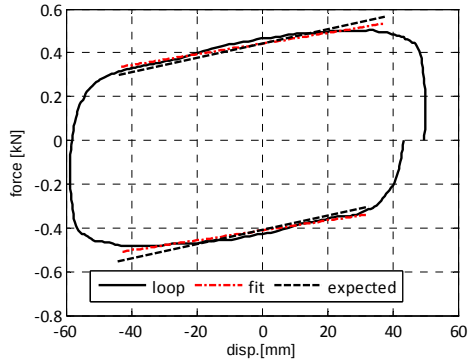

Figure 5.40 - test 10 L cycle 2

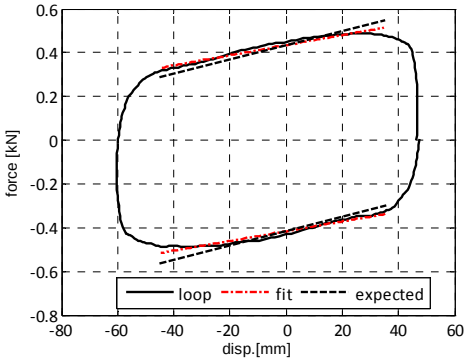

Figure 5.41 - test 10 L cycle 5

5.4.3 General considerations

The results presented above show the dynamic response of the isolated system and allow to understand that the effects of reduction of the actions is more evident when the friction coefficient is lower; however the isolation system seems to provide a proficient level of action reduction. The close overlap between the experimental results and the mechanical model is worth noting (e.g. Figure 5.40 and Figure 5.41). Indeed it can be pointed out that the experimental value of the stiffness of the system (slope of the red dashed line in the cycles graphs) fits the expected value of stiffness (black dashed line in the same graphs) with a good level of accordance. It is also remarkable that the shape of the loops follows as well the mechanical model with good accordance: it is clearly visible that the response of the devices follows two straight paths (positive direction and negative direction) with increasing forces and displacements, and the change of direction of motion is identified by a vertical segment.

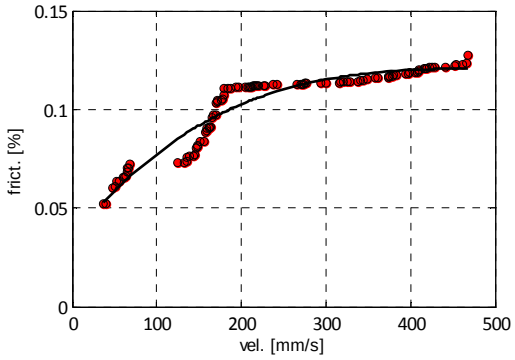

Figure 5.42 - global friction coefficient NL tests

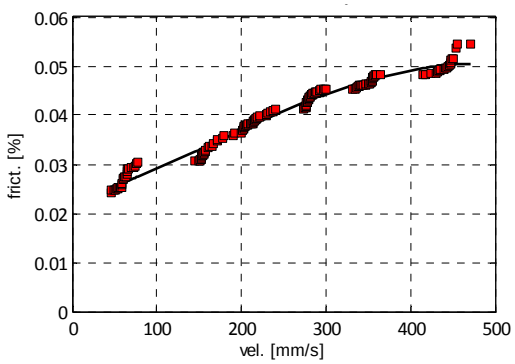

Figure 5.43 - Global friction coefficient L tests

An important aspect that needs to be pointed out is the coefficient of friction calculated from the experimental tests; the global results obtained from the tests carried out at FIP is depicted in Figure 5.42 and Figure 5.43, that are respectively referred to non lubricated and lubricated tests; it is worth noting that the value of friction coefficient reaches 12% for the non lubricated tests, while the maximum level of friction obtained from tests lubricated is almost 5%. These results are particularly important and some remarks need to be made because, as it will be shown in the following, determination of the coefficient of friction of the system is a critical aspect and it strongly affects predictions of the dynamic response. In this experimental campaign, the particular set up of the tests, in which the motion is restrained in the perpendicular direction by means of two rails, it is impossible to eliminate the component of energy dissipation even though the model is provided with wheels that reduce uncontrolled energy dissipation due to impact; hence it affects the value of the coefficient of friction which unavoidably includes this contribution; the result is an overestimate value. Furthermore the value of friction, which is one of the target of these tests, is one of the variables for the numerical models that are usually applied in the design phase of the isolation system; it is hence evident how much it can affect the final prediction of the response.

5.5 Experimental tests at SRMD

As it was previously stated, the experimental campaign of tests, carried out at SRMD testing facility, in San Diego, had two main targets: the first was an investigation about the general behavior of double concave curved surface slider, re designed to fit situations with low vertical load and reduced space of application. This in order to describe their mechanical behavior and properties, and also to understand in which way their response can be considered similar to the traditional double concave curved surface sliders.

The second important target was to describe the effects of the interaction between the isolation system and the typology of objects studied, since their peculiarities in geometry and inertia characteristics require an accurate analysis of the possible effects that the dynamic of the system may cause. With these objectives a model was built, based on the geometrical characteristics of the statues of the case study. As it will be described in the following the model is modular and the single parts can be assembled together to cover a wide range of different geometrical and inertia configurations.

5.5.1 Modular blocks system

The basic idea of the model that was designed and built for these experimental tests is “modularity”. Since the variety of objects and conditions that needed to be simulated with these tests is very wide, it was almost mandatory to design a specimen that could fit the most of the situations and, above all, the one represented by the case study of “Galleria dell’ Accademia”. The model was then designed considering the statues of the case study and their geometrical and inertia features, keeping always the possibility to assemble it with a different layout, in order to approximate a different condition.

The model consists in four blocks of reinforced concrete with two different shapes: one block (“footing block” in the following) represents the base of the statue, three blocks with same dimensions (“body blocks” in the following) represent the body of the statue. The body blocks have 9 going through holes that allow the passage of 9 threaded bars. The bars can be anchored in the footing block and tightened up on top of the assembled body. The final configuration can be modified by moving the body blocks in order to obtain the desired condition of inertia and position of the center of mass.

Figure 5.44- casting of the body blocks

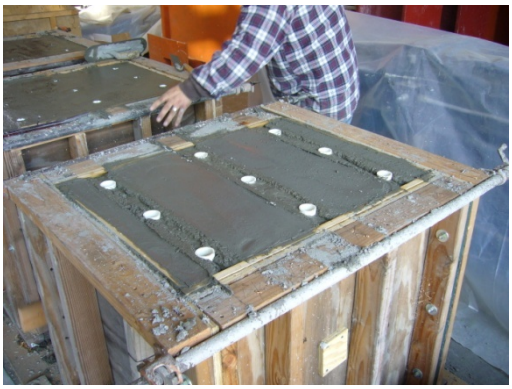

Figure 5.45 - casting of the body block

Figure 5.46 -casting of the footing block

An overview of the elements and of the measures of the model is given in Figure 5.44, Figure 5.45 and Figure 5.46

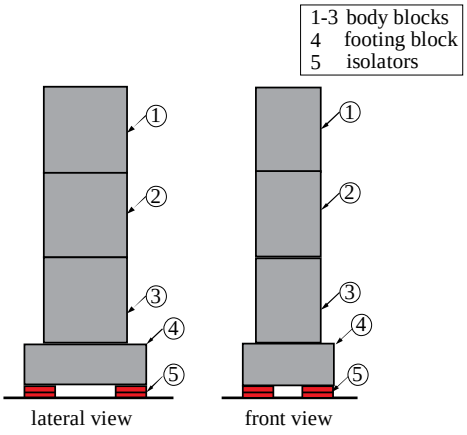

Figure 5.47 - modular blocks of the model

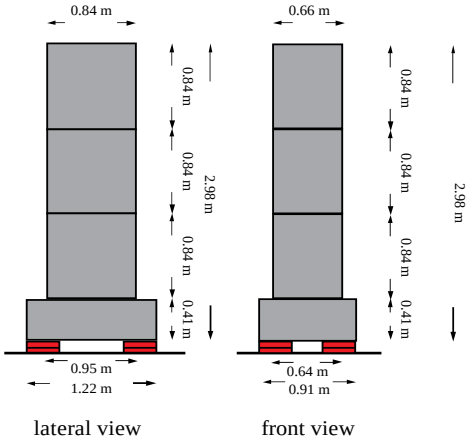

Figure 5.48 - dimensions of the blocks

The isolation system consists of four devices (par. 5.3) placed at the four corners of the footing block in order to obtain the maximum distance and hence to reduce the effects of rocking. This choice was made to represent the worst condition of set up, when the room for the intervention is very small.

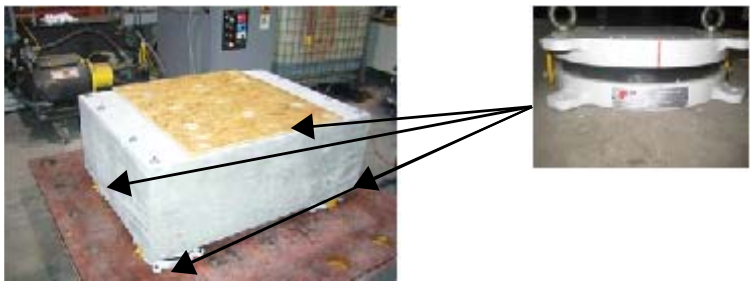

Figure 5.49 - position of isolators under the footing block

5.5.2 Comparisons between the model and the case study

As mentioned above the model was designed with the purpose of resembling the statues of the case study, assuming that they are rigidly connected to the base, in order to prevent the triggering of dynamic phenomena pointed out in the rigid body approach. Geometrical features of the model were designed in order to best fit the geometry, inertia and mass of the statues, a general overview of the accordance between the model and the case study is given in Figure 5.50.

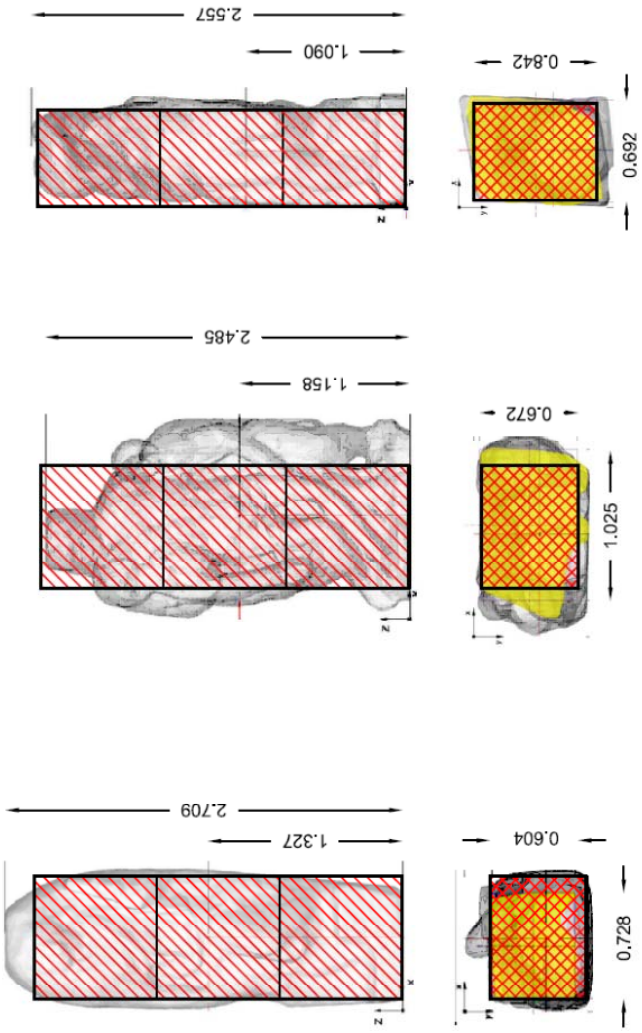
2.557
1.090
0.842
0.692
2.485
1.158
0.672
1.025
2.709
1.327
0.604
0.728

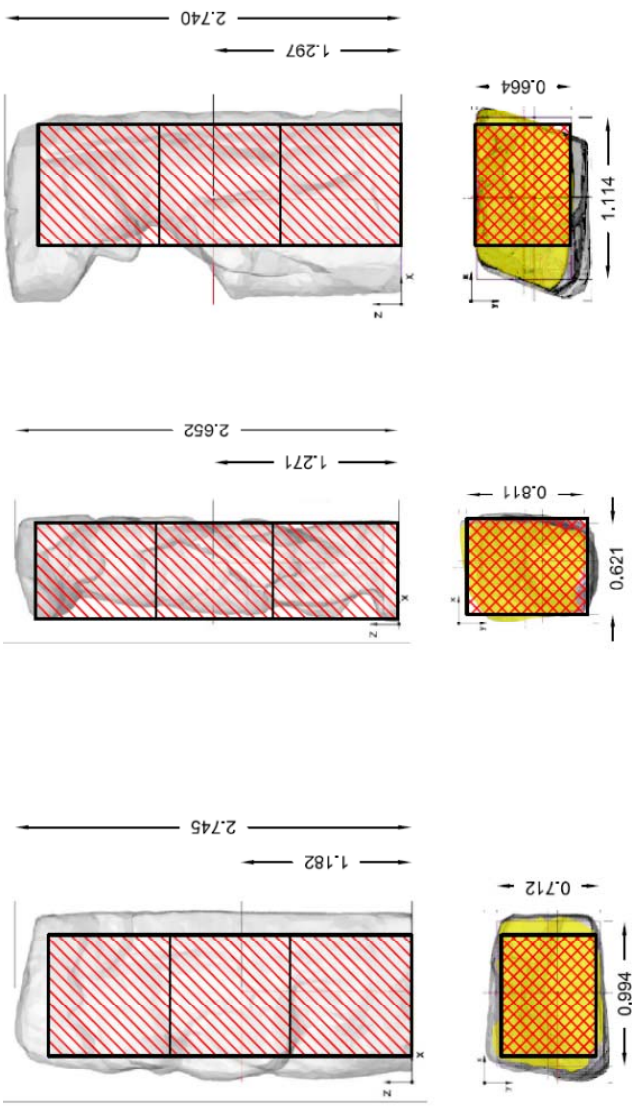

Figure 5.50 -geometrical comparison between the model and the statues

As described in Figure 5.48, each block is 0.83 x 0.66 x 0.83 m and the weight is respectively 1056 kg, 1056 kg and 1047 kg, the footing element is 1.21 x 0.91 x 0.38 m with a weight of 1065 kg. The geometry of the model fits properly the case study. An important assumption was made about the footing block: it was previously said that nature of the base block is often uncertain (it can be hollow or full); such an uncertainty is very influential on the behavior of the object because it changes the position of the center of mass and the total mass of the system, which are fundamental parameters for the dynamic response of the system. It was then decided to align the value of the mass of the model to the case study; the footing block was then designed as a full block of concrete , with base dimensions of a typical basement but with reduced height in order to keep the mass constant. As it is visible from picture Figure 5.50 the statues have different geometrical features (Prigione Atlante has, for example, a clear eccentricity of the mass in the upper part); the modular system built for the tests allows to assemble different final configurations to better fit each case, considering also the possibility to use only one or two of the body blocks. Some examples of possible configurations are given in Figure 5.51.

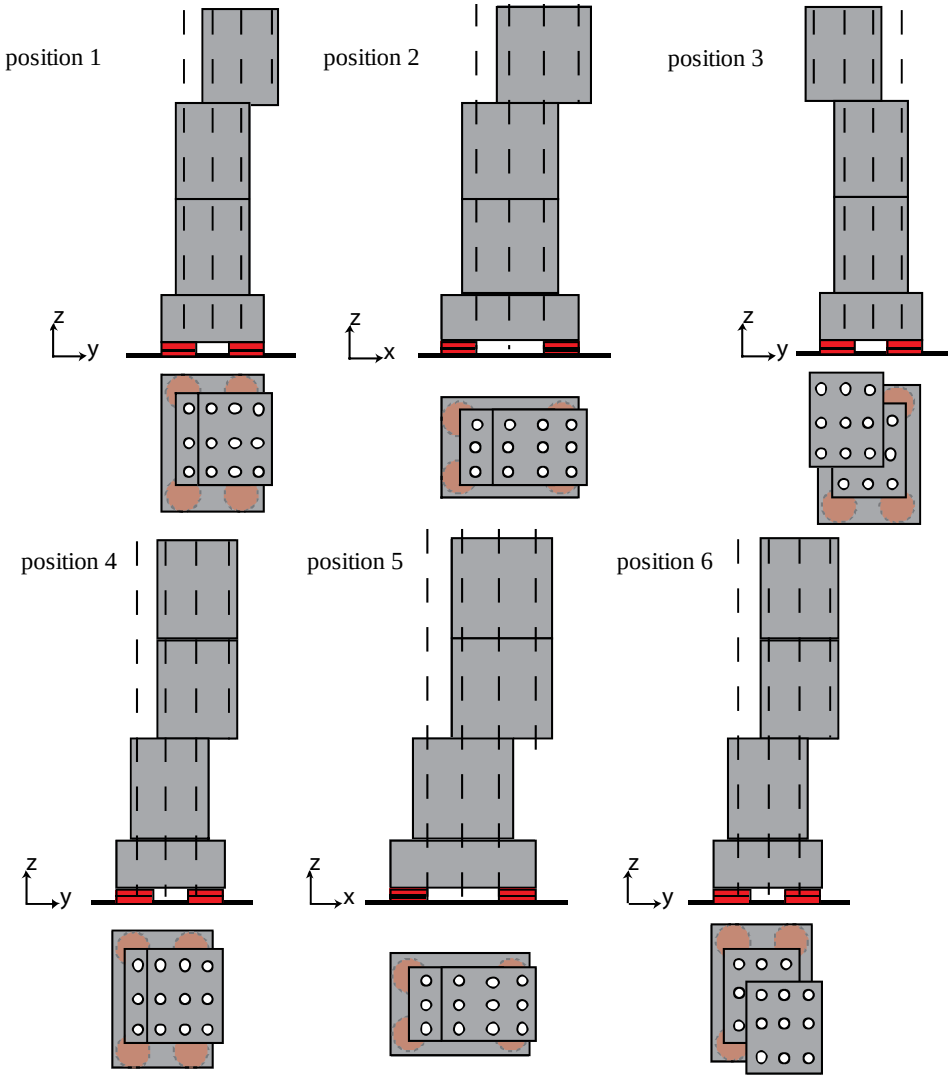

Figure 5.51 - examples of possible configurations of the blocks

In Table 5.3 geometrical features of the statues are compared to those of the different configurations of the model (Table 5.4), in order to show the level of accordance between the two:

Table 5.3 - geometrical features of the statues of the case study

	S Mat	Pie	Gio	Rid	Brb	Atl	Min	Max	Avg
H [m]	1.327	1.163	1.090	1.182	1.271	1.297	1.090	1.327	1.222
B_{x1} [m]	0.415	0.449	0.349	0.500	0.358	0.561	0.349	0.561	0.439
B_{x2} [m]	0.313	0.576	0.343	0.496	0.263	0.553	0.263	0.576	0.424
B_x [m]	0.728	1.025	0.692	0.996	0.621	1.114	0.621	1.114	0.863
e_x [m]	0.051	0.063	0.003	0.002	0.048	0.004	0.002	0.063	0.028
λ_x [-]	3.645	2.269	3.150	2.374	4.092	2.329	2.269	4.092	2.976
B_{y1} [m]	0.399	0.414	0.546	0.426	0.525	0.403	0.399	0.546	0.452
B_{y2} [m]	0.199	0.258	0.296	0.295	0.286	0.261	0.199	0.296	0.266
B_y [m]	0.603	0.672	0.842	0.721	0.811	0.664	0.603	0.842	0.719

	S Mat	Pie	Gio	Rid	Brb	Atl	Min	Max	Avg
e_y [m]	0.103	0.078	0.125	0.065	0.120	0.071	0.065	0.125	0.094
λ_y [-]	4.403	3.460	2.588	3.277	3.134	3.907	2.588	4.403	3.462

Table 5.4 - geometrical features of the configurations of the model

	pos 1	pos 2	pos 3	pos 4	pos 5	pos 6
H [m]	1.257	1.257	1.257	1.257	1.257	1.257
B_x [m]	0.838	0.838	0.838	0.838	0.838	0.838
B_y [m]	0.660	0.660	0.660	0.660	0.660	0.660
λ_x [-]	3	3	3	3	3	3
λ_y [-]	2.54	2.54	2.54	2.54	2.54	2.54
e_x [m]	0.00	0.10	0.10	0.00	0.19	0.19
e_y [m]	0.08	0.00	0.08	0.16	0.00	0.16

With reference to Table 5.3 and Table 5.4 the symbols used respectively represent:

- H = is the height of the center of mass;
- B_{x1},B_{x2} , B_{y1} , B_{y2} = are the lengths of the segments obtained from the projection of the center of mass on the base of the statue;
- B_x , B_y = are the total dimensions of the base of the statue;
- e_x , e_y = are the values of the eccentricity of the center of mass along the two horizontal directions;
- λ_x , λ_y = are the values of the coefficient of slenderness.

Table 5.5 - inertia of the statues of the case study

	S Mat	Pie	Gio	Rid	Brb	Atl	Min	Max	Avg
I_x [m^5]	0.767	0.654	0.738	0.771	0.809	0.840	0.654	0.840	0.763
I_y [m^5]	0.782	0.703	0.730	0.805	0.797	0.858	0.703	0.858	0.779
i_x [m]	0.705	0.614	0.483	0.954	0.551	1.207	0.483	1.207	0.752
i_y [m]	0.734	0.710	0.473	1.039	0.534	1.258	0.473	1.258	0.791

Table 5.6 - inertia of the configurations of the model

	pos1	pos2	pos3	pos4	pos5	pos6	min	max	avg
I_x [m^5]	0.802	0.784	0.802	0.802	0.784	0.802	0.784	0.802	0.796
I_y [m^5]	0.815	0.677	0.677	0.652	0.677	0.677	0.652	0.815	0.696
i_x [m]	0.759	0.751	0.759	0.759	0.751	0.759	0.751	0.759	0.756
i_y [m]	0.765	0.698	0.698	0.684	0.698	0.698	0.684	0.765	0.707

Similarly the parameters presented in Table 5.5 and Table 5.6:

- I_x I_y = are the values of the inertia moment about the central axis
- i_x i_y = = are the values of the inertia radii.

Data summarized in Table 5.5 and Table 5.6 show that there is a good accordance between the model and the case study both in terms of geometry and inertia; it is worth noting that all data given in the above tables are referred to the statue without base and to the three body blocks. another important feature that needs to be compared is the total mass of the bodies which is given in the following:

- **Smat** = 3235 kg;
- **Pie** = 4324 kg;
- **Gio** = 2396 kg;
- **Rid** = 4590 kg;
- **Brb** = 2271 kg;
- **Atl** = 3880 kg.

The three block elements, instead, provide a weight of 3159 kg. When the condition of the statue fixed to the base is considered the values of the geometric parameters change. This situation provides lowering of the center of mass and a variation of the inertia parameters. However the correspondence between the model and the case study is preserved. The most relevant difference between the model and the real cases is about the base; in fact for the "Prigioni" the footing can have different characteristics: it is, in general, around 0.75 m high sometimes it is made out of stone plates, assembled to obtain an hollow cavity that keeps the global center of mass high, and sometimes it is just a filled block; plane dimensions vary according to the dimension of the object placed on it, in order to obtain a plan area wide enough. In the testing set up, instead, the base is made of a filled concrete block. In order to keep the value of the global mass similar to the case study, the decision of reducing the height of the base was taken. Actually the height of the base block is 40.6 cm and with a mass of approximately 1050 kg, which is close to the value of the real bases. Rocking phenomenon and the effects due to inertia of forces on the system are reduced by this choice, because of the lower position of the center of mass, the reduction is though considered reasonable.

5.5.3 Possible layouts and configurations

As it will be described in the following several tests were carried out with different objective of investigation: five different configurations were adopted each one with a specific target. In the following the definition of the configurations given in this paragraph will be used.

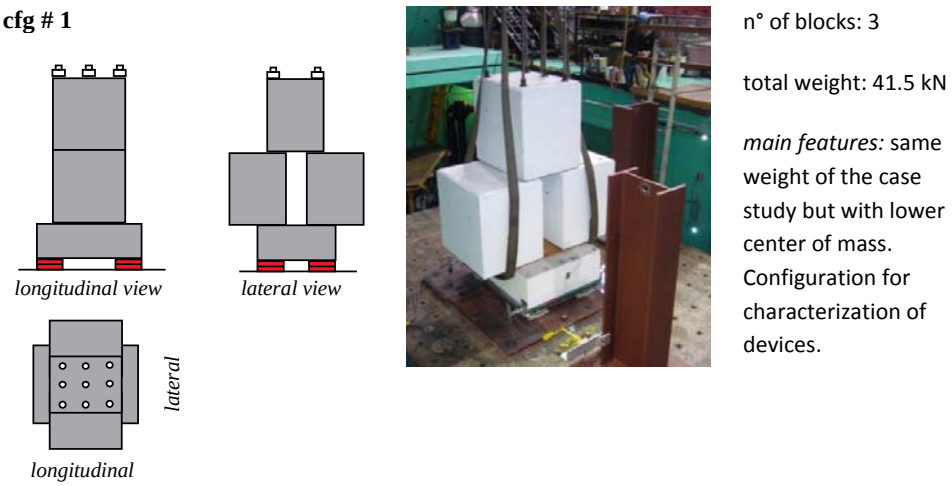

Figure 5.52 - configuration 1 a)sketch, b)set up, c) details

cfg # 2

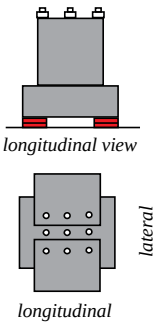

n° of blocks: 2

total weight: 30.9 kN

main features: low center of mass and lower weight.

Figure 5.53- configuration 2 a)sketch, b)set up, c) details

cfg # 3

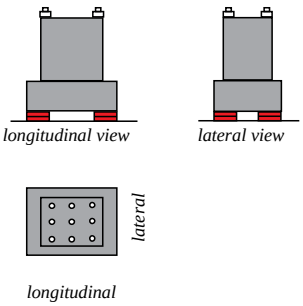

n° of blocks: 1

total weight: 20.6 kN

main features: another condition with low center of mass.

Figure 5.54- configuration 3 a)sketch, b)set up, c) details

cfg # 4

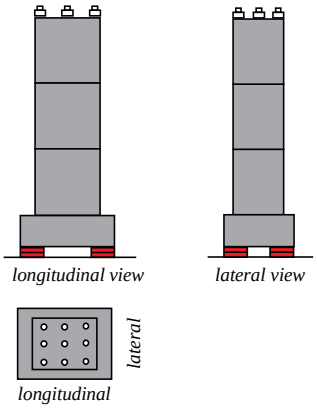

n° of blocks: 3

total weight: 41.5 kN

main features: high position of the center of mass

Figure 5.55 - configuration 4 a)sketch, b)set up, c) details

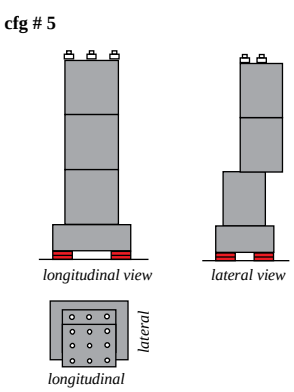

n° of blocks: 3

total weight: 41.5 kN

position of the center of mass:

main features: eccentricity along the lateral direction

Figure 5.56 - configuration 5 a)sketch, b)set up, c) details

Configurations from 1 to 3 are referred to the characterization of the devices, a series of tests carried out to investigate about the mechanical characteristics of the devices such as friction coefficient and stiffness, and their relations with the values traditionally used for bigger friction pendulum devices. A second group of tests was carried out in configuration 4 and 5, which resemble the geometrical characteristics of the case study; these tests were carried out to investigate the dynamic response of an isolated system with the features of a statue.

5.5.4 Testing protocol description

5.5.4.1 Data acquisition

Data acquired during the tests are accelerations and displacements; the layout of sensors was designed in order to allow the reconstruction of the dynamic response of the isolated system, considering also the average response of the devices; indeed the devices were not singularly monitored but accelerations and displacements, recorded during the tests are always referred to the isolated system. Even though this solution does not provide the most precise result for studying the devices it allows to understand the response of the system under an horizontal and a vertical input.

This paragraph summarized the layout of the acquisition devices for the different configurations, in the following, when referring to sensors, the nomenclature presented here will be recalled:

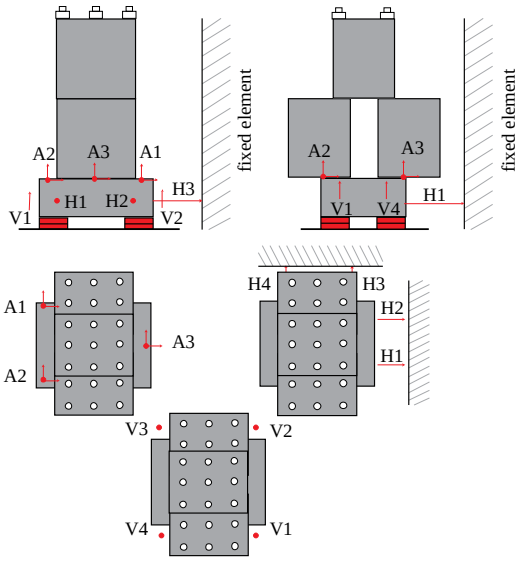

Figure 5.57 - sensors layout configuration cfg#1

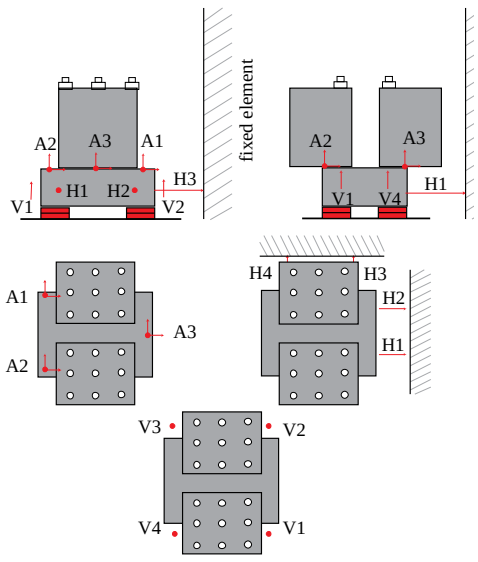

Figure 5.58 - sensors layout configuration cfg#2

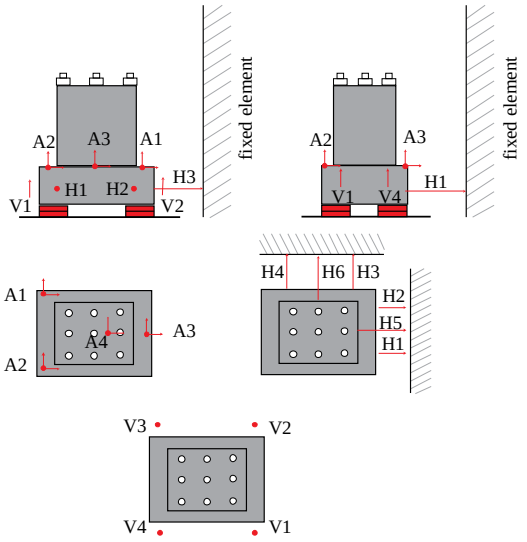

Figure 5.59 - sensors layout configuration cfg#3

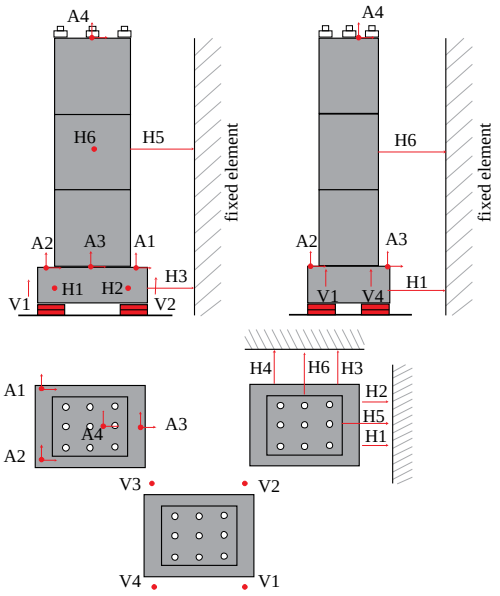

Figure 5.60 - sensors layout configuration cfg#4

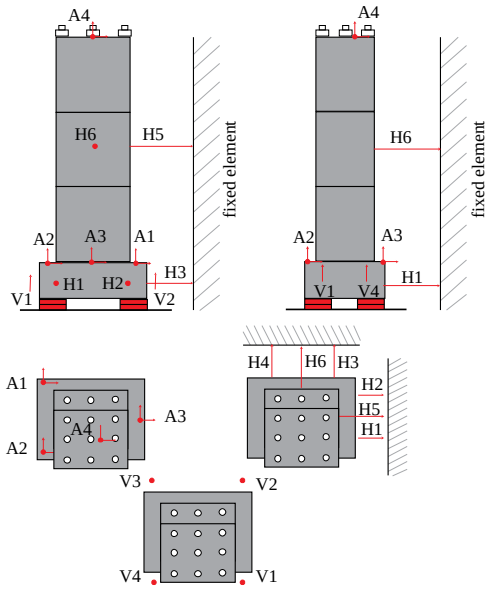

Figure 5.61 - sensors layout configuration cfg#5

Sensors tags:

A_i = triaxial accelerometers;

H_i = unidirectional string potentiometers for horizontal displacements;

V_i = unidirectional sensors for vertical displacements.

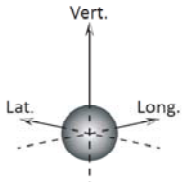

Figure 5.62 - reference system for data acquisition devices

5.5.4.2 Details about the input and the tests

For this experimental campaign sinusoidal inputs were used to investigate the response of the system. The chosen inputs have the same level of displacements and a variation in the frequency of the input is given in order to provide different velocities and accelerations. The nomenclature of the inputs is the following:

D1 = displacement level 1, 60 mm

V1,V2 = velocity level, respectively 200 mm/s and 300 mm/s;

D_i NN_V_i = full definition of the input, displacement level, multiplier of the velocity level, velocity level itself.

VERT1,VERT2 = vertical action (only for test 17 and test 18)

A summary of both horizontal and vertical inputs applied is given in Table 5.7 and Table 5.8:

Table 5.7 - horizontal inputs specifications

input name	amplitude		frequency	Pgv		Pga
	[in]	*[mm]*	*[Hz]*	*[in/s]*	*[mm/s]*	*[g]*
D1V1	2.36	60.00	0.53	7.86	200.00	0.07
D1_05_V1	2.36	60.00	0.265	3.93	100.00	0.02
D1_08_V1	2.36	60.00	0.424	6.29	160.00	0.04
D1V2	2.36	60.00	0.8	11.86	300.00	0.15
D1_15_V2	2.36	60.00	1.2	17.79	450.00	0.34

Table 5.8 - vertical inputs specifications

input name	amplitude		frequency	Pgv		Pga
	[in]	*[mm]*	*[Hz]*	*[in/s]*	*[mm/s]*	*[g]*
V1	0.78	19.81	1.53	7.50	190.46	0.19
V2	0.39	9.91	2.17	5.32	135.06	0.19

The summary of the carried out tests, with the correct order of performance is given in Table 5.9, which summarizes the single tests including details about the input function, the geometrical configuration tested and the direction of application of the input. In general three complete cycles were applied to the structure (with exception for test 20), assuming this number is high enough to assure a full development of the steady state response.

In order to provide a smooth beginning and end of the motion phenomenon, without sudden and sharp dynamic effects an entrance and an exit half cycles were also included in the input; an example of the typical input function is given in Figure 5.63, where the three cycles for the input D1 V1 are highlighted in different colors and the entrance and exit loops are depicted in black.

Table 5.9 – test summary

N°	LON	LAT	VERT	PGD	PGV	PGA	CONFIGURATION					DIR
				[mm]	[mm/s]	[mm/s^2]	1 [LCM]	2 [LCM+]	3 [LCM-]	4 [HCM]	5 [HCME]	
1	D1V1			60	200	0.07	N L					LON
2	D1V1			60	200	0.07	X					LON
3	D10_5V1			60	100	0.017	X					LON
4	D10_8V1			60	160	0.05	X					LON
5		D10_8V1		60	160	0.04	X					LAT
6	D1V2			60	300	0.15	X					LON
7	D11_5V2			60	450	0.35	X					LON
8		D10_5V1		60	100	0.017	X					LAT
9		D1V2		60	300	0.15	X					LAT
10	D10_8V1			60	160	0.04		X				LON
11	D10_8V1			60	160	0.04			X			LON
12	D10_8V1			60	160	0.04				X		LON
13	D10_8V1			60	160	0.04				X		LON
14		D10_8V1		60	160	0.04				X		LAT
15	D11_5V2			60	450	0.35				X		LON
16		D11_5V2		60	450	0.35				X		LAT
17	D10_8V1		VERT 1	60/19.8	160/190	0.04/0.19				X		LON
18	D10_8V1		VERT 2	60/9.91	160/135	0.04/0.19				X		LON
19	D10_8V1	D10_8V1		60	160/160	0.04/0.04				X		2D
20	D11_5V2	D10_8V1		60	300/160	0.35/0.04				X		2D
21	D10_8V1			60	160	0.04					X	LON
22		D10_8V1		60	160	0.04					X	LAT
23	D10_8V1	D10_8V1		60	160/160	0.04/0.04					X	2D
24	D11_5V2	D10_8V1		60	300/160	0.35/0.04					X	2D

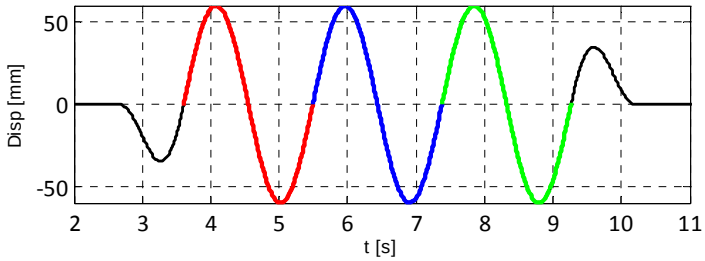

Figure 5.63 - D1 V1 input

5.5.5 Results and comments

In this paragraph a selection of interesting results of the experimental tests will be described, for brevity just the most significant will be presented.

5.5.5.1 Standard results

Stiffness:

A comparison between the values of stiffness obtained from the experimental data and the theoretical value given for the friction pendulum model is described in the following; the theoretical value is W/R* and the experimental value is obtained by calculating the slope of the best fitting straight line that approximates the behavior of the cycle force displacement, in the range between the 75% of the maximum and the minimum displacements. This comparison points out the difference between the expected behavior and the measured one. Even though it is important to mention that the approximation with a straight line neglects possible local oscillations in stiffness that, as seen from other results of these experimental tests, are often present. However it can be useful to study this parameter in order to get a general overview of the dynamic behavior .

Results shown are divided into two groups: the first one is for tests carried out in configuration cfg#1, with the total vertical load acting and a lower position of the center of mass, and the second one considers configurations cfg#4 and cfg#5, characterized by the high position of the center of mass, that resembles the geometrical layout of the case study.

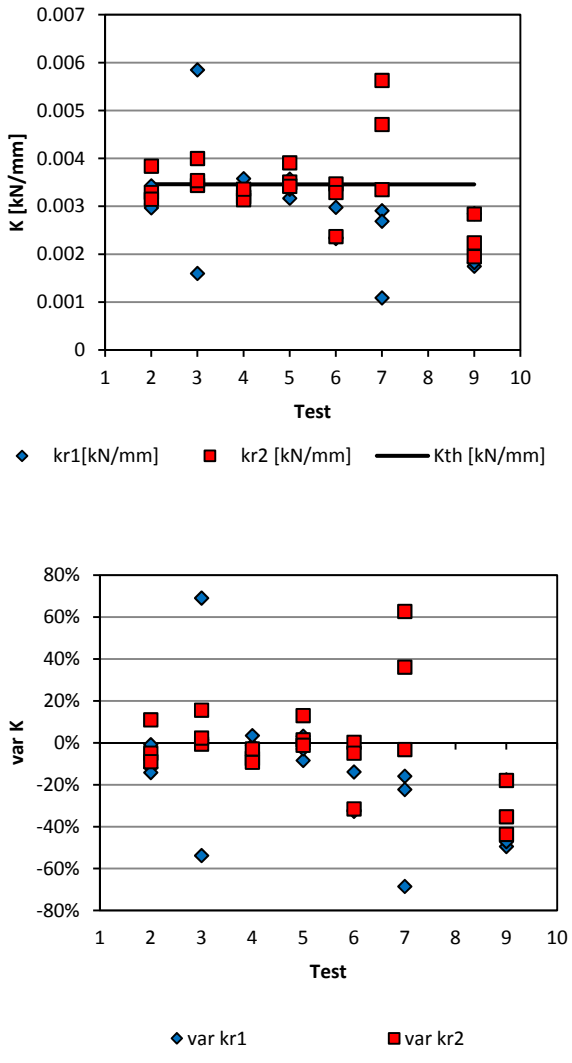

Figure 5.64 - tests cfg1 a) stiffness b) variation of stiffness from the expected value

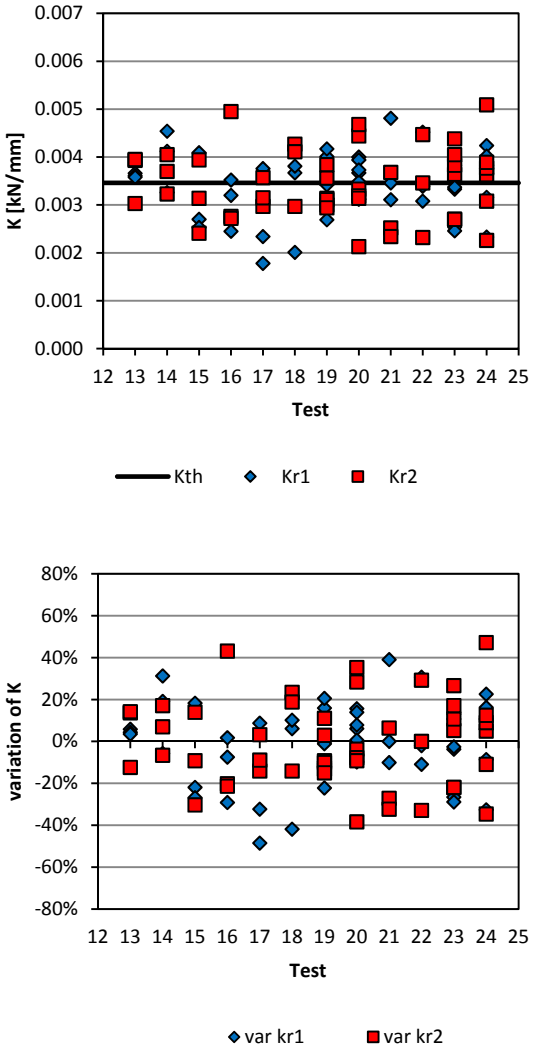

Figure 5.65 - tests cfg4 a) stiffness b) variation of stiffness from the expected value

Data show in some cases , such as test 7 and test 3, a great scatter, despite the fact that they on average distribute around the theoretical expected value. The peak recorded values can be justified by the shape of the cycle: it is worth to remind that stiffness is evaluated as the slope of the best fitting straight line of data. It will be shown in the following that intense oscillations of the force are present, so the experimental trend is far from a straight line; when these oscillations have a high frequency and keep around a mean value the result obtained is closer to the average. On the other hand when only a wide oscillation is present the fitting line slope is highly influenced and the obtained value has a great variation from the average.

The two groups of tests were carried out with the same vertical load, hence the pressure conditions can be considered the same; data appear to be more scattered for the second group (Figure 5.65) of tests, this behavior could be explained by the influence of the position of the center of mass. It is important to point out the presence of several outliers as shown in the boxplots of Figure 5.66

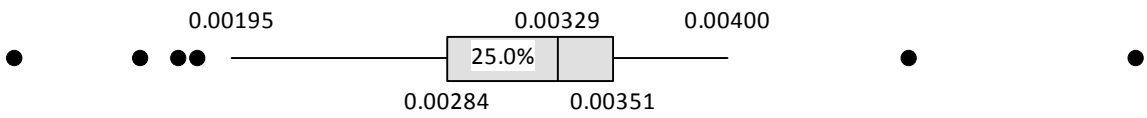

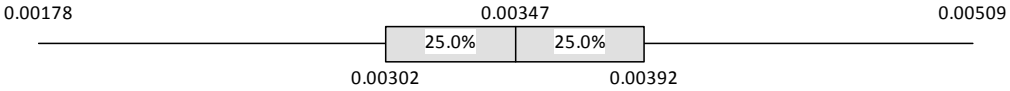

Figure 5.66 - boxplots of stiffness a) test 2-9, b) test 13-24

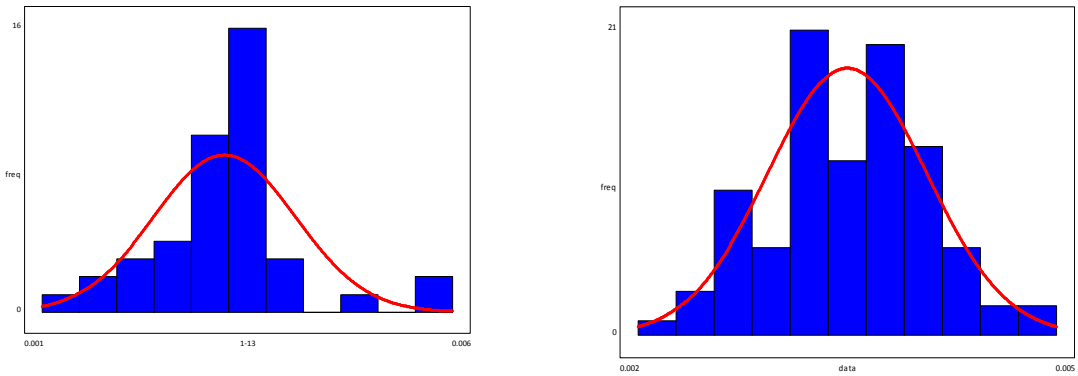

Figure 5.67 - histograms for stiffness frequency a) test 2-9, b) test 13-24

Although these results provide a general overview rather than details, it can be observed that tests with a lower center of mass have a lower spread. Several outliers and a lower median value on the other hand can be noted. Some further notable observations include tests 17-18 where vertical action was also given as an input, and tests 19 – 20, in which the input is bidirectional along the principal directions. It is worth noting that the values of stiffness obtained from these tests have particularly small values if compared to those in traditional applications of friction devices, this is mainly due to the reduced vertical load, which is a characteristic issue for this problem.

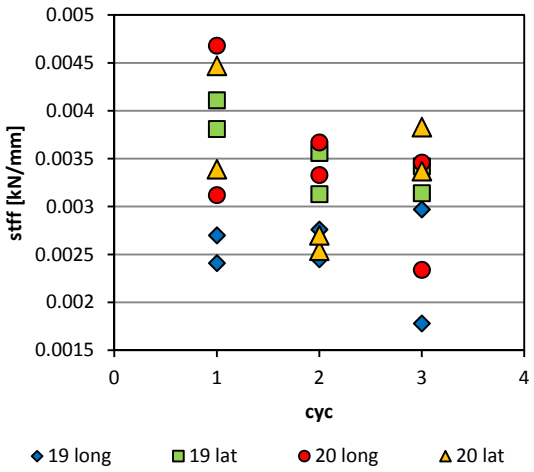

Figure 5.68 - test 19 and 20 stiffness vs cycle

In Figure 5.68 the value of stiffness for each cycle is given for tests 19 and 20. In this case values are depicted considering the different cycles of the test, it can be observed that the first cycle is more scattered this is a general issue for the first cycle which is a sort of transition from the rest condition to the motion one, furthermore, as it will be explained in the following, it is an effect of the presence of two directions of motion at the same time. The highest value of stiffness is reached for longitudinal component of test 20, which is subjected to the strongest input. When stiffness is depicted for tests with vertical action an average increase of the value can be pointed out, furthermore

results are more scattered compared to the tests without vertical action. This aspect could be due to the effect of the vertical acceleration on the vertical load on the devices:

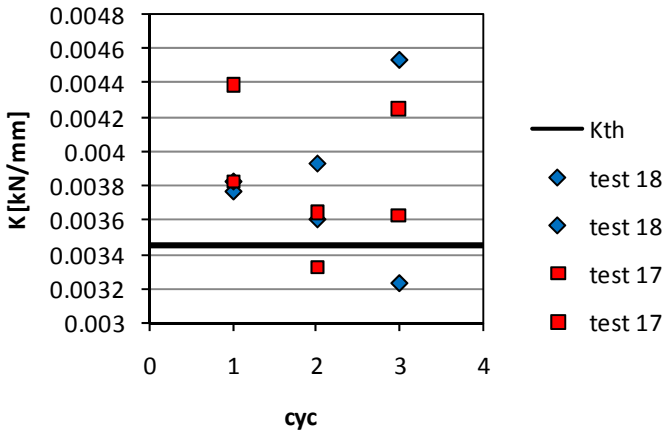

Figure 5.69 - variation of stiffness for tests 18 and 17

Friction

The coefficient of friction is an important parameter for the dynamic behavior of this type of devices. The value of friction is connected to relative sliding velocity. An expression, derived from experimental data, is given in (36). In this paragraph some results of the experimental tests are described to facilitate the understanding of some important aspects of the dynamics of the isolated system. Moreover, a correct evaluation of the coefficient of friction allows for a more educated use of this parameter in the phase of numerical modeling. Similarly, in regards to evaluation of stiffness, tests are analyzed first according to the geometrical configuration, that is subdividing the results into two groups according to the height of the center of mass. Then the second group will be studied considering the possible effect of other characteristics on the dynamic behavior of the system. Different methods to evaluate friction were used for this assessment:

μ_{EDC} = value of friction evaluated by means of the energy dissipated per cycle;

μ_{int} = value of friction coefficient evaluated as intersection of the best fit straight line with the vertical axis of forces in the force acceleration cycle;

μ_{eff} = intersection of the force displacement cycle with the vertical axis.

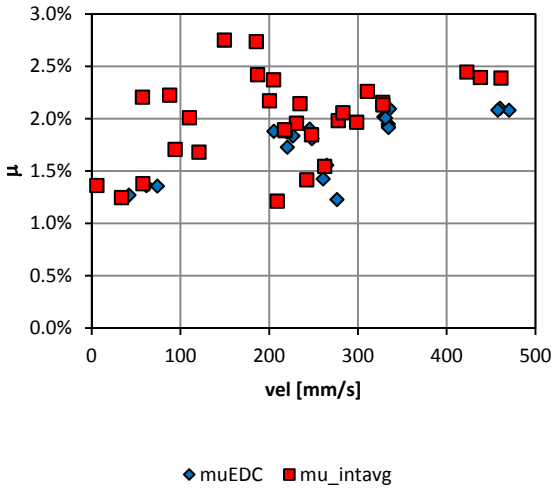

Figure 5.70 - test 2-9, friction vs velocity

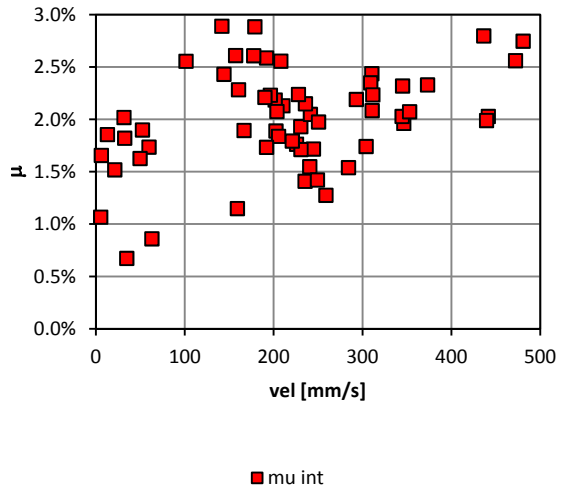

Figure 5.71 - friction (evaluated as μ_{int}) vs velocity for test 2-9

Graphs in Figure 5.70 and Figure 5.71 show a general connection between velocity and friction. In particular for high velocities (v > 300 mm/s) the value of friction reaches a maximum value of 2.5%. It is worth noting that in the velocity interval 100 mm/s 200 mm/s, a coefficient of friction slightly lower than 3% is measured; if the same graph is plotted not considering the average value of μ_{int} the trend is that shown in Figure 5.71. If the only tests with vertical load W = 41.5 kN are considered (i.e. tests 2, 3, 4, 5, 6, 7, 8 and 9), friction coefficient has a behavior much closer to the one described by the expression (5.4), as it is shown in Figure 5.72:

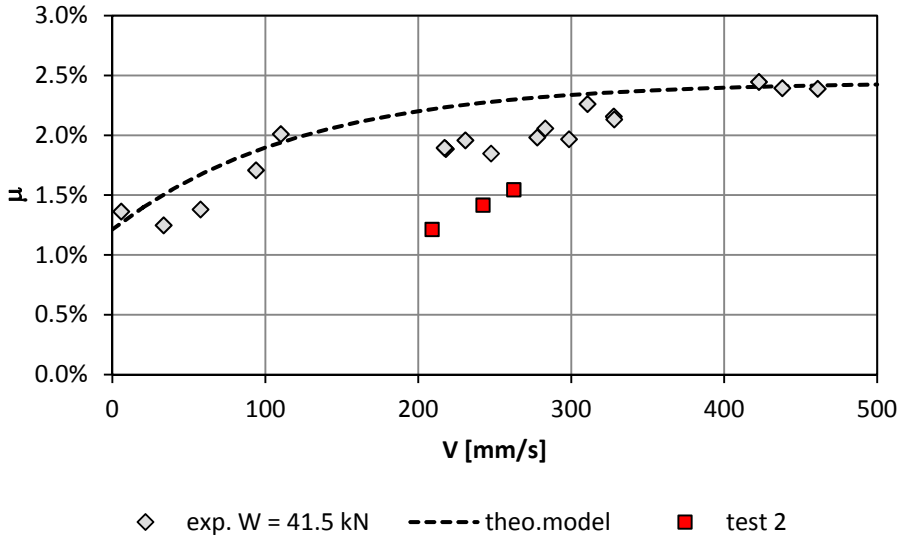

Figure 5.72 - friction (evaluated as μ_{int}) vs velocity for test from 2 to 9

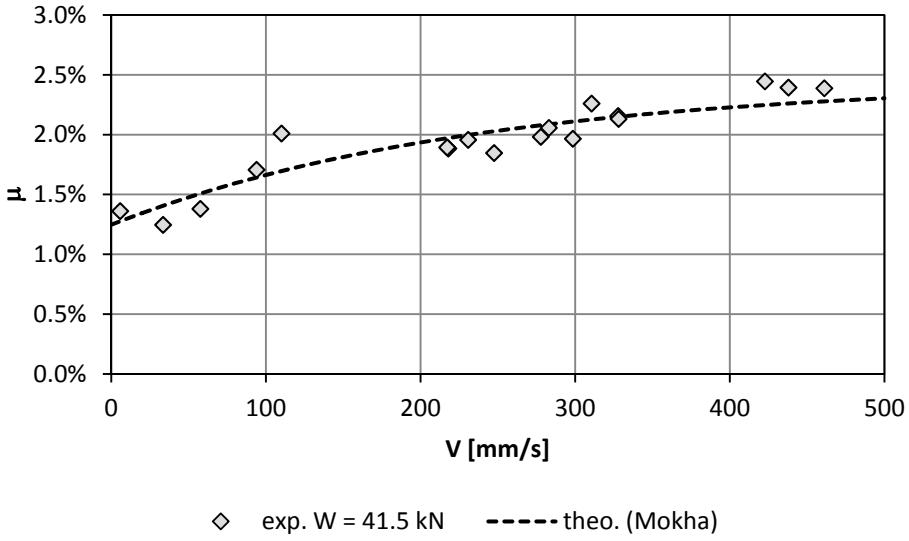

Figure 5.73 - friction coefficient vs velocity from 3 to 9

It is moreover interesting to note that the accordance between the experimental data and the theoretical behavior is more evident when the results of test number 2 are not considered: indeed the outcome for the friction value is lower than the general trend, but this can be explained with the fact that lubricant was applied immediately before this test and it was probably not perfectly spread on the surfaces.

So it can be stated that, friction value for a vertical load of 41.5 kN, corresponding to a pressure of 4.37 MPa can be assumed as μ_s = 1.5% and μ_f = 2%, with a variability that can make it reach the value of μ_f = 2.5%; other particular situations will be investigated in the following in order to find out a correlation between some characteristic features of the tests and the value of the coefficient of friction.

If the same considerations are extended to the second group of experimental tests (higher position of the center of mass) the results are those depicted in Figure 5.74; values of friction are divide into $\mu_{int\ 1}$ and $\mu_{int\ 2}$ which are the two

values corresponding to the two intersections of the best fitting line with the vertical axis, respectively in the positive and in the negative semi plan:

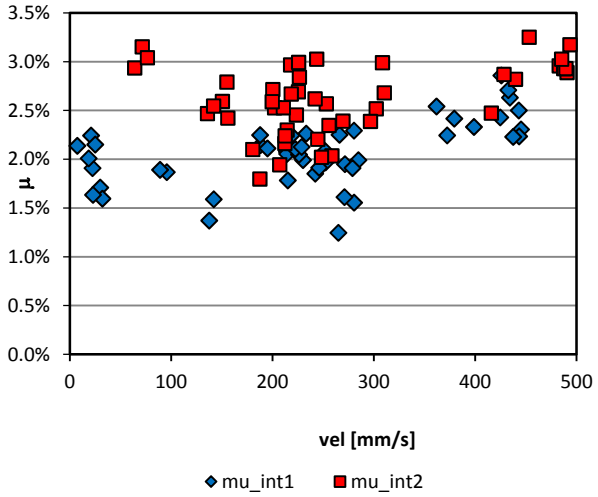

Figure 5.74 - tests 13-24 μ vs velocity

The global trend shows results similar to those obtained for the previous group of tests, with a tendency for high velocities to reach a value of the coefficient of friction μ = 2.5 % - 3%. If tests with peculiar features (i.e. vertical action, bidirectional input) are neglected the result obtained is:

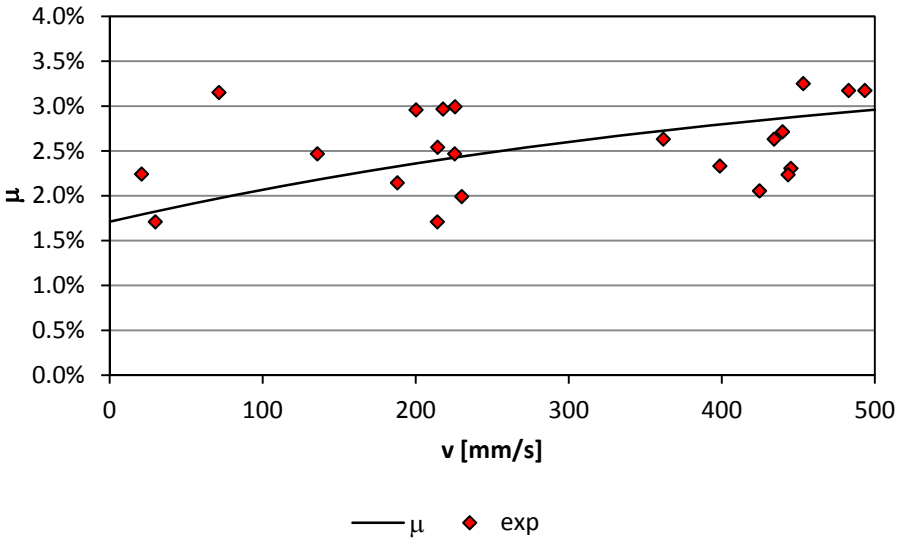

Figure 5.75 - tests 13 - 16 μ_{int} vs velocity

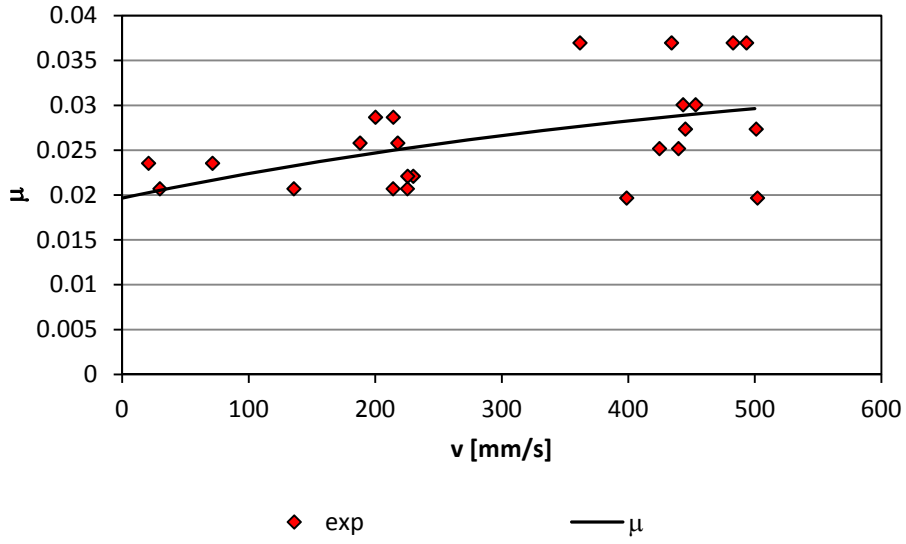

Figure 5.76 - tests 13-16 μ_{eff} vs velocity

Unidirectional tests with configuration cfg#4 do not show a good accordance between the theoretical model and the experimental data, as visible in Figure 5.75. The lines of best fit are obtained for a coefficient α=0.0017, resulting from the experimental data. As it was stated above, friction can be evaluated with different methods, Figure 5.76 depicts the same results of Figure 5.75, but considering the effective value of the friction coefficient. However in general results fit the expected trend. It is worth noting that the variation of the coefficient of friction is not so high, even though, compared to the results obtained for the previous configuration, we have a higher friction value for slow velocities.

Let's observe what happens when the coefficient of friction is monitored for tests 19 and 20, as previously did for stiffness.

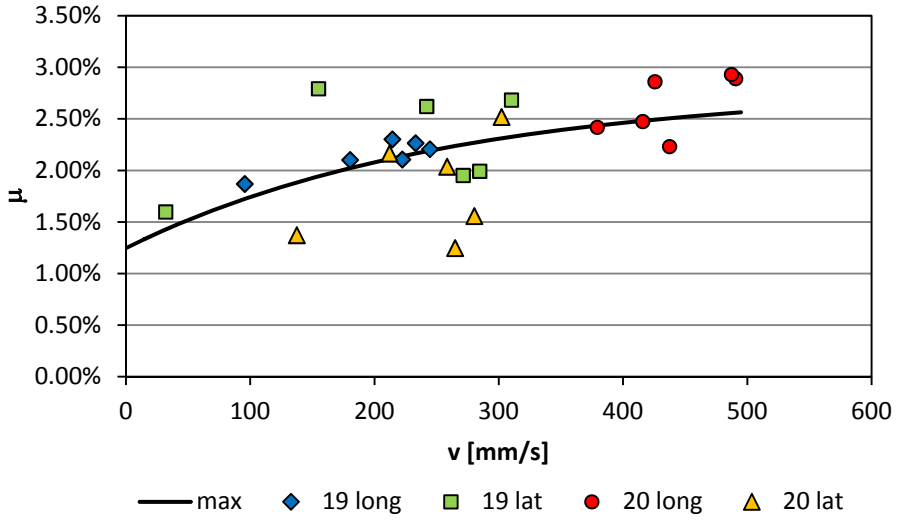

Figure 5.77 - test 19 friction vs velocity

In the part concerning the numerical model of the device and its application to the case study some further considerations about the influence of the variation of coefficient of friction on the response of the system will be presented.

Energy Dissipated Per Cycle

EDC is a parameter for assessing the energy dissipated by the device in motion and it is connected to the friction of the system. It is calculated as the area included in the force displacement cycle.

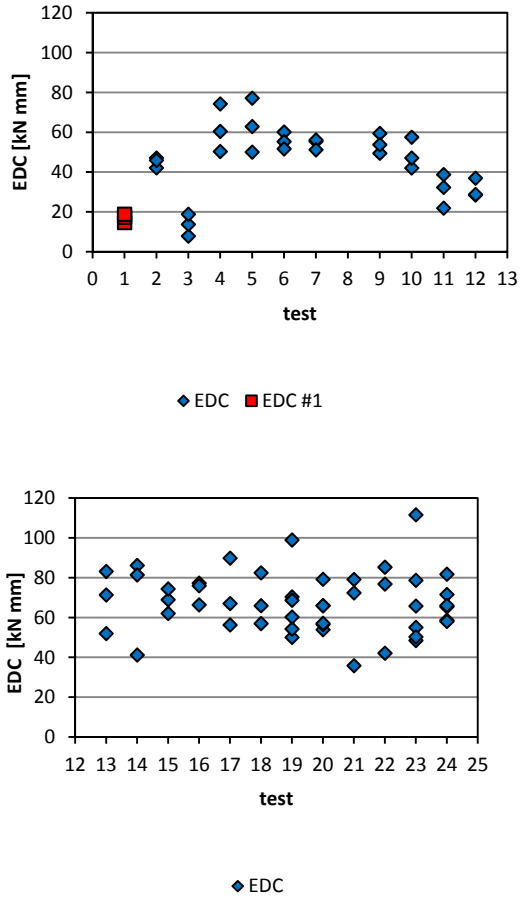

Figure 5.78 - EDC vs test

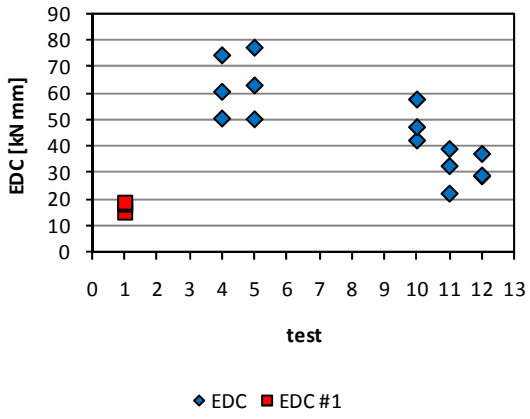

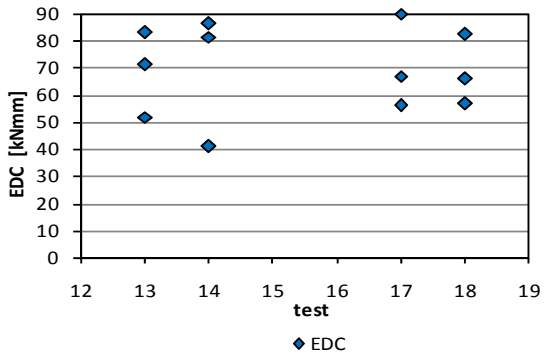

Figure 5.79 - EDC vs test input d1 0.8 v1

Figure 5.78 and Figure 5.79 depict the values of EDC evaluated for each of the three cycles of the tests, divided from 1 to 13 and then to 13 to 24. The red markers show the value of the index for test number 1, carried out with non lubricated devices. In this case the energy dissipation is lower than the other tests in which the surfaces are lubricated: dissipation is connected both to friction coefficient and to displacements, even though the non lubricated friction coefficient is higher than the lubricated one the system experiences very low displacements that reduce the quantity of dissipated energy. A similar observation can be done for test number three, in which the input is D1 0_5V1, and the devices dissipate a small amount of energy due to the reduced differential displacements between the base and the isolated system. Indeed the input acceleration is not high enough to produce a fully developed differential motion between the surfaces.

5.5.5.1.1 Accelerations and displacements

Monitoring of some characteristic aspects of the dynamic response of an isolated system provides a clear idea of the efficiency of the technical solution. In particular, the most important parameters to be observed are displacements and accelerations, that are directly connected to the forces acting on the system. The following charts present a comparison between the input acceleration and the acceleration measured on the top of the footing block, importantly the value of acceleration considered in the comparisons is the average between the records of the three accelerometers A_1,A_2 and A_3:

$$A_{x\,avg=}\ \sum_{i=1}^{3}\frac{A_{iX}}{3};\ A_{y\,avg=}\ \sum_{i=1}^{3}\frac{A_{iY}}{3};$$

Where x and y respectively are the longitudinal and the lateral directions.

Test 1 D1 V1 non lubricated longitudinal

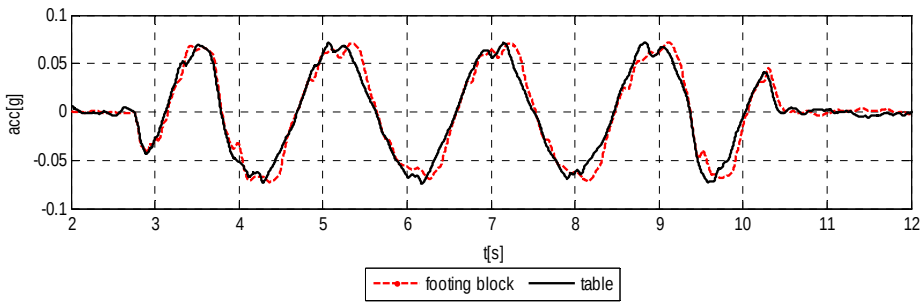

Figure 5.80– horizontal accelerations test #1

The dynamic behavior of the isolated system with non lubricated sliding surfaces shows that the application of such a solution gives no benefit to the system; indeed the acceleration given as an input at the base of the system is completely transmitted to the footing of the targeted isolated object. This happens because the input level is lower

than the breakaway force, i.e. F0 = μ W, or from another point of view, the friction level is too high to allow the motion, in the case of Figure 5.80 the limit is not overcome and the system moves rigidly with the ground.

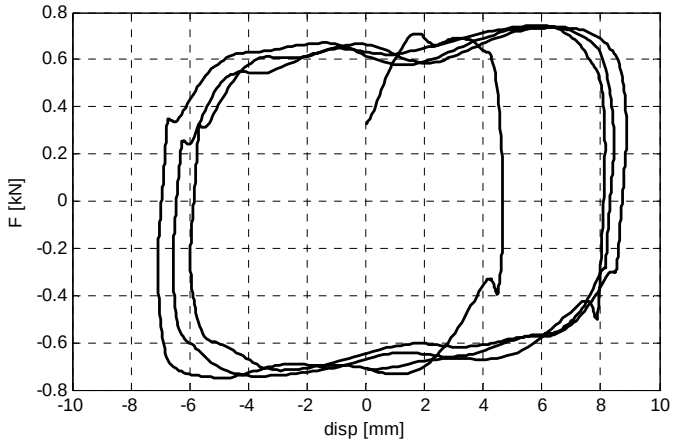

Figure 5.81– force displacement test #1

Figure 5.81 shows the behavior of the average force displacement cycle for one isolator, it can be pointed out that displacements are very small and do not reach the maximum value of 1 cm; on the other hand the amplitude of the maximum force allows a good dissipation of energy, which is represented by the area described by the cycle. As it will be shown and described in the following some particular aspects of the dynamic behavior of the system appear from this graph.

Test 2 D1 V1 lubricated longitudinal

The first test was performed with "dry surfaces", i.e. the sliders and the sliding surfaces were directly in contact and the coefficient of friction governing the motion was that of the interface between the two materials. This coefficient of friction seemed to be too high to provide an effective level of isolation, considering the assumed weakness of the objects to be isolated. Therefore the following tests were performed applying a layer of lubricant to reduce the value of the friction coefficient and to reduce consequently the level of the breakaway force, to produce an easier triggering of movement. It is worth noting that a reduced level of friction from one side allows the activation of the dynamic response of the system, but from the other side, it also increases the maximum displacement because of the lower dissipation of energy.

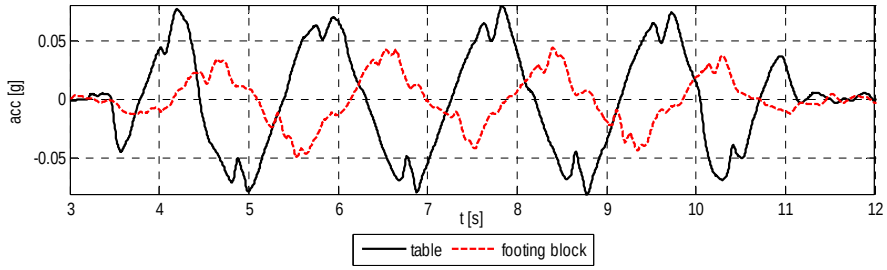

Figure 5.82 - horizontal accelerations test #2

It can be noted that, for the same horizontal input acceleration, the lubricant application gives a reduction of the acceleration transmitted to the body, even if the input level belongs to the range of the "low accelerations": Figure 5.82 an input of 0.07g is given, and it is filtered to 0.05g above the isolated plan. This means that there is a reduction of almost 30%.

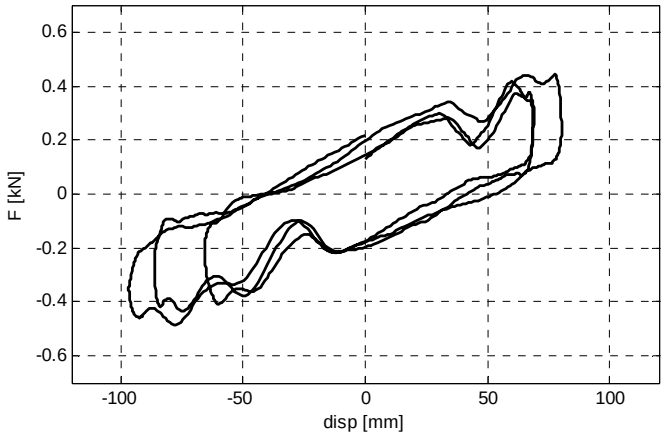

Figure 5.83 - force-displacements test #2

The behavior of forces and displacements is depicted in Figure 5.83, the maximum displacements, if compared to those obtained from the previous test, reach much higher value, due to the application of a reduced coefficient of friction the displacements increase. It is interesting noting that the response shows wide oscillations when the displacements are around 50 mm.

Test 4 D1_08_V1 lubricated longitudinal

The application of a lower acceleration, with a peak of 0.04g, points out that the reduction of the action is almost zero: the acceleration transmitted to the body reaches the same level of the one given as an input, this means that for this level of input the isolation system does not improve the level of safety of the isolated object. However a dynamic effect can be pointed put, in fact the response of the system is shifted in time of 0.5 seconds and it is possible to point out the instant in which the acting force exceeds the breakaway force (4.3 seconds, Figure 5.84)

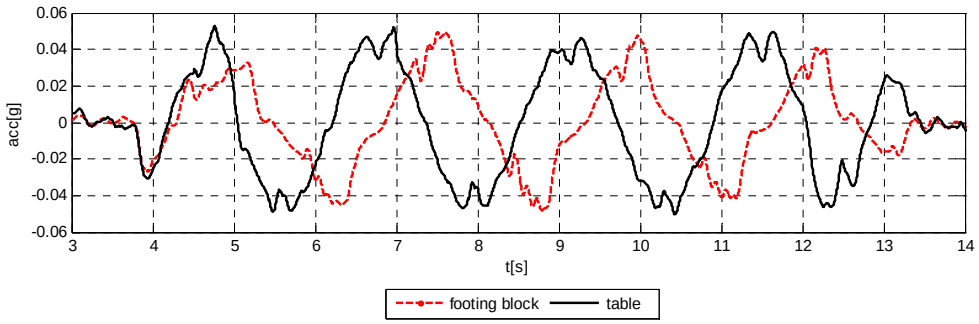

Figure 5.84 - horizontal accelerations test #4

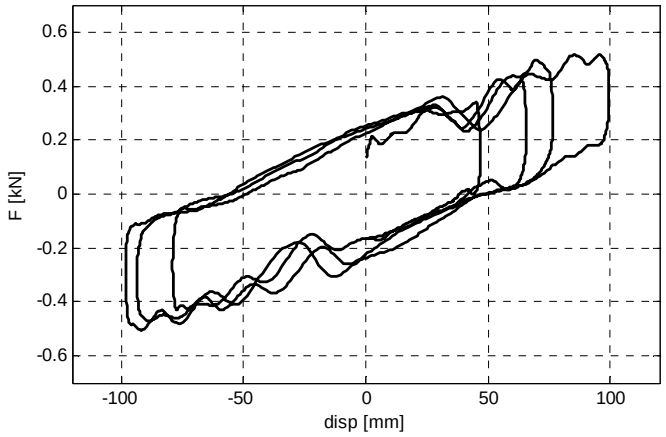

Figure 5.85 - force-displacement test #4

Test # 4 shows a force displacement cycle with maximum displacement of +/- 100 mm; the inclined branches of the loop, which from the mechanical model must be straight, are characterized by several and wide oscillations.

Test 5 D1_08_V1 lubricated lateral

The dynamic behavior of the isolated system changes according to the direction of application of the input: in the case of Figure 5.86, the application of the same input applied in test#4 gives a dynamic response with more intense local oscillations of the footing block; the general trend of the horizontal acceleration follows on a quality level the one of the input but with more stressed local oscillations, this effect can be caused by different factors: the lower inertia of the specimen along the lateral direction and the lower distance between the bearings and the low level of the input acceleration. These concepts will be discussed in detail in the following of this work.

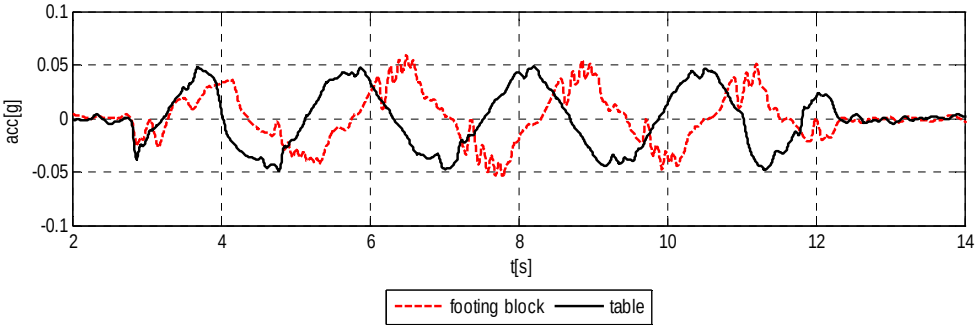

Figure 5.86 - horizontal accelerations test #5

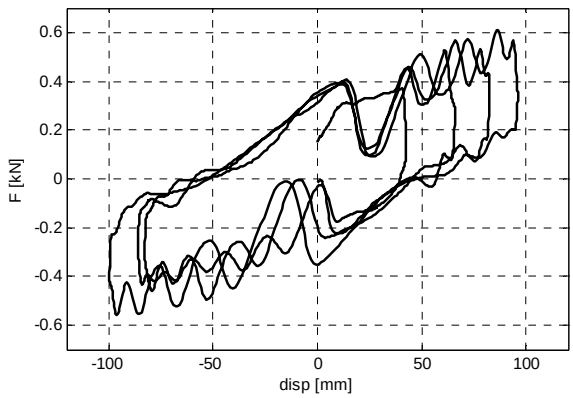

Figure 5.87 - force displacement test #5

Test 5 which is carried out along the lateral direction is characterized by a force displacement cycle with more local oscillations before the maximum (and minimum) force and displacements cycle are reached.

Test 6 D1_V2 lubricated longitudinal

The input for test#6 is characterized by a higher base acceleration, which reaches the value of 0.15g: the positive effect of actions reduction appears more clear, the maximum level of transmitted acceleration is still 0.04g, moreover the response of the system seems not to be affected by phenomena of local oscillation as much as the previous examples. This behavior is probably due the higher level of acceleration of the input, that is far from the limit that divides the fixed motion field from the one of relative motion between the sliding surfaces: this limit is given by the friction coefficient.

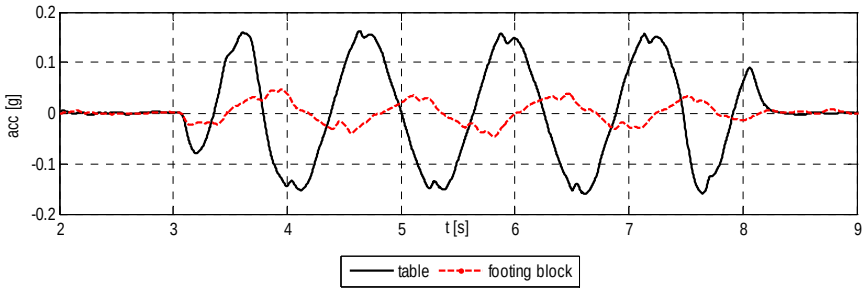

Figure 5.88– horizontal accelerations test #6

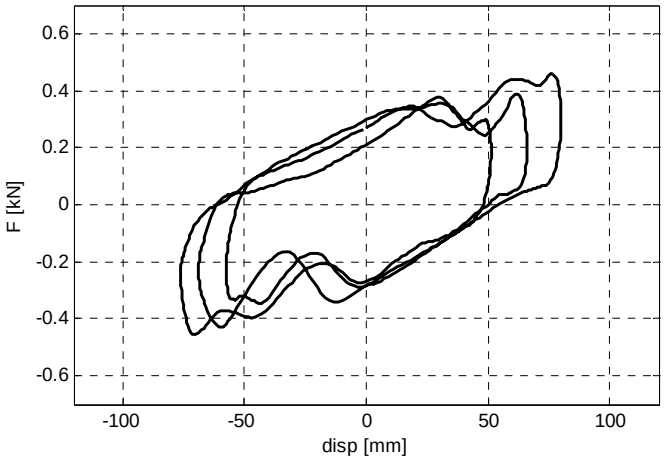

Figure 5.89– force displacements test #6

Test 7 D1_15_V2 lubricated longitudinal

Test # 7 provides an increment of input up to the value of 0.35g: the response of the system is again under 0.05g with an excellent level of reduction of actions; on the other hand the local oscillations, even though are still visible, appear of much lower intensity

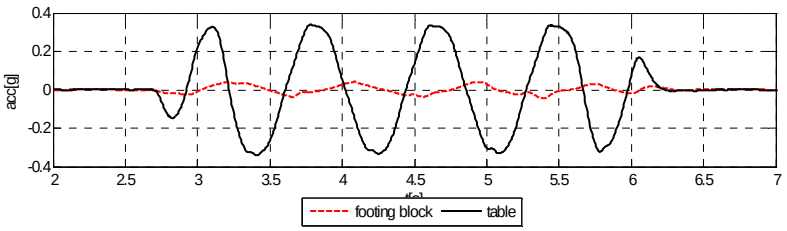

Figure 5.90- horizontal accelerations test #7

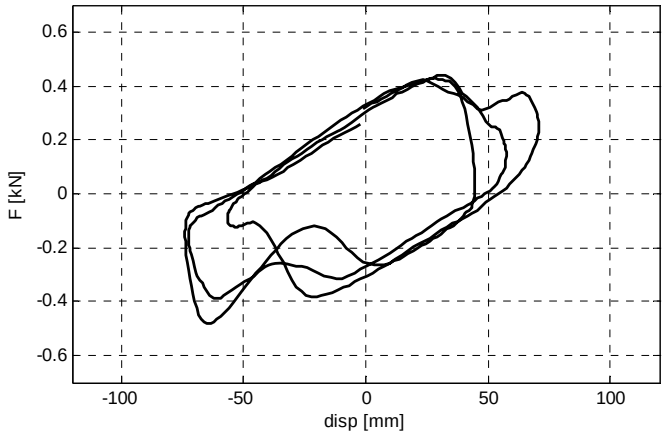

Figure 5.91- force displacements test #7

From test 13 on the reference configuration is 2 ”cfg#4”, with center of mass in the highest position, but without any horizontal eccentricity; this configuration was designed to fit the inertial and geometrical features of the statues of the case-study sample of “Galleria dell ‘Accademia”. The following part gives some general and brief remarks about the tests conducted in this configuration, leaving the more detailed description and observation to the following part.

Test 13 D1_08_V1 lubricated longitudinal (CFG#4)

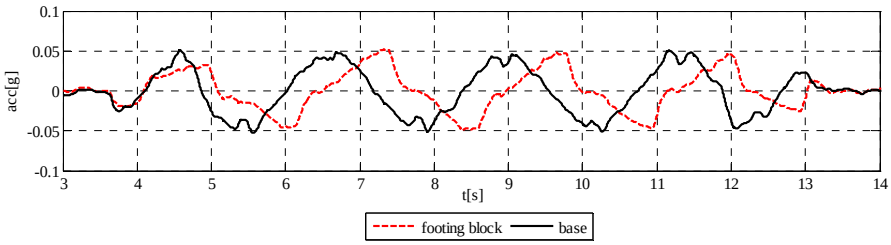

Figure 5.92- horizontal accelerations test #13

Test#13 applies the same horizontal action as test#4, along longitudinal direction as well; the absence of action reduction can be observed, even if, during the first oscillation, when acceleration reaches the level of 0.02g (Figure 5.92) there is the activation of the relative motion of isolator’s surfaces, responsible for the shift in the period of the response.

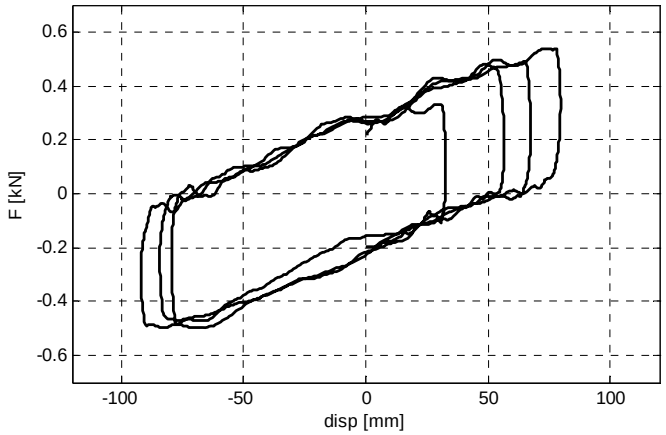

Figure 5.93- force displacement test #13

Test 15 D1_15_V2 lubricated longitudinal (CFG#4)

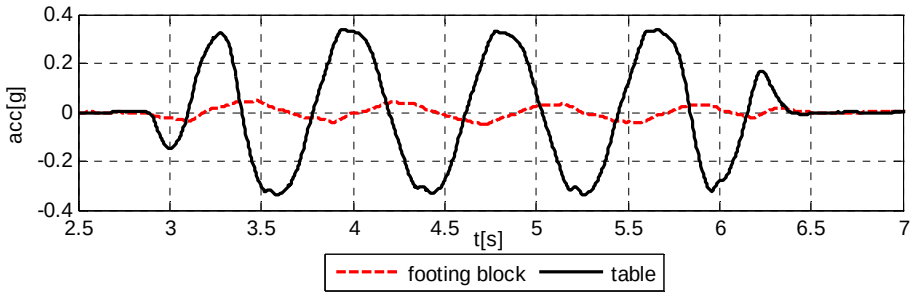

Figure 5.94- horizontal accelerations test #15

Test# 15 applies the strongest acceleration (0.35g), the comparison between the accelerations given as input and those read as an output, show a strong reduction of the action transmitted to the base of the isolated structure; as in test#7 local oscillations are reduced.

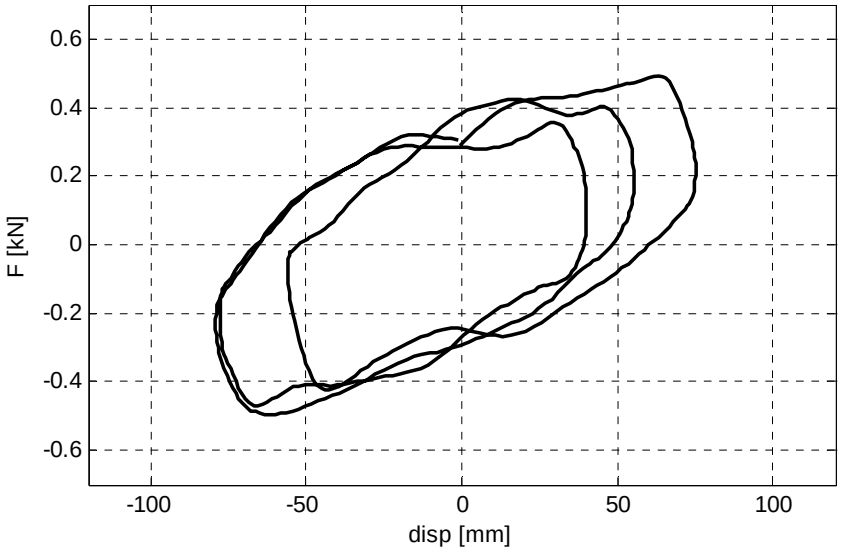

Figure 5.95- force displacement test #15

Test 17 D1_08_V1 longitudinal VERT1 vertical direction, lubricated(CFG#4)

Test 17 applies the horizontal input D1_08_V1 simultaneously to the vertical input VERT 1, which is characterized by a frequency f_{vert1} = 1.25 Hz. The intensity of the vertical acceleration was set in accordance with two important aspects: the first one is the vertical peak ground acceleration of the site of the case study, the second is the frequency of the input that needs to be sufficient to provide an adequate number of vertical oscillations during an horizontal one. Details about the input displacements features are depicted in

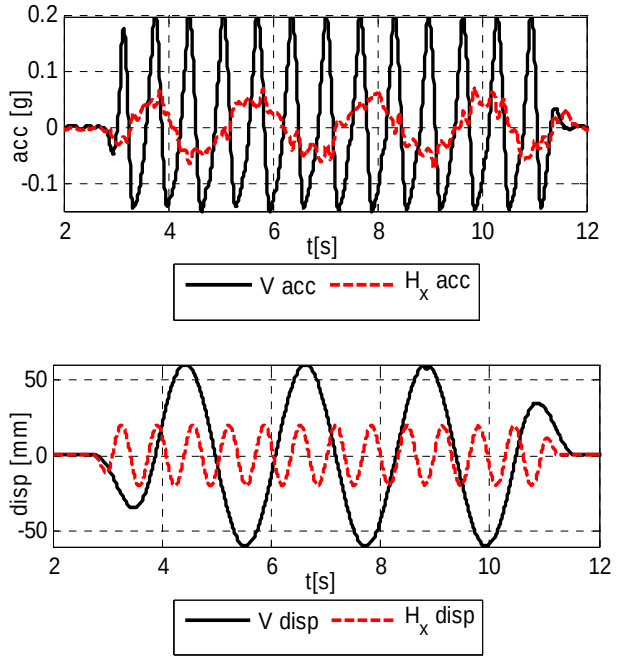

Figure 5.96 - input details test 17 a) accelerations, b)displacements

One of the most important parameters that needs to be checked is the transmitted acceleration. What is important to investigate is indeed the real efficiency of the system, and how it is affected:

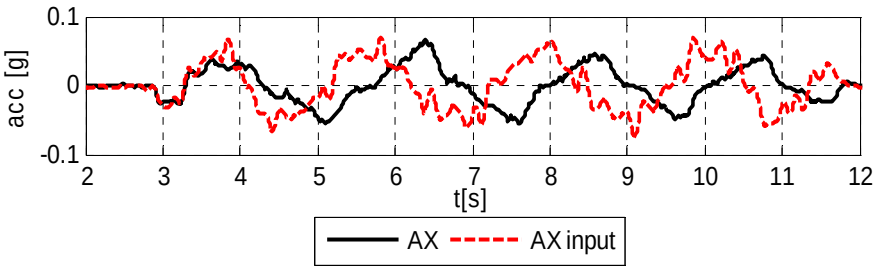

Figure 5.97 - comparison between input and output accelerations, test 17

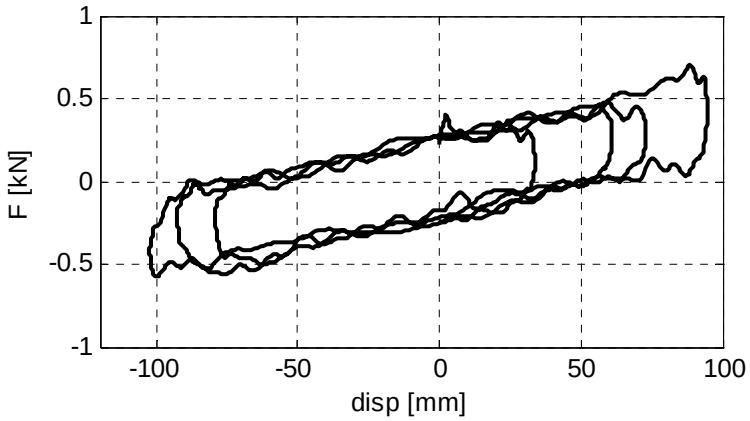

Figure 5.98 - test 17 force displacement cycle

Test 20 D1_1.5V1 longitudinal D1_0.8V1 lateral lubricated(CFG#4)

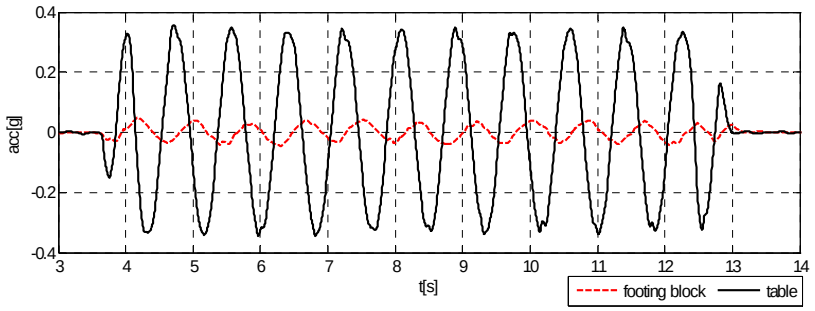

Figure 5.99 - longitudinal accelerations test #20

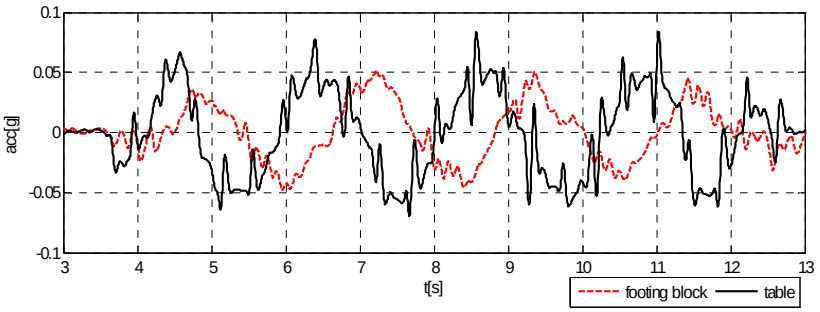

Figure 5.100- lateral accelerations test #20

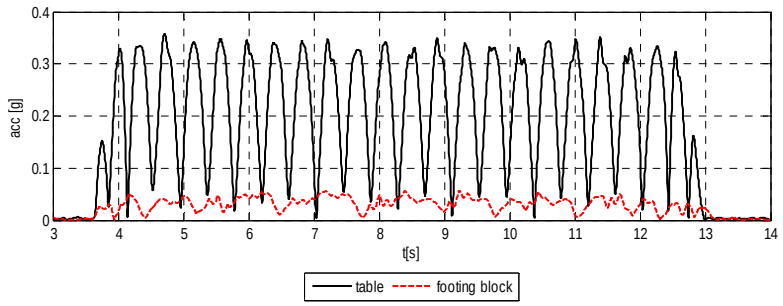

Figure 5.101- combined accelerations test #20

Test#20 applies two inputs along the longitudinal and lateral directions at the same time. Test#20 though uses two different functions: D1_1.5V2 longitudinal and D1_0.8V1 along the lateral direction; the longitudinal input reaches 0.35 g and the lateral one 0.04g. The effects of the application of the isolation system are positive and the output accelerations recorded take the value of 0.04 g.

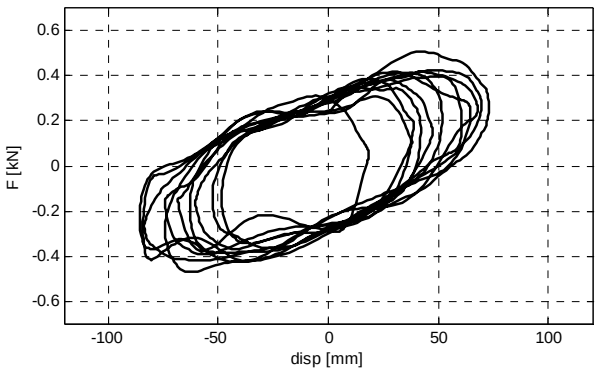

Figure 5.102- longitudinal force displacement test #20

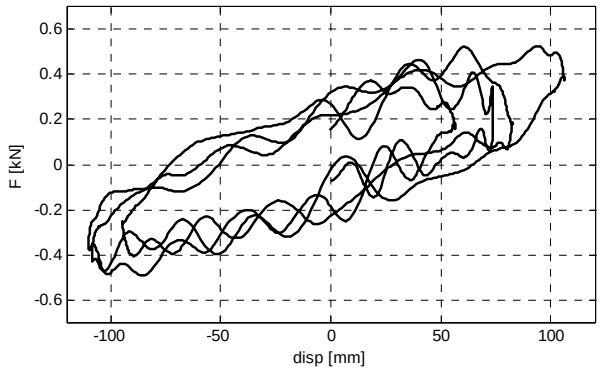

Figure 5.103- lateral force displacement test #20

The presence of two actions at the same time has strong effects on the response of the system, some particular details of the response are visible in Figure 5.102 and Figure 5.103: the lateral component is clearly affected by local oscillations that modify the stiffness of the system instant by instant, the effect is also non symmetric considering the two different directions of motion: local oscillations have different frequency and amplitude in the upper and lower straight parts of the loop; the maximum displacement, is also increased (as it will be shown in the following) along the lateral direction.

The effects of the interaction are hence potentially dangerous for the response because they can induce an unexpected behavior that could cause failure of the system.

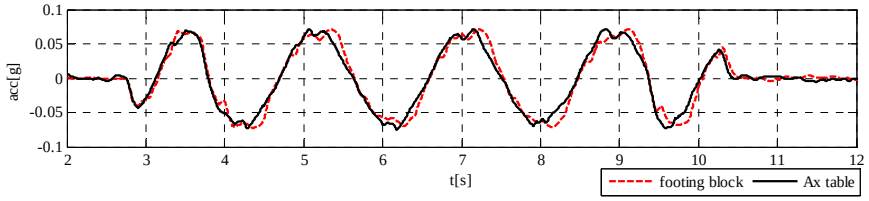

Figure 5.104- horizontal accelerations test #1

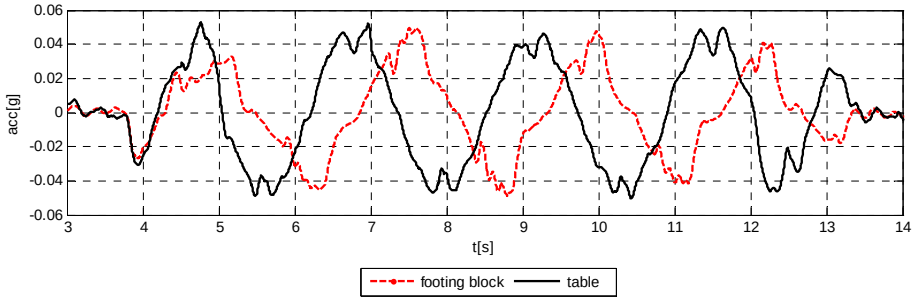

Figure 5.105- horizontal accelerations test #4

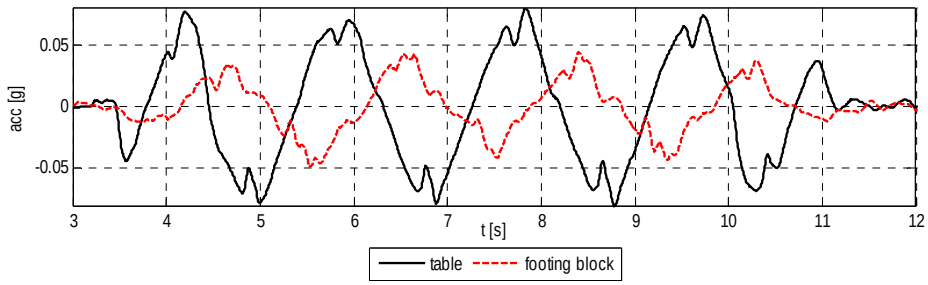

Figure 5.106- horizontal accelerations test #2

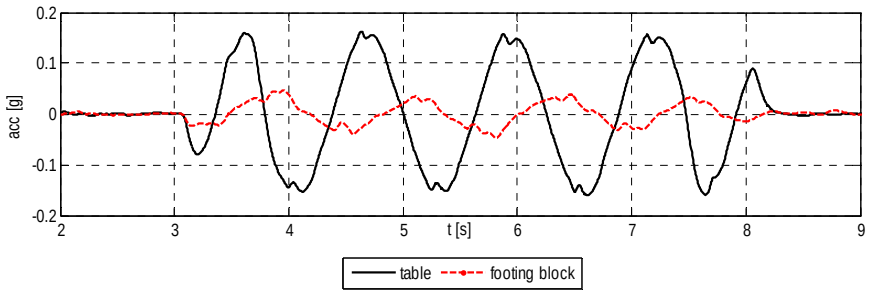

Figure 5.107- horizontal accelerations test #6

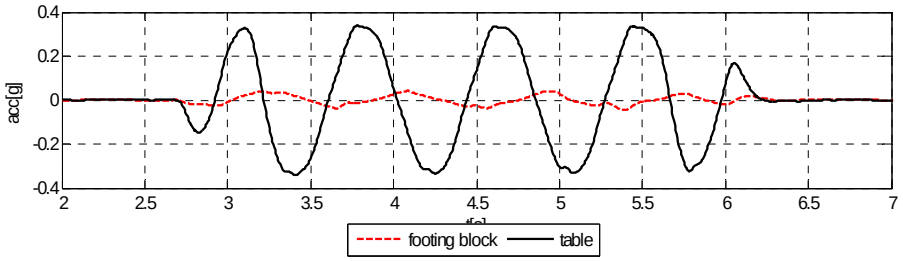

Figure 5.108- horizontal accelerations test #7

The comparison between test#1 and test#2 shows that the choice of application of lubrication with the purpose of reducing the coefficient of friction allows to reduce the value of the "activation acceleration" (hence of the breakaway force) of the system: in this way the relative sliding between the surfaces begins for lower levels of action. In fact the input acceleration of 0.07g generates an output of 0.05 g in test#2, while in test#1 the value of output acceleration is exactly the same as the input. For this reason the choice that is made is to apply lubrication in the following tests. If the comparison with the results obtained from test#4 is added (Figure 5.105), which has an input peak ground acceleration of 0.04g, it can be observed that the value of the maximum acceleration transmitted to the body is not reduced by the isolators and that the only remarkable effect is on the dynamic response is a time shift of the output of the system. The lower input acceleration also causes an amplification of local oscillations in the output. This is connected to several phenomena acting together: such as the "stopping" of the sliders during the motion, the different geometrical layout of the system, the configuration of the bearings and their layout and also the intensity of the input. For the last one in particular it was observed that the closer the input accelerations are to the value of static friction coefficient the higher are these effects. Thus whenever the input is not high enough to keep the motion far from stopping, the object experiences local oscillations that need to be taken into account because they might cause the exceeding of the artistic limit state. This facet is the logical consequence considering that friction is one of the governing parameters of this type of systems. Furthermore, it also confirms the choice for lubricated surface in order to keep this phenomenon reasonably under control.

The expected action reduction is more clear when the value of the horizontal input increases: test#6 (Figure 5.107) gives as an input a value of PGA of 0.15 g that are reduced around 0.05 g of output. The general trend is characterized

by local variations of output acceleration. If the acceleration is increased at the base of the system, up to the value of 0.35 g (test#7), it can be observed that the output accelerations still reach the maximum value of 0.05 g, with a very good effect of isolation for reduction of the input actions.

If these latest remarks are summarized and depicted (Figure 5.109), in particular observing the interaction between the maximum input acceleration and the maximum output acceleration, it can be observed that in general the reduction of action has an increasing trend with the increase of the ground acceleration, but with an upper limit; the graph shows the results obtained from tests 2, 4, 6, 7, 13 and 15. It can be underlined a difference between the accelerations transmitted to the system from test 4 and test 13 (Figure 5.109, triangle markers): both the tests were carried out with the same input signal (PGA = 0.04g).The same remark is valid for tests 15 and 7 (Figure 5.109, square markers), carried out along the longitudinal direction but with a peak ground acceleration of 0.35 g. This effect can be justified by the effect of the local oscillations of acceleration; for the tests with lower input indeed the difference is more evident, and since the only variation in the two tests is the position of the center of mass it can be assumed that, with low accelerations the local oscillations due to the unexpected stopping of the motion of the devices are more intense, hence in the condition of configuration cfg#4 they are more evident.

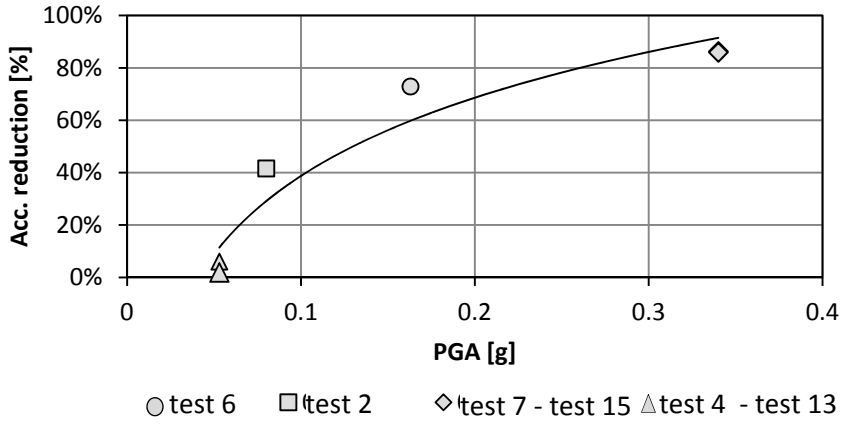

Figure 5.109– accelerations reduction

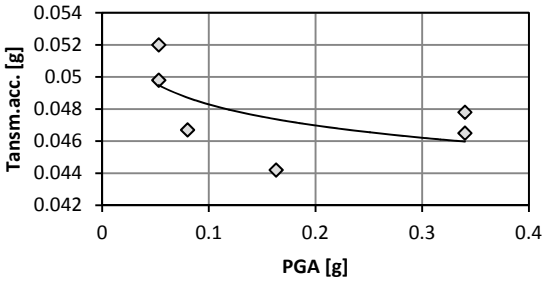

Figure 5.110– transmitted accelerations

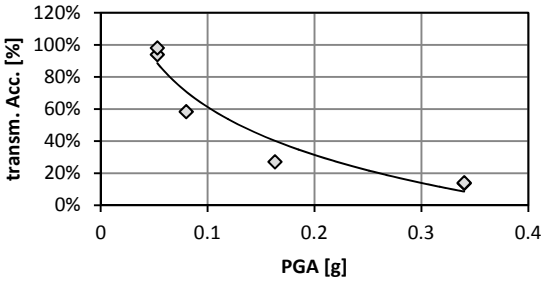

Figure 5.111 - transmitted accelerations (%)

Table 5.10 – summary of acceleration reductions

test	max A [g]	max A top [g]	PGA exp. [g]	PGA meas.[g]	var. accel. [%]
2	0.0467	-	0.07	0.08	42%
4	0.0498	-	0.04	0.05	6%
6	0.0442	-	0.15	0.16	73%
7	0.0465	-	0.35	0.34	86%
13	0.052	0.057	0.04	0.05	2%
15	0.0478	0.051	0.35	0.34	86%

Tested levels of acceleration are not always extremely high, but it must be considered that, the objects that are under study, often allow very low levels of stress, so the transmitted forces must be very low and the "activation" of the system should be kept at low levels as well. On the other hand the reduction of forces generates higher displacements, connected to the reduction of friction and dissipation, that must fit the availability of space of the exhibition hall.

5.5.5.1.2 Actions reduction for bidirectional tests

When bidirectional inputs are considered the reduction of actions is very important. Indeed, as it was shown before for displacements, the dynamic response of the system to contemporary actions along different directions cannot be handled as a combination of single unidirectional actions. It was already observed that displacements significantly increase, in particular along the transversal direction; some results for accelerations are summarized in the following considering unidirectional tests 13, 14 and 15 and comparing them to test 19 and 20, that are respectively bidirectional combinations of:

test 19 = 13 long +14 lat

test 20 = 15 long + 14 lat.

Table 5.11 – accelerations reductions, bidirectional tests

	Max A [g]	Min A [g]	Max Ass [g]	Diff [%]	Diff [%]
13	0.0518	-0.0478	0.0996		
14	0.0514	-0.522	0.1036		
15	0.047	-0.047	0.094		
19 Long	0.040	-0.033	0.073	-22.8	-31.0
19 Lat	0.0567	-0.0473	0.104	10.4	-9.5
20 Long	0.049	-0.045	0.094	3.6	-4.8
20 Lat	0.051	-0.047	0.098	-1.2	-8.8

Table 5.11 shows that output accelerations for bidirectional tests are in general different from the unidirectional ones,: if test 13 and test 19 are compared it can be observed a reduction of the maximum positive acceleration and of the minimum negative acceleration: there is a reduction of the amplitude (calculated as the difference between the maximum and the minimum acceleration) of the output signal. Instead the lateral direction for the test 19 shows an increasing of the transmitted acceleration if compared to the corresponding unidirectional one.

Comparing the longitudinal direction of test 20 with test 15 it can be underlined an increased positive acceleration and a reduction of the negative one: the amplitude of the response is the same for the two tests, even though what is important in this case is the maximum absolute value of acceleration, which is connected to the maximum value of the force on the object. Along the lateral direction test 20 shows a reduced amplitude of acceleration and, at the same time, a reduction of both the negative and the positive acceleration. It's important to underline that for bidirectional tests the transmitted acceleration does not exceed the limit of 0.05 g.

5.5.5.1.3 Actions reduction for tests with vertical component of the action

Tests 17 and 18 were carried out with the presence of vertical action, characterized by the parameters summarized in Table 5.8. In terms of maximum acceleration transmitted to the system it is worth noting that, as for the other tests with the same input function, the effect is visible but not very intense. For a more accurate description of the result, the recorded acceleration for test 17 can be compared to the same parameter of test 13:

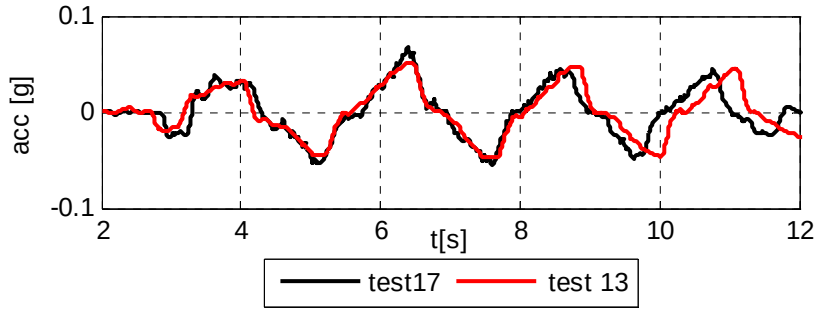

Figure 5.112 - comparison between output accelerations, test 13 and test 17

the responses depicted are in general similar even though test 17 is characterized by a higher number of local oscillations in the acceleration record. Moreover a clear difference in the period of oscillations is visible.

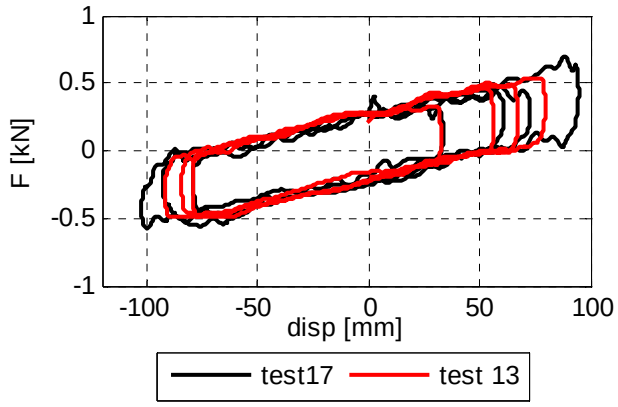

Figure 5.113 - force displacement cycle test 17 and test 13

Despite the fact that the difference between forces is not high for test 17 and test 13, a significant increment of the displacements can be highlighted from Figure 5.113. Indeed the maximum absolute displacement for test 13 is :

D_{max_13} = 92.0 mm

while the same parameter for test 17 is

D_{max_17} = 102.4 mm

This comparison shows the displacement increases of 10.1 %. It is important to highlight once again that a good prediction of displacements and forces is fundamental for a reliable design of the isolation system. , The above stated results demonstrate that in case that the design phase is performed without considering the presence of a vertical component, displacements can be underestimated.

Test 18 is characterized by the same horizontal input but with a vertical component of motion, named VERT2 with a frequency f_{vert2} = 2.17 Hz. The comparison between the input and output acceleration is given in

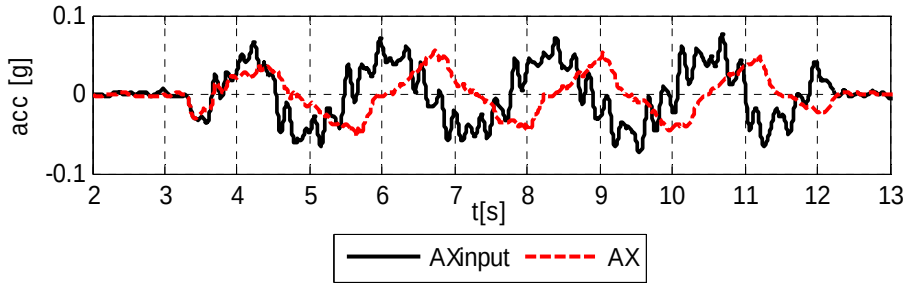

Figure 5.114 - comparison between input and output accelerations, test 18

A comparison between the output accelerations of test 13 and test 18 highlights that the efficiency of the isolation system in terms of reduction of transmitted acceleration is good although the presence of a vertical input; it is interesting to note that the response, in presence of a vertical acceleration input is subjected to an increasing of the oscillation period:

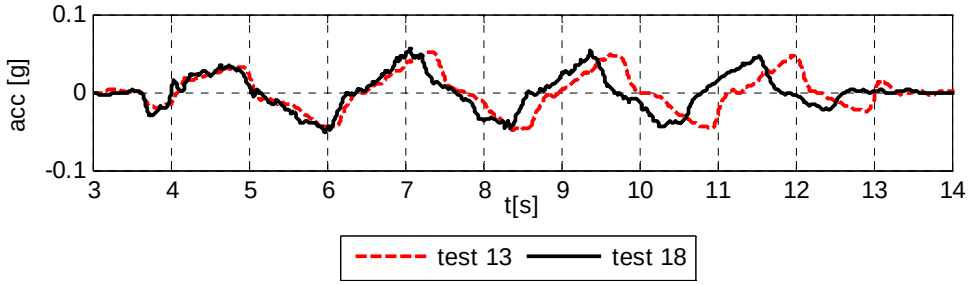

Figure 5.115 - comparison between output accelerations, test 13 and test 18

the general trend of the force – displacement cycles is very similar between test 18 and 13 even though, also in this case, an increase in displacements can be underlined:

The maximum absolute displacement for test 13, as mentioned before is:

D_{max_13} = 92.0 mm

while the same parameter, measured for test 18 is:

D_{max_18} = 92.0 mm

Despite the fact that maximum absolute displacement is the same for both tests, it is worth noting that each cycle of the test with vertical action shows displacements higher than the corresponding horizontal ones. In this case the fact that there is no amplification of the displacement can be due to the fact that the inputs are not at the same phase in time.

5.5.6 Non Standard results

The experimental tests also pointed out some responses of the devices that were unexpected, and gave some hints to investigate more in depth behavioral aspects that are not often considered. Many of the aspects emerging from the tests are inconsistent with the mechanical model known from current literature. This means that, despite the fact that the general behavior is similar to the theoretical one, the presence of "confounding effects" needs to be investigated to properly consider the application of seismic isolation devices. In particular for nontraditional purposes, such as the one studied in this dissertation. In the following part some of the tests that were previously discussed will be presented again, this time focusing attention on some of the above mentioned behaviors and stressing the importance of taking care of design details.

5.5.6.1 Increased displacements in bidirectional tests

Test 19 is bidirectional with the same input along both the principal directions. Application of bidirectional inputs opens up several questions about design aspect and the interpretation of results. The input function used for this test was D1_0.8V1 applied along the two main directions of the motion: longitudinal and lateral. The two inputs have a difference in the phase angle (90°) in order to provide a variation in the direction of application of motion instant by instant; a graphic description of the plane input and of the two time histories is given in Figure 5.116

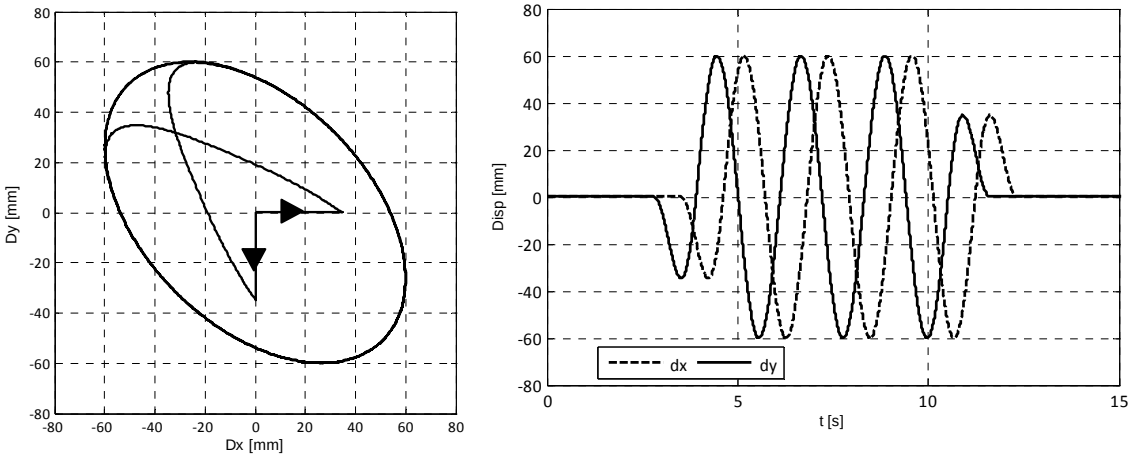

Figure 5.116 - test#19, a) plane input, b) time history inputs

A first interesting comment can be made when observing the output of test#19 along the two directions (Figure 5.117): despite the fact that the input is perfectly symmetric the output is not and a wider displacement is recorded along the lateral direction. This behavior is associated with the fact that the isolated object is not symmetric in the two direction so it can be stated that geometry of the isolated system influences the response.

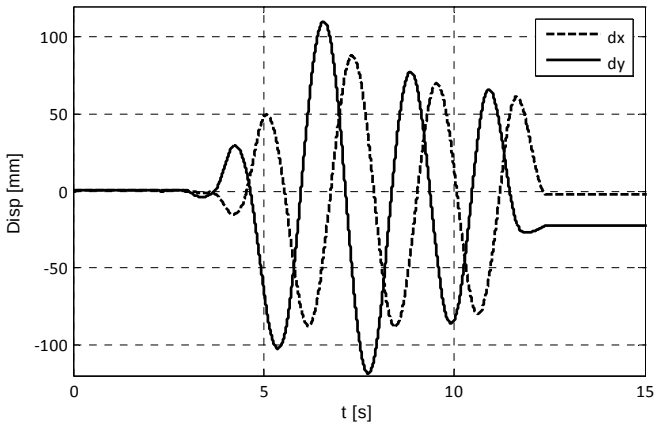

Figure 5.117 - displacements test#19

A first and rough evaluation of the effect of a bidirectional input can be obtained with the comparison between the bidirectional response and the corresponding unidirectional tests: the results obtained are depicted in figure:

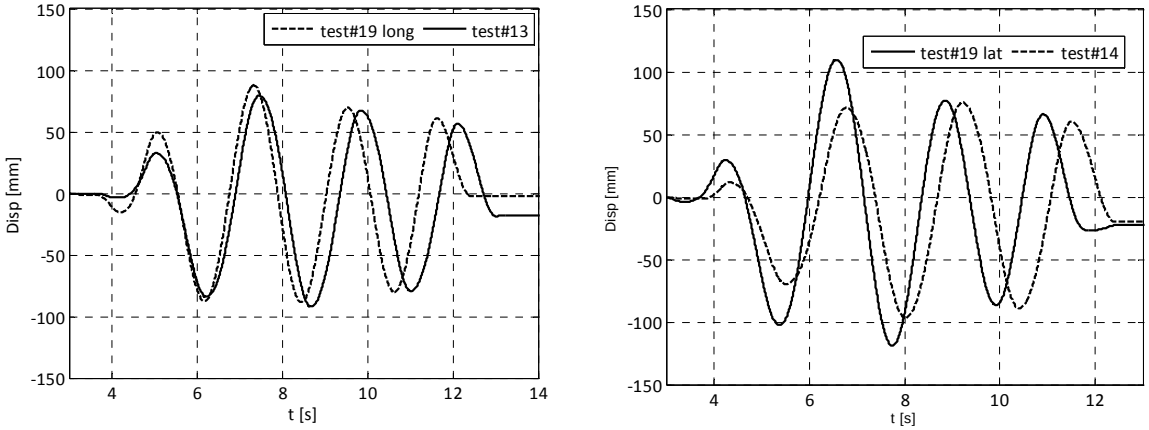

Figure 5.118 - comparison between bidirectional and unidirectional displacements

It can be observed that the component of the motion along the longitudinal direction has an increment of the maximum positive displacement and a reduction of the minimum negative displacement, while along the transversal direction there is an increment of both the positive and the negative displacement; from Table 5.12 it can be noted that increments along the longitudinal direction can be compared, as an order of magnitude, to the perpendicular effect of test 14, on the other hand lateral displacements reach a maximum value that cannot be justified with the perpendicular displacement of test 13.

The response for the bidirectional input shows a larger magnitude of displacements, in particular along the lateral direction; results are also compared in Table 5.12:

Table 5.12 - comparison between unidirectional and bidirectional displacements

Test	Max D [mm]	Min D [mm]	Var [%]	Var [%]
13	79.5	-92.8		
14	75.6	-96.8		

Test	Max D [mm]	Min D [mm]	Var [%]	Var [%]
19 long.	87.9	-88.3	10.5	-4.1
19 lat	110	-119	44.9	22.7

When a unidirectional input is given the system moves mainly along the direction of the input, but it was also observed the presence of a perpendicular displacement, as it is shown in Figure 5.119 and Figure 5.120.

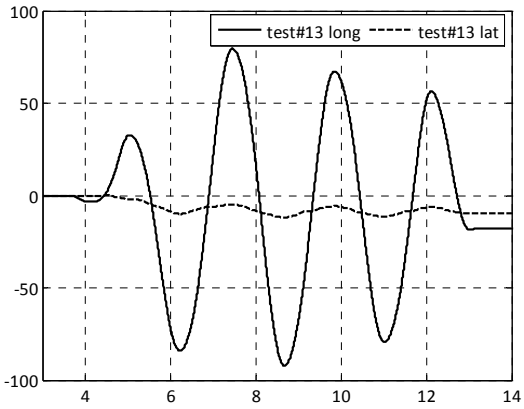

Figure 5.119 - longitudinal and lateral component test #13

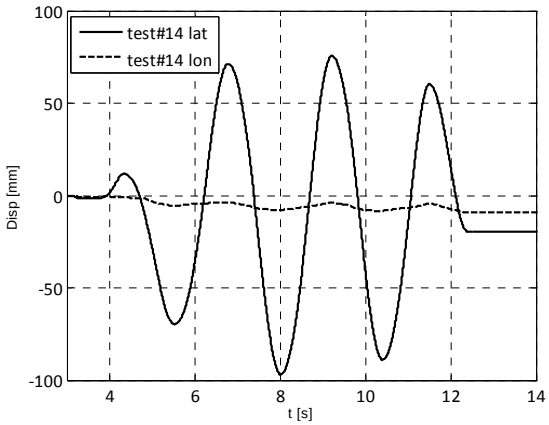

Figure 5.120 - longitudinal and lateral component, test#14

The perpendicular component of displacements is the result of a translation and of oscillations around a new point of equilibrium, different from the initial one, for instance test#13 shows an average translation of 8 mm and oscillations around this equilibrium point with amplitude ±3 mm; for test#14 the perpendicular component of the displacement is around 6 mm and oscillations around that value have amplitudes of ± 2 mm. This phenomenon can be justified with the non perfect symmetry and the imprecision in the assembly of the specimen, it can be also connected to the difference in the mechanical characteristics of the devices, for instance slightly different values of the coefficient of friction that cause differences in the response of the single devices.

Table 5.13 – horizontal displacements test 13 e 14

Test	maxD paral. [mm]	maxD perp. [mm]	%
13	-92	-11.8	12.8
14	-96.8	-9.25	9.5

Values of the maximum displacements for the horizontal tests are summarized in Table 5.13: the amplitude of perpendicular displacements is high (12.8% and 9.5% respectively) but it is not enough to justify the increased lateral displacement for test #19.

If the displacements are depicted considering the plane X-Y and compared with the maximum tolerable displacement the result obtained is depicted in Figure 5.121

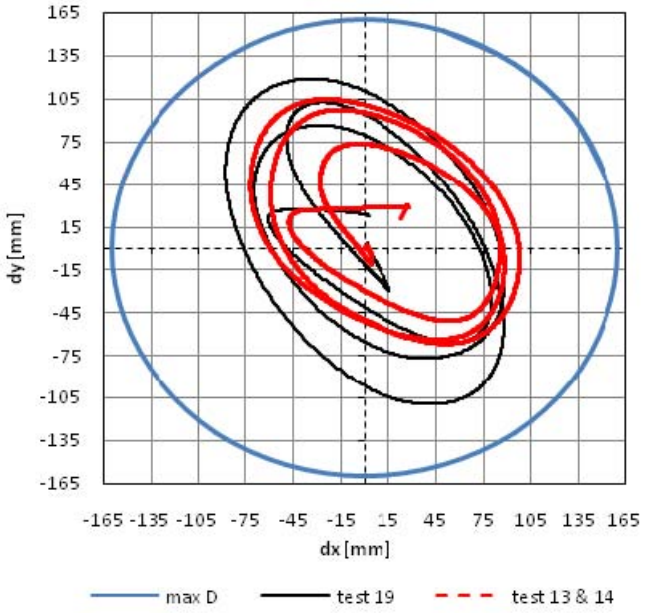

Figure 5.121 - comparison displacements test 19 and test 13 and 14 combined

It is interesting to compare the red line and the black line in Figure 5.121, they respectively represent the X-Y (longitudinal and lateral) displacements of test 19 and the combination of test 13 and 14 (13 long + 14 long, 13 lat + 14 lat, considering the proper phase angle). The results obtained from the superposition of the unidirectional tests is completely different from the result obtained from the bidirectional test; it is moreover clear from the above mentioned picture that the approach of superposition of unidirectional tests underestimates the maximum displacement and it provides a result that is not on the safe side.

Another interesting aspect is the presence of a residual displacement, pointed out by the trajectory of the center of mass which moves from the origin of the system but does not end the motion in the same position: residual displacement of 22 mm is recorded along the lateral direction; this result highlights the fact that there might not be a perfect re centering of the sliders after the motion.

Differences between unidirectional and bidirectional tests can be observed also in the hysteresis loops, that can give an overview of the behavior of the system in terms of forces and displacements; it should be reminded though, that the accelerations and the displacements obtained from the tests are referred to the average behavior of the system; indeed the acceleration (and hence the force) is measured above the isolated plan and then used for evaluating an average force on the device.

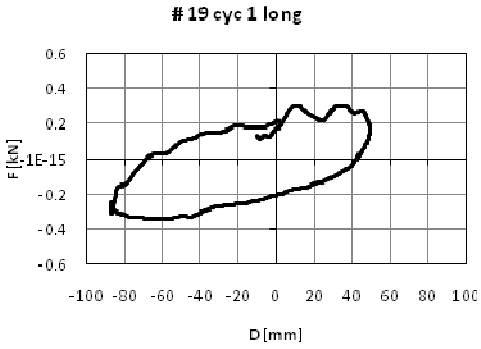

Figure 5.122 - cycle n° 1 longitudinal test 19

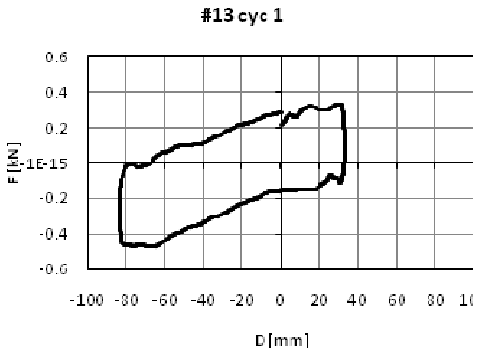

Figure 5.123 -cycle n° 3 longitudinal test 13

Figure 5.124 - cycle n° 2 longitudinal test 19

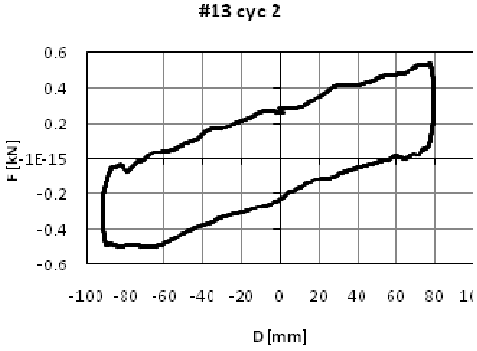

Figure 5.125 -cycle n° 3 longitudinal test 13

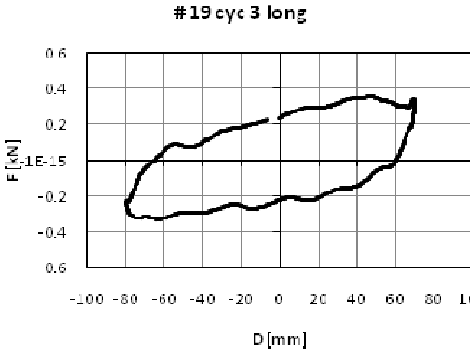

Figure 5.126 - cycle n° 3 longitudinal test 19

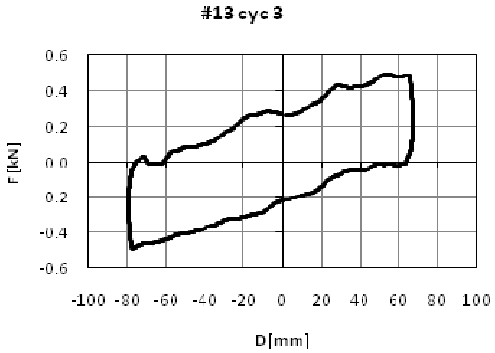

Figure 5.127 -cycle n° 3 longitudinal test 13

The six graphs presented from Figure 5.122 to Figure 5.127 depict the single cycles in the longitudinal direction for tests 19 (left column) and test 13 (right column).The difference is immediately visible: the bidirectional tests have a smoother shape, in particular in the range of high displacements, where the inversion of the direction of motion is not as well defined as in the corresponding unidirectional test (in the right column of graphs the maximum and minimum displacements always correspond to a reduction of force at almost the same value of the displacements; this is due to the fact that while the motion in the unidirectional test is only in one direction). Another interesting aspect emerges from the comparison between the results: the straight part of the cycle, which represents the stiffness of the system ($\frac{W}{R^*}$) is well defined for the unidirectional test, while the corresponding part of the bidirectional cycle shows oscillations and variations of slope, as it will described more in detail in the following. The same comparisons in the lateral direction, between test 19 and test 14 are presented in the following:

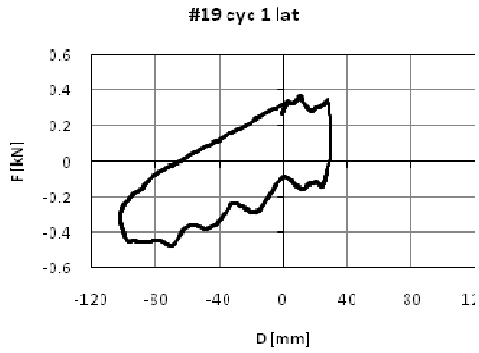

Figure 5.128 - cycle n° 1 lateral test 19

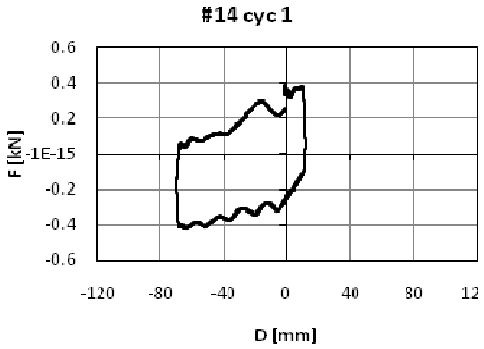

Figure 5.129 - cycle n° 1 lateral test 14

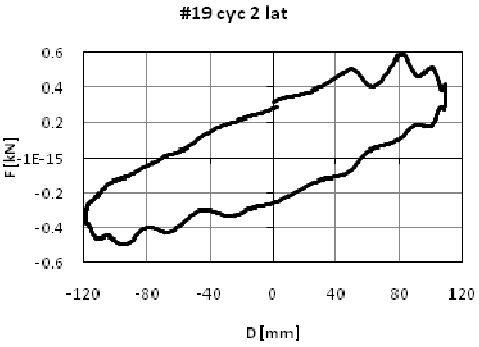

Figure 5.130 - cycle n° 2 lateral test 19

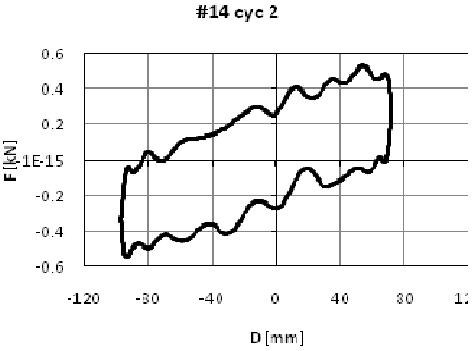

Figure 5.131 - cycle n° 2 lateral test 14

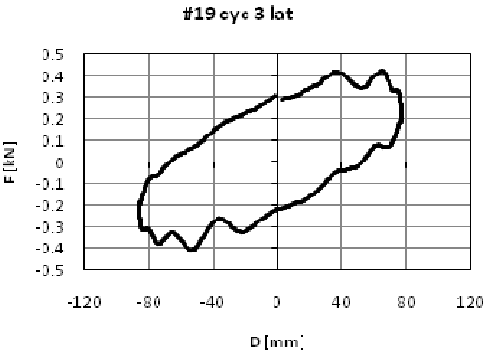

Figure 5.132 - cycle n° 3 lateral test 19

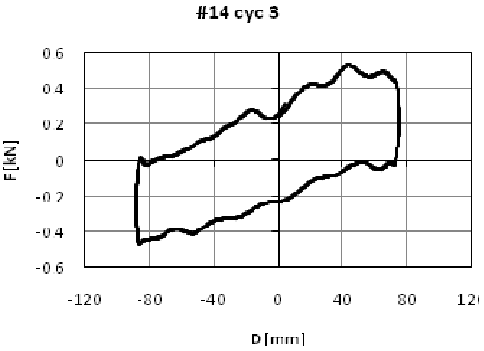

Figure 5.133 - cycle n° 3 lateral test 14

Motion along the lateral direction is characterized first of all by a different geometrical layout because of the different distance between the isolators (914.4 mm longitudinal, 609.6 mm lateral) and the dimension of the specimen itself (base block: 1210 mm longitudinal, 914 mm lateral). Graphs from Figure 5.128 to Figure 5.133 depict the force displacement cycle for lateral direction of test 19 (left column) and test 14 (right column). Oscillations recorded in the part of the cycle with "constant stiffness" that were pointed out along the longitudinal direction are more evident along the lateral one. An additional test including bidirectional input was carried out, it is classified as test 20, the input functions are D1 1_5V2 along the longitudinal direction and D1_0.8V1 along the lateral direction. Inputs have the same maximum displacement and different frequency, the longitudinal input is applied with 8 cycles (instead of 3) to allow the superposition of the input in the other direction.

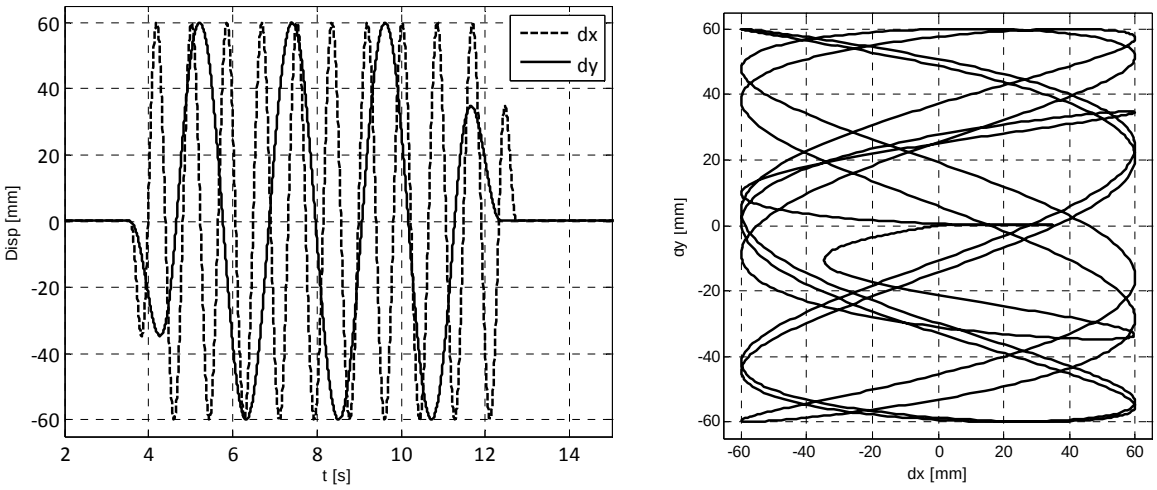

Figure 5.134 - test 20 input details a) time history, b) plane XY

The input functions applied in test 20 are depicted in Figure 5.134, both the representation over time and the plotting of the two input functions on the plane XY. Figure 5.135 shows the response in terms of displacements along the longitudinal and lateral directions.

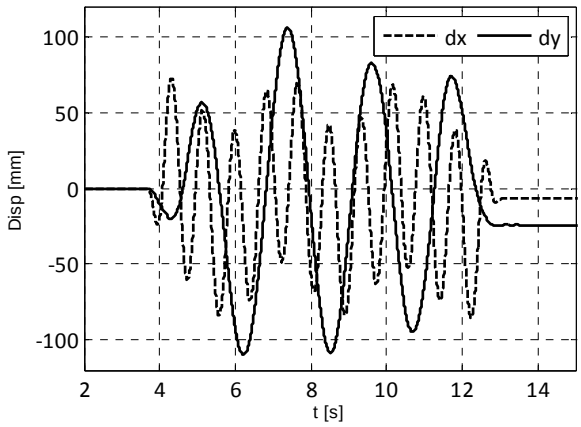

Figure 5.135 - test 20 displacement response

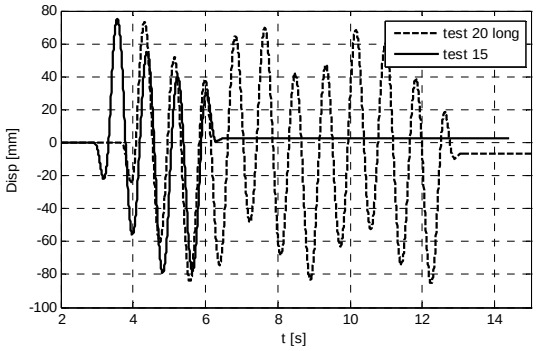

Figure 5.136 - longitudinal displacement for test 20 and test 15

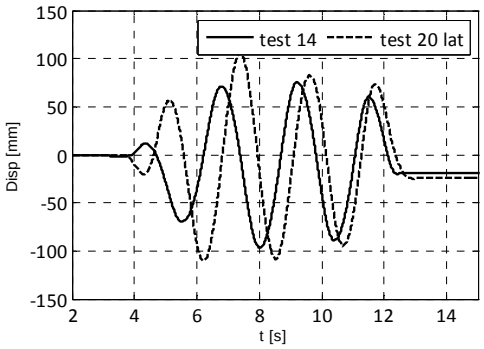

Figure 5.137 - longitudinal displacement for test 20 and test 14

The effect of the action along two directions at the same time is more evident along the lateral direction: the maximum recorded displacement for test 15 is indeed reduced if compared with the one obtained in test 15, on the other hand the perpendicular component, if compared with test 14, shows an increase of the displacements. Results are summarized in Table 5.14:

Table 5.14 – comparison between unidirectional and bidirectional results

Test	Max D [mm]	Min D [mm]	Var [%]	Var [%]
14	75.6	-96.8		
15	75.1	-79		
20 long.	72.9	-85.5	-2.9	8
20 lat.	106	-110	40	13.5

As it was stated for test 19 the increased displacement can be due to the perpendicular displacement that is present in the unidirectional tests, results are depicted Figure 5.137 and summarized in Table 5.14

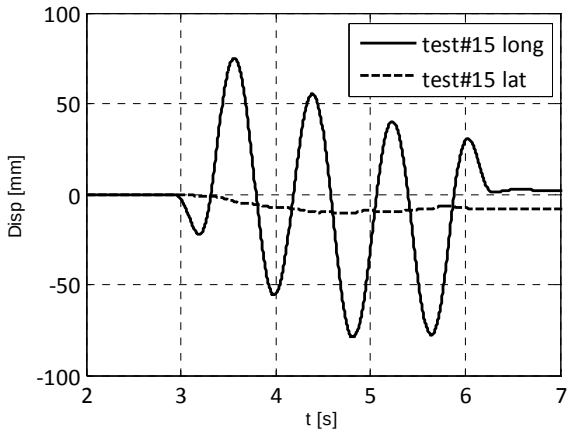

Figure 5.138 - test #15 displacements

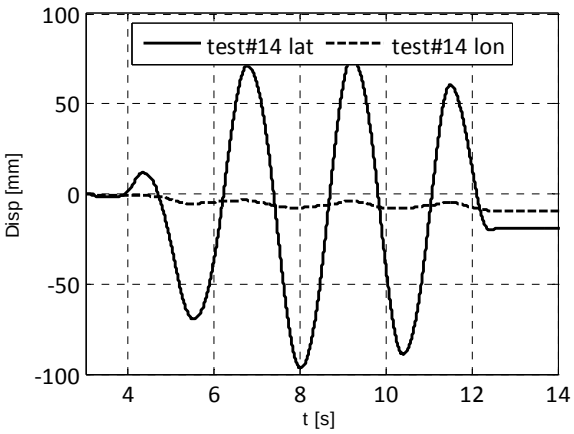

Figure 5.139 – test #14 displacements

A comparison between the recorded output for test 20 and the combination of tests 14 and 15 (obtained from the same procedure described for test 19) demonstrates how, as it was previously stated, an approach to the dynamic response of a system subjected to bidirectional input, considering the sum of the single components, is often not on the safe side and it can be cause of errors in the design phase.

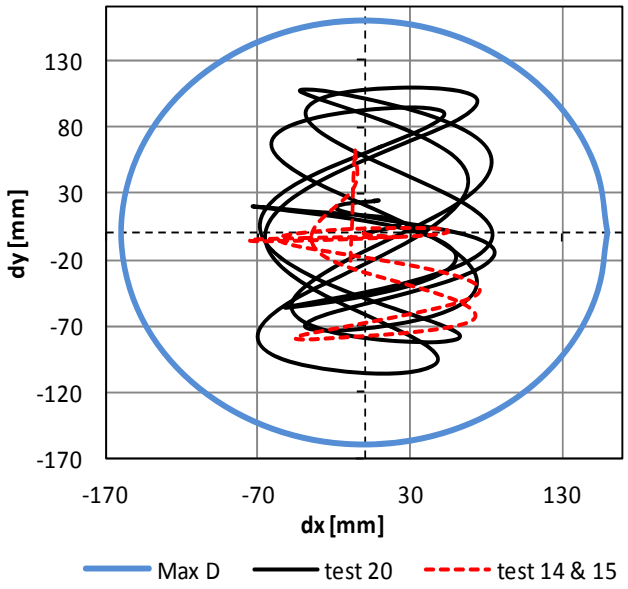

Figure 5.140 - plane displacements test 20

Further information about the response of the dynamic system that is object of study can be obtained from the analysis of force displacement cycles; in pictures from Figure 5.141 to Figure 5.152 the single cycles are depicted and compared with the corresponding unidirectional cycles, in order to point out differences and peculiar behaviors:

Figure 5.141 - cycle n° 1 longitudinal test 20

Figure 5.142 - cycle n° 1 longitudinal test 15

Figure 5.143 - cycle n° 2 longitudinal test 20

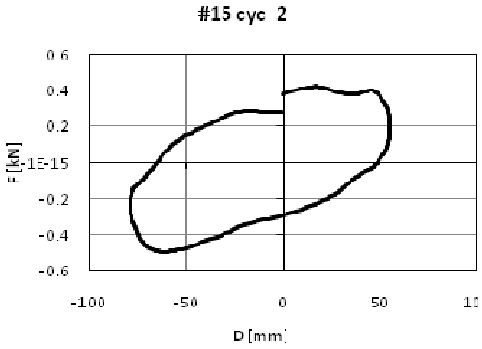

Figure 5.144 - cycle n° 2 longitudinal test 15

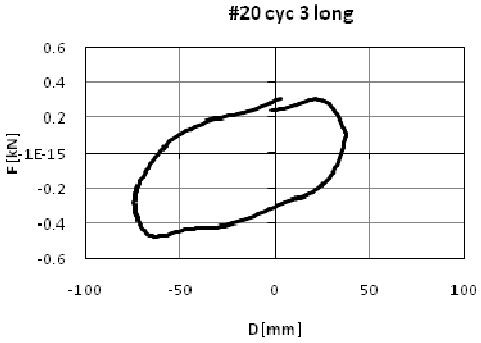

Figure 5.145 - cycle n° 3 longitudinal test 20

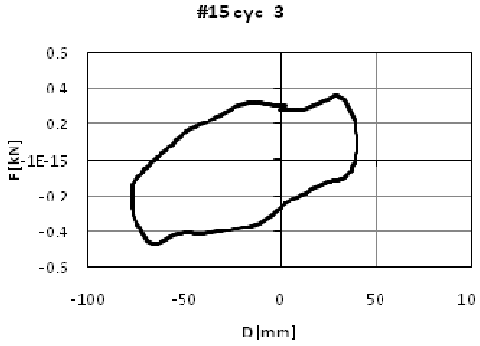

Figure 5.146 - cycle n° 3 longitudinal test 15

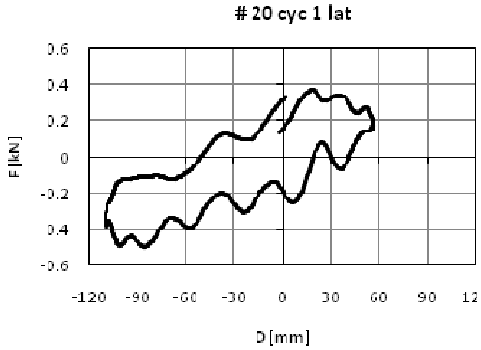

Figure 5.147 - cycle n° 1 lateral test 20

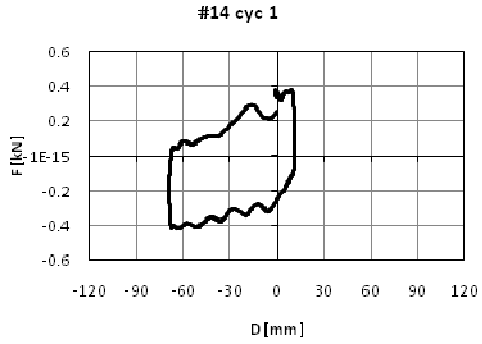

Figure 5.148 - cycle n° 1 lateral test 14

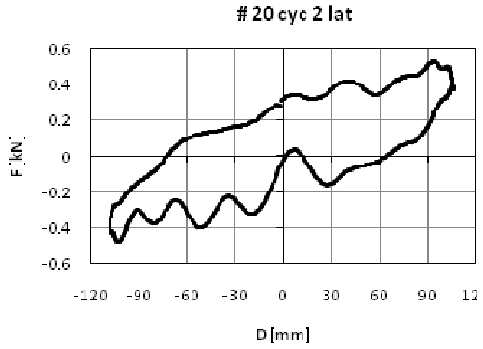

Figure 5.149 - cycle n° 1 lateral test 20

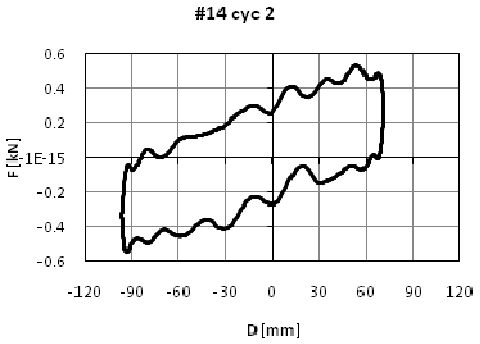

Figure 5.150 - cycle n° 2 lateral test 14

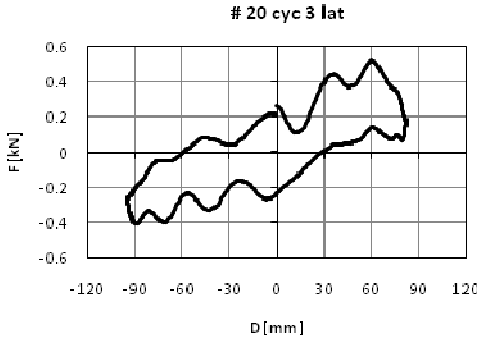

Figure 5.151 - cycle n° 3 lateral test 20

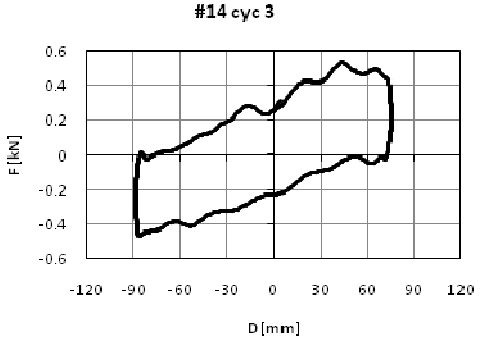

Figure 5.152 - cycle n° 3 lateral test 14

Graphs from Figure 5.147 to Figure 5.152 show the comparison between the longitudinal response of tests 15 and 20 along the longitudinal direction. The maximum and minimum displacements are almost the same and the maximum and minimum forces are very similar as well: the two responses have the same general behavior even though, as it was stated for test 19 the shape of the loop for the unidirectional test is sharper and similar to the theoretical mechanical model. This aspect is due to the fact that, when the inversion of direction of motion occurs, there is the perpendicular component of motion that is non null, and there is still a component of velocity. The response shows more differences along the lateral direction (in accordance to what shown for test 19), the unidirectional response, although diffused local oscillations are present, follows in general a trend similar to the theoretical mechanical model. The lateral component of test 20, instead, shows loops that are far from the expected behavior, they are characterized by diffused and wide local oscillations and sudden changes in the stiffness of the system; more details about this aspect will be given in the following.

Such a difference in terms of shape of the hysteresis loop corresponds to a difference in terms of dissipated energy. It is evident in fact, that the area of the cycle in the case of the bidirectional test, if the same displacement is considered, is smaller because of the curve shape of cycles around the maximum displacements zone (and also because of local oscillations). This behavior can be explained by comparing the traditional model that describes the hysteresis loop and the real behavior of the devices. The traditional model for the friction pendulum is given in relation (5.1); it properly describes the for unidirectional tests, as depicted in Figure 5.153 and Figure 5.154:

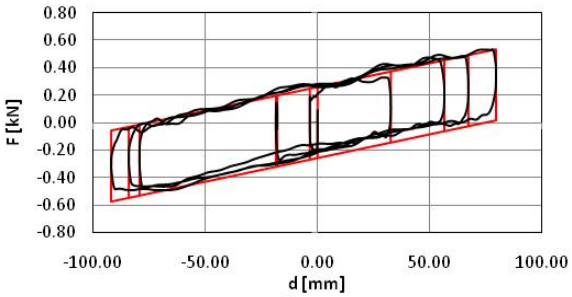

Figure 5.153 - hysteresis loop test 13 longitudinal, experimental (black line) and theoretical (red line) results

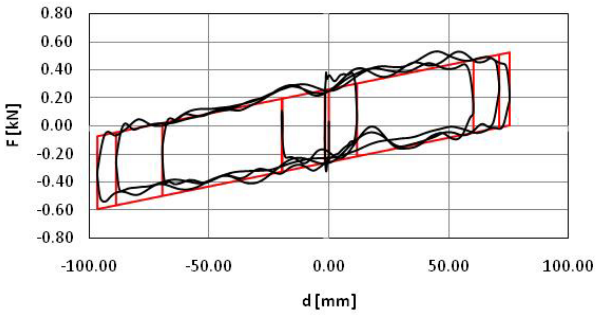

Figure 5.154 - hysteresis loop test 14 lateral , experimental (black line) and theoretical (red line) results

Graphs show a good accordance between the mechanical model described and the experimental results. It is worth noting that this statement is valid for the average behavior, since local oscillations are present, but this aspect will be studied more in detail in the following. When the same model is applied to fit the results obtained from the bidirectional test the comparison gives the following results:

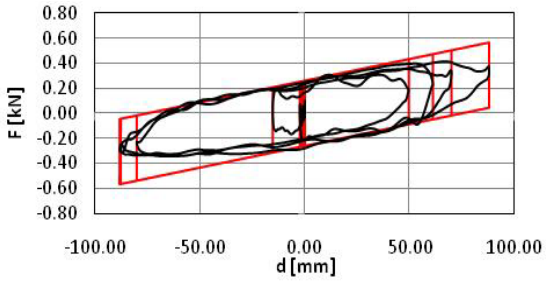

Figure 5.155 - hysteresis loop test 19 longitudinal , experimental (black line) and theoretical (red line) results

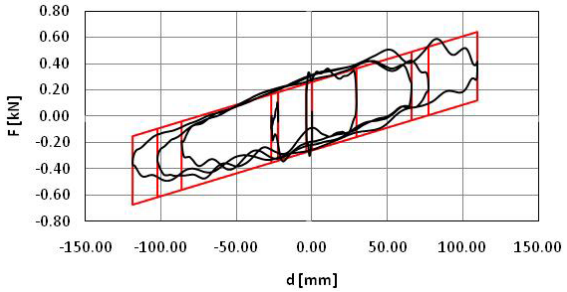

Figure 5.156 - hysteresis loop test 19 lateral, experimental (black line) and theoretical (red line) results

It is evident how the above described model does not properly match the real response of the system. The areas of the loops close to the maximum and minimum displacements are indeed less smooth for the bidirectional tests than for the modeled response. Furthermore, when the inversion of the motion is considered, a value of

$$F = 2\,\mu\,W \tag{5.5}$$

is expected. The real value of force that can be measured from the bidirectional tests is summarized in the following table:

Table 5.15 – comparison for the force value at motion inversion

	2μW [kN]	
Cyc	**13**	**19**
1L	0.437	0.31
1R	0.404	0.242
2L	0.555	0.351
2R	0.475	0.356
3L	0.472	0.347
3R	0.491	0.408

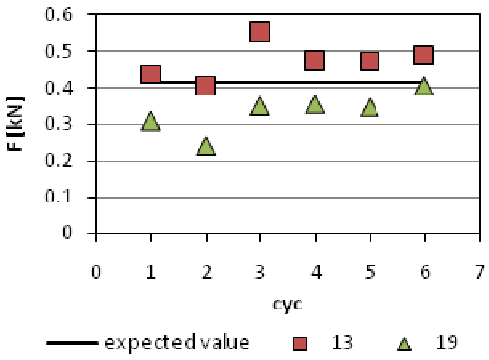

Figure 5.157 - comparison for the force value at motion inversion

The summary gives, for each cycle of tests , values of the force evaluated for the maximum (R-right) and minimum (L-left) displacement. It can be observed that the value of the force is always greater in the unidirectional tests. This difference can be justified by the presence, in the bidirectional tests, of two components of motion, that contribute at same time to reach the value of activation of motion, hence the presence of two components must be included for the calculation of the limit friction force surface. A model such the one described in can be assumed:

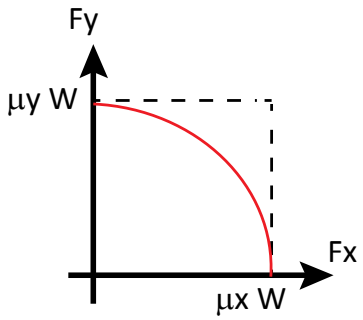

Figure 5.158 - friction model

the two dashed lines describe friction thresholds for the single directions, longitudinal and lateral: once the value of limit friction is reached the sliding motion start, but with this model the interaction between the two components is not considered at all. If a different model is assumed, for instance a quadratic surface, the value of the limit force to reach for activating sliding is:

$$F \geq \mu_i * W = \sqrt{(\mu_x W)^2 + (\mu_y W)^2} \qquad (5.6)$$

the components of the friction coefficient along the two directions can be assumed to be proportional to the corresponding velocity components. The model that describes the behavior of force with displacement, which is also that implemented in the software used for the numerical analyses, can then be modified considering these assumption.

Results are described in Figure 5.159 and Figure 5.160

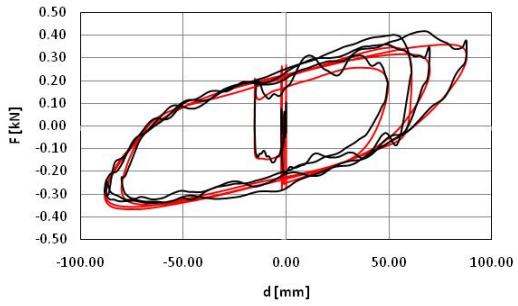

Figure 5.159 - comparison between experimental (black line) results and modified model (red line)

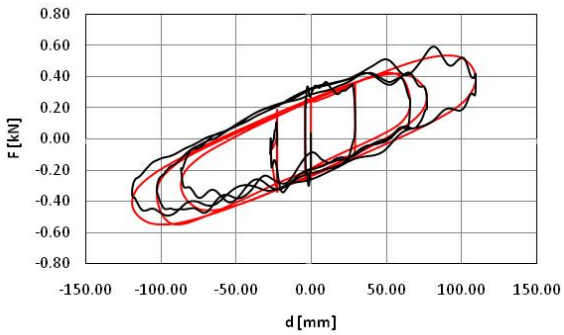

Figure 5.160 - comparison between experimental (black line) results and modified model (red line)

As shown in the graphs above the modified model provides a good accordance between the experimental results and those obtained with the model. The general trend of the modified model is also connected to lower energy dissipation than that foreseen by the traditional model, as it can be clearly seen from the comparison depicted in Figure 5.163

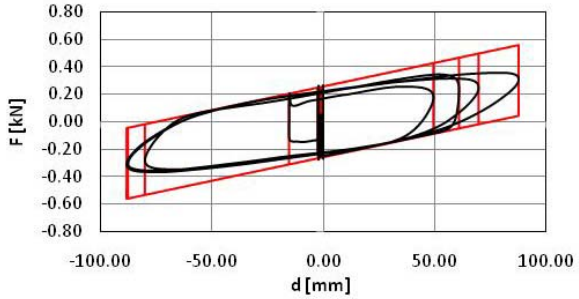

Figure 5.161 - comparison between traditional (red line) and modified model (black line), test 19 longitudinal direction

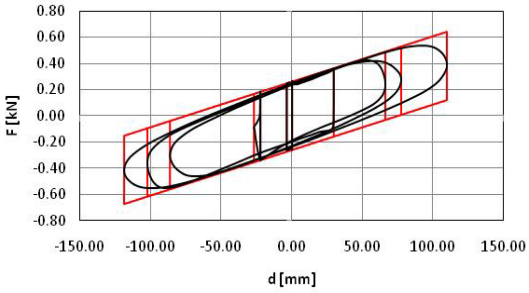

Figure 5.162 - comparison between the traditional (red line) and the modified model (black line), test 19 longitudinal

Interesting considerations can be made when the EDC parameter is taken into account; a good accordance is found if the value of the dissipated energy for the experimental data and the unidirectional model is considered for test 13:

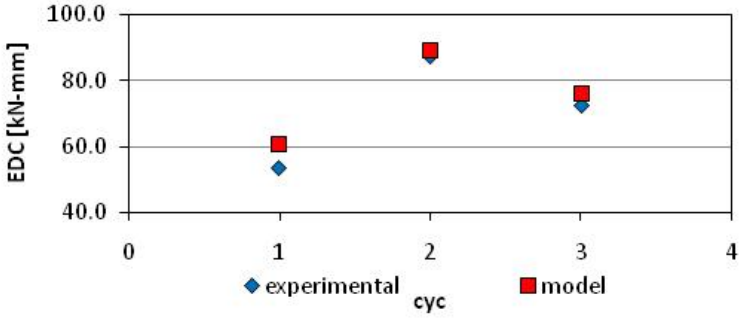

Figure 5.163 - comparison between experimental EDC and expected EDC, longitudinal direction test 13 unidirectional model

Differences that appear in the dissipated energy are mainly due to the effects of local oscillations, that affect the value of the area of the cycle. When the same control parameter is monitored for the bidirectional tests, for instance longitudinal direction of test 19, it can be observed that the value is noticeably lower than the one predicted by the traditional model. On the other hand, when the model that accounts the two directions of motion is considered, the accordance level is higher:

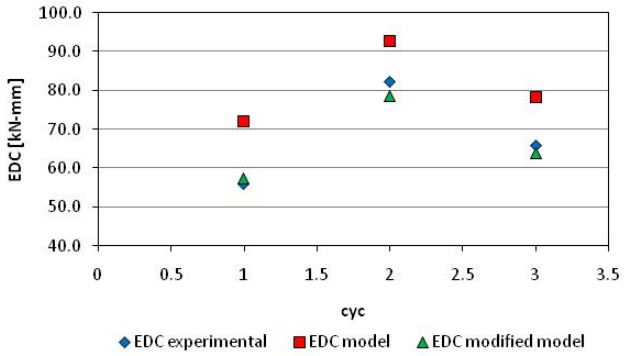

Figure 5.164 **- EDC values comparison**

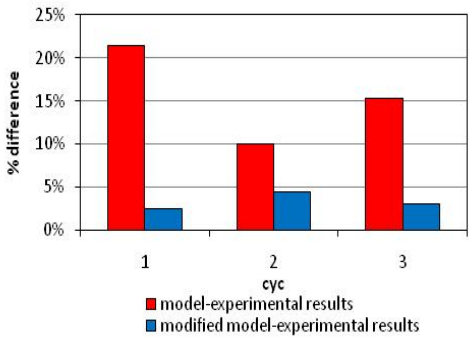

Figure 5.165 EDC value comparison (%)

5.5.6.1.1 Rocking

Rocking is an interesting phenomenon which has significant effects on the dynamic response of the system; one of the aims of these experiments was in fact to point out some correlations between the behavior of an isolated system and the effects connected to rocking.

This phenomenon was studied in particular for configuration cfg#4 which allows the study of differential displacements between the base of the isolated system and the upper part of the model. The following results and considerations are given for tests 13, 14, 15 and 16, unidirectional respectively along the longitudinal (13, 15) and the lateral direction (14, 16); the analysis of the response in terms of displacements, for the system subjected to different load conditions the presence of differential displacements can be pointed out. The differential displacement for test 13, for instance, is depicted Figure 5.166:

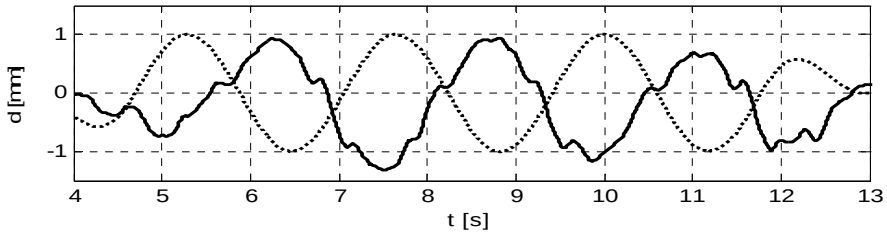

Figure 5.166 - differential displacements test 13 (solid line), normalized input (dashed line)

With reference to Figure 5.166, the dashed line represents the ground displacement normalized with respect to its maximum value, while the solid line represents the difference between the measured displacement at the base and the half height measurement point.

The result shows a sinusoidal trend, with a period similar to that of the input load. the maximum measured displacement is around 1 mm, considering that the difference is measured between horizontal displacement sensors H1 and H2 (H3 and H4 for the lateral direction) and H5 (H6 for the lateral direction) .

Similarly it is possible to depict the same parameter for test 15, which is longitudinal as well, with maximum acceleration 0.35 g:

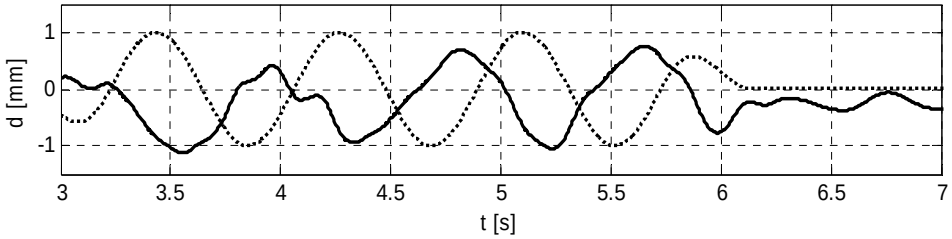

Figure 5.167 - differential displacements test 15 (solid line), normalized input (dashed line)

maximum displacement has still a maximum value of 1 mm, although the ground acceleration is 7 times higher than before; this underlines the efficiency of the isolation system in terms of reduction of transmitted actions.

When the same results are depicted also for the lateral test 14 and 16, which are characterized by the same input functions of test 13 and 15 the presence of rocking can be similarly observed but with other secondary effects, connected to the direction of motion along the direction with the lower moment of inertia and the lowest distance between the bearings:

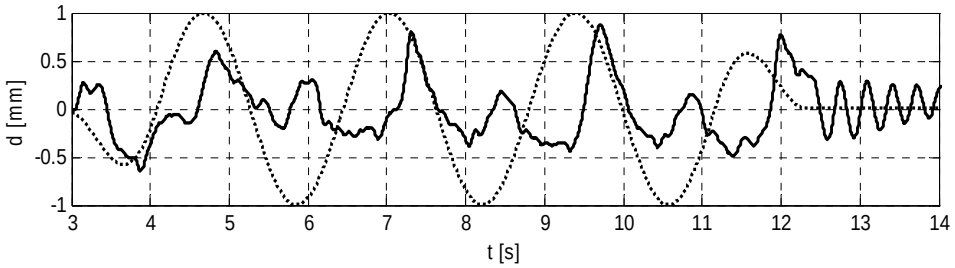

Figure 5.168 - differential displacements (solid line) test 14, normalized input (dashed line)

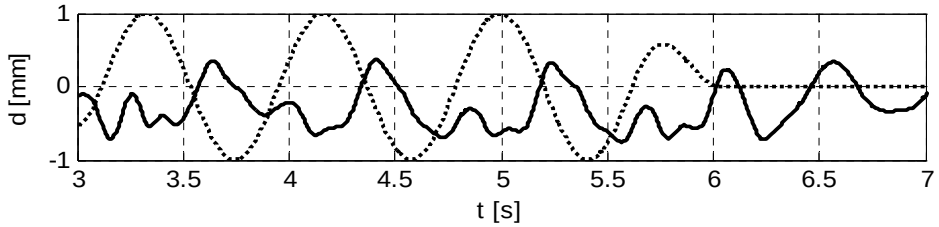

Figure 5.169 - differential displacements (solid line) test 16 ,normalized input (dashed line)

The amplitude of the oscillations is in this case lower and the response is influenced by secondary effects that make the result less clear than in the perpendicular direction. It is worth noting the presence of differential displacements also when the input is over. This phenomenon can be present either as free oscillations or as residual displacement, as it can be observed from previous graphs. A justification can be found in the lack of horizontal alignment of the isolation plan, due to the different displacement of the sliders inside the devices, that can modify the vertical position of the devices with the extreme limit of losing the contact of one of the four bearings; this behavior will be described with more details in the following. One of the aspects connected to rocking is the variation of vertical load on the single devices: such a variation consequently leads to a variation of the stiffness of the isolator. As a result of this behavior a rotation around the vertical axis can be experienced by the system, as it is shown in figure:

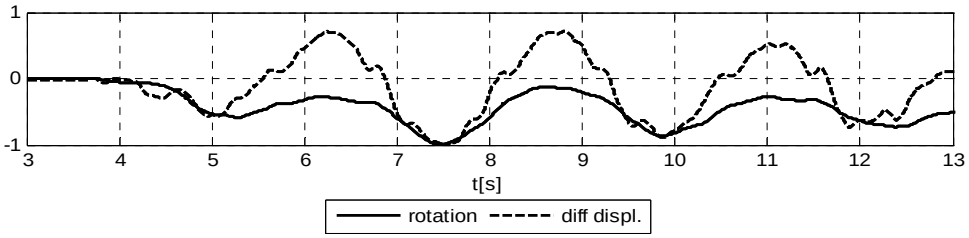

Figure 5.170 - rotation about vertical axis test 13

with reference to the above depicted graph the dashed line represents the differential horizontal displacement, normalized with respect to its maximum absolute value, while the solid line represents the value of the rotation angle around the vertical axis. Rotation of the system about the vertical axis is connected to the horizontal rocking, as it can be observed from figure. A similar result is obtained for test 15.

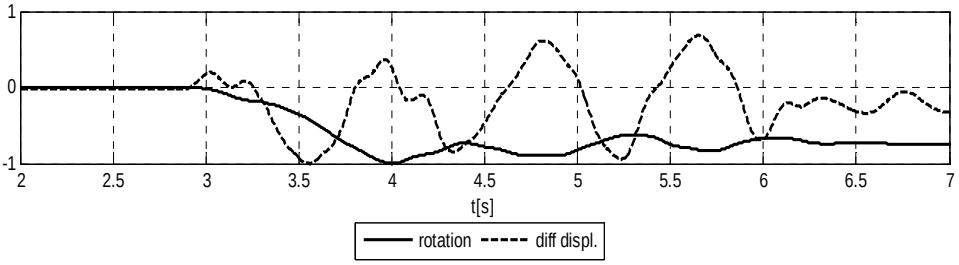

Figure 5.171 - differential displacements test 15

It is worth noting that the presence of horizontal displacements, free oscillations and rotations about the vertical axis demonstrate how, despite the starting condition of the system is that of a correct relative positioning of the sliders in the devices (i.e. slider perfectly centered), they are subjected to a different relative displacement that causes these potentially dangerous phenomena, as pointed out in the following sketch:

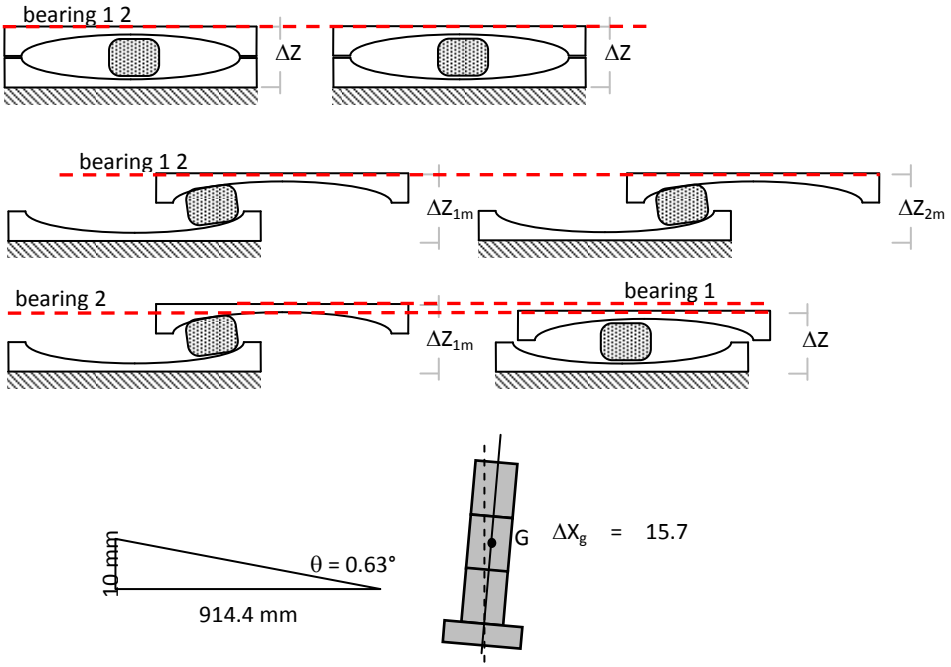

Figure 5.172 - vertical behavior of the devices

The above described phenomenon of different alignment of the sliders can be represented with a plot of the vertical displacements on the horizontal displacement of the base block. Concerning test#13, for instance, results are depicted below:

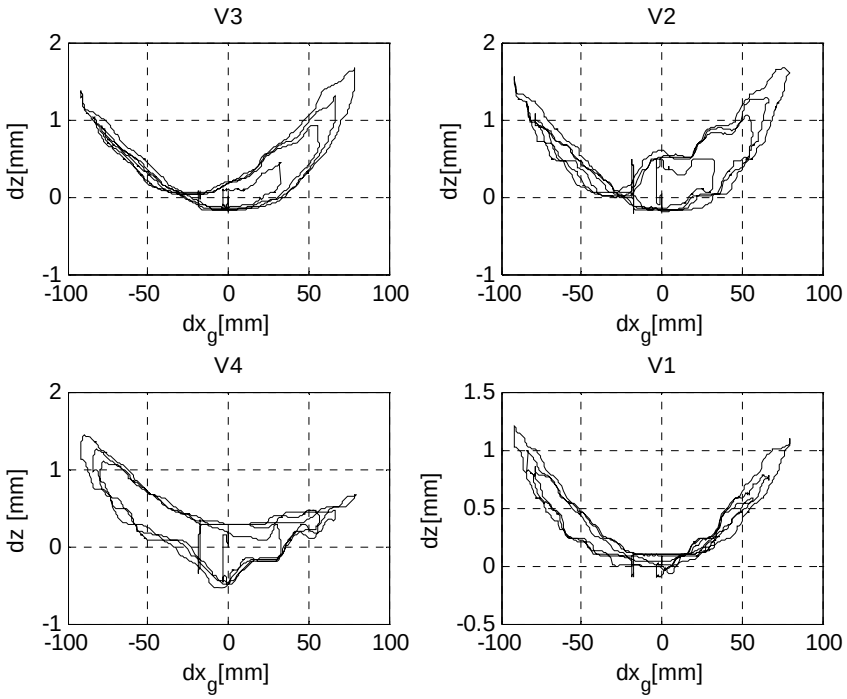

Figure 5.173 - vertical displacements of single isolators, test 13

The four graphs represent the vertical displacements versus the average horizontal displacement for each corner of the base block, from these plots it is visible how, for the same horizontal displacement, the vertical one can be very different. This demonstrates how the vertical displacement of the single corners is different during motion. Moreover the response shows a sort of loop-like behavior that is explained by a displacement of the slider perpendicularly to the main direction of motion. Indeed, despite the fact that a unidirectional test is considered, a perpendicular displacement was already pointed out. Such a displacement causes a variation in the position of the slider which does not follow the central path anymore, but moves along a parallel linear path. This new sliding path is characterized by a different vertical height, the phenomenon, that justifies the behavior depicted in the graphs above, is described in the following sketch.

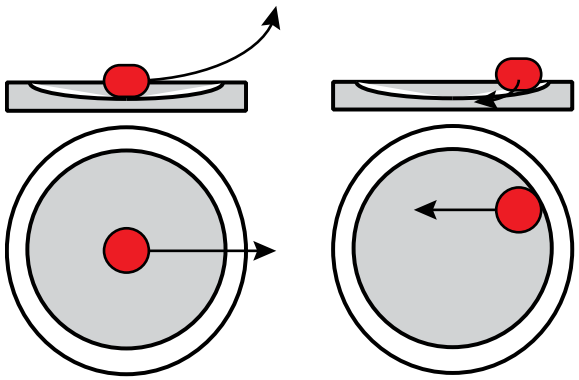

Figure 5.174 vertical displacements of single isolators, sketches

Similar results are presented for test 15:

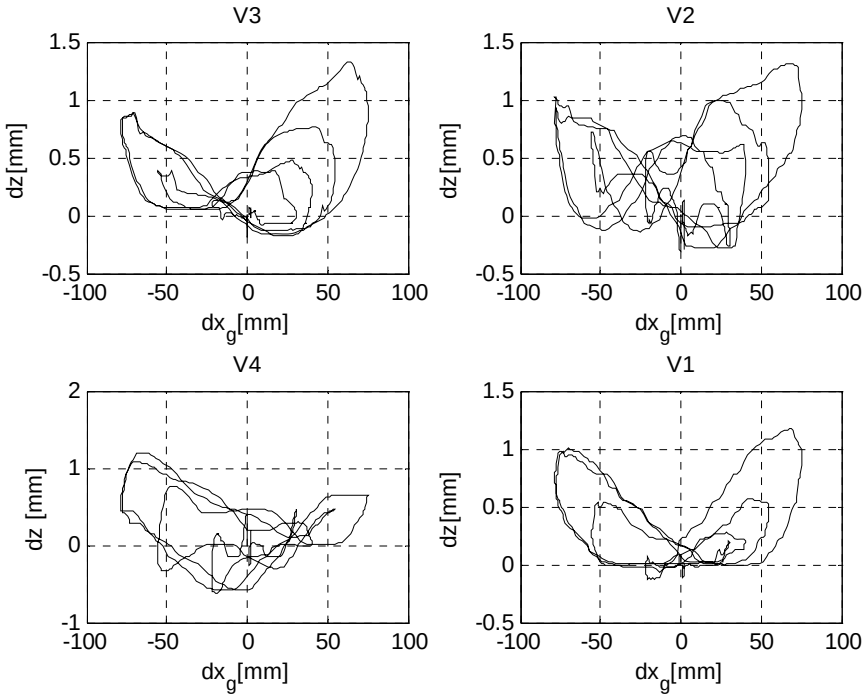

Figure 5.175 - vertical displacements of single isolators, test 15

The above described effect is more evident for test 15, where the effect of rocking behavior can be pointed out from the response of the horizontal differential displacements and from the vertical displacements of the system. Such a behavior affects the mechanical characteristics of the isolation system and is strongly connected with several other effects that will be mentioned in the following.

The influence of the vertical action on rocking phenomenon is evident. It is clear that a vertical component of the acceleration could both reduce or amplify inertial effects on the isolated object. In terms of the present study the interesting aspect is the potential increasing of the displacements of the isolated object that would need to be considered for an accurate design phase. The following graph depicts the differential displacements between the base and the top of the specimen:

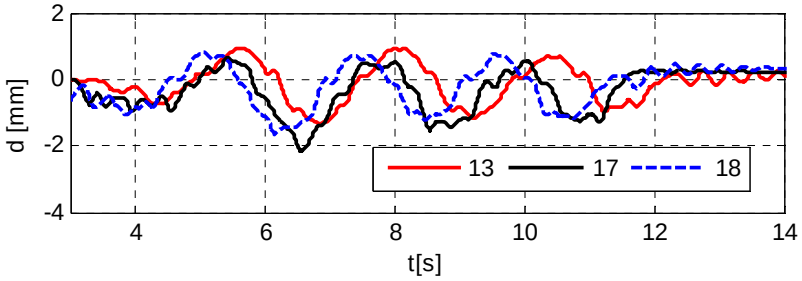

Figure 5.176 - differential displacements

The results depicted above show how the presence of vertical action influences the rocking effect, indeed the maximum differential displacement is increased both in test 17 and 18, in particular in test 17 it has a more evident effect:

	Test 13	**Test 17**	**Test 18**
MAX D [mm]	1.3	2.2	1.7

Diff.%		70%	30%

It is also worth noting that both the tests with vertical input show free oscillations, which means that modification in the vertical alignment of the devices occurred; this effect can also be pointed out from the vertical displacements behavior:

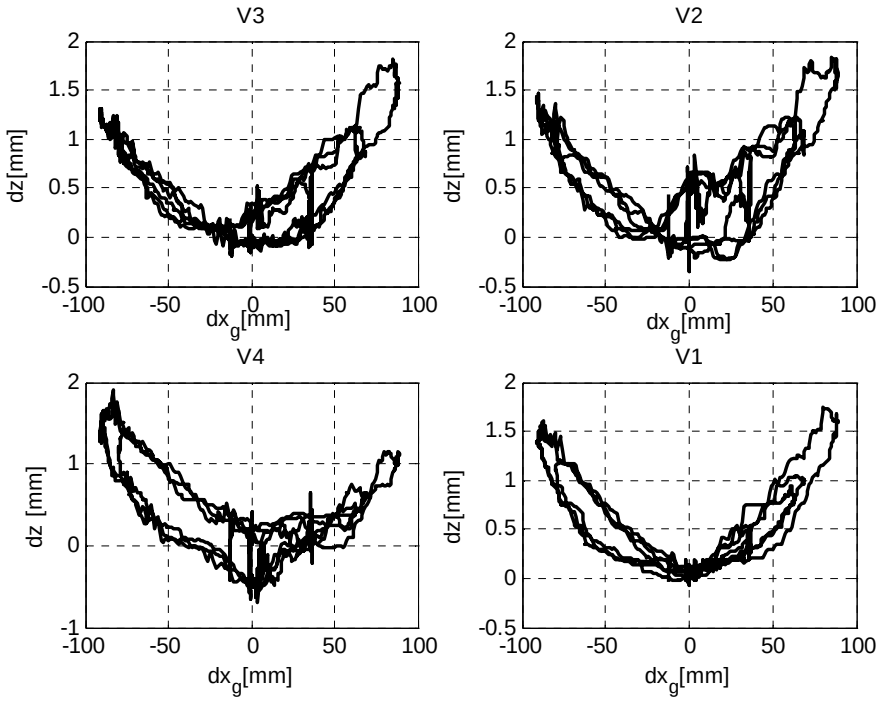

Figure 5.177 – vertical displacements test 17

5.5.6.2 Reduction of the maximum design displacement

The above described phenomenon opens up an important and delicate issue that needs to be pointed out, in fact the motion of the slider along a path that is not centered implies a reduction of the maximum displacement that the device can experience:

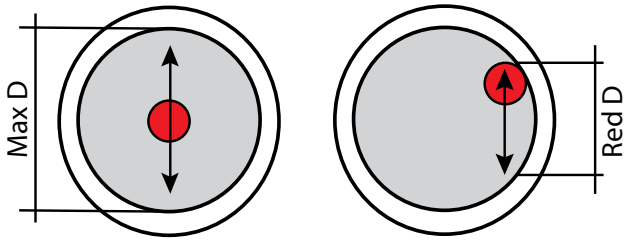

Figure 5.178 - reduction of maximum displacement

When unidirectional tests are considered a reduced perpendicular displacement is involved, this displacement causes a reduction of the maximum displacement that can be neglected (for test 13, for instance the reduction of the stroke of the device is about 2 mm), but in case of bidirectional tests the variation becomes important and it can cause high reduction of the maximum stroke.

In test 19 the maximum lateral displacement is D_y = 119 mm that can be divided between the upper and the lower surfaces, with this assumption the maximum displacement of the slider is D_y = 59.5 mm, considering that the maximum half displacement is 85 mm this lateral translation of the sliders reduces the stroke from 85 to 40 mm. This is of course the worst scenario possible, and it describes the worst condition in which the system can be, but even if present with a lower intensity this aspect cannot be neglected.

5.5.7 Suspects and further investigation

Some of the aspect that emerged so far from the analysis of the results, are only partially answered. More detailed analysis needs hence to be performed to point out the correct cause-effect relations. However such phenomena have evidently interesting facets that are worth to point out even though only with a qualitative description that can provide an idea of the phenomenon.

5.5.7.1 Variation of stiffness

An important aspect that emerged from the tests is the variation of stiffness of the system. The theoretical model proposed by (36), describes the paths of force displacement cycles, that the system follows from maximum to minimum displacements, with straight lines characterized by a constant slope. This is a function of the curvature of the sliding surfaces and of the vertical load acting on the device (for double concave curved surface sliders with different coefficient of friction for the two surfaces, slope can have two different values); the assumptions on which this model is based consider that the motion is regular and no stop of the different elements occurs. Sometimes these assumptions are too strong in a real situation, in particular for systems in which numerous devices are applied, and where the position of the center of mass induces overturning moments. To these aspects one must add the effects of inertia of the isolated system, that can influence the contribution of vertical load on each device and then can cause variation on the response and, as a consequence of the whole system.

Some of the tests, instead, show an oscillatory behavior in these parts of the cycles, in which it is often possible to highlight short segments with constant slope; as an example of this behavior longitudinal cycle 1 and cycle 2 for test 20 are depicted in Figure 5.179 and Figure 5.180:

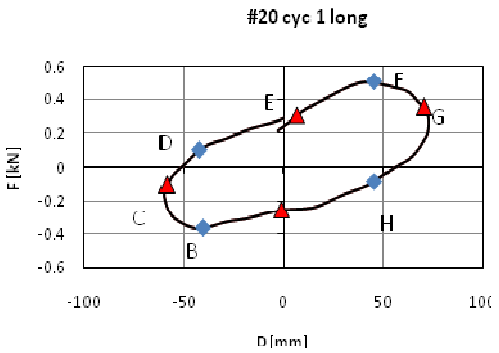

Figure 5.179 - variation of stiffness, cyc 1 test 20 longitudinal

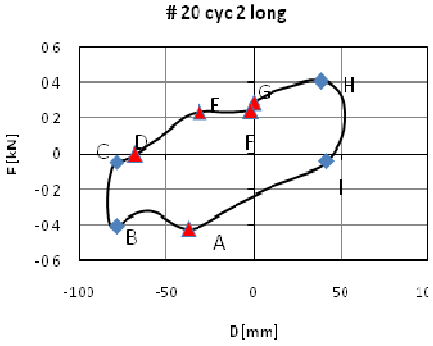

Figure 5.180 - variation of stiffness, cyc 2 test 20 longitudinal

For cycle 1 of test 20 the slope of the "straight" part has a great variation, and it can be approximated with different segments. Stiffness of the different segments can be compared to the theoretical value of stiffness evaluated as $K_{th} = \frac{W}{R^*}$ = 0.0034 kN/mm:

EF = 0.0054 kN/mm;
BA = 0.0036 kN/mm;
AH = 0.00329 kN/mm;
CD = 0.00139 kN/mm;
DE = 0.0043 kN/mm.

The same values can be calculated for cycle 2 and compared to the theoretical value given above:

DE = 0.0068 kN/mm ;
EF = 0.00034 kN/mm;
GH = 0.00345 kN/mm;
AI = 0.00488 kN/mm.

It is interesting to note that stiffness is very variable and it reaches values that are double the theoretical one, confirming the hypothesis that in some phases of the motion the relative displacement between the slider and one of the surfaces is absent.

For other segments (such as E –F Figure 5.180) stiffness decreases and the slope is almost zero. It can be remarked that, although the average stiffness can be compared with the theoretical one, when the behavior is investigated in detail it appears to be variable and affected by oscillations. Thus, the aspects that influence this behavior are multiple: the variation of vertical load due to rocking, the presence of "bouncing" and numerous others.

5.5.7.2 "Bouncing effect"

Bouncing is a dangerous phenomenon that is generated by non perfect sliding of the sliders on the curve surfaces. Based on the theoretical model of double concave curved surface slider, described in (35), the movement of the slider on both surfaces occurs concurrently, when the friction coefficients are equal. The experimental results highlight that this condition is seldom verified. The minute differences between the friction coefficients of both surfaces in conjunction with the mechanical characteristics of the two curve surfaces can induce different behaviors leading to a response completely different from modeled predictions. Furthermore, if the problem is observed from the point of view of the global system, the variation of vertical load previously underlined in the "rocking phenomenon analysis", leads to differences between the single devices that influence the dynamic response of the system.

A great issue is that all these phenomena interact with each other. The non synchronous sliding of the surfaces, for instance, affects the behavior of the slider that does not perfectly match one of the two surfaces anymore, causing an unpredictable distribution of pressure between slider and sliding surface, which can cause the instantaneous arrest of the device, due to pointing of the slider on one of the two surfaces, as depicted in Figure 5.135. Such a condition causes inertial oscillations that reduce the efficiency of the isolation system, it also increases the possible rocking effects and the oscillations of the system.

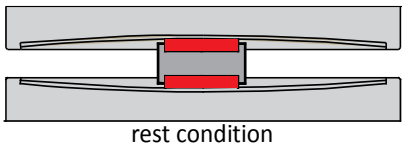

Figure 5.181 - device in rest condition

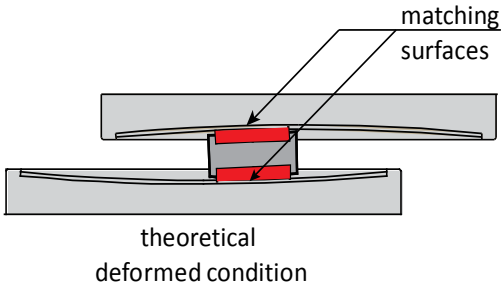

Figure 5.182 - device in a deformed condition

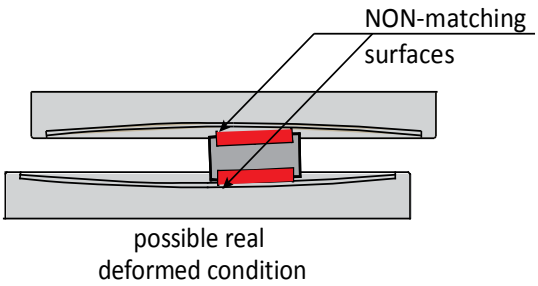

Figure 5.183 - device in a deformed condition

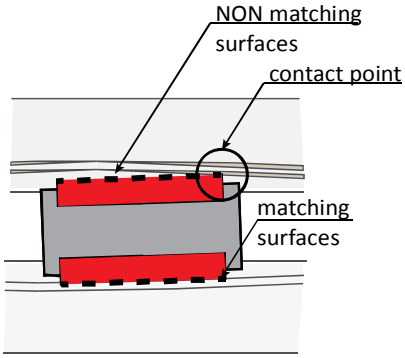

Figure 5.184 - pointing of the slider

The pointing of the slider produced by non correct matching of the surfaces can be removed or sensibly reduced by means of a design detail that allows slider's surfaces to follow device's surfaces curvature for each possible condition. The application of a hinge, as described in , would allow differential rotation of both the halves of the slider:

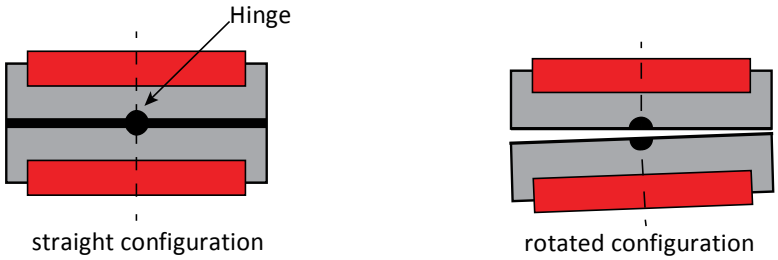

Figure 5.185 - slider with internal hinge, possible configurations a) undeformed, b) deformed

5.5.8 Conclusions and remarks

Experimental results show that the application of isolation devices for art objects with reduced dimensions and vertical load can be useful and produce positive results; indeed tests showed a good reduction of transmitted actions to the isolated object.

In order to set an adequate threshold of activation of the system with a minimum action level that does not generate any dangerous situation, the choice of application of lubricant is made. Such a solution helps with the reduction of the force that activates sliding in the devices but, on the other hand, allows greater displacements that needs to be taken into account during the design phase.

In general a maximum transmitted acceleration of 0.05 g was found. This upper limit is independent from the maximum acceleration of the input signal. Hence it can be stated that, as a solution to reduce the transmitted forces, such a type of isolation device, is an efficient choice.

Other interesting aspects emerged from the analysis of the tests, in particular numerous unexpected issues were found. In the following the aspects that showed to have significant effects on the general response are briefly summarized:

- effect of bidirectional inputs: it was found that bidirectional actions influence the maximum displacements of the system, by means of the reduction of the dissipation of energy. The modified mechanical model was also described, in order to describe the presence of simultaneous bidirectional actions which reduce the friction limit forces;
- rocking phenomena were underlined in the response of the system. The presence of these oscillations induces differences in the vertical displacements and vertical load of the devices. In particular a variation of the vertical load causes changes in the stiffness of the single devices, hence an uneven distribution among the bearings leads to potential rotation about the vertical axis, that results in higher horizontal displacements;
- rocking phenomenon is also emphasized by the presence of vertical action, which produces wider differential displacements between the base and the top of the statue and also an increasing of the horizontal displacements of the system itself;
- differences in the behavior of the single sliders were pointed out. This particular aspect can induce a differential vertical displacement between the single isolators that causes the loss of vertical alignment of the isolated structure, an increased horizontal displacement and, as an extreme case, the loss of contact of one or more of the devices. Such a situation causes unexpected dynamic response of the system which experiences local oscillations and changes in the equilibrium condition. Such a problem is more evident when the system is hyperstatic and with a high torsional stiffness: a possible solution to this can be the application of three isolators instead of four, which needs to be properly analyzed considering all the possible implications that it might have in the stability of the system.
- It was also pointed out that sliders can be in a position that is not perfectly centered, in this case the maximum stroke of the device can be significantly reduced:
- It was proven that the theoretical condition of simultaneous and regular sliding of the two sliding surfaces is not always verified; irregular initiation of motion can occur, caused by differences in the mechanical characteristics of the elements (i.e. friction coefficient of the surfaces);

- it was proven that the relative displacement between the slider and the surfaces can stop during the motion, this causes a modification of the system, which in some phases of the motion can behave as a single concave curved surface slider; a possible solution to this problem can be, where the maximum predictable displacements allow it, the choice of a single concave system instead of the double concave;
- the irregular relative movement between slider and sliding surface, in conjunction with the absence of an internal hinge in the slider, that can help the matching of the different surfaces, causes potential phenomena of pointing and stopping of the slider that moves without continuity, and generates oscillations that were named as "bouncing". A possible solution for better matching of the surfaces is the introduction of a hinge in the slider to better fit the possible different positioning of the slider.

In general it can be stated that the application of seismic isolation devices can be an efficient solution for single objects that need a mitigation of the seismic vulnerability condition. It must be noted that the application of such a solution, in particular the above described one, with DCCSS, must be studied and designed carefully because of the different aspects, besides the simple reduction of the horizontal actions, that it involves.

5.6 Numerical models

As it was previously mentioned, DCCSS has been studied and widely applied in the case of ordinary civil structures; it was though seldom considered for applications as the one proposed in this work. Part of this work was dedicated to highlight how, in condition of real applications, they show dynamic behaviors that may affect the general response of the system, and affect their efficiency.

Presence of these aspects makes the application of existing mechanical models and numerical models more difficult and, from some points of view, less reliable than what it is for traditional applications, because it can lead to a bad esteem of the design parameters.

5.6.1 Prediction tests based on F.I.P. tests results

According to the results obtained from the first series of experimental tests, carried out at FIP facility (par. 5.4), some preliminary numerical tests were performed, with the objective of a qualitative prediction of the responses of the tests performed at Caltrans SRMD facility in San Diego.

The mechanical model adopted is that implemented in the general purpose Finite Element software SAP2000 (37), and it has largely been validated. Results shown in the following concern the response of the experimental model in configuration cfg#1, subjected to the main input functions, used as inputs in the experimental tests. The sliding surfaces are assumed to be lubricated, because this condition will be the one chosen for a practical application, because of the advantages connected to this technical choice.

Besides the geometrical parameters involved, that are well defined (i.e. the curvature radii of the sliding surfaces and the maximum stroke of the isolators), the variability of other parameters can affect the numerical response and hence lead to an erroneous esteem of the response.

For this first application parameters values are set as:

- μ_f = 5%

The value is chosen considering the results obtained from the first series of tests, as depicted in Figure 5.43:

- K_1 = 51 K_2= 51*W/R = 51*0.003458 kN/mm = 0.1763 kN/mm

Initial stiffness, which characterizes the slope of the first part of hysteresis cycles and of the unloading phase, is evaluated according to the relation proposed by Naeim and Kelly ;

- ξ = 0.5% - 5%.

The value of the numerical damping is a choice that , as it will be shown, can affect the response of the model. In order to model a situation as closest as possible to reality, some analyses are carried out to assess the effects of

this parameter on the outcomes. It seems anyway reasonable to choose a value between the 0.5%, which simulates a damping close to zero, and 5%, which is given for general structural damping. The first value is justified by the fact that, since the objects targeted with the isolation system studied in this work are in general single block bodies, dissipative phenomena are very reduced. On the other hand, when the experimental multi-block system is modeled, there are possible relative displacements between the single blocks, due to the particular configuration of the structure, that can lead to friction dissipative phenomena. For this reason the maximum value is assumed as an upper limit.

The sensitivity of the response does not seem to be in general strong, as it is depicted in Figure 5.186:

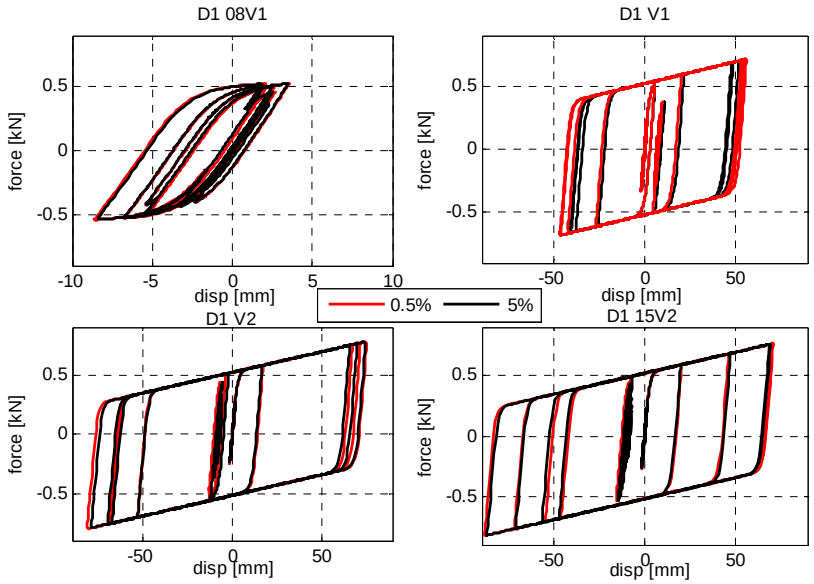

Figure 5.186 - comparison between results obtained with different values of numerical damping ξ

As it was expected displacements obtained with the lower value of numerical damping are higher, even though the difference is very low:

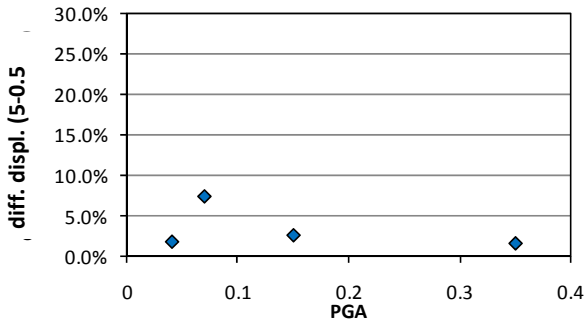

Figure 5.187 - variation of the maximum displacement for different values of ξ

The effect of numerical damping in this configuration of mechanical parameters does not affect much the predicted response.

Some important observations can be made from the comparison between the numerical and the experimental results: it instead, shows how an accurate evaluation of the involved mechanical parameters in the assessment of the response is fundamental for a reliable prediction of the dynamic behavior of the system:

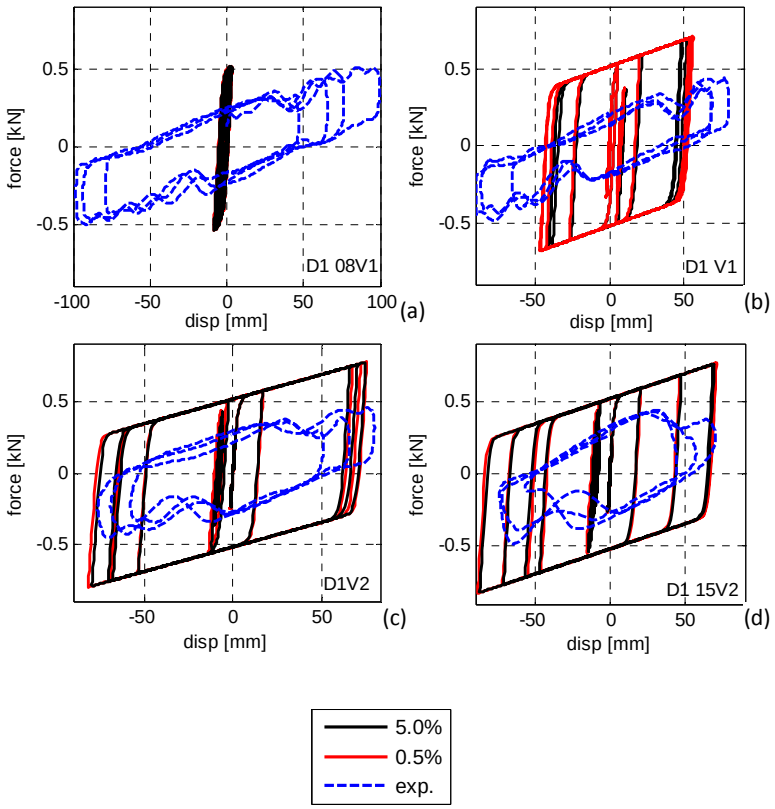

Figure 5.188 - comparison between numerical and experimental results: (a) D1 08V1; (b)D1 V1; (c) D1 V2; (d) D1 15V2

Results in Figure 5.188 depict the low accordance between the numerical prediction and the experimental results: the difference could be due to numerous factors, one of them can be an erroneous selection of the mechanical parameters. The first difference that can be pointed out is visible in the upper left graph, in which it can be observed that, for input D1 08V1, the experimental model experiences a full motion, while the numerical response shows reduced relative displacements, due to the fact that transmitted force barely overcomes the static friction force ($F_0 = \mu W$).

This is due to a wrong assessment of the coefficient of friction: the value of 5%, obtained from the experimental tests, clearly over evaluates the actual coefficient of friction of the system; this remark confirms what was already stated about the result obtained: friction evaluated with that particular set up is highly influenced by the dissipation of energy caused by the restrain system (described in 5.4.1) This is also confirmed by the other graphs of Figure 5.188, in which, independently from the input that is considered, the experimental cycles intersect the vertical axis for a lower value than the numerical ones.

On the other hand it can be noted that the stiffness K_2 is in general well represented, even though local oscillations are not described by the implemented model.

Despite the fact that, as the input intensity increases the experimental displacements are more accurately described, the numerical responses give an erroneous evaluation of the energy dissipated by the system: the area of the numerical cycles is higher than the experimental one. It was already stated how the wrong description of dissipative phenomena can lead to hazardous misevaluations in the design phase, and this aspect clearly appears from graph in Figure 5.189 . This figure depicts a comparison between the dissipated energy for the numerical solution (which represents the condition $\xi = 0.5\%$) and the experimental tests:

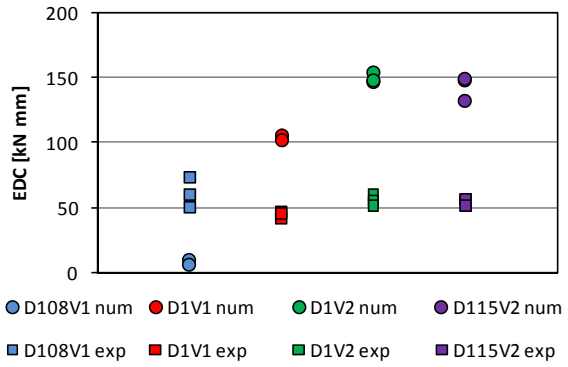

Figure 5.189 -comparison between numerical and experimental EDC

Results for the first test, D1 08V1, show that the dissipation of energy is very low for the numerical solution, due to the reduced relative displacement measured, besides this case the experimental tests always give a dissipation of energy lower than the one evaluated with the numerical model: it is reasonable to affirm that a numerical model characterized by this value of coefficient of friction overrates the dissipative capacity of the isolation system.

In Figure 5.190 a summary of the displacement behavior is depicted:

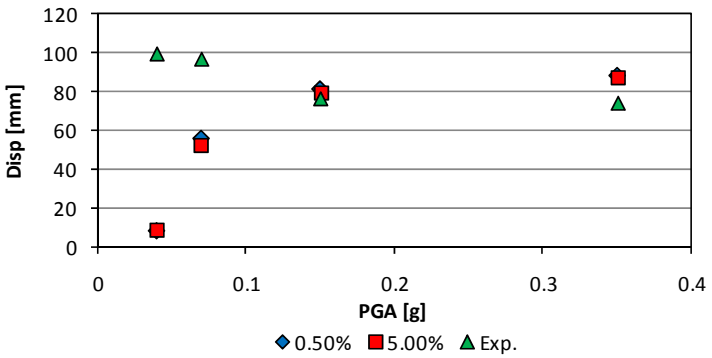

Figure 5.190 - comparison between numerical and experimental results, displacements

For the low levels of acceleration D1 08V1 and D1 V1 results obtained from the numerical model give highlight how coefficient of friction influences the response, in particular it is worth noting how it sets the threshold between the initiation of the movement and the fixed condition; indeed in this example the predicted response follows the ground motion, while in the experimental case the isolation system starts working and provides relative displacements.

As it was stated above, the parameters that mostly influence the response are the value of initial stiffness, damping ratio and the coefficient of friction. A series of sensitivity analyses and parametric evaluation were carried out and it was decided to increase the value of the initial stiffness from $K_1 = 51 * K_2$, as proposed by Naeim and Kelly (35) for isolators of standard dimensions, to $K_1 = 150 * K_2 = 519$ N/mm, considering the reduced dimensions of the applied isolation devices. Indeed the displacement that is acceptable for a level of force equal to the breakaway force, needs to be adequate to the features of the targeted isolated object: the acceptable "yielding" displacement for an art object cannot be the same for bridges or buildings. Furthermore the value of K_2 depends on the vertical load acting on the device, which for the case study of statues is reduced (also for other objects or devices that can be targeted with this system): this implies that, to obtain a dynamic response comparable to that of the traditional devices, the value of the coefficient needs to be adequately increased.

Assuming the above mentioned value for the initial stiffness a parametric evaluation on the coefficient of friction was performed. Results of the numerical and of the experimental tests were then compared. A summary is given in Figure 5.191:

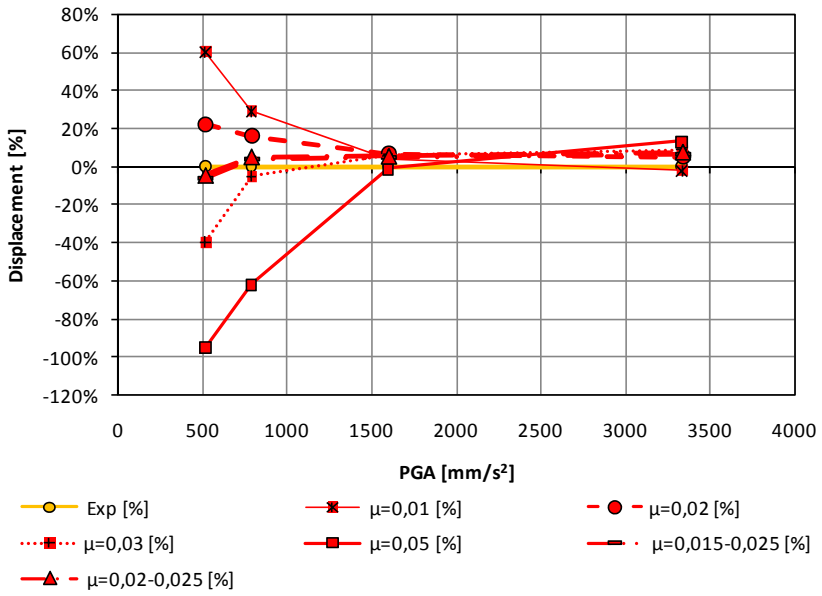

Figure 5.191 - variation of maximum displacements, cfg#1, K1 = 519 N/mm

5.6.2 Model parameters fitting to SRMD results

In order to assess the correct values of the mechanical parameters to adopt for the modeling of the case study of the "Galleria dei Prigioni" and also evaluate the unexpected effects emerged from the experimental results, some sensitivity analyses on the main mechanical parameters of the models were performed. Results obtained from the second series of experimental tests was then compared to the results of the numerical analyses.

The model adopted for this preliminary application represents the configuration of tests named cfg#1, an example is depicted in Figure 5.192

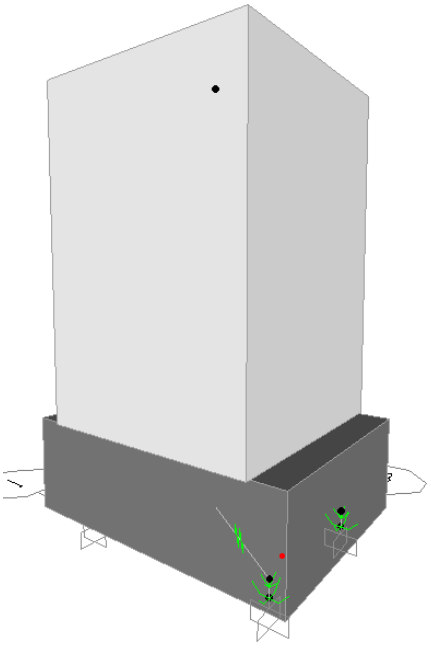

Figure 5.192 - sketch of the model representing configuration cfg#1

The parameters assumed for the mechanical characteristics of the devices were opportunely changed from the previous example.

First of all the real coefficient of friction for the lubricated case is lower than that assumed in the previous example, as it is shown in Figure 5.190. In this case coefficients of friction (respectively fast and slow) are assumed:

μ_f ; μ_s = 0.025 – 0.02;

also according to what was obtained from the analyses of the tests results showed in 5.5.5.

For what concerns the value of the initial stiffness the value of 519 N/mm is assumed, for the above explained reasons.

The other fundamental feature that needs to be analyzed is the coefficient of damping ξ to use in the analyses. A variable ξ ,between 0.5% and 5% was previously considered; in this case the layout of the experimental model is characterized by two interface surfaces which can experience a relative displacement, with a consequent dissipation of energy due to friction phenomena; this means that a value of damping coefficient close to zero is probably too small to describe that level of dissipation but on the other hand a value of 5% may be too high and lead to erroneous evaluations of the response. The graph depicted in Figure 5.193 shows the variation in terms of percentage of numerical results obtained with different values of the damping ratio ξ, from the value registered for the corresponding experimental test:

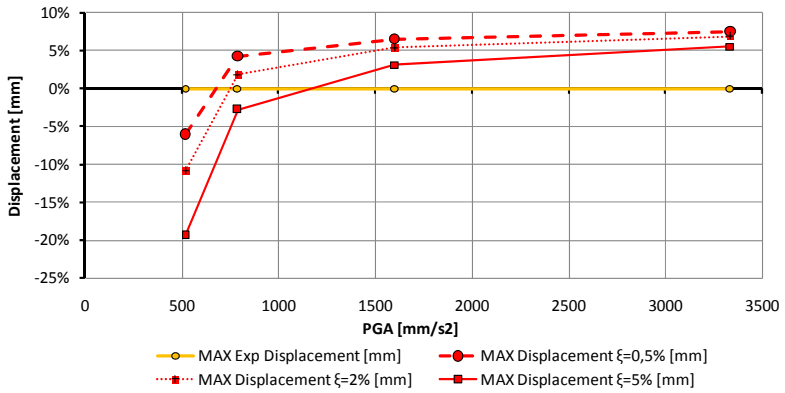

Figure 5.193 - Maximum displacements for different values of the damping ratio

For the lowest value of ground acceleration the predicted displacement is lower than the measured one; the difference between experimental and numerical response decreases with the increasing acceleration: it is interesting to highlight how, for ground acceleration of 0.07g (second level of acceleration) the damping ratios of 0.5% and of 2% provide a higher displacement than the experimental one, while model with 5% still has a lower displacement than the experimental. As the acceleration increases the numerical displacements tend to the same value, with a general difference of 5% from the experimental result.

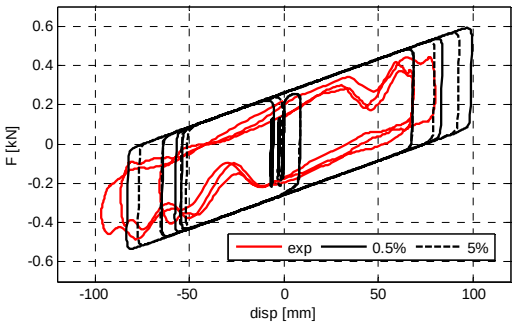

Figure 5.194 - comparison between experimental and numerical results, input D1V1

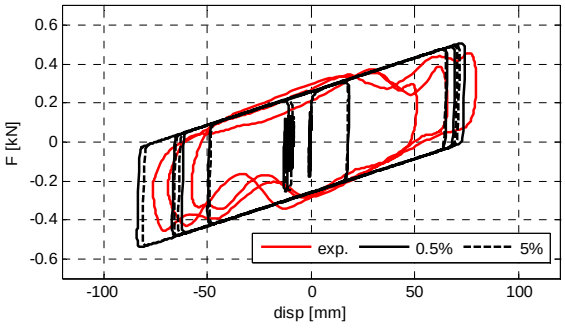

Figure 5.195- comparison between experimental and numerical results, input D1V2

A comparison between experimental tests and numerical results in terms of hysteresis loops is depicted In Figure 5.194 and Figure 5.195, for different levels of ground acceleration and, for the numerical results also considering damping ratio of 0.5% and 5%. The numerical response fits the experimental response with reasonable accordance in terms of maximum displacements and maximum forces experienced by the system; for the input D1V1, depicted in Figure 5.194, it is worth noting that coefficient of friction $\mu = 0.025$ is probably slightly too high (numerical loops intercept the vertical axis for higher levels of force then the experimental ones) but displacements are caught with a good level of approximation, even though they are slightly underestimated. This aspect is probably due to the higher dissipation of energy caused by the higher coefficient of friction of the model.

Table 5.16 - comparison between maximum displacements

D1V1	**MaxD [mm]**	**MinD[mm]**	**Abs [mm]**
Exp	80	-96	96
num 0.5%	100	-80.2	100
num 5%	92.78	-77.5	92.78
D1V2	**MaxD [mm]**	**MinD[mm]**	**Abs [mm]**
Exp	79	-76	79
num 0.5%	73.78	-82.7	82.7
num 5%	71.78	-80.49	80.49

The evaluation of the coefficient of friction is significant for the results, as it was just shown, even after an accurate experimental assessment of its value the variability it can have effects on the quality of the results.

Although the general behavior is described with good accordance by the numerical model, there are several aspect that it neglects: local oscillations visible in the experimental response are not present in the numerical outcomes and variation of stiffness during the motion are just two of the numerous effects that influence the response.

Some preliminary comparisons between numerical and experimental results for test number 19, carried out in configuration cfg#4, are presented in the following. In particular the hysteresis cycle along X and Y direction and the displacements of the system on plane XY show some interesting aspects of the behavior of the system.

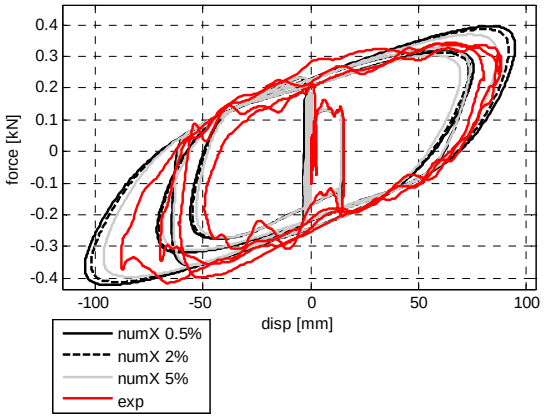

Figure 5.196 - test 19 cycle X

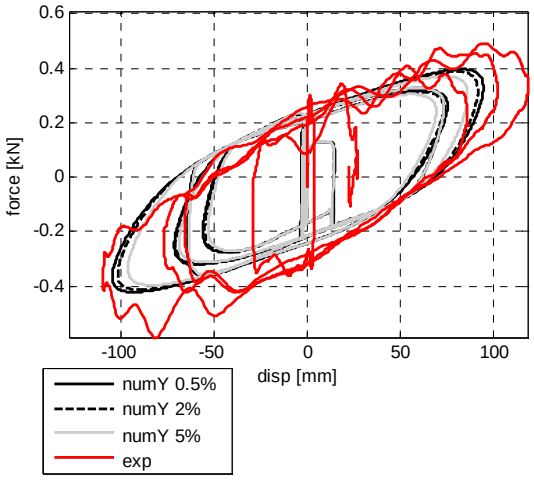

Figure 5.197 - test 19 cycles Y

Figure 5.196 and Figure 5.197 depict respectively the hysteresis loop along X and Y directions, it can be noted how, for the longitudinal direction X the numerical model provides results that can be considered on the safe side from the point of view of maximum displacement and maximum force transmitted to the object. Furthermore, comparing these results with the different levels of damping assumed, it can be stated that the 2% and 5% properly fit the experimental results. It is worth noting that the typical curve shape of responses to bidirectional inputs is well approximated by the mechanical model of friction, which is presented and described in 5.5.6.1. Results obtained along the perpendicular direction Y do not present the same accordance, indeed as it can be observed from Figure **5.197**, the numerical response underestimates the experimental results both in terms of forces and accelerations. Along the longitudinal direction, in particular, the effect of local oscillations can be highlighted; local oscillations do not affect the general trend, but they influence the local response of the system with potentially dangerous actions for the targeted isolated object.

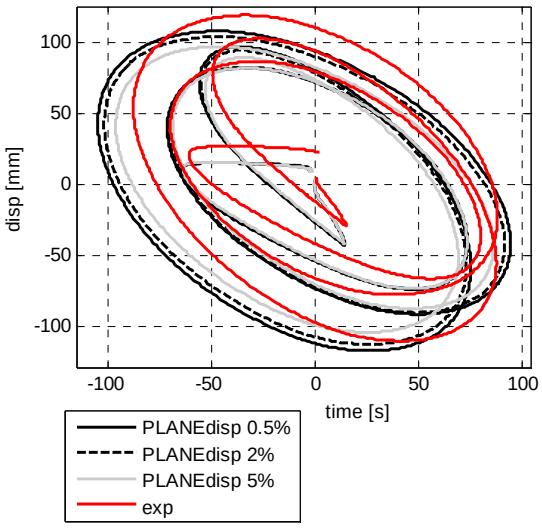

Figure 5.198 - displacements in plane

Figure 5.198 show the comparison between numerical and experimental displacements of the system in the plane X Y.

Table 5.17 - comparison between displacements

T19	MaxDx [mm]	MinDx [mm]	Abs [mm]
Exp	87.87	-88.26	88.26
num 0.5%	94.6	-104.95	104.95
num 2%	91.7	-101.95	101.95
num 5%	86.26	-96.32	96.32
T19	**MaxDy [mm]**	**MinDy [mm]**	**Abs [mm]**
exp	109.56	-118.8	118.8
num 0.5%	107.6	-116.5	116.5
num 2%	103.63	-111.94	111.94
num 5%	96.63	-103.61	103.61

5.6.3 Analyses on 3D models of statues

One of the objectives pursued in this work is an assessment of the efficiency of the above described intervention of mitigation. This aspect is important for a potential phase of decision: it is fundamental to understand whether the system works or not for the specific case and whether its application is worth.

Preliminary results described in the following present an example of two statues of the case study equipped with the system of double concave curved surface slider described in 5.3. Four devices are positioned at the four corners of the pedestal of the statue; this configuration represents one of the possible layouts of a real application. Analyses are performed on 3D finite element models.

The first objects targeted with the analyses are the statues of "San Matteo" and the "Barbuto" that probably, as it was previously mentioned, represent the most interesting statues of the case study because of their health condition and of the uncertainty about the mechanical properties of the material. The objects are considered rigidly restrained to the base.

The inputs selected for this preliminary application are:

- D1 1,5 V2 applied along the weak direction (as for the previously described test number 15);

- D1 0,8 V1 applied along X and Y direction (as for the previously described test 19);

- Earthquake 1916,(used as input in section 3.7.7.2) considering both components along the X and Y components.

The mechanical properties of the isolation system were chosen according to the results obtained from the mechanical modeling of the tests carried out at SRMD:

μ_f ; μ_s = 0.025 – 0.02;

ξ = 0.5%

From these first results some preliminary considerations can be made. The comparison between the stress pattern obtained in the objects demonstrates how for medium values of acceleration, i.e. test 15 with a peak ground acceleration of 0.35g, the application of the isolation system provides a good reduction of the stress level and of the maximum differential displacement between the top and the bottom of the statues indeed the application of the isolation system for the statue of the "Barbuto" reduces the stress level from the value of 0.74 MPa to 0.14 MPa

Also for the statue of San Matteo the effect of the isolation system is evident, the maximum tensile stress measured in the object, when it is considered fixed to the ground, is 0.79 MPa, while, after the application of the isolation system the maximum value of measured stress is 0.09 MPa

It is worth noting that this level of acceleration is considered a medium high level for the Italian territory.

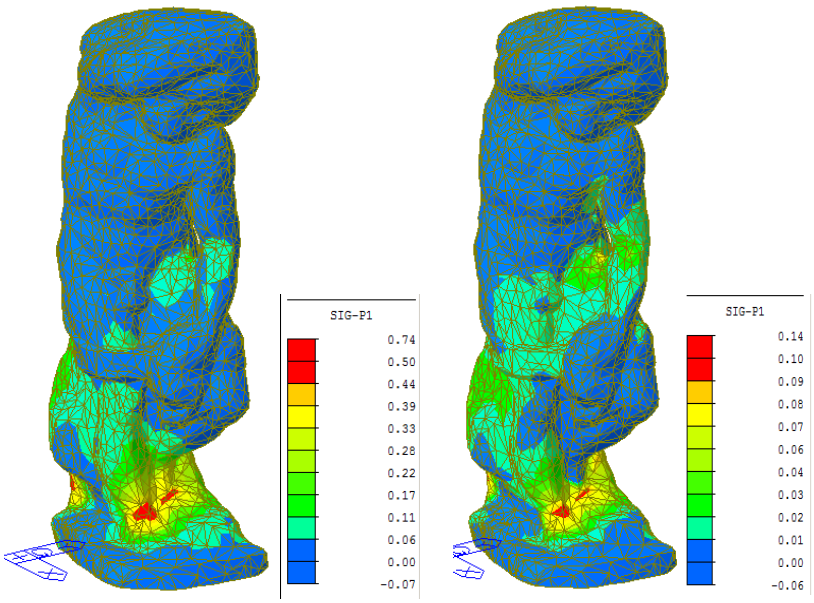

Figure 5.199 - Barbuto stress level, D1_1,5V2 input, a) non isolated b)isolated

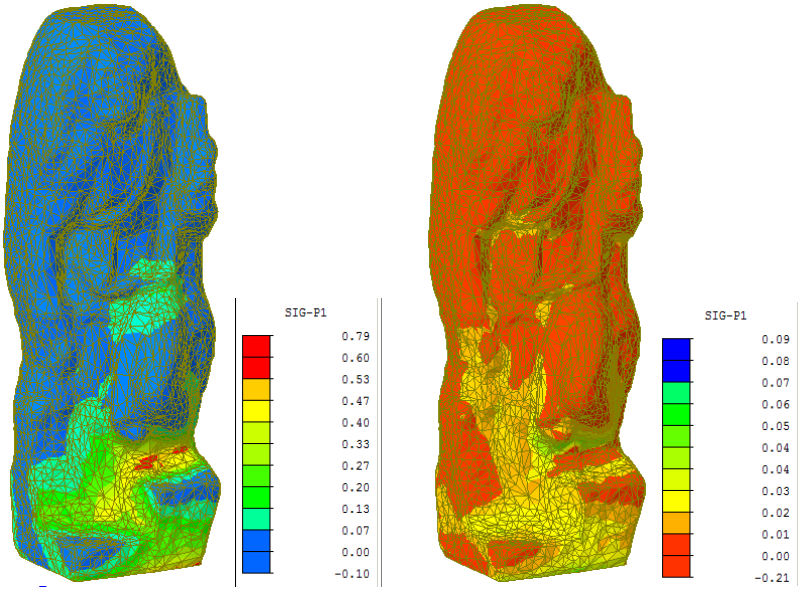

Figure 5.200 - San Matteo stress level [MPa], D1_1,5V2 input, a) non isolated b)isolated

Table 5.18- summary of stresses and displacements

TEST 15		σ_{max} [MPa]	Δ disp [mm]
BARBUTO	Ground	0.74	0.07
	Isolated	0.14	0.02
SMATTEO	Ground	0.79	0.06
	Isolated	0.09	0.01

When the bidirectional input of test 19 is applied, in which the maximum acceleration along both directions is 0.04g. the improvement of the conditions of the objects given by the introduction of the devices is not significant: the stress level measured on the fixed object and on the isolated object is not different; almost the all input is transmitted to the

statue, from Figure 5.201 it can be noted that the maximum tensile stress level decreases from 0.16 to 0.13 MPa. These results are in agreement with what expected from the experimental results.

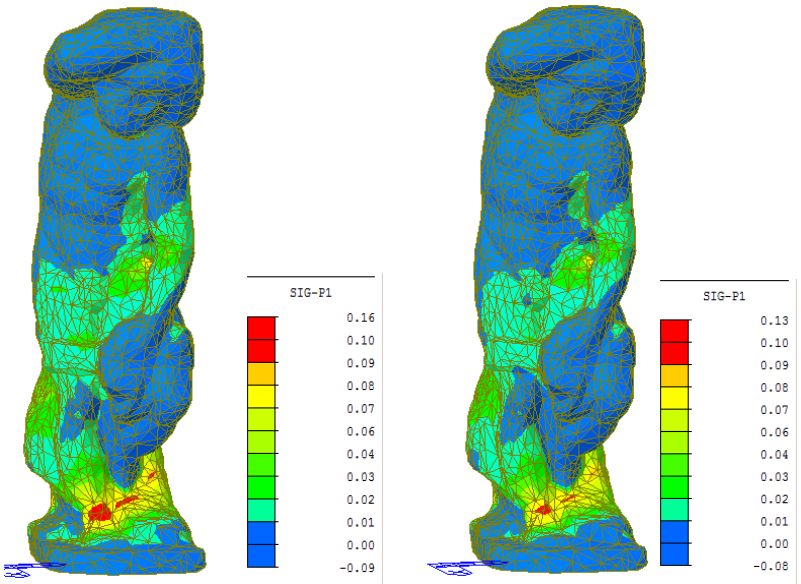

Figure 5.201- Barbuto stress level [MPa], D1_0,8V1 input, a) non isolated b)isolated

In section 3.7.7.2 it was shown the results of the application of recorded earthquakes, compatible to the response spectrum of the site, to the statues considered as rigidly fixed to the ground; in the following the same input (record 1916) will be applied to the isolated system in order to provide a first overview of the effects of this system for the reduction of the stress level in the objects.

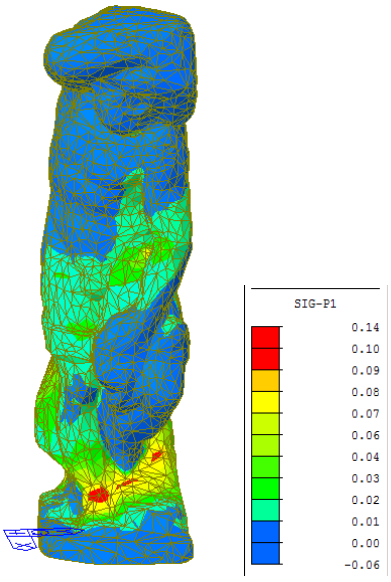

Figure 5.202 - Barbuto stress level [MPa], D1_0,8V1 input, a) isolated

The stress level displayed in Figure 5.202 reached 0.65 MPa, compared to that depicted inFigure 3.79, 0.14 MPa, shows that the application of the isolation system is efficient since it reduces the stress in the most stressed zone which is still the one of the ankles and corresponds to a reduction of the resisting section of the statue.

From these first results it comes out the importance of the ground acceleration for the decisional phase: the application of isolation systems in sites prone to low level of earthquake needs to be carefully evaluated, considering first of all the type of the object that to protect and, after that, the technical and economic efforts necessary to set up such a system. An acceleration of 0.05g, which is considered a low level for the Italian territory, would not justify the introduction of isolation systems since the improvement in the conditions of the objects is not significant. On the other hand, medium

levels of acceleration showed that the application of an accurately designed isolation system can reduce its vulnerability within acceptable levels.

Furthermore it is worth noting that the presented models do not take into account the real behavior of the isolators. As it was underlined in 5.5.6 strong local effects due to different dynamic phenomena are present and could influence the general response of the system.

6. Conclusions

The involvement and support of this project by the Italian ministry for artistic and cultural goods (MiBAC) should be acknowledged again. This project aims to define new guidelines to deal with the seismic vulnerability assessment and mitigation of different types of cultural goods.

In this dissertation a brief review of the risk framework was presented. Its main aspect were described and compared to the principles proposed by the "Guidelines for assessment and mitigation of seismic risk on cultural heritage" published by MiBAC, with the main intent to propose an extension of these standards, which only deal with masonry structures, to movable art objects. The presented work focuses mainly on the proposal of a procedure inspired to the principles given in the Guidelines and it adapts them to the peculiar features of these objects.

In the first part a comparison with the above mentioned norms and the risk framework is described. This is meant to be an introduction to the problem of the assessment of seismic vulnerability and to its position within a risk analysis framework. The numerous similarities between the traditional risk management approach and the one presented by the norms let understand the common roots of the two methods and they highlight the fact that, since knowledge from different fields is involved, the extension of the methodology that will be presented needs to be strictly connected to that presented in the original risk assessment framework.

Afterwards the principles of guidelines are described and applied to the case study of Venetian bell towers: such an application was aimed to explain the criteria of the code, with particular attention to simplified models. It emerged how the standards can be useful for drawing a priority list of intervention and how they can pinpoint critical situations that require more accurate analyses. On the other hand, the application also revealed the sensitivity of the results to the mechanical model chosen and to the parameters involved in the evaluations. These results are fundamental for the procedure to extend the criteria to art objects as one of the most challenging tasks is the definition of reliable, but at the same time simple, mechanical models. Models need to involve a small number of significant parameters either geometrical or mechanical; the choice has necessarily to be the most objective possible.

The next part deals with the proposal of the assessment criteria: the steps for a complete understanding of the problem are described in detail, with particular attention to those of the "path of knowledge" that can mostly affect the quality of the outcome of further analyses. The problem is dealt with both from a theoretical point of view, with an accurate description of each significant step, and also from the practical one. Indeed the entire methodology is applied step-by-step to the case study of the Galleria dell'Accademia, in Florence and in particular to "Sala dell'Ottocento" and "Galleria dei Prigioni".

First of all the reference action is dealt with: new limit states for art objects are defined: the new Artistic Limit State is proposed. Additionally, the reference period of the characteristic actions that are connected to the ultimate limit state is then defined, with attention to the safeguard of people surrounding the targeted object.

The accuracy of the survey is one of the most significant aspects that is taken into account; different levels of accuracy were studied in order to highlight the interaction between the level of detail chosen, the reliability of the results and the choice for a proper safety coefficient. It came out that the higher accuracy of the geometrical survey does not mean neither always a safer result nor always a less safe one.

Another important aspect that was considered is the material survey; art objects are indeed made out of very different materials and with such different characteristics that a reliable evaluation of the mechanical properties is in general a hard task. For this reason a specific procedure for the survey of stone materials is proposed as an example, highlighting those aspects that can mostly affect the outcomes in terms of seismic safety levels.

A significant aspect of this work is the proposal of possible mechanical models to apply to art objects: different approaches were indeed proposed. The targeted artifact can be studied, either as a rigid body or as a deformable body according to its geometry and restraint conditions. Whenever the body is simply supported it is free to develop a dynamic response that can be described with the known relation that govern rigid body phenomena. These phenomena were studied, focusing in particular on rocking and overturning aspects; besides the “typical” solution to the problem, considered in literature with static formulas, also other aspects were taken into account: the presence of vertical action and the possibility to deal with a non symmetric body. In order to investigate the rigid body phenomena, the above mentioned relations were studied by means of a specifically developed numerical tool that can solve non linear rocking equations for non symmetric objects subjected to general horizontal and vertical input. Such a tool was applied both as a feedback for the static formulas presented before and as a tool to describe the dynamic response of a specific object, for a more detailed level of analyses. Results obtained from the application showed the adequate reliability of the simplified formulas, which provide results that are reasonably on the safe side. On the other hand, whenever a more detailed description of the dynamics of the system is required, the integration of the equation of motion seems to be quite a reliable instruments that can provide a description of the motion of the object in time.

From the point of view of the procedure it was then proposed that, when triggering of motion is predicted, one of the possible technical solutions is to connect it to the ground (or to the supporting surface). Such a solution implies that the stress level into the artifact needs to be checked, since the entire seismic action is transmitted to the object through the anchorage devices. Different methods can be adopted to proceed with the stress levels checking, in particular in this dissertation the renderings obtained with 3D laserscanner survey were adopted to implement 3D Finite Element models of the statues exhibited in Galleria dei Prigioni. The attention was focused on those that, for particular reasons (i.e. uncertainties on materials conditions) are in a health state that needs to be investigated. Analyses were performed assuming bi directional inputs along the principal directions of the objects; they revealed that, for the case study, the stress level induced by the reference action does not exceed the mechanical limits set for the considered material. Despite the fact that stress levels are not dangerously high, the diffused uncertainties about materials and about the actual health condition of the objects, joined to the procedural structure of this work lead to the decision of the application of some mitigation techniques to reduce the seismic vulnerability.

Hence the last part of this work deals with the aspect of mitigation of seismic vulnerability. Different approaches to this problem are presented: quick methods for interventions of mitigation on a large scale are presented, with hypothesis for the application of low cost and easy to apply techniques that aim to improve the safety condition of a large number of objects. Furthermore a significant part of the mitigation section is dedicated to the discussion of the application of seismic isolation devices for the case of art objects. In particular it was proposed to apply a technical solution that involves the application of a well established technology, reshaped to fit the peculiar conditions of art goods.

It was decided, in co operation with an Italian producer, to apply double concave curved surface slider devices. Such a solution required a first phase of re-design of the devices to fit the particular needs of light weight and reduced room of application, then two series of experimental tests were carried out with the purpose to characterize the mechanical parameters of the devices and also to study the dynamic response of a system resembling the statues of the case study. Both the targets were proficiently pursued, and the outcomes showed that, after an accurate redesign phase, the reduction of the seismic action transmitted to an isolated object is efficient. Despite this general encouraging result it was also highlighted the fact that, in areas characterized by a-low reference seismic action, the efforts to set up this technical solution may not be worth the benefit they give. The choice for the application indeed needs to take into account numerous aspects, connected to the difficulty of application in museums that are often classified as “historical” themselves or to the objective lack of room. Hence the choice for this solution must be accurately evaluated.

The experimental phase also highlighted some interesting and unexpected behaviors that these type of devices present, when applied to a real system: results showed the presence of several phenomena that produce a behavior slightly different from the theoretical one; these aspects may influence the response and the effects on the targeted object, which is a significant aspect also considering the fact that artifacts are in general much delicate. Presence of non continuous motion of the two faces of the isolators, potential stopping of the sliders during motion, reduction of the stroke of the devices emerged from the analyses: these aspects need to be studied with more attention and with specific tests aimed to underline either the effects they have on the target isolated object and the causes that generate them.

Concluding, it should be remarked that the efficiency and the applicability of the proposed procedure was demonstrated throughout this dissertation. Moreover the quality of results obtained from its application seems to be reasonably good in the context of a vulnerability assessment environment. Similarly the mitigation part also resulted in good outcomes, but there is opportunity to further investigate and improve the actual proposal. Several further possible developments are presented and described, in particular for the optimization of the devices proposed in the dissertation.

Appendix A – Bayes' Rule

In the Bayesian interpretation the probability P(A) of the event A is formulated as a *degree of belief* that A will occur. The degree of belief is a reflection of the state of mind of the individual person in terms of experience and preferences. The Bayesian statistical interpretation of probability is personal-dependent but the subjectivity should be based on experience from previous trials, like in the frequentistic definition of P(A), as well as considering the objective nature of the problem, like in the classical definition (39).

Given two sets A and B with assigned probabilities P(A) and P(B) respectively, the conditional probability of B given A is defined as:

$$P(B|A) = \frac{P(A \cap B)}{P(A)} \tag{A.1}$$

where $A \cap B$ is the intersection sets that proves $P(A)$ is greater than zero.

Considering that the whole set $\Omega = A_1 \cup A_2 \cup \dots A_n$ composed by n mutually exclusive subsets A_i, and let X be an arbitrary se; the *total probability* theorem provides:

$$\begin{aligned} P(X) &= P(X \cap A_1) + P(X \cap A_2) + \cdots P(X \cap A_n) \\ &= P(X|A_1)P(A_1) + P(X|A_2)P(A_2) + \cdots P(X|A_n)P(A_n) \end{aligned} \tag{A.2}$$

From (A.1) it is $P(X|A_i)P(A_i) = P(X \cap A_i) = P(A_i|X)P(X)$, implying that:

$$P(A_1|X) = \frac{P(X|A_i)}{P(X)} P(A_i) \tag{A.3}$$

The above formula presents the denominator for the Bayes' rule:

$$P(A_i|X) = \frac{P(X|A_i)P(A_i)}{\sum_j P(X|A_j)P(A_j)} \tag{A.4}$$

showing how one conditional probability depends on its inverse. In other terms, it is derived how the probability $\mathrm{P(A_i|X)}$ of an event $\mathrm{A_i}$ given observed evidence X is related to the probability of that evidence given the event $\mathrm{P(X|A_i)}$.

Using (A.4), the priory probability of an event $\mathrm{P(A_i)}$ is updated by the observation of the evidence X defining the posteriori probability $\mathrm{P(A_i|X)}$.

References

1. **Faber, M.H.** *Risk and safety in civil engineering – Lecture Notes.* ETH Zürich : s.n., 2007.

2. **Pliefke, T., Sperbeck, S. e Urban, M.** *The probabilistic risk management chain - General concept and definitions.* Braunschweig : GRK 802, 2007.

3. **Grossi, P. and Kunreuther, H.** *Catastrophe modelling: a new approach to managing risk.* s.l. : Springer, 2005.

4. **Baker, J.W. and Cornell, C.A.** *Uncertainty specification and propagation for loss esti-mation using FOSM methods.* Berkeley : University of California, 2003. PEER Report 2003/07.

5. *Some proposals for a first step towards a Per-formance Based Wind Engineering.* **Paulotto, C., Ciampoli, M. and Augusti, G.** Stoos, Switzerland : s.n., 2004. IFED International Forum in Engineering Decision Making: First Forum.

6. **Olivato, G.** *Managing Wind Risk On Long Span Roofs.* 2010.

7. *Rocking Response of Rigid Blocks to Earthquake.* **Yim, CS, Chopra, A. e Penzien, J.** 1980, Earthquake Engineering and Structural Dynamics, p. 565-587.

8. *Compatible acceleration and displacement spectra for seismic design codes.* **Bommer, J.J., A.S., Elnashai e A.G., Weir.** Auckland : s.n., 2000.

9. **Lazzarini, L e Laurenzi Tabasso, M.** *Il restauro della pietra.* s.l. : Cedam, 1986.

10. **Griffith, A.A.** The phenomena of rupture and flow in solids. *Philosophical Transaction of the Royal Society of London.* 1921.

11. **G., Irwin.** Analysis of stresses and strains near the end of a cracking transversing a plate. *Journal of Applied Mechanich.* 1957, 24.

12. **Antonelli, F., et al.** Provenance of the ornamental stones used in the baroque church of "S.Pietro in Valle" and commentary on their state of conservation. *Journal of Cultural Heritage.* 2003, Vol. 4.

13. **L., Lazzarini e Antonelli, F.** La determinazione dell'origine delle pietre e dei marmi usati in antico. L'identificazione del marmo costituente manufatti antichi. [aut. libro] L. Lazzarini. *Pietre e marmi antichi.* s.l. : Cedam, 2004.

14. *Motions of rigid bodies and criteria for overturning by earthquake excitations.* **Ishyiama, Y.** 1982, Earthquake Engineering and Structural Dynamics, p. 635-650.

15. **Housner, G.W.** The behavior of inverted pendulum structures during earthquakes. *Bulletin of Seismological Society of America.* 1963, Vol. 53, 2.

16. **Lowry, M., Farrar, B.J., Armendariz,D. e Podany, J.** A review of the protection of objects in the J.Paul Getty Museum from earthquake damage. [aut. libro] J. Podany. *Advances in the Protection of museum collections from earthquake damage: papers from a Symposium held at the J.Paul Getty Museum at the Villa.* Malibu : Getty Pubblications, 2006.

17. *Criteria for Initiation of Slide, Rock, and Slide-Rock Rigid Body Modes.* **Shenton, H.W.** 1995, Journal of Engineering Mechanics, p. 690-693.

18. *Overturning criteria for non-anchored non-symmetric rigid bodies.* **Boroschek, Ruben L. and Romo, David.** Vancouver : s.n., 2004. 13th World Conference on Earthquake Engineering.

19. **Augusti, G., Ciampoli, M e L., Airoldi.** Protezione sismica degli oggetti d'arte: uno studio preliminare. *Ingegneria Sismica.* 1993, Vol. 1, X.

20. *Initiation of motion of a free-standing body to base excitation.* **Tung, C.C.** 36, s.l. : Wiley Interscience, 2007.

21. **Caliò, I. e Marletta, M.** Passive control of the seismic rock response of art objects. *Engineering Structures.* 2003, Vol. 25.

22. **Purvance, Matthew D.** *Overturning of Slender Blocks: Numerical Investigation and Application to Precariously balanced Rocks in Southern California.* Reno : s.n., 2005.

23. **MATLAB.** *The performance language software for technical computation.* 2002.

24. **Makris, N. e D., Konstantinidis.** Seismic response analysis of multidrum classical columns. *Earthquake engineering and structural dynamics.* 2005, 34.

25. **D, Gasparini e E.H., Vanmarke.** *SIMQKE:A program for Artificial Motion Generation.* Boston (MA) : Department of Civil Engineering Massachussets Institute of Technology, 1976.

26. **Priestley, M.J.N, G.M., Calvi e M.J., Kowalsky.** *Displacement Based Seismic Design of Structures.* s.l. : IUSSPress. ISBN: 88-6198-000-6.

27. **Iervolino I., Galasso C. e E., Cosenza.** REXEL: computer aided record selection for code-based. *Bulletin of Earthquake Engineering.* 2010, Vol. 8, 2.

28. **Agbabian, M.S., et al.** Evaluation of earthquake damage mitigation methods for museum objects;. *Studies in conservation.* 1991, Vol. 36.

29. **Berto, L., et al.** Assessment of seismic vulnerability of art objects: the "Galleria dei prigioni" sculptures at the Accademia Gallery in Florence. *Journal of Cultural Heritage.* 2012.

30. **Attanasio, D., Rocchi, P. e Platania, R.** The Fantiscritti provenance of the David's Marble: new data supporting an old hypotesis. *Exploring David.* Firenze : Edizioni Giunti, 2004.

31. **Gorogoni, C. e Pallante, P.** Sulla provenienza del marmo dell'Adolescente dell'Hermitage. *Critica d'arte.* 2001.

32. **IMIM, (internazionale marmi emacchine).** *THe tuscan marbel identities.* Signa (FI) : s.n., 2010.

33. **Scesi, L., Papini, M. e Gattinoni, P.** *Geologia applicata, il rilevamento geologico tecnico.* s.l. : Ed.Ambrosiana, 2006.

34. Direttiva P.C.M. 12 Ottobre 2007 per la valutazione e riduzione del rischio sismico del patrimonio culturale tutelato, S.O. n 25 della G.U. n. 24 del 29 Gennaio 2008, update 9 febbraio 2011.

35. **Naeim, F. e J.M., Kelly.** *Design of Seismic isolated Structures: from theory to practice.* s.l. : John Wiley and Sons, Inc., 1999.

36. **Fenz, D. e M., Constantinou.** Behaviour of the double concave Friction Pendulum bearing. *Earthquake engineering and Structural Dynamics.* 2006, 35.

37. **Constantinou, M., A., Mokha e A., Reinhorn.** Teflon Bearings in Base Isolation II: Modeling. *Journal of Structural Engineering.* 1990, Vol. 116, 2.

38. **Structures, Computer and.** *CSI reference manual, for SAP, ETABS, and SAFE.* Berkeley : s.n., 2008.

39. **Faber, M.H.** *Statistics and probability theory – Lecture Notes.* ETH Zürich : s.n., 2006.

40. *Guidelines For Seismic Protection of Museum Contents.* **Augusti, G. e M.Ciampoli.** Acapulco : s.n., 1996. Proceedings of 11th World Conference on Earthquake Engineering.